STAR

Bell Laboratories

NASA CR-122389

# FINAL REPORT ON

## REDUCTION AND ANALYSIS OF PARTICLE DATA FROM IMP F (EXPLORER 34) AND IMP G (EXPLORER 41)

by
**W. L. Brown, L. J. Lanzerotti, et. al.**

Contract NAS 5-9102

## DECEMBER 31, 1971

Period Covered June 1965 - December 1971

(NASA-CR-122389) REDUCTION AND ANALYSIS OF PARTICLE DATA FROM IMP F (EXPLORER 34) AND IMP G (EXPLORER 41) Final Report, Jun. 1965 - W.L. Brown (Bell Telephone Labs., Inc.) 31 Dec. 1971 249 p CSCL 03B G3/29

N72-21831 thru N72-21848 Unclas 24396

prepared by
Radiation Physics Research Department
Bell Telephone Laboratories, Incorporated
Mountain Avenue, Murray Hill, New Jersey 07974
Dr. W. L. Brown—Principal Investigator
on behalf of
Western Electric Company, Incorporated
83 Maiden Lane, New York, N.Y. 10038
for
Goddard Space Flight Center
Greenbelt, Maryland 20771
Dr. F. B. McDonald—Technical Monitor

| 1. Report No. | 2. Government Accession No. | 3. Recipient's Catalog No. |
|---|---|---|
| 4. TITLE AND SUBTITLE<br>FINAL REPORT ON REDUCTION AND ANALYSIS OF PARTICLE DATA FROM IMPF (EXPLORER 34) AND IMPG (EXPLORER 41) | | 5. Report Date<br>December 31, 1971<br>6. Performing Organization Code |
| 7. Authors<br>W. L. Brown, L. J. Lanzerotti, et. al. | | 8. Performing Organization Report No. |
| 9. Performing Organization Name and Address<br>Bell Telephone Laboratories, Incorporated<br>Murray Hill, New Jersey 07974<br>on behalf of<br>Western Electric Company, Incorporated<br>New York, New York 10038<br>Dr. W. L. Brown - Principal Investigator | | 10. Work Unit No.<br>11. Contract or Grant No.<br>NAS 5-9102<br>13. Type of Report and Period Covered<br>Final Report |
| 12. Sponsoring Agency Name and Address<br>National Aeronautics and Space Administration<br>Goddard Space Flight Center<br>Greenbelt, Maryland 20771<br>Dr. F. B. McDonald - Technical Monitor | | 14. Sponsoring Agency Code |
| 15. Supplementary Notes | | |

16. Abstract

This report consolidates material prepared by investigators who participated in the analyis of particle data acquired by Bell Laboratories particle detection equipment on Explorer 34 and Explorer 41 satellites. Results of studies contained in this report concern the propagation and composition of Solar flare particles measured in interplanetary space by the two satellites. This material has been presented at meetings in the form of talks and papers and in articles appearing in numerous scientific journals.

| 17. Key Words | 18. Distribution Statement |
|---|---|
| Explorer (IMP F&G) Particle Data Analysis<br>Solar Flare Electrons, Protons, and<br>Alpha Particles | |

| 19. Security Classif.(of this report) | 20. Security Classif.(of this page) | 21. No. of Pages | 22. Price |
|---|---|---|---|
| | | | |

## PREFACE

This is the final report on the reduction and analysis of data obtained from particle detection equipment flown on the Explorer 34 (IMP F) and Explorer 41 (IMP G) spacecraft. The equipment on Explorer 34 successfully acquired data from launch on 24 May 1967 until reentry in May 1969. The particle detection equipment on Explorer 41 successfully acquired data from launch on 21 June 1969 until the end of January 1970, after which time, due to a failure in a spacecraft power supply, the high energy particle identifier modes in the equipment became inoperative. From February 1970 to the present time this equipment has successfully acquired low energy proton, alpha particle, and electron data in interplanetary space and in the magnetosphere.

The data obtained from the equipment on both IMP satellites have been utilized predominately for studies of solar flare particle composition and propagation and for studies of particle penetration into the magnetosphere. Many of these analyses have involved data correlations using data obtained from Bell Labs equipment on the ATS-1 satellite and data from spacecraft experiments conducted by other groups.

In accordance with original plans, all scientifically significant information derived to date from the data reduction and analysis work has been disseminated. This has been accomplished by means of talks at scientific meetings and articles presented in scientific publications, the latter of which are all included in this report. It is expected that analysis work on the Explorer 34 and Explorer 41 data will continue indefinitely under Bell System sponsorship. It is fully intended that future results of scientific importance stemming from this work will be shared with the scientific community at large.

TABLE OF CONTENTS

TABLE OF CONTENTS (Continued)

TABLE OF CONTENTS (Continued)

TABLE OF CONTENTS (Continued)

LIST OF ILLUSTRATIONS

LIST OF ILLUSTRATIONS (Continued)

LIST OF ILLUSTRATIONS (Continued)

LIST OF ILLUSTRATIONS (Continued)

LIST OF ILLUSTRATIONS (Continued)

LIST OF ILLUSTRATIONS (Continued)

LIST OF ILLUSTRATIONS (Continued)

LIST OF ILLUSTRATIONS (Continued)

LIST OF ILLUSTRATIONS (Continued)

LIST OF TABLES

N72-21832

# CHAPTER 1

## A SATELLITE SOLAR COSMIC RAY SPECTROMETER WITH ON-BOARD PARTICLE IDENTIFICATION

L. J. Lanzerotti, H. P. Lie and G. L. Miller*


### ABSTRACT

The design and calibration results of a satellite based solar-cosmic ray particle identifier system utilizing a field effect transistor analog multiplier for the IMP F and G spacecraft are described. A discussion is made of the effectiveness of particle separation by such a particle identifier used in on-board data processing.


### INTRODUCTION

The increasing number of energetic particle-producing solar flares during the approaching period of solar maximum provide more frequent opportunities for the study of solar flare particles, their spectral distributions and isotopic abundances, and their interplanetary propagation. The experiments that were conceived and instrumented by Bell Telephone Laboratories for the Interplanetary Monitoring Platforms (IMP) F and G spacecraft were designed to provide fast (few minute or less) time resolution during a solar particle event for the energy spectra of low energy electrons, protons and alpha particles as well as information on the possible presence of deuterons, tritons and $He^3$. In order to avoid telemetering each event for subsequent analysis on the ground, an on-board particle identifier was used as a key element in the design. In addition to providing fast time resolution, the identifier also provides a means of improving the statistics for the detection of rare particle types.

### EXPERIMENT

The identification of particle type and the measurement of the particle energy spectrum is performed in the IMP experiments using a four element solid state detector telescope and the associated electronics as shown in the block diagram of Figure 1. The detector telescope is axially symmetric with the symmetry axis perpendicular to the spin axis of the satellite. The first two detectors (active areas of 0.43 and 0.96 $cm^2$, respectively) are totally depleted n-on-p diffused silicon diodes[1]. The last two detectors are lithium-drifted silicon detectors (active areas of 0.96 $cm^2$ each) vacuum encapsulated in a windowless package. A set of lithium detectors similarly encapsulated and flown on the ATS-1 and ATS-2 satellites have been previously discussed[2].

The detector stack is preceded by a defining collimator of 20° half-angle, which gives an effective geometrical solid angle of 0.37 ster. Titanium and nickel foils in front of the first detector serve as light shields and primarily determine the lower limits on the heavy particle energies that can be observed. The detector stack and collimator are housed in an aluminum shielding block that stops high-energy particles incident from the rear or sides of the telescope.

The electronics of the experiment is built up using hybrid tantalum thin-film microcircuit modules previously described elsewhere[3]. Proton and alpha particles up to an energy of approximately 4 meV/nucleon are distinguished by the amount of energy deposited in stopping in the first two detectors of the telescope. Above this energy particle species other than electrons are distinguished by the use of a pulse multiplier as a particle species identifier. Electrons are identified in the lithium detectors by their lack of sufficient energy loss to produce a logic pulse in the thin detector electronics (see Table 1; in addition, Ref. 4 gives a detailed summary of the electron characteristics of the ATS experiments which are similar to the IMP experiments).

Since the experiment was designed to measure the energy spectra of six different particle species, telemetry limitations required that the experiment operate in a number of sequential modes. During each satellite telemetry sequence (10.227 sec) a particular set of coincidence requirements and pulse height and multiplier discrimination requirements is established for the pulses from the various detectors. Each time a particle event satisfying these conditions occurs during a 9.28 sec counting interval within the sequence period, the pulse heights from the detectors in coincidence are summed and analyzed in a five channel pulse height analyzer. The digital data from the analyzer are read out at the end of each counting interval. A list of the modes of the experiment and their characteristics are shown in Table 1.

### THE MULTIPLIER

The purpose of the multiplier is to produce electronically, from the detector signals, the approximate relationship for particle energy loss,

$$P = RMZ^2, \qquad (1)$$

where M and Z are the mass and charge of the incident particles, respectively, and R is an

*Bell Telephone Laboratories, Incorporated, Murray Hill, New Jersey

energy dependent factor. In the experiments, Eq. (1) was achieved by forming the product

$$P = \Delta E[(E-\Delta E) + K_1\Delta E + K_2] \qquad (2)$$

where E is the total energy of the incident particle and $\Delta E$ is the energy lost in a dE/dx detector. As will be seen below and in Figure 5, proper choices of $K_1$ and $K_2$ made R vary by less than ±10% over the IMP F and G energy ranges.

Numbers of different schemes have been used in the past to provide the function of analog multiplication. These include the use of accurate squaring circuits[5] together with the relation $(a+b)^2 - (a-b)^2 = 4ab$, log-antilog systems[6], voltage controlled attenuators[7], and field-effect-transistor bridges[8]. Of these methods the field-effect-transistor approach appeared to be the most attractive one for satellite use from the viewpoint of simplicity, speed, and power consumption.

The basic scheme employed for the formation of the product is shown in Figure 2. Here, one input provides a symmetrical push-pull voltage signal to drive the FET gates, while the other input provides a symmetrical push-pull current drive to the channels. The use of a current drive to the channels is important, as indicated in Ref. 8, in providing automatic temperature compensation for the multiplier bridge gain.

The field-effect transistors selected for use in the bridge were Siliconix Type 2N2608. These are P-channel junction devices having a channel resistance at zero gate voltage of ~500 Ω and a pinch-off voltage of ~4 V.

High quality 10 mh 1:1 transformers were available for use in the electronics of the experiment, providing a simple means of realizing the required symmetrical driving and difference-taking functions required in Figure 2.

The multiplier circuit is shown in detail in Figure 3. Here the FET bridge Q4, Q5, Q6, Q7 is driven from T1 and T2. The gate generator source impedance is ~2.7K (small compared with the gate impedance) while the channel source impedance is the reflected collector impedance of Q2, (large compared with the channel resistance). Finally the FET bridge output sees the reflected input impedance of the A1 operational amplifier (low compared to the bridge impedance) so the basic bridge driving and receiving impedance conditions are satisfied.

The single-clipped $\Delta E$ and $(E-\Delta E)$ input signals are differentiated by $C_1R_1$ and $C_2R_2$ respectively, thereby providing double clipped current drive to the virtual grounds at the emitters of Q2 and Q3. (Double clipping is necessary to prevent baseline shifts at the secondaries of the transformers.)

Some of the double clipped $\Delta E$ voltage signal is used to drive the emitter follower Q1. A moment's inspection of the circuit shows that the input to the Q3 emitter is of the form $(E-\Delta E) + K_1\Delta E$ while a fraction K2 of the $\Delta E$ signal is added directly to the multiplier bridge output at the input to A1. The overall output signal is therefore of the form

$$\Delta E[(E-\Delta E) + K_1\Delta E] + K_2\Delta E$$

or

$$V_0 = G\Delta E[(E-\Delta E) + K_1\Delta E + K_2] \qquad (3)$$

where G is a constant representing the overall multiplier gain.

In practice, as indicated in Table 1, different detectors were used to provide the $\Delta E$ and $(E-\Delta E)$ signals in different modes of the experiment. For this reason additional linear gating was needed to provide alternative values for the constants $K_1$ and $K_2$ of Eq. (2).

This additional gating is shown in Figure 4. Logic signals applied to the base of Q12 either result in the saturation of Q8 and Q9 while turning off Q10 and Q11, or else perform the converse function. In this way the K factors of Eq. (2) are either set by potentiometers P1 and P2 or else by P3 and P4 depending on the experimental mode.

For functional testing purposes it is possible to saturate all four transistors Q8 through Q11 simultaneously by suitably raising the potential at the "multiplier balance check" input. Under these conditions the multiplier output is given by $\Delta E(E-\Delta E)$, with no additional factors, and the bridge balance can then be checked by driving each input in turn with the other input short-circuited.

In operation the basic circuit of Figure 3 provides an output within ~1% of the calculated output, in ~1 μs, over a temperature range of -10°C to +40°C. The power consumption is ~12 mW. (The logical switching shown in Figure 4, and the operational amplifier A1, consume additional power not included in this figure.)

## FACTORS DETERMINING PARTICLE SEPARATION

In an experiment such as this in which the number of protons being detected is much larger than the number of other particles being searched for, it is important that the particle identifier make as few errors as possible in the mass analysis. The prime sources of particle identifier error are a) fluctuations due to noise in the particle detection process, b) variation of the multiplier output with particle energy, and c) rate effects. The effects of particle channeling and entrance angle on the size of the $\Delta E$ pulse are not important sources of identifier error in this experiment.

The signal-to-noise ratio in the particle detection process is due primarily to noise from

the dE/dx detector. This detector is usually made as thin as possible so that it can be penetrated by low energy, heavy particles. However, as the detector thickness is reduced, the detector capacitance increases, causing a corresponding increase in the noise level. At the same time, of course, the $\Delta E$ signal decreases. Thus, the signal-to-noise ratio rapidly becomes worse as the dE/dx detector is made thinner.

A more serious source of signal fluctuations arises from the statistical nature of the amount of energy lost by a particle in traversing the dE/dx detector. For example, ~16 MeV protons, which deposit ~250 keV in detector 1, exhibit fluctuations in $\Delta E$ of ~60 keV FWHM. The electronic noise in this detector (with which a field-effect preamplifier is used) is 35 keV FWHM. Since the $\Delta E$ signal varies over a large range (small for high energy protons and large for low energy alphas) the accuracy of particle identification is inherently energy and particle dependent. Hence, the limits set on the thickness of a dE/dx detector used as an input to a particle multiplier must be chosen to be consistent with the goals of a given experiment.

Even when optimum values of $K_1$ and $K_2$ in Eq. (2) are used for a given set of detectors in coincidence, the multiplier output is energy dependent (see Figure 5). This is due to the fact that only an approximate calculation is used in determining $MZ^2$. This also limits the energy range over which the multiplier output will be unambiguous. A discussion has recently been given of the above problems in connection with a multiplier used for particle identification on rocket experiments[9].

Degradation with counting rate is perhaps the most important factor influencing the quality of particle separation. Both pulse-on-pulse pileup, and pulse-on-tail pileup (baseline shift) will cause an otherwise perfect multiplier to identify particles incorrectly. Pulse-on-pulse pileup causes two particles to appear to be a single particle of larger mass, whereas baseline shift makes particles appear to have smaller masses.

## RESULTS

Extensive checks and calibrations were performed both on the multiplier and the experiments as a whole. Values of $V_o$ as a function of energy, using the actual circuit value parameters of $K_1$ and $K_2$, were calculated for each species of particle using range-energy relations for protons[10,11] and alpha particles[11] in aluminum and adapting them to silicon. The calculations were then compared to the actual output of the multiplier (measuring $V_o$ directly) due to accelerator-produced protons, deuterons, and alpha particles over a wide energy range.

The results of these comparisons for Modes D, E,F,G,P are shown in Figure 5, where the theoretically calculated curves are plotted as solid lines and the experimentally determined points are plotted as open circles. The upper and lower limit settings of the single channel analyzer at the multiplier output for each particle species are shown to the left of the curves. The agreement between the calculated curves and the experimental values of the multiplier performance is quite good over the particle energy ranges measured. The proton points are observed to turn up slightly at the higher energies. Similar behavior might be expected in the deuteron and alpha data at the higher energies as well.

The results of the measurements of the performance of the IMP G experiment are shown in Table 2, which lists the fraction of the incident particles which were incorrectly identified. In general, Modes M, N and O exhibit cleaner particle identification because the thicker dE/dx detector used results in an improved signal-to-noise ratio. The most striking difference occurs in the contamination of the deuteron modes by high energy protons. Here the contamination resulting from the use of detector 2 as the dE/dx detector (Mode N) is a factor of 6 less than when detector 1 is used (Mode E).

As shown in Fig. 5 for Modes D,E,F,G and P (the identifier windows are similar for Modes M, N and O) the particle identification windows are set to minimize proton contamination of deuterons, and to leave the proton and alpha windows wide enough to accomodate small gain shifts, should they occur. The effect of this can clearly be seen in comparing the results of proton contamination of deuterons with the deuteron contamination of protons in Table 2.

As Table 2 indicates, the contamination of $He^3$ by alphas is much worse than the contamination of protons by deuterons. This arises from an unforseen effect of the detector-collimator geometry. The area of detector 1 was made less than the area of the collimator and subsequent detectors in order to reduce its capacitance, and hence the resulting electronic noise. However, this then allows particles to traverse the edge of the active region of the detector, producing an anomalously low $\Delta E$ signal. This causes a low mass tail on the multiplier pulse for all multiplier modes using detector 1.

Figure 6 shows the rate dependence of particle separation expressed as ratios of the deuteron mode rates to proton mode rates for 6 MeV incident protons. Although not shown in the figure because of insufficient statistics for the modes plotted, some degradation in particle separation may be observed for rates as low as 1000 counts/sec.

A pileup rejector of the type which rejects pulses having an improper shape was incorporated in each of the experiments to reduce the effects of pileup. Unfortunately, these particle calibrations of the experiments have shown the pileup rejector to be relatively

ineffective, for reasons which are not yet clear. However, since these particular experiments are not expected to encounter particle rates much exceeding 1000 counts/sec, the rate problem is not considered serious.

The response of the detector telescope as a function of angle of the incident protons and alpha particles is shown in Figures 7a and 8a, respectively. The contamination of protons in the deuteron mode, Mode E, and of alphas in the $He^3$ mode, Mode G, as a function of incident proton and alpha angle is shown in part b of each of the figures. The proton angle data and the alpha angle data were obtained for incident particle rates of ~3000 counts/sec.

Although the angle data presented is for only one energy of each particle type, similar results are also obtained at other energies. Even though the proton contamination of Mode E may be slightly larger at an angle of 20° than at an angle of 5°, neither the proton contamination of Mode E nor the alpha contamination of Mode G became worse at the larger incident angles.

## SPACE CHECKS AND PERFORMANCE

The complexity and precision required of the experiment made extensive in-flight checks mandatory. The spectrum of the multiplier output is monitored by two modes in each data sequence. In these modes (C and L, see Table 1) the output of the multiplier is analyzed in the five channel analyzer. The five channel levels are set to monitor outputs corresponding to protons, deuteron, tritons and alphas. In addition, one channel monitors the valley between the proton and deuteron channels in order to check the width of the proton multiplier peak.

During a special calibration sequence, occurring every six hours, two additional internal checks are made. First, the detectors are exposed to natural radioactive sources of alphas and electrons. Second, a ramp pulser connected to all detector preamplifiers causes counting in all modes sufficient to detect electronic drifts on the order of one per cent.

An example of the space performance of the IMP F experiment, which does not have as good particle separation as the IMP G experiment, is shown in Figure 9. The experiment was measuring the flux of solar protons and alpha particles emitted from the series of three solar flares on day 143 (May 23), 1967. The half hour average of the D,E,F,G and P mode counting rates measured on day 145 near the peak of the fluxes are plotted as open bars on the graph. A representative 12 MeV proton calibration result for the IMP F experiment is normalized to the D-Mode rate and is plotted as darkened bars on the graph.

The data in Figure 9 certainly shows that the experiment performs in space as it does on the ground and that unambiguous separation of the protons and alphas is obtained. Although it will not be discussed in this paper, it should be remarked that the precise interpretation of the response of E, F and G modes must, of course, consider the ground-based alpha calibration results and the calibration results over all energies as well as the results shown in Figure 9.

## SUGGESTED IMPROVEMENTS

While the performance of the multiplier as a space-borne particle identifier has proved adequate for the experiments on the IMP F and G spacecraft there are notable improvements that could be incorporated into future versions of such particle identification systems. The most obvious of these would be the use of the newer and enormously improved n-channel FET devices, such as the 2N4416, for the multiplier elements. These would provide higher bridge gain, shorter "solution times"[8], and less spurious feed-through due to the reduced gate-channel capacitance.

Further advantages would accrue from the use of an effective pulse-on-pulse pileup rejector which would reduce incorrect particle identification at high counting rates. Use of direct coupling and d.c. restoration[12,13,14] should produce significant improvements in the effects of pulse-on-tail pileup.

A very interesting possibility for substantial improvement in the multiplier output vs. energy curves has been suggested by Radeka[15]. This depends on the observation that suitably cascaded multipliers and adders can be employed to approximate power-series expansions. In this way, very accurate "curve fitting" can be performed to analyze the output signals of cascaded thick and thin detectors.

All of these approaches are viable schemes which only require effort for their development. Whether such effort would be justified depends on overall judgments regarding the relative importance of on-board particle identification, together with its reduced telemetry bandwidth requirements, vs. the simpler but possible less statistically significant scheme of telemetering all events and identifying the different particle types on the ground.

## ACKNOWLEDGMENTS

We acknowledge with pleasure the constant encouragement of W. L. Brown, the help of I. Hayashi in the electronic design, and the assistance of W. M. Augustyniak, W. F. Flood, R. W. Kerr and W. Wallis in the long calibration runs. We also acknowledge the hospitality of R. Bercaw and R. Blue of the NASA Lewis Research Center who twice made their cyclotron facility available for portions of the alpha particle calibrations.

## REFERENCES

1. T. C. Madden and W. M. Gibson, IEEE Trans. Nucl. Sci., NS-11, 254 (1964).

2. I. Hayashi, H. E. Kern, J. W. Rodgers and G. H. Wheatley, IEEE Trans. Nucl. Sci., NS-13, 214 (1966).

3. F. E. Curran, I. Hayashi, L. V. Medford and G. L. Miller, IEEE Trans. Nucl. Sci., NS-13, 326 (1966).

4. L. J. Lanzerotti, Nucl. Instr. and Methods, 61, 99 (1968).

5. W. L. Briscoe, Rev. Sci. Instr., 29, 401 (1958).

6. M. G. Strauss and R. Brenner, Rev. Sci. Instr., 36, 1857 (1965).

7. L. W. Swenson, Nucl. Instr. and Methods, 31, 269 (1964).

8. G. L. Miller and V. Radeka, NAS-NRC Report, Publication 1184 (1964), p.104.

9. T. Doke, K. Nagata, S. Nakagawa, A. Sasaki and M. Tsukuda, ISAS Report No. 426, Univ. of Tokyo (1968).

10. R. M. Sternheimer, Phys. Rev., 115, 137 (1959).

11. Tables of Nuclear Data (1960), Part III, Sec. I - Ranges and Energy Loss of Charged Particles in Matter.

12. L. B. Robinson, Rev. Sci. Instr., 32, 1057 (1961).

13. R. L. Chase and L. R. Poulo, IEEE Trans. Nucl. Sci., NS-14, 83 (1966).

14. E. A. Gere and G. L. Miller, IEEE Trans. Nucl. Sci. NS-14, 89 (1966).

15. V. Radeka, private communication.

TABLE 1

| Mode | Coincidence Condition | Identified Particle | Approximate Energy Range MeV | 5 Channel Energy Spectrum | Remarks |
|---|---|---|---|---|---|
| A | 1 $\bar{2}$ - - | Heavily ionizing | $0.6 < p < 1.9$<br>$1.7 < \alpha < 9.0$ | 1 | |
| B | 1 2 $\bar{3}$ - | Heavily ionizing | $1.9 < p < 4.0$<br>$9.0 < \alpha < 12$ | 1+2 | |
| C | 1 2 3 $\bar{4}$ | | | 1x(1+2+3) | Multiplier check-Modes D,E,F,G,P |
| D | 1 2 3 $\bar{4}$ | p | $4.0 < p < 18.0$ | 1+2+3 | |
| E | 1 2 3 $\bar{4}$ | d | $5.0 < d < 20$ | 1+2+3 | Particle Identifying Modes |
| F | 1 2 3 $\bar{4}$ | t | $5.5 < t < 25$ | 1+2+3 | |
| G | 1 2 3 $\bar{4}$ | $He^3$ | $11 < He^3 < 72$ | 1+2+3 | |
| P | 1 2 3 $\bar{4}$ | $\alpha$ | $16 < \alpha < 80$ | 1+2+3 | |
| H | - $\bar{2}$ 3 $\bar{4}$ | e | $.3 < e < 3$ | 3 | |
| I | - - 3 4 | Lightly ionizing | $2 < e$<br>$18 < p$ | 3 | |
| J | - - - - | | | | Singles check |
| K | - 2 $\bar{3}$ | Heavily ionizing | $2.2 < p < 4.0$<br>$8.8 < \alpha < 12$ | 2 | |
| L | - 2 3 $\bar{4}$ | | | 2x(2+3) | Multiplier check-Modes M,N,O |
| M | - 2 3 $\bar{4}$ | p | $4.0 < p < 18$ | | Particle Identifying Modes |
| N | - 2 3 $\bar{4}$ | d | $5.0 < d < 20$ | | |
| O | - 2 3 $\bar{4}$ | t | $5.5 < t < 25$ | | |

TABLE II

Fraction of incident particles incorrectly identified in the other particle modes

| Incident particle | Proton | Deuteron | Triton | Helium 3 | Alpha |
|---|---|---|---|---|---|
| Protons | | .002<br>.0002 | .001<br>.0002 | ~.0002<br>~.00002 | ~.0001<br>~.00002 |
| Deuterons | .04<br>.01 | | .02<br>.0005 | ~.0001<br>~.00002 | ~.00005<br>~.00002 |
| Alphas | .0002 | .0004<br>.0002 | .001<br>.0002 | .02<br>.01 | |

The two numbers for each case are for the most favorable and least favorable incident particle energies for incident rates up to ~3000 counts/sec.

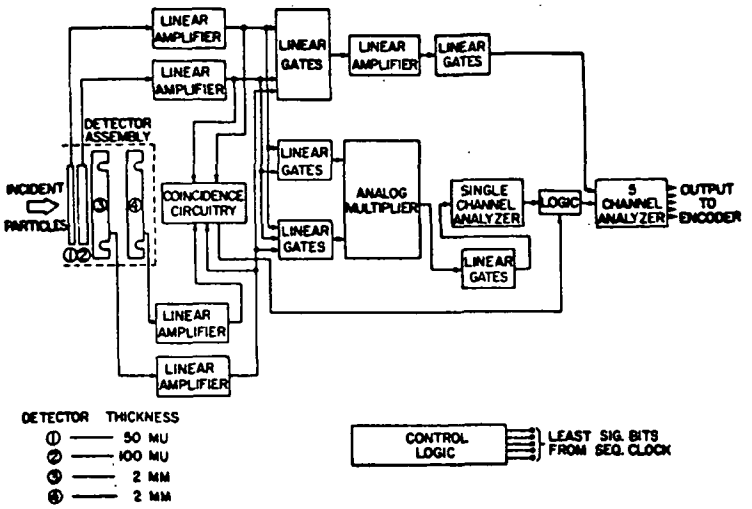


Fig. 1 - Block diagram of the detector telescope and electronics for the BTL IMP F and G experiments.

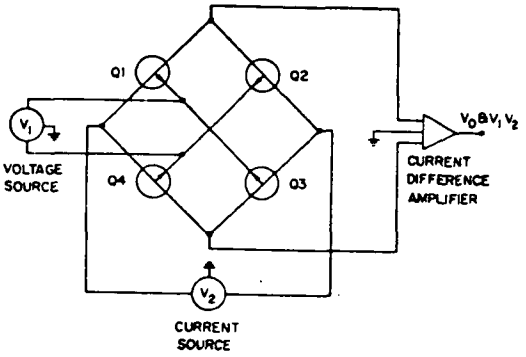


Fig. 2 - Basic FET bridge employed to effect analog multiplication.

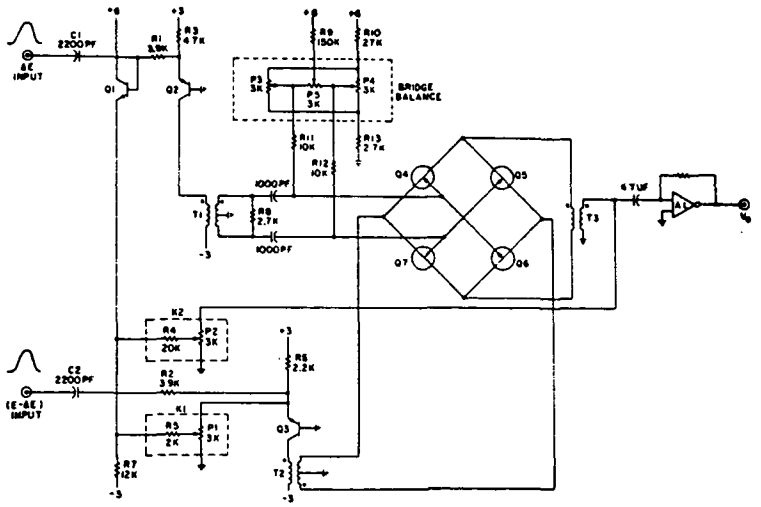


Fig. 3 - Detailed schematic of the multiplier. The four FET transistors used in the bridge have pinch-off voltages and channel resistances (at zero gate voltage) matched to ±5%.

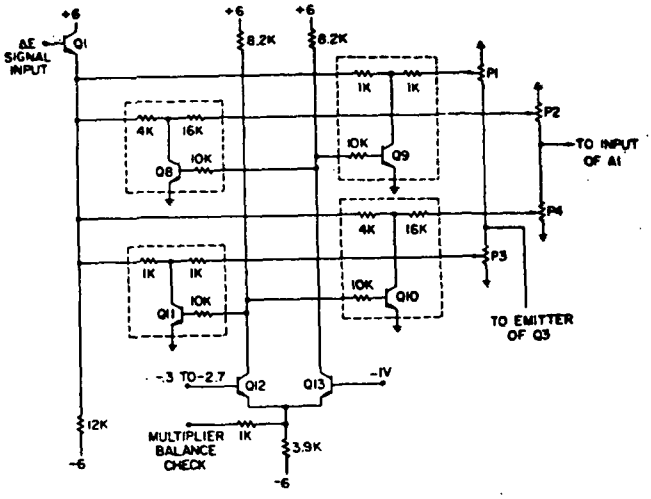


Fig. 4 - Scheme employed to provide different multiplier K factors in different modes of the experiment.

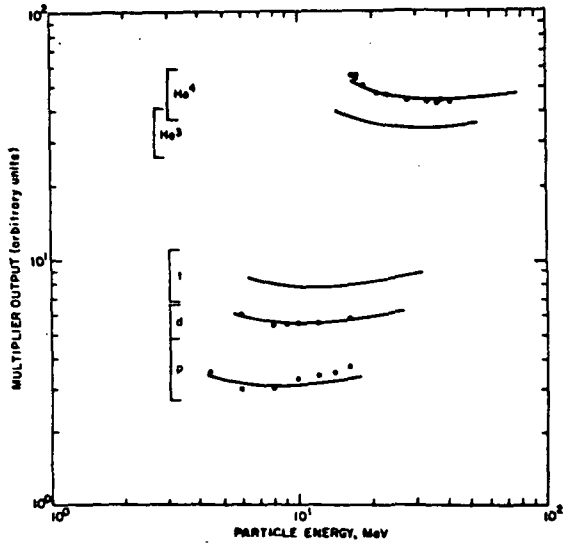


Fig. 5 - Comparison of the calculated and experimental values of the multiplier response in Modes D(p), E(d), F(t), G($He^3$) and P($He^4$) for IMP G. The open points correspond to the experimentally determined multiplier outputs using accelerator-produced particles.

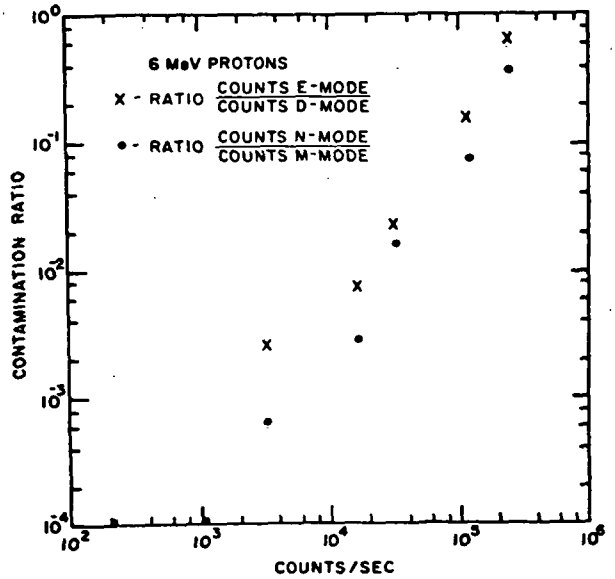


Fig. 6 - Rate dependence of the proton contamination in the IMP G deuteron modes - Mode E and Mode N.

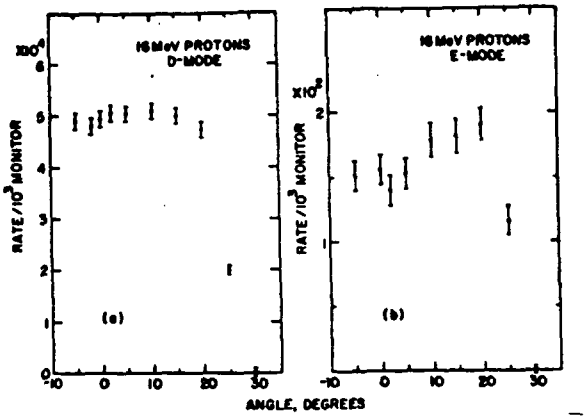


Fig. 7 - (a) D-Mode angle response of the detector telescope to 16 MeV protons (IMP G). (b) E-Mode angle response of the detector telescope to 16 MeV protons (IMP G).

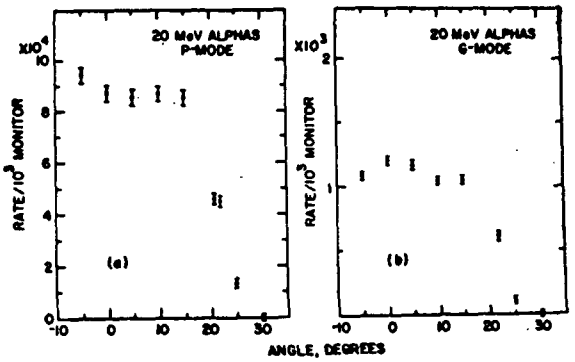


Fig. 8 - (a) P-Mode angle response of the detector telescope to 20 MeV alphas (IMP G). (b) G-Mode angle response of the detector telescope to 20 MeV alphas (IMP G).

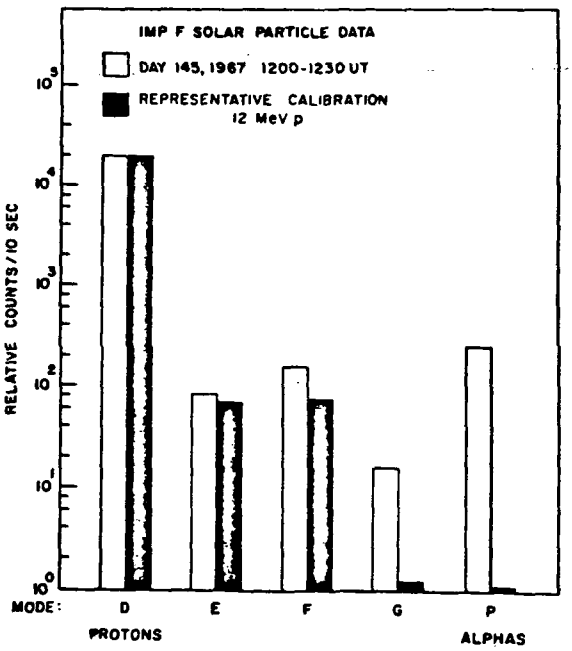


Fig. 9 - Response of the IMP F experiment in Modes D, E, F, G, and P to solar protons and alphas. Representative 12 MeV ground-based proton calibration results are normalized to the D-Mode rate.

N72-21833

# CHAPTER 2

## PENETRATION OF SOLAR PROTONS AND ALPHAS TO THE GEOMAGNETIC EQUATOR

L. J. Lanzerotti
Bell Telephone Laboratories, Murray Hill, New Jersey

Simultaneous spectral observations of low-energy solar particles in interplanetary space and in the magnetosphere on the equator strongly imply that these particles have essentially free access to the outer magnetosphere through a very effective diffusion mechanism which preserves the spectral shapes and the flux magnitudes. These observations further imply that measurements of solar-particle arrival time over the polar caps are not sufficient to distinguish between open or closed magnetosphere models.

A number of investigators making measurements over the polar caps[1] have observed that the low-energy solar protons have cutoff energies that depend on latitude in a manner that departs significantly from the predictions of Störmer's theory[2] and subsequent modifications to more realistic field models.[3] Recent measurements of >40-MeV solar protons at the equator at $L < 5R_E$ were shown also to have cutoffs below the classical Störmer values.[4] Krimigis, Van Allen, and Armstrong,[5] utilizing simultaneous data from an interplanetary satellite and a low-altitude, polar-orbiting satellite, have reported evidence of "essentially immediate access" of 0.5- to 4.2-MeV solar protons to the earth's polar caps. They interpret these results as favoring an "open" magnetosphere model[6] over a more closed model with magnetic merging at several A.U. in the magnetotail.[7]

Reported here are extensive simultaneous spectral measurements of both low-energy solar protons and alpha particles outside the magnetosphere on IMP F (Explorer 34) and inside the magnetosphere on the equatorial satellite ATS-1 during both quiet and disturbed geomagnetic conditions. The observed rapid penetration of both enhanced solar protons and alphas to the equatorial region at $6.6R_E$, the observed preservation of the spectral shapes, and the observed diurnal effects in the protons strongly suggest that there is continuous diffusion of these interplanetary particles across the magnetosphere boundary and deep into the magnetosphere during all times when a source of these particles is present in interplanetary space. The diurnal effect also implies that these solar particles are geomagnetically trapped for several longitudinal drift periods. These observations of solar particle penetration into the outer regions of the magnetosphere cast serious doubt on the validity of interpreting polar-cap measurements of solar protons strictly in terms of open or closed magnetosphere models.

The ATS-1 satellite (launched 6 December 1966) is a geostationary, spin-stabilized satellite (with the spin axis parallel to the local magnetic field) stationed at 150°W, 0°N and at a geocentric distance of $6.6R_E$. The Bell Telephone Laboratories (BTL) experiment flown on ATS-1 consists of a six-element solid-state detector telescope oriented perpendicular to the spin axis of the satellite. By use of the particle $dE/dX$ characteristics and appropriate logic circuitry, the experiment is capable of distinguishing between protons and alphas. The half-angle of the detector telescope collimator is 20°; the flux measured by the BTL experiment is the spin-averaged flux of those particles with pitch angles close to 90°.[8,9] ATS-1 local time is obtained by subtracting 10 h from the universal time.

IMP F, launched 24 May 1967, is a spin-stabilized (with the spin axis perpendicular to the ecliptic plane) polar-orbit satellite with an apogee of approximately $34R_E$. The BTL experiment consists of a four-element solid-state telescope oriented perpendicular to the spin axis. The half-angle of the detector telescope collimator is also 20°; the flux measured by the experiment is the spin-averaged flux of particles in the ecliptic plane. Protons and alphas up to an energy of approximately 4 MeV/nucleon are distinguished by the energy deposited in the first two detectors of the telescope and subsequently measured in a five-channel analyzer. Particle species above this energy are distinguished by the use of an on-board pulse multiplier.[10]

$\frac{1}{2}$-h averages of the interplanetary (IMP, 1.2-2.5 MeV) and magnetosphere (ATS, 1.9-2.8 MeV) proton data for days 164-181, 1967, are plotted in Fig. 1. The data for days 220-225, 1967, are plotted in Fig. 2. The periods when the IMP satellite was within $10R_E$ of the earth are indicated. The 6-h counting rates for time intervals centered about ATS local times of noon, 1800, mid-

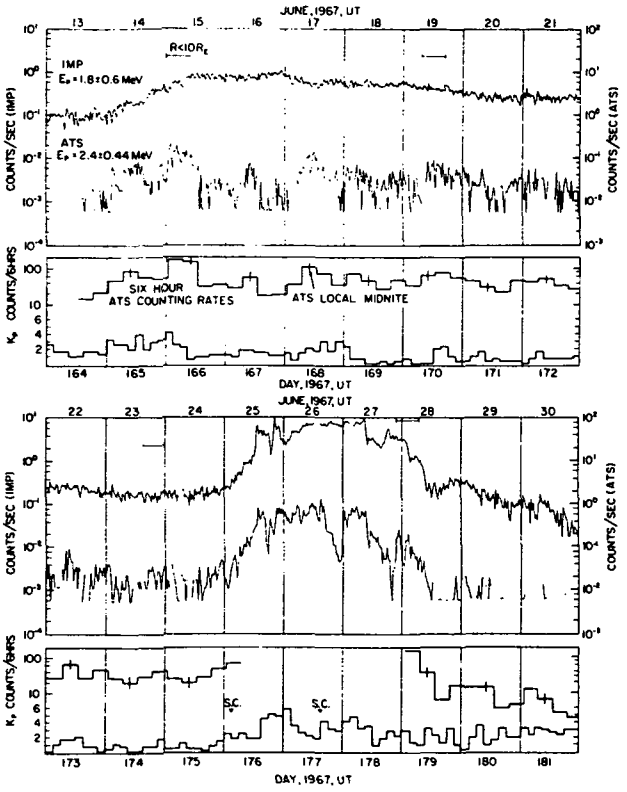


FIG. 1. Simultaneous interplanetary and equatorial magnetosphere solar-proton data—June, 1967.

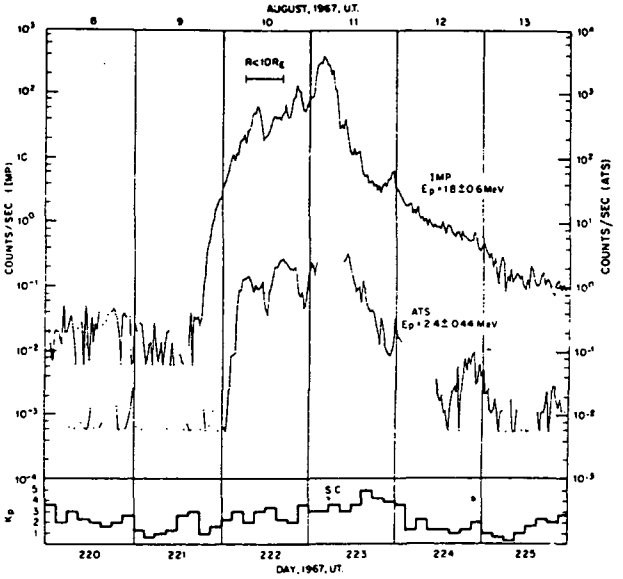


FIG. 2. Simultaneous interplanetary and equatorial magnetosphere solar-proton data—August, 1967.

night, and 0600 are plotted immediately below the $\frac{1}{2}$-h averaged data in Fig. 1. Plotted at the bottom of both figures are the 3-h-averaged $K_p$ data indicating the geomagnetic activity in the time intervals discussed.

The data plotted in Fig. 1 correspond to the 18-d period between 13 June and 30 June which followed the three solar-flare particle events on 23 and 25 May and 6 June 1967.[11,12] The interplanetary flux of 1.2- to 2.5-MeV protons from day 164 to day 176 is larger than is normally observed. From days 167 to 176 the interplanetary proton fluxes decayed by approximately a factor of 5. This same overall decay was also observed in the proton fluxes inside the magnetosphere.

The 6-h ATS proton data in Fig. 1 show a diurnal variation during most of the rather quiet geomagnetic period up to day 176. During this entire period a diurnal effect similar to that reported previously,[11] and opposite to these proton variations, was observed in the electron data. The maximum in the proton diurnal fluxes generally occurred in the 6-h interval centered around local midnight and the minimum generally occurred in the 6-h interval centered around local noon. This is the same type of proton diurnal behavior observed during portions of the 25 January solar event.[13,14] During the two geomagnetically very quiet days 174 and 175, when the interplanetary fluxes were low, the diurnal effect was reversed with more protons measured at local noon than at local midnight.

Figures 3(a) and 3(b) show 6-h-averaged proton spectra from IMP and ATS centered about 1200 (noon) and 2400 (midnight) day 167, ATS local time. The higher energy ATS proton fluxes at both times are approximately equal to the interplanetary fluxes; both spectra fall off at the lower energies, with the largest falloff occurring at local noon. The effective $L$ value at the ATS altitude during these two local time periods is different because of the solar-wind distortion of the magnetosphere.[15] Since magnetic field data from ATS were not yet available, the diurnal variations in the electron fluxes observed by the BTL experiment[9] were used to estimate indirectly the amount of magnetosphere distortion. The electron diurnal variations during days 167 and 168 were compared with available simultaneous electron and magnetic-field data obtained during the first two weeks of 1967. These comparisons were used with Roederer's computations of a model magnetosphere[15,16] and indicated that on day 167 the magnetosphere boundary was near $10.5R_E$ and that the ATS satellite was measuring protons near $L = 6.0$ at local noon and $L = 6.6$ at local 2400(midnight).

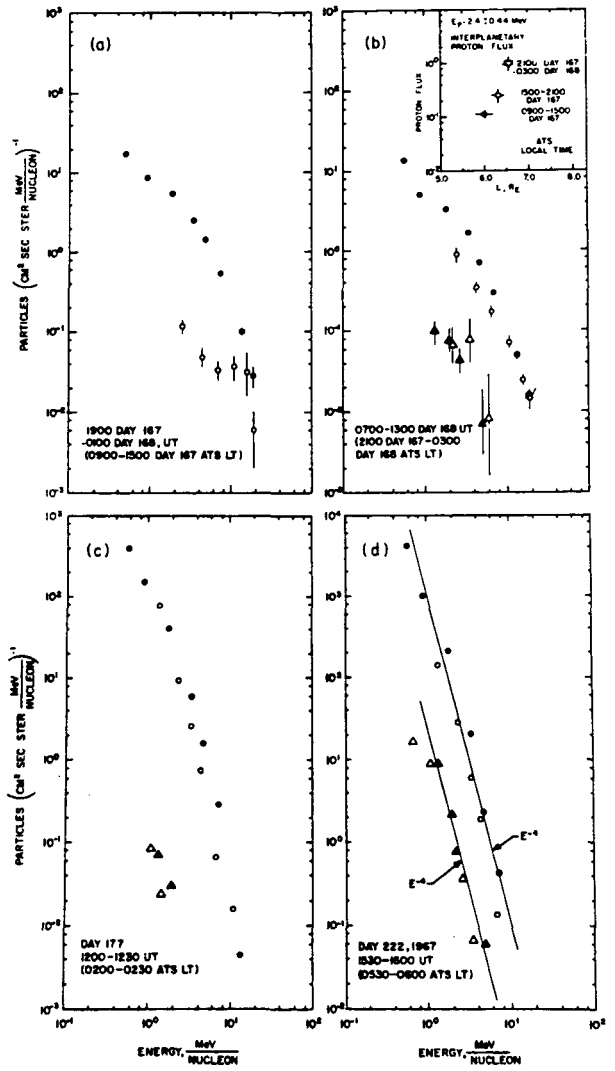


FIG. 3. Interplanetary (solid points) and equatorial magnetosphere (open points) particle fluxes. Circles correspond to protons; triangles correspond to alpha particles. The data points in the inset in (b) are protons.

The inset in Fig. 3(b) shows the 1.9- to 2.8-MeV ATS proton data plotted as a function of $L$ during day 167 ATS local time in order to indicate the relationship of the ATS proton fluxes to the same energy proton fluxes measured on IMP. This plot suggests that the magnetosphere fluxes and spectra at approximately $L = 7$ would be equal to the interplanetary fluxes and that the proton intensities decrease strongly below $L \sim 7$.

The increase in the flux of interplanetary protons observed near the beginning of day 176 (Fig. 1) apparently resulted from the reappearance after one solar rotation of the region associated with the 28 May solar-flare event.[12] At the time of the flux increase IMP F was outbound at a distance of $\sim 30 R_E$, an angle to the ecliptic of ~23°, and a sun-earth-probe angle of ~80° east, while ATS-1 was at approximately 1400 local time.

The proton increase in interplanetary space was accompanied within $\frac{1}{2}$ h by an increase in the proton fluxes measured at ATS. (The timing uncertainties are not instrumental but statistical, due to the gradual interplanetary increase.) The drop in fluxes on day 179 also occurred simultaneously within $\frac{1}{2}$-1 h both outside and inside the magnetosphere. Although there is not always a one-to-one correspondence during the entire event (the larger dip in the ATS flux during the latter part of day 177 occurred at the time of the second sudden commencement storm; a similar dip was observed during the 28 May event[12]), the overall correspondence between the interplanetary flux increases and decreases and the simultaneous equatorial magnetosphere response is indeed striking.

The solar proton event shown in Fig. 2 occurred during an August geomagnetically quiet day while IMP F was inbound at a distance of $20 R_E$ with an ecliptic angle of 23° and an earth-sun-probe angle of ~35° east. ATS-1 was approximately at local 0800 at the time of the interplanetary proton increases and observed the first flux increase some six hours later, at approximately 1400. Hence, during the geomagnetically quiet period after the solar protons were initially observed in interplanetary space there was an approximately 6-h time delay before the protons were seen inside the magnetosphere. However, within 3-4 h after the protons were first observed on ATS-1 (while the geomagnetic disturbance was increasing), the interplanetary and the magnetosphere proton increases and decreases again had a striking resemblance.

Proton and alpha spectra during a period of enhanced fluxes of both day 177 and day 222, 1967, are shown in Figs. 3(c) and 3(d). During both periods the proton and alpha fluxes inside and outside the magnetosphere were approximately equal. Both the proton and alpha spectral shapes were very similar; there was no evidence of a low-energy falloff.

The electron diurnal data observed by the BTL experiment during days 164-175 imply that the ATS experiment was measuring particles on closed longitudinal drift shells. Hence the "inverse" diurnal variation in the quiet-time proton data implies that the protons were stably trapped

for a time period of the order of a few longitudinal drift periods ($\tau_D \sim 8$ min for 1-MeV protons at synchronous altitude) and that their source was beyond $L \sim 7$. The facts that no magnetosphere protons were observed when the interplanetary source was absent and that a proton and alpha enhancement in the magnetosphere did not persist after the source was absent also imply that the protons and alphas are trapped for only a few drift periods and certainly not for more than a few hours. The fact of proton trapping rules out the possibility that these protons entered the magnetosphere by field-line connection either to the magnetotail[7] or to interplanetary space over the poles.[6] The rapid access of the enhanced interplanetary particles to the equatorial region further rules out access via the geomagnetic tail where the merging in the tail is believed to take place at several A.U.

The observed "inverse" diurnal effect and the observed rapidity with which the equatorial regions of the magnetosphere respond to an enhanced interplanetary flux of protons and alphas strongly suggest that a diffusion mechanism is continually operative in the outer magnetosphere and not just at the times of magnetic sudden commencements or sudden impulses.[17] The interplanetary-magnetosphere response-time difference observed between quiet and disturbed geomagnetic times is indicative that the diffusion mechanism is probably stronger during a more disturbed condition. In addition, during a disturbed geomagnetic condition, the magnetosphere boundary is closer than during a more quiet period. Furthermore, the similarity of the particle spectra observed inside and outside the magnetosphere, particularly during the times of enhanced fluxes, implies that the diffusion mechanism preserves the spectral shapes of the interplanetary protons and alphas. The similarity of the magnitude of the magnetosphere particle fluxes to the enhanced interplanetary source fluxes over a wide energy range suggests that the diffusion mechanism violates the first adiabatic invariant.

During the geomagnetically quiet times, the value of $L$ near ATS local noon was ~6, corresponding to a geomagnetic latitude of ~63° at the surface of the earth. During geomagnetically active times much higher flux values of protons were observed at the ATS altitude and some protons were thus presumably seen at lower $L$ values, corresponding to lower latitudes. It is possible that the latitude lowering for low-energy solar particles observed on polar-orbiting satellites during geomagnetically disturbed conditions is simply a reflection of the fact that solar particles can diffuse faster and with more intensity to lower equatorial altitudes during these times. These protons are then rapidly pitch-angle scattered so that they are seen at the lower altitudes over the polar caps and in the auroral zones. The short trapping times attributed here to the equatorially mirroring particles could then be due to a combination of particle loss due to pitch-angle scattering and diffusion back out of the magnetosphere.

In conclusion, the simultaneous solar proton and alpha-particle observations discussed above strongly imply that there is a very effective continuous diffusion of the interplanetary-source particles into the outer equatorial magnetosphere. The strength of the diffusion is strongly dependent upon the intensity of the geomagnetic activity. The observations also imply that these particles are geomagnetically trapped for only a few longitudinal drift periods. Finally, the existence of a diffusion mechanism for producing rapid solar-particle penetration into the outer regions of the magnetosphere and the short trapping time of these particles strongly imply that measurements of the solar-particle arrival time in interplanetary space and over the polar caps are not sufficient to distinguish between open or closed models of the magnetosphere.

The authors would like to thank Dr. W. L. Brown, Dr. C. S. Roberts, Dr. M. Schulz, Dr. A. Hasagawa, and Dr. A. Eviatar for a number of profitable comments, suggestions, and discussions. I would also like to thank Professor P. Coleman and Professor W. Cummings for the use of their January 1967 ATS-1 magnetic field data.

---

[1]Detailed references are contained in G. A. Paulikas, J. B. Blake, and S. C. Freden, J. Geophys. Res. 72, 2011 (1967).

[2]C. Störmer, Polar Aurora (Oxford University Press, New York, 1955).

[3]See, e.g., R. Gall, J. Jiménez, and L. Camacho, J. Geophys. Res. 73, 1593 (1968), and references contained therein.

[4]R. W. Filius, to be published.

[5]S. M. Krimigis, J. A. Van Allen, and T. A. Armstrong, Phys. Rev. Letters 18, 1204 (1967).

[6]J. W. Dungey, Phys. Rev. Letters 6, 47 (1961).

[7]F. C. Michel and A. J. Dessler, J. Geophys. Res. 70, 4305 (1965).

[8]L. J. Lanzerotti, Nucl. Instr. Methods 61, 99 (1968).

[9]L. J. Lanzerotti, C. S. Roberts, and W. L. Brown, J. Geophys. Res. 72, 5893 (1967).
[10]L. J. Lanzerotti, H. P. Lie, and G. L. Miller, to be published.
[11]A. J. Masley and A. D. Goedeke, Can. J. Phys. 46, S766 (1968).
[12]L. J. Lanzerotti, to be published.
[13]G. A. Paulikas, J. B. Blake, and S. C. Freden, Trans. Am. Geophys. Union 49, 276 (1968).
[14]C. S. Roberts, W. L. Brown, L. J. Lanzerotti, and E. J. Gleckner, Trans. Am. Geophys. Union 49, 275 (1968).
[15]J. G. Roederer, J. Geophys. Res. 72, 981 (1967).
[16]J. G. Roederer, private communication.
[17]M. P. Nakada and G. D. Mead, J. Geophys. Res. 70, 4777 (1965).

N72-21834

# CHAPTER 3

## Penetration of Solar Particles to Ionospheric Heights at Low Latitudes

Ganguly and Rao recently presented evidence for the possibility of the penetration of high energy solar particles to ionospheric heights at the equator[1]. Their letter, based on ionospheric absorption data obtained at Calcutta (geomagnetic latitude 12° 15′ N), together with optical observations of solar flares and tabulated proton flux data, is very interesting in the light of extensive work recently on the penetration of solar particles to low magnetospheric $L$-values ($L \sim 4$–$7\ R_E$) at the equator[2-7]. Because the observations of Ganguly and Rao would have a profound and far-reaching impact on current ideas of the mechanisms for the access of such solar particles to the geomagnetic equator[2-4,6], the ionospheric and solar evidence presented by the Calcutta group has been examined carefully. We conclude that there is little basis for their contention that solar particles can penetrate directly to low altitudes and thus influence ionospheric absorption at the equator.

Ganguly and Rao present perhaps their most conclusive evidence in their Fig. 2. They plot, as a function of time, the night-time absorption (for 4·7 MHz) and the "proton flux ($E > 60$ MeV) measured by Explorer 33" for the period 1400 UT August 1 to 0300 UT August 2, 1967. Proton data ($E \sim 60$ MeV) measured by the Bell Laboratories instrument on ATS-1 at the equator (150° W geographic longitude) at synchronous altitude were examined for evidence of a solar particle enhancement occurring around the time reported in ref. 1. No evidence for such an enhancement was found.

The $E > 60$ MeV proton data from the solar proton monitoring experiment on Explorer 34, published routinely in the ESSA bulletin *Solar Geophysical Data*[8], were examined for a proton enhancement as presented by the Calcutta group. During the time period discussed by Ganguly and Rao, Explorer 34 was at perigee and thus measuring the electron radiation belts by electron pile-up in the proton channels[9]. It was found that the $E > 60$ MeV data presented by Ganguly and Rao were equal to the fluxes reported by the Explorer 34 solar proton monitoring experiment during its perigee-pass through the radiation belts. Hence we conclude with respect to the "correlation" presented in Fig. 2 of the letter by Ganguly and Rao that: (1) ATS-1 data give no evidence of a solar proton enhancement at high altitudes at the equator; (2) Ganguly and Rao were evidently using Explorer 34 and not Explorer 33 data in their comparison; (3) the data they plotted were the perigee-pass data when the satellite detector was measuring the radiation belts.

We have examined the optical flare data and the solar proton data from ATS-1 and Explorer 34 during the three

periods of anomalous absorption presented in Fig. 1 of Ganguly and Rao. The optical flare data which we used were those in the master list of flares and subflares compiled by World Data Center A and published in *Solar Geophysical Data*[10]. Although not stated explicitly in their caption to Fig. 1, Rao informs us that the data were plotted in Indian Standard Time (IST = UT + 5·5 h).

The flare that occurred between 0337 and 0352 UT, February 11, 1968, was classified as −N (ref. 10). The flare that occurred between 0416 and 0439 UT, February 14, 1968, was classified as 1B (ref. 10). No evidence of high energy solar protons was observed at synchronous altitude on ATS-1 at the time of either of the two absorption events which Ganguly and Rao associated with these flares. Explorer 34, located in the magnetotail, also measured no high energy solar protons. A small flux of low energy ($\leq 5$ MeV) solar protons was observed on both ATS-1 and Explorer 34 throughout February 14. The flare that Ganguly and Rao reported as occurring between 0820–0840 UT, February 7, 1968, was classified as 1F in the list of "Small or Unconfirmed" flares[10]. No solar protons in any energy range were observed on either satellite during this day.

We conclude with respect to the three February 1968 flare events in Fig. 1 of Ganguly and Rao that the solar proton data do not support the authors' contentions that high energy protons contribute to low altitude equatorial absorption at Calcutta. We further note that the three February 1968 flares used by Ganguly and Rao were smaller than the flares that generally produce high energy proton fluxes at the Earth.

In summary, we find the evidence for correlation of proton events with low altitude equatorial absorption to be invalid, and find the supporting flare data to be unconvincing and unsupported by spacecraft measurements.

We thank Miss E. Ruth Hedemann of the McMath-Hulbert Observatory, University of Michigan, for comments on optical flare reporting and publication, and Dr. M. Rao for comments on the first draft of this letter.

L. J. LANZEROTTI

Bell Telephone Laboratories,
Murray Hill, New Jersey 07974.

T. E. GRAEDEL

Bell Telephone Laboratories,
Whippany, New Jersey 07981.

[1] Ganguly, S., and Rao, M., *Nature*, **225**, 169 (1970).
[2] Fillius, R. W., *Ann. Geophys.*, **24**, 821 (1968).
[3] Lanzerotti, L. J., *Phys. Rev. Lett.*, **21**, 929 (1968).
[4] Paulikas, G. A., and Blake, J. B., *J. Geophys. Res.*, **74**, 2161 (1969).
[5] Paulikas, G. A., and Blake, J. B., *J. Geophys. Res.*, **75**, 734 (1970).
[6] Lanzerotti, L. J., *Proc. Third ESRO Symp.* (G. Reidel Pub. Co., 1970).
[7] Lanzerotti, L. J., Montgomery, M. D., and Singer, S., *J. Geophys. Res.*, **75**, 3729 (1970).
[8] *Solar Geophysical Data, IER-FB-282*, 147 (US Dept Commerce, 1968).
[9] *Solar Geophysical Data, IER-FB-294 (Supp.)*, 64 (US Dept Commerce, 1969).
[10] *Solar Geophysical Data, IER-FB-288*, 103 (US Dept Commerce, 1968).

# CHAPTER 4

## Penetration of Solar Protons into the Magnetosphere and Magnetotail

L. J. LANZEROTTI

*Bell Telephone Laboratories, Murray Hill, New Jersey 07974*

M. D. MONTGOMERY AND S. SINGER

*University of California, Los Alamos Scientific Laboratory, Los Alamos, New Mexico 87544*

Three sets of satellite measurements are used to compare solar proton fluxes in the magnetotail, in the outer magnetosphere, at synchronous altitude, and in interplanetary space. Comparisons of the interplanetary and magnetosphere proton fluxes show that outer magnetosphere disturbances play a strong role in the initial access of near-90° pitch angle protons to synchronous altitude. One comparison of the magnetotail and synchronous altitude fluxes suggests that the synchronous altitude fluxes may not always result from a scattering of the protons in from the tail. The interplanetary magnetotail proton comparisons further confirm the results of Montgomery and Singer (1969), who found that delays in the proton access to the magnetotail were always present.

### INTRODUCTION

One of the more current and important studies in the analysis of solar particle data is the attempt to understand the configuration of the geomagnetic field by analyzing the means or modes of access of the particles into the magnetosphere and magnetotail [*Krimigis et al.*, 1967; *Lin and Anderson*, 1966; *Williams and Bostrom*, 1967; *Filius*, 1968; *Kane et al.*, 1968; *Konradi*, 1968; *Lanzerotti*, 1968*b*; *Blake et al.*, 1968; *Williams and Bostrom*, 1969; *Vampola*, 1969; *Paulikas and Blake*, 1969; *Anderson and Lin*, 1969; *Montgomery and Singer*, 1969; *Hudson and Anderson*, 1969; *Evans and Stone*, 1969; *Bostrom*, 1970; *Lanzerotti*, 1970; *Paulikas*, 1970]. Generally, the studies have concerned themselves with the access of low-energy solar protons (~0.5–10 Mev), although *Lin and Anderson* [1966] and *Anderson and Lin* [1969] discussed electron access to the geomagnetic tail, *Vampola* [1969] discussed solar electrons over the polar caps, and *Lanzerotti* [1968*b*] discussed solar alpha particle access to synchronous altitude. It now seems quite clear that the question of access is very complicated and that the use of particle data will not give an answer as to whether the geomagnetic field is 'open' or 'closed' far behind the earth.

A major difficulty arises when low-energy solar particles are used as probes of the magnetosphere configuration because of the question of whether the magnetosphere is truly 'quiet' when the first solar particles arrive at the earth and are seen to penetrate into the polar cap, the synchronous altitude, or the magnetotail. A second difficulty arises because the small interplanetary proton enhancements often used as 'probes' for observing access time delays are frequently accompanied by solar wind or interplanetary magnetic field changes which could disturb the magnetosphere. The effects of magnetosphere and magnetotail disturbances and distortions *have seldom been considered* quantitatively or qualitatively in the analyses of proton access.

Instead of using the low-energy particle data as 'proof' of a given static magnetospheric configuration, it is more significant to use the data comparisons to discuss fundamental physical processes operating in the magnetotail and magnetosphere. It seems quite likely that even during moderately disturbed conditions there may be sufficient electric and magnetic noise in the outer magnetosphere, in the neutral

point region, and in the tail to cause solar particles to 'diffuse' (with greatly variable diffusion coefficients) into the magnetotail and magnetosphere. The conclusion of *Montgomery and Singer* [1969] that both diffusion and direct access of protons into the magnetotail appear to be effective at various times is a succinct summary of the present state of affairs. It also appears that fairly rapid diffusion (such as a few scatterings of the particle gyro radius) across the magnetopause or through the tail and then in the magnetosphere seems to be required to bring solar particles to the synchronous orbit. [*Lanzerotti,* 1968*b*, 1970; *Paulikas and Blake,* 1969].

This paper is an initial report on a current study investigating the temporal structure of solar protons detected on three satellites (in the outer magnetosphere and interplanetary space, at synchronous altitude, and in the magnetotail). These data comparisons (1) show that the initial onset of the solar particle enhancements at synchronous altitude apparently results from a large disturbance and/or noise in the outer magnetosphere [*Lanzerotti,* 1970]; (2) indicate that the synchronous altitude proton fluxes may not always result from a scattering of the particles in from the magnetotail; (3) indicate that the proton fluxes in the midlatitude outer magnetosphere and the magnetotail are generally quite similar; and (4) confirm the results of *Montgomery and Singer* [1969], who always found time delays for proton penetration of the tail.

## Observations

The proton particle instrumentation on Vela 4, ATS 1, and Explorer 34 (IMP F) (see data plotted in Figure 1) were previously described in the literature .[*Singer et al.,* 1969; *Lanzerotti* 1968*a*; and *Lanzerotti et al.,* 1969]. The Vela 4A spacecraft traversed the tail region during 0600–2400 UT. At 0600 UT the solar-magnetosphere latitude and longitude of 4A were ~9° and 184.2°, respectively; the coordinates had changed to −40.9° and 230.9°, respectively, by 2400 UT. The Explorer 34 satellite was in the magnetosphere from ~0500 UT until it entered the magnetosheath at ~1410 UT (D. H. Fairfield, private communication). Explorer 34 crossed the bow shock at ~1700 UT and had a solar-magnetosphere longitude close to 0°. ATS 1 local time is UT −10 hours; the ATS 1 local time orientation is

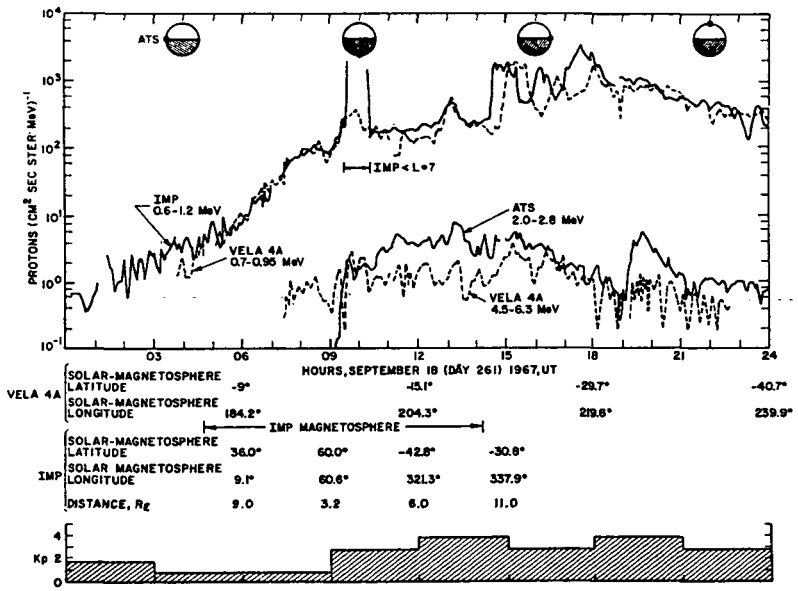


Fig. 1. Solar proton fluxes as measured by the Explorer 34, Vela 4A, and ATS 1 satellites on September 18, 1967. The solar-magnetosphere location of Vela 4A, the perigee pass of Explorer 34, and the temporal locations of ATS 1 are indicated. The *Kp* index is plotted to give an indication of the magnetosphere disturbances.

shown schematically at the top of Figure 1. It should be stressed that the ATS-1 instrument, oriented perpendicular to the local magnetic field, measures particles that mirror near the equator.

The particular time period of Figure 1 was especially selected for this report because of the relative locations of the satellites during the solar particle enhancements and because of the structure in the enhancements during the last half of the day. During the September 18 perigee pass of the polar-orbiting Explorer 34 satellite, the spacecraft traversed the outer region of the magnetosphere, with the perigee occurring on the nightside of the earth.

*Outer magnetosphere and magnetotail observations.* It is evident (Figure 1) that during the period from ~0500 until Explorer 34 was at high latitudes over the south pole, the 5-min average 0.6- to 1.2-Mev solar proton fluxes in the outer region of the magnetosphere and the the 0.7- to 0.95-Mev fluxes in the magnetotail tracked one another in amplitude (on the average) quite well. Data were not acquired during the Explorer 34 perigee from ~0930 to ~1015 UT.

From ~1030 to ~1245 UT the outer magnetosphere fluxes were generally larger than the proton fluxes (0.7–0.95 Mev) observed in the tail. An enhancement in the fluxes, centered at ~1315 UT, was observed nearly simultaneously both in the magnetotail and in the outer regions of the magnetosphere close to the boundary. Just prior to the large flux enhancement at ~1430 UT, the Explorer 34 satellite passed into the magnetosheath. The large enhancement occurred ~24 min. later in the magnetotail fluxes (0.7–0.95 Mev) with approximately the same flux width and magnitude as that observed in the magnetosheath. This enhancement was also in the higher energy protons measured on Vela (4.6–6.3 Mev) and on Explorer 34 (4.4–5.0 Mev), although these data are not shown in Figure 1. The magnitude of the higher energy enhancements was also approximately equal at the two satellites and showed a time delay between the magnetotail and magnetosheath comparable to that observed at lower energies.

Two subsequent enhancements were observed by Explorer 34. The first, with the satellite in the magnetosheath, peaked at ~1610 UT; the second, with the satellite in interplanetary space, peaked at ~1730 UT. These enhancements were also subsequently seen in the Vela magnetotail data (0.7–0.95 Mev). However, the time delay in observing the last enhancement was nearly an hour. In addition, the magnetotail intensities of each of these subsequent enhancements were progressively diminished, and the distinguishing structures progressively obliterated. After ~1900 UT, the interplanetary and magnetotail flux magnitudes tracked one another quite well (on the average) for the remainder of September 18.

The second interplanetary enhancement (~1610 UT) was also measured delayed in the higher energy proton channel (4.5–6.3 Mev) in the magnetotail. The third large enhancement was not seen in this proton channel. This is probably due both to the fact that (1) the interplanetary enhancement above ~5 Mev as measured by Explorer 34 (not shown) was reduced in magnitude compared with the ~0.6 Mev enhancement, and (2) the magnetotail access mechanism produced a large flux reduction from the interplanetary amplitude observations.

*Synchronous altitude observations. Lanzerotti* [1970] attributes the usual rapid access of interplanetary protons to synchronous altitude to the existence of a generally disturbed state of the outer magnetosphere. He also indicates in a qualitative way that the electron fluxes at the synchronous altitude can be used to indicate the general state of disturbance at 6.6 $R_E$. The 2-min average electron fluxes measured in two electron channels $E >$ 0.4 and $>1.9$ Mev on ATS 1 on September 8 are plotted in Figure 2.

The relationship of the magnitude of the synchronous altitude diurnal variation to stormy magnetosphere conditions (as measured by *Kp*) and the relationship of increases or decreases in the electron fluxes to increases or decreases in the local magnetic field intensity are discussed by *Lanzerotti et al.* [1967], *Brown* [1968], and *Paulikas et al.* [1968]. Whether the electron fluxes increase or decrease compared to increases or decreases of the local magnetic field intensity depends, among other considerations, on the local electron radial gradient as well as the rapidity of the field changes. In general, however, increases (decreases) in the local mag-

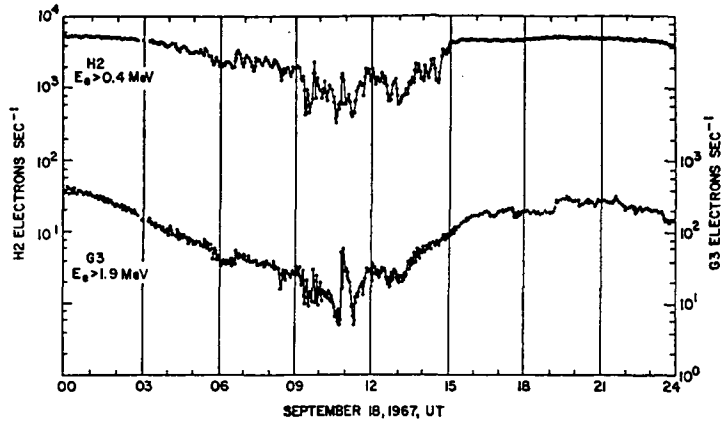


Fig. 2. Two-minute average $E > 0.4$ and $E > 1.9$ Mev electron rates measured on the ATS 1 satellite on September 18, 1967. The data are used to indicate the local ATS 1 magnetosphere disturbances during the solar proton observations.

netic field intensity are accompanied by increases (decreases) in the local electron fluxes. This corresponding behavior of the electron fluxes is often termed an 'adiabatic' change. The ATS 1 satellite is beyond the maximum of the outer electron belt. Generally, because of the steeper radial gradient of the higher energy electron fluxes, these fluxes undergo larger changes than the lower energy fluxes for a given local field intensity change.

Until the sharp decrease in the electron fluxes at ~0915 UT, the interplanetary solar proton enhancement was not observed at synchronous altitude (for near-90° pitch angle particles). The increase in flux intensity to between one quarter and one half the Explorer 34 intensities was quite sharp after the initial onset (which corresponded in time to the apparent decrease of the local field intensity).

No substorms were in progress at the time of the ATS 1 flux onset. An inspection of several high-latitude magnetograms (College, Barrow, and Dixon Island) and the Honolulu low-latitude magnetogram showed qualitatively that an increase in the 'noisiness' of the magnetic field began at approximately the same time as the particle onsets. These additional disturbances are also reflected in the increase in *Kp* during the 0900–1200 UT interval (Figure 1).

It is also interesting that the proton flux enhancement in the magnetotail and outer magnetosphere at ~1315 UT occurred at the same time and with essentially the same temporal width at synchronous altitude. This increase in the proton fluxes in three widely separated places inside the magnetopause was accompanied by a small decrease in the local ATS 1 electron fluxes (small expansion of the local field). The large interplanetary and magnetotail flux enhancements at ~1730 were not observed at the synchronous altitude.

## Discussion and Conclusions

The excellent preservation in the magnetotail of both the flux magnitude and temporal width of the large 1430 UT interplanetary enhancement argues for the non-diffusive penetration of solar particles into the tail. The ~24-min time delay implies an entry to the magnetotail ~0.05 AU behind the earth. The successively longer time delays in the magnetotail appearance of the next two interplanetary enhancements could also be due to direct particle access into the tail at larger distances (0.1 AU and 0.15 AU, respectively). The reduced amplitudes of these two enhancements could be due to dispersive processes in the more distant magnetotail. Both the longer delay times and the reduced amplitudes, however, do not rule out the possibility that these succeeding two magnetotail enhancements could be attributed to a diffusion of the solar particles across the tail.

*Behannon and Ness* [1966] show a correla-

tion between the magnetotail field intensity and *Kp*. The successively longer time delays for the appearance of the three interplanetary disturbances between 1400 and 1800 UT inside the magnetotail could be due to a continued increase in the magnetotail field strength as the general high level of magnetic activity persisted. The increased field intensity could cause the protons to either enter further and further down the tail and/or cause the diffusion time across the tail to increase.

Although *Paulikas and Blake* [1969] show little correlation between the solar proton intensities at synchronous altitude and the local ATS field magnitude, it is nevertheless significant that both the initial onset of protons observed at ATS 1 and the general magnetosphere-wide enhancement at ~1315 were accompanied by changes in the synchronous altitude electron fluxes (thus implying changes in the local magnetic field intensity). Both of these local changes were perhaps indicative of more wide-spread magnetosphere disturbances, as suggested by the noisiness of the ground magnetometer data.

The explanation of the peak in the ATS 1 proton fluxes, beginning at ~1915 UT, represents a real challenge. A temporary increase in the accessibility of protons to synchronous altitude at the time of the 1915 UT enhancement seems the most plausible explanation. Indeed, a gross magnetosphere field configuration change is suggested by the increase in the fluxes of high-energy electrons during the proton enhancement (Figure 2). This flux change, however, suggests an *increased* field intensity, which implies that ATS 1 was therefore *deeper* inside the magnetosphere. Given the measured proton spectrum, and if the proton radial gradient was negative (as it should be due to the interplanetary source, and as is suggested by the flux decreases as the satellite moved toward the noon side of the magnetosphere), then the proton fluxes would tend to decrease rather than increase.

The accessibility could also be enhanced by an increase in the amount of electromagnetic noise in the outer magnetosphere and near-tail regions. The increased *Kp* value during this time suggests an increased magnetosphere disturbance. However, *Kp* is generally a rather poor indicator of solar particle transmission to synchronous altitude [*Paulikas and Blake*, 1969; *Lanzerotti*, 1970]. In addition, an examination of the high time resolution ATS 1 electron fluxes (not shown) does not indicate an enhancement of outer-magnetosphere noise at the ATS 1 location during the 1915 UT flux increase.

There is another possible explanation for the synchronous altitude flux increase if the large ATS 1 enhancement at ~1915 UT is associated with the third large interplanetary enhancement (~1715 UT) because of the temporal, somewhat broadened, shape of the former. If this is a proper identification, then it seems unlikely that in this case these protons resulted from a scattering in of particles from the tail, because the percentage synchronous altitude increase is much larger than the third magnetotail increase that allegedly produced it. (The lack of a corresponding magnetotail peak at ~1915 UT is real and is not produced by differences in instrumental response.)

If the ATS 1 enhancement at ~1915 UT did not result from an enhanced accessibility or from scattering in from the tail, then it may have resulted from other processes for which no evidence exists in the data examined here. One such possible process could be a very delayed access of the interplanetary particles (~1715 UT) across the magnetopause and deep into the magnetosphere.

*Acknowledgments.* We thank Dr. D. H. Fairfield for supplying the magnetopause and shock crossing data from Explorer 34 and Dr. W. L. Brown for helpful comments on the manuscript.

The Los Alamos portion of this research was performed as part of the Vela Nuclear Test Detection Satellite Program, which is jointly sponsored by the Advanced Research Project Agency of the Department of Defense and the U. S. Atomic Energy Commission, and is managed by the U. S. Air Force.

## References

Anderson, K. A., and R. P. Lin, Observation of interplanetary field lines in the magnetotail, *J. Geophys. Res.*, *74*, 3953, 1969.

Behannon, K. W., and N. F. Ness, Magnetic storms in the earth's magnetic tail, *J. Geophys. Res.*, *71*, 2327, 1966.

Blake, J. B., G. A. Paulikas, and S. C. Freden, Latitude intensity structure and pitch angle

distributions of low energy solar cosmic rays at low altitude, *J. Geophys. Res., 73,* 4927, 1968.

Bostrom, C. O., Entry of low energy solar protons into the magnetosphere, *Proceedings of the Third ESRO Symposium on Intercorrelated Satellite Observations Related to Solar Events,* to be published, D. Reidel, Dordrecht, Holland, 1970.

Brown, W. L., Energetic outer belt electrons at synchronous altitude, in *Earth's Particles and Fields,* edited by B. M. McCormac. p. 33, Reinhold Publishing Corporation, New York, 1963.

Evans, L. C., and E. C. Stone, Access of solar protons into the polar cap: A persistent north-south asymmetry, *J. Geophys. Res., 74,* 5127, 1969.

Filius, R. W., Penetration of solar protons to four earth radii in the equatorial plane, *Ann. Geophys., 23,* 821, 1968.

Hudson, P. D., and H. R. Anderson, Nonuniformity of solar protons over the polar caps on March 24, 1966, *J. Geophys. Res., 74,* 2881, 1969.

Kane, S. R., J. R. Winckler, and D. J. Hoffman, Observations of the screening of solar cosmic rays by the outer magnetosphere, *Planet. Space Sci., 16,* 1381, 1968.

Konradi, A., 135–1650 kev solar protons after the flare of July 7, 1966, observed in the magnetotail and magnetosheath, *J. Geophys. Res., 74,* 1158, 1969.

Krimigis, S. M., J. A. Van Allen, and T. P. Armstrong, Simultaneous observations of solar protons inside and outside the magnetosphere, *Phys. Rev. Lett., 18,* 1204, 1937.

Lanzerotti, L. J., Calibration of a semiconductor detector telescope for space experiments, *Nucl. Instrum. Methods, 61,* 99, 1968*a*.

Lanzerotti, L. J., Penetration of solar protons and alphas to the geomagnetic equator, *Phys. Rev. Lett., 21,* 929, 1968*b*.

Lanzerotti, L. J., Access of solar particles to synchronous altitude, in *Proceedings of the Third ESRO Symposium on Intercorrelated Satellite Observations Related to Solar Events,* to be published, D. Reidel, Dordrecht, Holland, 1970.

Lanzerotti, L. J., C. S. Roberts, and W. L. Brown, Temporal variations in the electron flux at synchronous altitudes, *J. Geophys. Res., 72,* 5893, 1967.

Lanzerotti, L. J., H. P. Lie, and G. L. Miller, A solar cosmic ray particle spectrometer with on-board particle identification, *IEEE Trans. Nucl. Sci., NS-16*(1), 1969.

Lin, R. P., and K. A. Anderson, Evidence for connection of geomagnetic tail lines to the interplanetary field, *J. Geophys. Res., 71,* 4213, 1966.

Montgomery, M. D., and S. Singer, Penetration of solar energetic protons into the magnetotail, *J. Geophys. Res., 74,* 2869, 1969.

Paulikas, G. A., J. B. Blake, S. C. Freden, and S. S. Imamoto, Observations of energetic electrons at synchronous altitude, 1, General features and diurnal variations, *J. Geophys. Res., 73,* 4915, 1968.

Paulikas, G. A., and J. B. Blake, Penetration of solar protons to synchronous altitude, *J. Geophys. Res., 74,* 2161, 1969.

Paulikas, G. A., Propagation of solar particles to the polar cap, in *Proceedings of the Third ESRO Symposium on Intercorrelated Satellite Observations Related to Solar Events,* to be published, D. Reidel, Dordrecht, Holland, 1970.

Singer, S., W. P. Aiello, J. P. Conner, and R. W. Klebesadel, The Vela 4 satellite energetic particle experiment, *IEEE Trans. Nucl. Sci., NS-16*(1), 1969.

Vampola, A. L., Energetic electrons at latitudes above the outer-zone cutoff, *J. Geophys. Res., 74,* 1254, 1969.

Williams, D. J., and C. O. Bostrom, Proton entry into the magnetosphere on May 26, 1967, *J. Geophys. Res., 74,* 3019, 1969.

Williams, D. J., and C. O. Bostrom, The February 5, 1965, solar proton event, 2, Low energy solar protons and their relation to the magnetosphere, *J. Geophys. Res., 72,* 4497, 1967.

# CHAPTER 5

## ACCESS OF SOLAR PARTICLES TO SYNCHRONOUS ALTITUDE

L. J. LANZEROTTI
*Bell Telephone Laboratories, Murray Hill, N.J., U.S.A.*

**Abstract.** When a source of solar-originated particles is present in interplanetary space, comparable fluxes of these particles with similar spectral characteristics are usually observed inside the magnetosphere at synchronous altitudes. The temporal and spectral changes in the access of these solar protons and $\alpha$ particles to synchronous altitude are discussed and reviewed. Possible consequences of the presence of substantial fluxes of low energy solar protons deep inside the magnetosphere are also discussed.

### 1. Introduction

A multitude of ground and satellite observations of solar proton fluxes at high latitudes have provided much convincing evidence that these protons have access to inner regions of the magnetosphere that would normally be prohibited by the Störmer theory (1955). These measurements and their relationship to theoretical particle trajectory calculations in model magnetospheres have been reviewed recently by Bostrom (1970), Paulikas (1970), and Hofmann and Sauer (1968).

Only recently have solar particle measurements been reported in the equatorial regions of the magnetosphere. Filius (1968) reported the access of solar protons (40–250 MeV) to 4 $R_E$ at the equator and showed that the Störmer theory could be modified to agree with his observations. Lanzerotti (1968b) reported measurements of solar proton and alpha particle fluxes (1–20 MeV/nucleon) at synchronous altitude (6.6 $R_E$) and compared their temporal and spectral characteristics to simultaneous measurements of the interplanetary fluxes. The significance of these measurements was that substantial cutoff lowering was observed for $\sim$1 MeV protons with near 90° pitch angles at the geomagnetic equator. Lanzerotti concluded that there must exist an effective diffusion process operative in the outer regions of the magnetosphere and/or the near regions of the geomagnetic tail that often preserves the spectral character and magnitude of the interplanetary fluxes after their penetration to the synchronous altitude. Paulikas and Blake (1969) have also reported the omni-directional intensity of solar protons at the synchronous altitude during a solar event in January, 1967. In addition to concluding that protons with energies greater than 21 MeV have essentially free access to synchronous altitude, they observed a diurnal effect in the fluxes of 5–21 MeV solar protons, with more protons observed near local midnight than near local noon. Lanzerotti (1968b) also observed such a diurnal effect in the 2.4 MeV proton fluxes.

This paper presents extensive measurements of the proton environment at synchronous altitudes. Most of the data are obtained from measurements made by the Bell Laboratories experiment on the ATS-1 satellite during the last half of 1967.

These measurements are compared to similar measurements obtained simultaneously by an instrument on the Explorer 34 (IMP F) satellite in interplanetary space. Since the ATS-1 satellite traverses all local times (solar-ecliptic longitudes) in a 24-hour period, and since the number of $\gtrsim 1$ MeV protons at synchronous altitude when interplanetary particles are not present is essentially zero, comparisons of the solar fluxes at this equatorial location with the interplanetary fluxes allows systematic investigations of the results of the particle access with other magnetosphere observations.

Due to the distortion of the magnetosphere by its interaction with the solar wind, the ATS-1 satellite does not remain on a line of constant magnetic field intensity $B$ during its daily traversal of all local times. Rather the satellite is located on lines of lower $B$ intensity at local midnight than at local noon. This fact, together with the observation that the satellite is always beyond the maximum of the outer electron zone gives rise to the familiar diurnal effect observed in the relativistic electron intensities (Lanzerotti *et al.*, 1967; Paulikas *et al.*, 1968). Also attributed to the distortion of the magnetosphere was the apparent diurnal effect (with the same sense as the electron fluxes) reportedly observed in the 0.3 to 10 MeV outer zone trapped proton fluxes by Armstrong and Krimigis (1968) using data from the elliptical orbit satellite, Explorer 33.

## 2. Experiments

The ATS-1 satellite (launched December 6, 1966) is a geostationary, spin-stabilized satellite (with the spin axis parallel to the local magnetic field) stationed at 158°W, 0°N and at a geocentric distance of 6.6 $R_E$. The Bell Telephone Laboratories (BTL) experiment flown on ATS-1 consists of a 6-element solid-state detector telescope oriented perpendicular to the spin axis of the satellite. By use of the particle $dE/dx$ characteristics and appropriate logic circuitry, the experiment is capable of distinguishing between protons, $\alpha$'s, and electrons. The half-angle of the detector telescope collimator is 20°; the flux measured by the BTL experiment is the spin-averaged flux of those particles with pitch angles close to 90° (Lanzerotti, 1968a). ATS-1 local time is obtained by subtracting 10 hours from the universal time.

The IMP F satellite, launched May 24, 1967, is a spin-stabilized (with the spin axis perpendicular to the ecliptic plane) polar-orbit satellite with an apogee of approximately 34 $R_E$. The BTL experiment consists of a 4-element solid-state telescope oriented perpendicular to the spin axis. The half-angle of the detector telescope collimator is also 20°; the flux measured by the experiment is the spin-averaged flux of particles in the ecliptic plane. Protons and $\alpha$'s up to an energy of approximately 4 MeV/nucleon are distinguished by the energy deposited in the first two detectors of the telescope and subsequently measured in a 5-channel analyzer. Particle species above this energy are distinguished by the use of an on-board pulse multiplier. Electrons $\gtrsim 300$ keV are detected by their $dE/dx$ characteristics and the appropriate logic circuitry (Lanzerotti *et al.*, 1969a).

## 3. Observations

The first figure contains the 1 hour average temporal history of 1.9 and 2.4 MeV proton fluxes measured in interplanetary space and at synchronous altitudes, respectively, from day 318 to day 360, 1967. Also plotted at the bottom of the figure are the hourly average AE and Dst indices and the 3-hour average $K_p$ index. The dark bars above the IMP data indicate periods when the Explorer 34 satellite was inside the magnetopause (D. H. Fairfield, private communication).

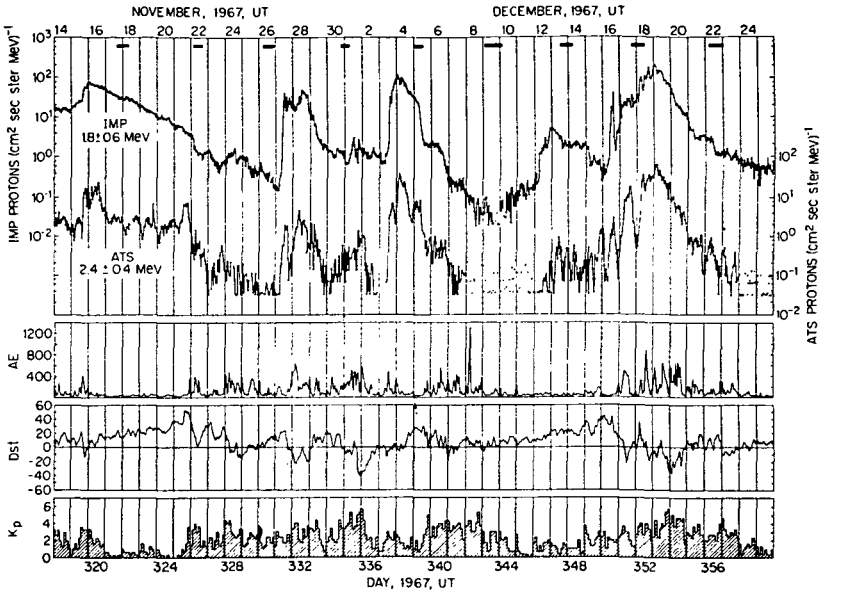


Fig. 1. 1-hour average Explorer 34 (IMP-F, interplanetary) and ATS-1 (synchronous altitude magnetosphere) proton fluxes from day 318 through day 359, 1967. The bars above the interplanetary data indicate periods when Explorer 34 was inside the magnetosphere.

This entire time period had appreciable fluxes of solar-origin interplanetary particles which are of interest in themselves. (In fact, the long period of interplanetary enhancements began on day 300, but continuous ATS coverage was not available during the entire period of day 300 to day 318.) This period was also moderately active geomagnetically as evidenced by the AE and $K_p$ indices. However, although there were two sudden commencements reported, there were no large geomagnetic storms, the largest Dst negative excursion being less than 50 $\gamma$.

The overall, quite striking, impression obtained from this figure is that whenever there are interplanetary fluxes present, there are also proton enhancements inside the magnetosphere at synchronous altitudes. The enhancements have approximately the same temporal appearances and magnitudes as the interplanetary fluxes and do not persist after the interplanetary fluxes are absent.

There are also gross differences between the interplanetary fluxes and the syn-

chronous altitude fluxes which will be discussed in detail later. The most striking of these are the decreases in the ATS fluxes that are often observed near local noon (2200 UT). The decreases are especially noticeable on days 331, 337, 338, 350, 351, 355, and 356, for example. Often the temporal histories of the flux decreases resemble PCA mid-day absorption recoveries (Leinbach, 1967).

A noticeable feature in the interplanetary data is the general absence of a modulation of the measured solar proton fluxes as the IMP satellite crosses the magnetopause. This feature of proton access to the magnetosphere is also discussed briefly later.

Expanded views of the 1-hour average ATS proton fluxes in several energy channels for a disturbed and a quiet geomagnetic period are plotted in Figures 2 and 3. Plotted at the bottom of each figure are the AE, Dst, and $K_p$ indices. The open and closed circles on each data plot indicate the ATS local noon and local midnight locations, respectively.

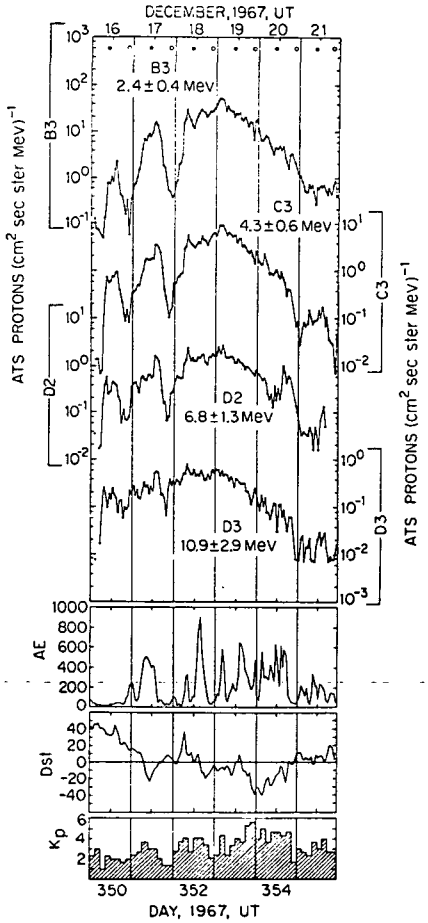


Fig. 2. 1-hour average ATS-1 proton fluxes from day 350 through day 355, 1967. This was a geomagnetically disturbed period.

During the geomagnetically disturbed period, days 350–355 (Figure 2), the diurnal variations in the proton fluxes were most pronounced at the lower energies. The diurnal minimum on day 351 was quite symmetrical about local noon in the 2.4 MeV proton channel, whereas both the symmetry and magnitude of the variations decrease at the higher energies.

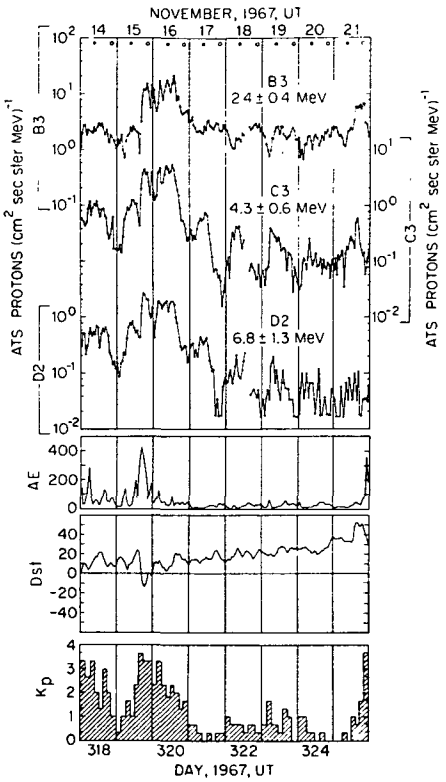


Fig. 3. 1-hour average ATS-1 proton fluxes from day 318 through day 325, 1967. The period including days 321–324 was a geomagnetically quiet period.

The temporal variations of the ATS proton fluxes during a quiet geomagnetic period, days 321–325 (Figure 3), were strikingly different than those observed in the data of Figure 2. The 2.4 MeV data show no decrease in the proton fluxes near local noon but rather small decreases near local evening on days 322–325. In contrast, the fluxes from the two higher energy proton channels plotted in the figure show significant decreases near local noon.

The hourly average electron fluxes for the disturbed and quiet periods are plotted in Figures 4 and 5. These data are shown in order to contrast the simultaneously measured electron diurnal variations (larger fluxes near local noon) with the proton diurnal variations seen in Figures 2 and 3 (larger proton fluxes near local midnight in general). It should be noted that even though no diurnal variations were observed in the proton fluxes on days 352–354, nevertheless, the electron flux intensities continued

to reflect the distortion of the magnetosphere as the ATS satellite traversed all local times.

## 4. Results

### A. DAILY VARIATIONS – DISTURBED CONDITIONS

Of great interest is the accessibility of the solar protons to synchronous altitude and the changes in the amount of accessibility with time, geomagnetic conditions, and energy of the protons. That indeed there are temporal changes in the accessibility was pointed out by Lanzerotti (1968b) and Paulikas and Blake (1969) and is seen clearly in Figures 1–3.

Although both the ATS-1 and IMP experiments measure proton fluxes in approximately the same energy ranges, the proton energy channels of the two experiments do not have the same energy widths nor do they have the same central energy values. In order to study the temporal variations of the ratio $R$ of the synchronous altitude fluxes to the interplanetary fluxes for a common set of energies, the following proce-

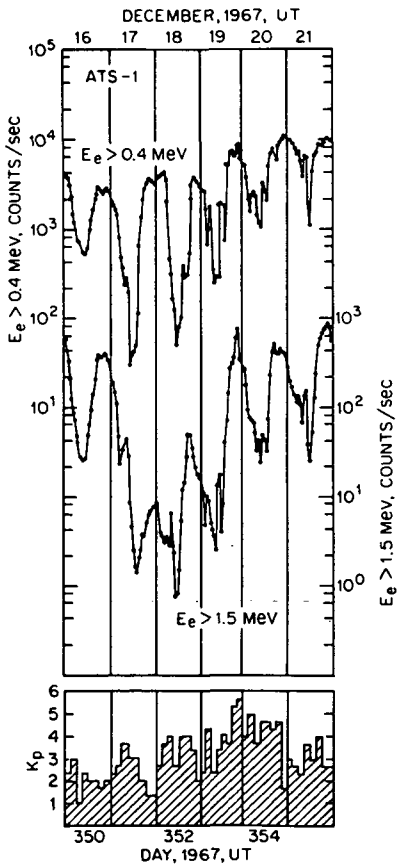


Fig. 4. 1-hour average data from two of the ATS-1 electron channels during the geomagnetically disturbed period, days 350–355, 1967.

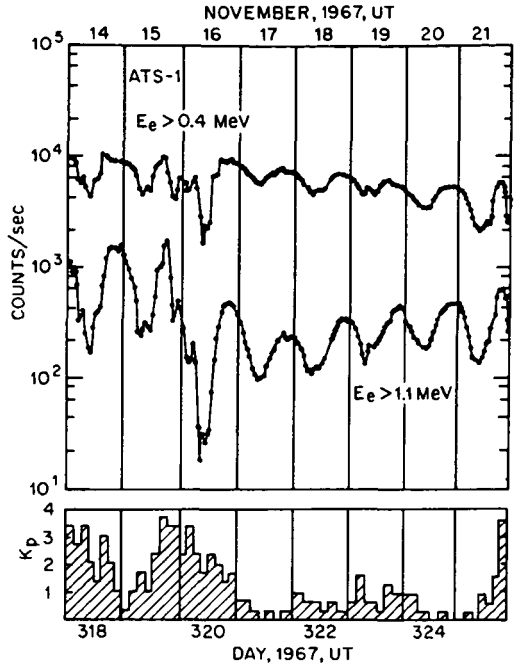


Fig. 5. 1-hour average data from two of the ATS-1 electron channels including the geomagnetically quiet period, days 321–324, 1967.

dure was adopted. The differential-in-energy proton flux values at given energies for each experiment were determined by linear interpolation between adjacent log(energy) values of the hourly-averaged log(flux) values. These flux values were then used in forming the ATS/IMP proton ratios.

It should be stressed that the ratio $R$ does not necessarily measure the transmission or accessibility of solar protons from the interplanetary source to the synchronous altitude. There is a continued loss of the synchronous altitude protons as well during the time the interplanetary source is present. Hence, $R$ measures the result of the sum of the transmission and loss processes present at synchronous altitude at any time.

Figure 6 contains five sets of equal energy ATS/IMP proton flux ratios for the geomagnetically disturbed period, days 350–355. As stressed in the introduction, for a symmetrically distorted dipole field, the ATS-1 satellite is effectively measuring particles further out in the magnetosphere at local midnight than it is at local noon. The effect of this distortion is seen on days 350–352 in the diurnal variation of $R$ in Figure 6. There are fewer protons at the ATS orbit at local noon than at local midnight. That is, there are fewer protons effectively further inside the magnetosphere.

The diurnal variation evident in Figure 6 is larger for the lowest energy protons. The ratio $R$ on day 351 is plotted in Figure 7 as a function of proton energy for ATS local times of noon, morning, and midnight. The fluxes near local midnight are essentially identical to the interplanetary fluxes at all energies. By local morning, the ATS-measured fluxes at all energies have decreased. It is clear that there is an energy

dependence to the decrease in $R$ at local noon; this energy dependence does not have a sharp cutoff.

After approximately the middle of day 352 UT, the value of $R$ remains nearly constant at $\sim 0.5$ for all energies in Figure 6. This indicates very clearly that the proton spectra both inside and outside the magnetosphere are essentially the same at all local times (Lanzerotti, 1968b).

The access of solar protons from the interplanetary source region to the ATS orbit could well be expected to have a dependence upon the plasma and field conditions in the outer magnetosphere. Likewise, the proton loss mechanisms at the synchronous altitude would also be expected to depend upon disturbances in the outer magnetosphere. Hence, the dependence of $R$ upon $K_p$ (Paulikas and Blake, 1969) and Dst were investigated. Since the AE index is perhaps a better indicator of disturbances in the outer magnetosphere than $K_p$, the dependence of $R$ upon AE was also studied.

It is quite clear from the data of Figure 2 that, due in particular to the large diurnal

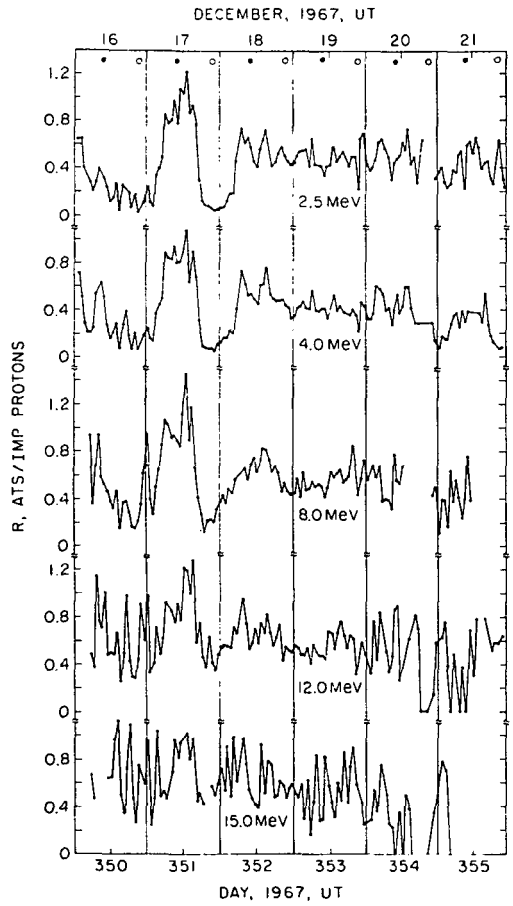


Fig. 6. Temporal plot of the ratio $R$ of the ATS-1 to Explorer 34 proton fluxes during the geomagnetically disturbed period, days 350–355, 1967.

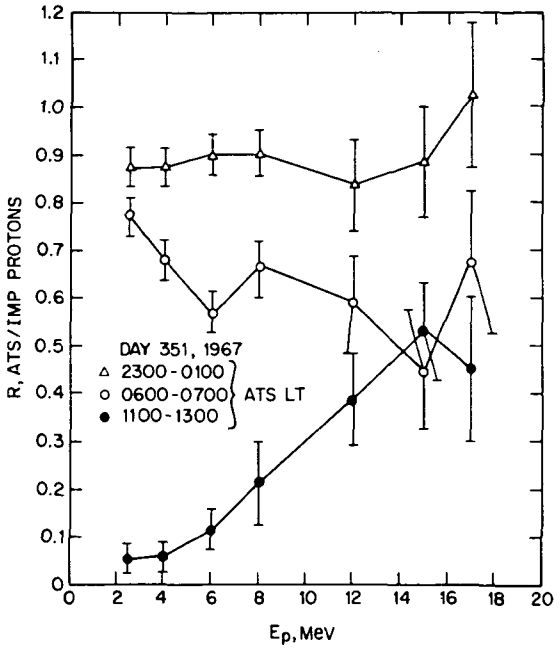


Fig. 7. Ratio $R$ as a function of energy and local time for day 351, 1967, a day when large diurnal variations in $R$ were measured.

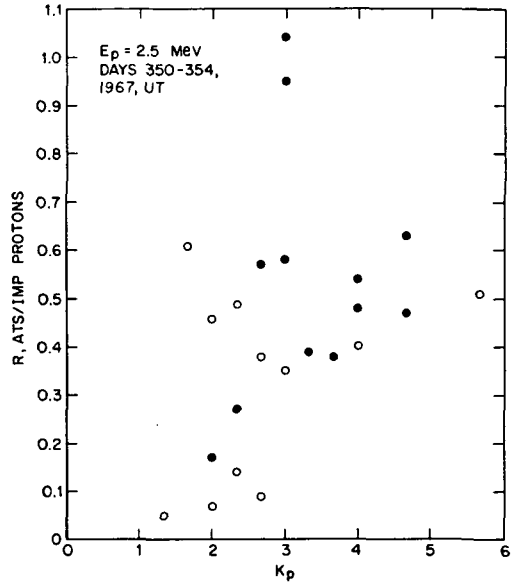


Fig. 8. $R$ as a function of the 3-hour average $K_p$ for 2.5 MeV protons – days 350–354, 1967. The open circles correspond to 3-hour average $R$ values around ATS local noon (2100–2400 UT and 0000–0300 UT). The solid circles correspond to 3 hour average $R$ values around ATS local midnight (0900–1200 UT and 1200–1500 UT).

variations, $R$ does not have a simple correlation with the indices measuring the amount of geomagnetic disturbance. In Figures 8, 9, and 10a are the 2.5 MeV proton ratios plotted as a function of $K_p$, AE, and Dst for days 350–354, 1969. The ratios for several hours spanning local noon and local midnight on each day are denoted by open and closed circles, respectively. For large values of either $K_p$ or AE, $R$ is generally large, as could well be expected. Most of the $R$-values $\gtrsim 0.4$ are observed to occur for negative Dst values (Figure 10a). Other than these observations, $R$ has little dependence upon the magnitude of the indices.

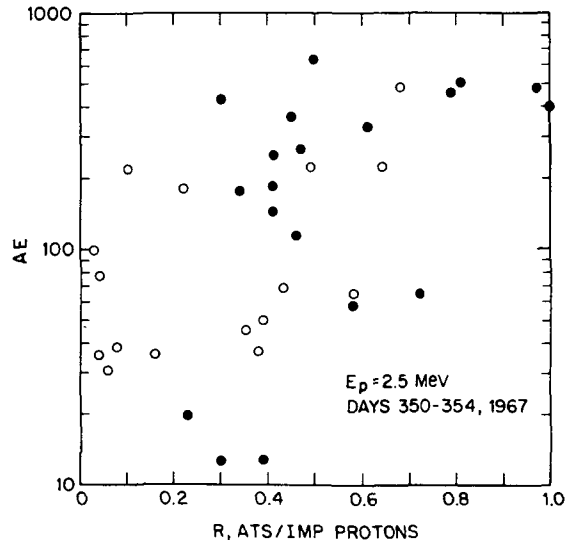


Fig. 9. $R$ as a function of the hourly average AE for 2.5 MeV protons – days 350–354, 1967. The open circles correspond to the hourly average $R$ values for 3 hourly periods around ATS local noon. The solid circles correspond to the hourly average $R$ values for 3 hourly periods around ATS local midnight.

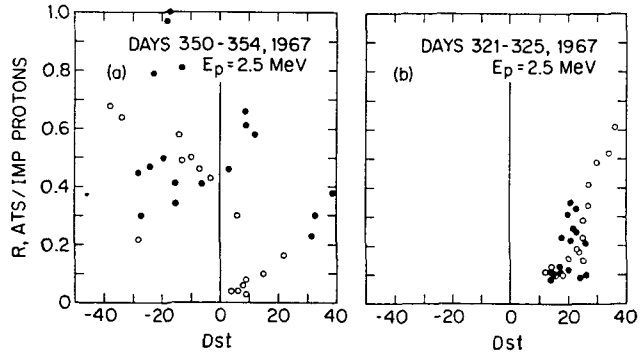


Fig. 10. $R$ as a function of the hourly average Dst for 2.5 MeV protons. – (a) days 350–354, 1967. – (b) days 321–324, 1967. The open circles correspond to the hourly average $R$ values for 3 hourly periods around ATS local noon. The solid circles correspond to the hourly average $R$ values for 3 hourly periods around ATS local midnight.

The ratios, $R$, for 6 different proton energies for days 318–325, 1967, are plotted in Figure 11. The 'quiet-time' (days 321–324) ratios show the opposite temporal changes from the disturbed period ratios (Figure 6) in that a larger diurnal variation is generally observed at the higher energies.

The distortion of the magnetosphere during these quiet-days can be estimated from the ATS magnetic field data, using the calculational results of Roederer (1969) for particle drift motion in a Williams-Mead model geomagnetic field. Since the magnetic field data were not available, estimates of the boundary stand-off distance and tail field strength were made by comparing the smoothly varying electron flux variations on day 321 (Figure 5) with similar electron daily variations in January, 1967, when the field data were available. Although this provides only a rough estimate, it was

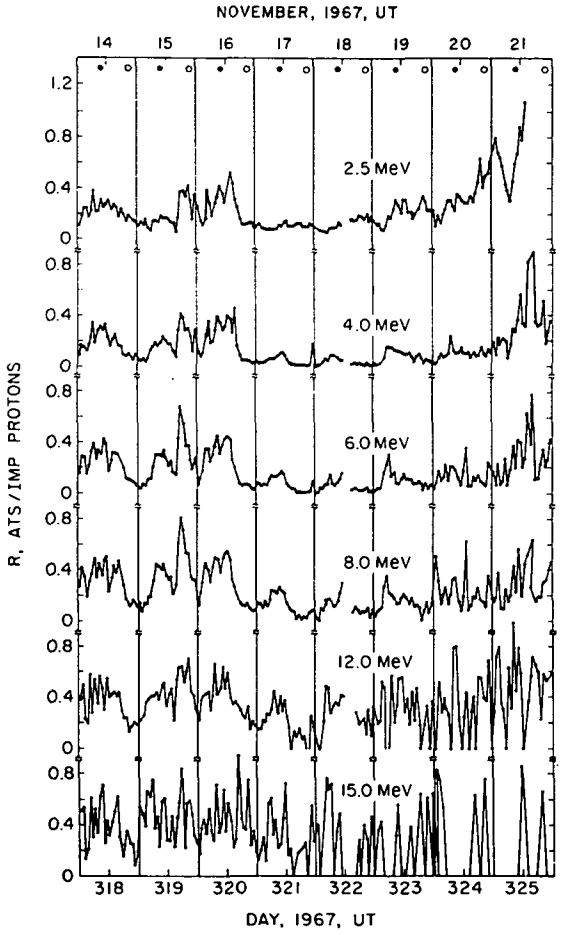


Fig. 11. Temporal plot of the ratio $R$ of the ATS-1 to Explorer 34 proton fluxes for a time period including the geomagnetically quiet period, days 321–324, 1967.

determined in this way that ATS was near $L \sim 6$ at local noon and near $L \sim 6.6$ at local midnight.

Using these results, a plot of $R$ as a function of $L$ is given in Figure 12 for four different proton energies. The radial gradient of the 2.5 MeV protons is constant over this $L$ range (as was evident from the data of Figures 3 and 11) while the fluxes of higher energy protons all increase at higher $L$-values. The largest radial gradients are observed in the highest energy fluxes. A similar result of a radial gradient increasing with $L$ was noted by Lanzerotti (1968b) for 2.4 MeV protons.

Plots of the ratio $R$ as a function of $K_p$ for 2.5 and 8.0 MeV protons during this period when $K_p \leqslant 1$ show no significant dependence of $R$ upon the value of $K_p$ (Figure 13). However, a striking temporal resemblance between the 2.5 MeV proton flux ratios and Dst during days 324–325 is observed in Figure 3. A plot of the quiet-time 2.5 MeV proton ratios and Dst in Figure 10b indicates an approximate linear

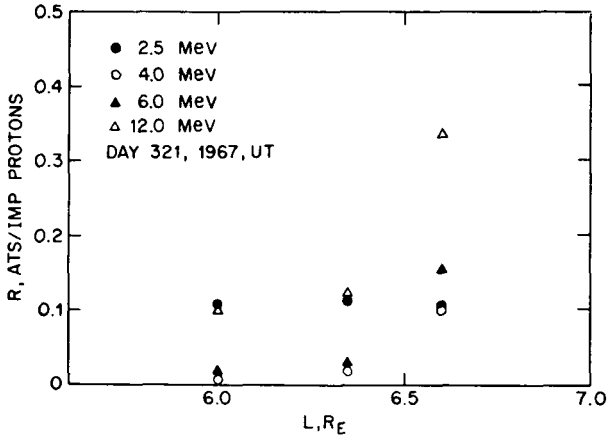


Fig. 12. Ratio $R$ as a function of $L$ for four different proton energies on the geomagnetically quiet day, day 321, 1967.

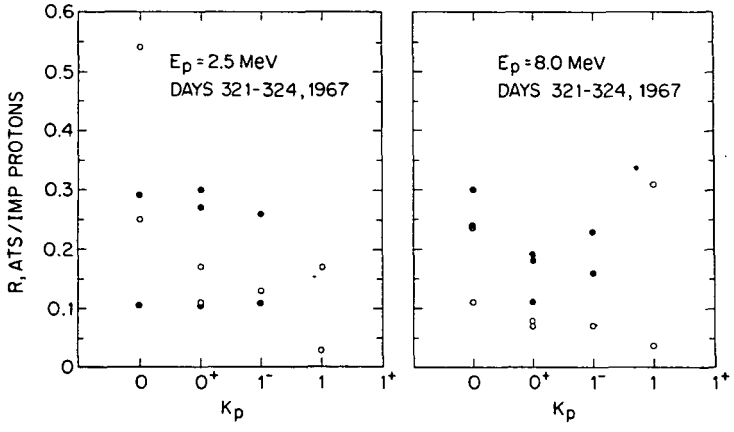


Fig. 13. $R$ as a function of the 3-hour average $K_p$ for 2.5 and 8.0 MeV protons – days 321–324, 1967. See caption of Figure 8 for time periods represented by open and closed circles.

relationship between $R$ and the magnitude of the Dst positive excursion, particularly for the hours around local noon (open circles).

### C. SOLAR PARTICLE ONSETS

It was quite evident from the data of Figure 1 that very frequently there is little or no delay between the observation of ~2 MeV solar protons in interplanetary space and their detection in the magnetosphere at synchronous altitude. Paulikas and Blake (1969) have also demonstrated this result for higher energy protons. Figure 14, taken from their paper, compares 21–70 MeV protons inside and outside the magnetosphere during the January, 1967, event.

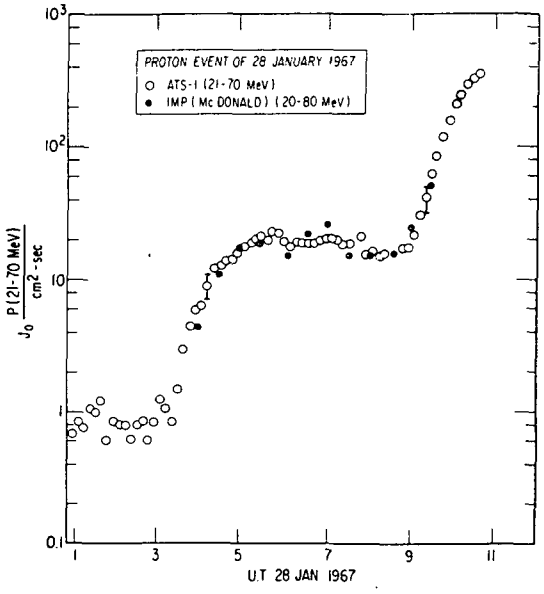


Fig. 14. 21–70 MeV protons observed at synchronous altitude and in interplanetary space on day 28, 1967. The $K_p$ indices for the half-day were 2, $4^-$, $4^-$, and $3^+$. (From Paulikas and Blake, 1969.)

However, Lanzerotti (1968b) and Lanzerotti *et al.* (1970), also observed events when there were substantial delays before the low energy interplanetary protons were initially seen inside the magnetosphere. Figure 15, reproduced from Lanzerotti (1968b) shows such a delay very clearly. Once the solar particles are finally observed at synchronous altitudes, however, their intensities increase very rapidly to values comparable to those of the interplanetary fluxes.

Figure 16 plots the onset times of the interplanetary and magnetosphere particles as a function of proton energy for the event shown in Figure 15. The onset times were determined using 10-minute average data and determining the first significant flux increase above the background statistical fluctuations. There is approximately a 7-hour time delay between the onset of the 800 keV protons inside and outside the magnetosphere. There also appears to be a small decrease of the access time delay

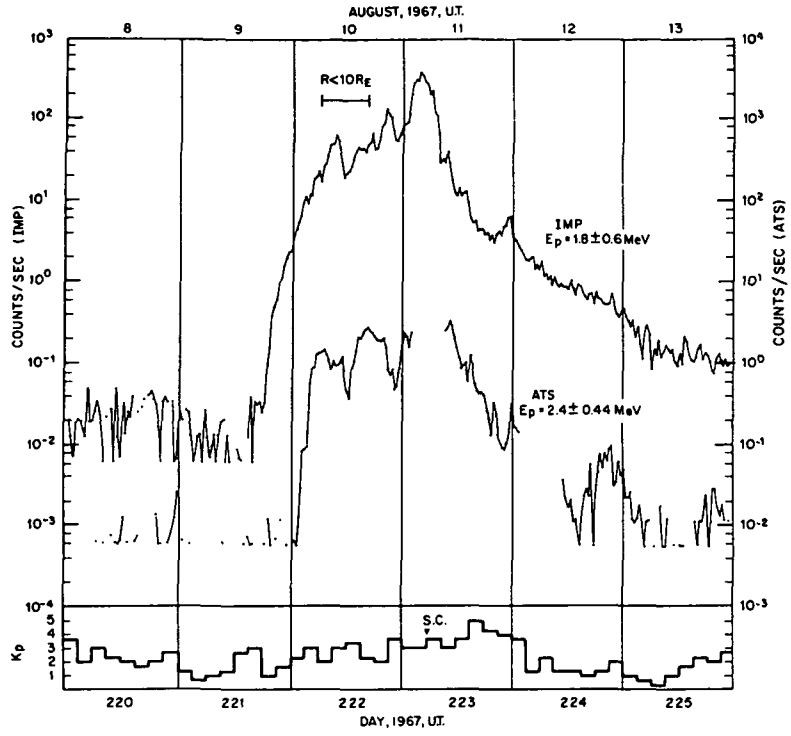


Fig. 15. Explorer 34 and ATS-1 proton fluxes during a solar event in August, 1967. (From Lanzerotti, 1968b.)

for the higher energy particles inside the magnetosphere with the 2.4 MeV protons being observed approximately 1½ hours before the 800 keV protons.

Although ATS magnetic field data were not available for this period, the measured ATS electron fluxes smoothly decreased in intensity during the first few hours of day 222, indicating a decrease in the local magnetic field intensity. Just after the first protons were observed, the electron fluxes decreased sharply, increased again, and were disturbed for the next hour to hour and one-half. The nature of these fluctuations in the electron flux intensities indicate fluctuations in the local magnetic field intensity (see Lanzerotti *et al.*, 1968, for a discussion of simultaneous field and particle changes). These disturbances of the local electron measurements indicate that the proton onsets were probably due to the onset of magnetosphere-wide disturbances. It is interesting to note, however, that the index AE had values of 350–400 during most of the first 4 hours of day 222 (when no solar particles were seen at ATS) and decreased to ~25 at ~0600 UT (when approximately full intensity solar fluxes were observed).

An investigation of all ATS particle data for days 27 and 28 and days 221 and 222, 1967, showed that the electron count fluctuations on days 27 and 28 were much more disturbed and had a much noisier character than did the electron fluxes on day 221 and the first few hours of day 222. This difference in the 'noisiness' of the electron

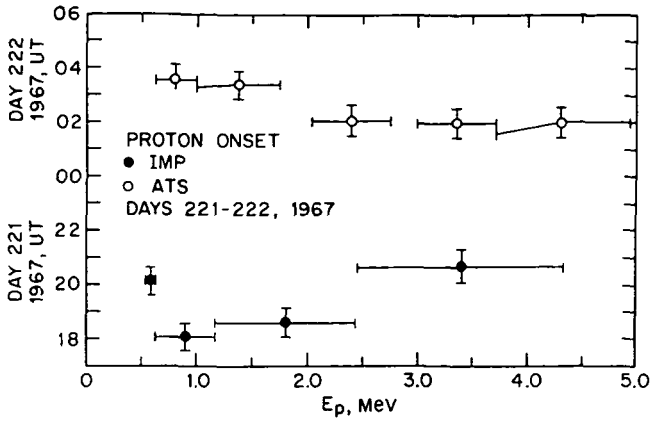


Fig. 16. Onset time as a function of proton energy for the interplanetary and synchronous altitude proton fluxes observed on days 221–222, 1967.

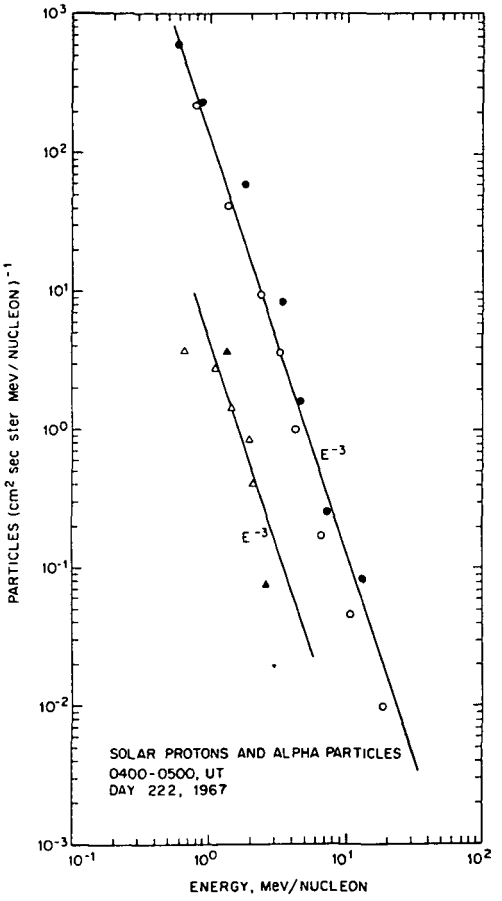


Fig. 17. Interplanetary and synchronous altitude proton and α spectra during hour 04, day 222, 1967. The circles denote protons; the triangles denote α-particles. Solid points are interplanetary fluxes; open points are magnetosphere fluxes.

fluxes undoubtedly reflects a basic difference in the intensity of disturbances in the outer magnetosphere. Outer magnetosphere disturbances such as those that produced the electron flux variations on days 27 and 28 undoubtedly control the initial and continued access of solar protons to the ATS orbit.

The interplanetary and magnetosphere proton and $\alpha$ spectra measured between 0400–0500 UT on day 222 are shown in Figure 17. These ATS data were measured only an hour after the first 800 keV protons were detected at synchronous altitudes. The spectra in Figure 17 very graphically show that shortly after the first magnetosphere particle onsets, the particle spectra inside and outside the magnetosphere are very similar.

## 5. Discussion

### A. MAGNETOSPHERE SHIELDING

The foregoing observations and results, comparing near 90° pitch angle proton fluxes at 6.6 $R_E$ geocentric radius to simultaneous measurements of interplanetary proton fluxes, indicate that solar protons generally have ready access to synchronous altitude. However, Figure 15 indicates that at times at the beginning of an interplanetary solar flux enhancement, the earth's magnetic field provides a very effective shield for several hours against the observation of near 90° pitch angle solar particles at the ATS altitude. Both of the 1967 solar enhancements in which significant synchronous altitude shielding was observed occurred following rather long periods of interplanetary quiet (Figure 15; Figure 19, below). Furthermore, as pointed out in the previous section, the absence of ATS electron flux variations prior to the day 221 proton enhancement suggested an absence of significant outer magnetosphere disturbances.

The extensive observations in Figure 1 indicate that there are at least moderately disturbed geomagnetic conditions during most of the time period accompanying the low energy solar particle enhancements. The geomagnetic activity is undoubtedly caused by the disturbed solar wind and interplanetary fields resulting from the energetic particle-producing solar processes. The proton 'shielding' observations in Figures 15 and 19, together with the geomagnetic disturbance observations in Figure 1, strongly suggest that the disturbances in the outer magnetosphere and/or the magnetotail provide the mechanisms for access of solar particles to synchronous altitude.

The 'shielding' observations at the onset of a solar particle enhancement which has occurred after a long period of interplanetary quiet suggest an important conjecture: there exists a 'quiet' state of the magnetosphere such that the trajectory calculations performed in realistic model magnetosphere geometries (using external fields as well as merely internal ones) in order to determine cutoffs for the low energy protons at the equator are perhaps valid. However, as was discussed, the magnetosphere is often disturbed by interplanetary processes accompanying or following the onset of solar flux enhancements. Thus, direct trajectory analyses that do not include outer zone noise and/or disturbances are probably unable to treat properly the problem of low energy solar particle access.

It is indeed interesting that during the 'quiet' geomagnetic period of days 321–324, although the fluxes observed inside the magnetosphere were low, they were non-zero. In fact, at the lowest energy, 2.5 MeV, the data suggest that the protons were stably trapped. The higher energy protons were also probably stably trapped (see next section). It is possible that the diffusion processes that move the interplanetary particles into the magnetosphere are still operative during a quiet period once protons have achieved access to the outer magnetosphere. Additionally, the proton loss processes may tend to zero intensity during a quiet period. It should be noted, however, that the radial gradient distributions of the higher energy protons were still opposite to those of the electrons, perhaps suggesting continued diffusion.

As has been pointed out by Lanzerotti (1968b), if solar protons can generally be found at synchronous altitudes during solar events, then they might be expected to be found everywhere in the outer magnetosphere, including the polar cap regions. Such a comparison has not been made. An important test of this hypothesis would be to compare polar cap and synchronous altitude data during a period when the magnetosphere is acting as a shield against the enhanced solar fluxes – such as day 222 (Figure 15) or day 261 (Figure 19, below).

### B. GEOMETRY OF ACCESS

Low energy protons mirroring near the equator at the ATS altitude are normally stably trapped in a standard magnetosphere (stand-off boundary distance of 10 $R_E$; tail field of 20 $\gamma$). This can be seen from the results in Figure 18 (computer program courtesy of J. G. Roederer). Plotted here are the tail field and boundary position limits so that 70° and 90° pitch angle protons detected at 6.6 $R_E$ altitude at local

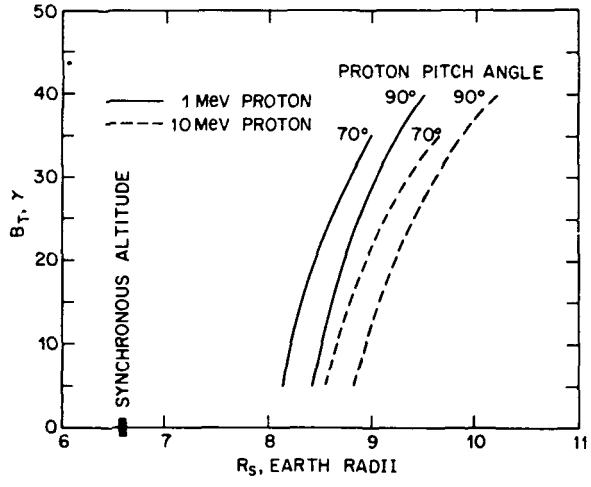


Fig. 18. Tail field ($B_T$) and stand-off boundary positions ($R_S$) as a function of proton energy and equatorial pitch angle such that a proton observed at local midnight would find the distant edge of its gyro-radius in the pseudo-trapping region. Magnetosphere parameters falling to the right and below a curve describe a magnetosphere configuration such that a proton with the given energy and pitch angle will complete a longitudinal drift period.

midnight would find the distant edge of their cyclotron orbits ($\sim 0.5\ R_E$ for a 1 MeV proton in a 50 $\gamma$ field) entering the pseudo-trapping region. Magnetosphere parameters falling to the right and below a curve in Figure 18 indicate that a proton with the given energy and pitch angle will complete a longitudinal drift period. If the magnetosphere configuration has parameters falling above and to the left of a curve, the proton will be lost out the dusk side of the magnetosphere.

The boundary and tail field limits on this plot seem merely to confirm the trajectory calculation findings that protons do not normally have access to the equatorial region of the magnetosphere at synchronous altitude. Some process must move their guiding centers by one or several gyro-radii in order that they be observed at the equator.

Theoretically, when the ATS satellite is at noon on the dayside, the cyclotron orbits of the near 90° pitch angle protons will not intersect a pseudo-trapping region during their longitudinal drifts. They will only become untrapped when the front boundary moves as close as one proton gyro radius to the satellite.

Smart *et al.* (1969), have recently shown, via trajectory calculations, that the vertically incident cut-off rigidities rapidly tend to zero for nightside latitudes in the region of the ATS field line. However, to get particles to mirror near the equator in order to be detected by the BTL ATS-1 experiment, scattering (or diffusion) of the pitch angles of the protons must take place. The means for accomplishing this is certainly not clear.

The question as to whether these solar particles are diffusing in everywhere across the magnetopause and/or through the magnetotail has not been satisfactorily answered yet. A recent paper by Williams and Bostrom (1969) suggested that the diffusion to synchronous altitude was predominantly via the neutral sheet and cusp region. This may indeed be a source for these particles. However, a recent data comparison by Lanzerotti *et al.* (1970), using ATS, IMP, and Vela magnetotail data has been made. Figure 19, taken from their paper, shows little relation between the Vela and ATS fluxes. However, a flux enhancement beginning at $\sim$1900 UT at ATS, approximately 2 hours following what appears to be the corresponding interplanetary enhancement, is scarcely seen at all in the magnetotail (at $\sim$1800 UT).

It was pointed out earlier that no modulations of the proton fluxes detected by the experiment on IMP F were generally observed as the satellite crossed the magnetopause. Although this might be expected because of the relatively large proton gyroradius, it is interesting that in the boundary crossing example shown in Figure 20 no diminution of the proton flux intensities is seen at $\sim 3.5\ R_E$ (2000 UT) inside the boundary at mid-latitudes. (The boundary crossing occurred at $\sim$1700–1710 UT.) In contrast, however, large, quasi-periodic fluctuations in the electron fluxes ($E_e > 0.44$ MeV) are observed for a substantial distance inside the magnetosphere boundary. The implications of these observations for particle access have not yet been fully explored. It should be pointed out, however, that the data of Lanzerotti *et al.* (1970), Figure 19, show appreciable fluxes of solar protons in the outer regions of the magnetosphere long before there are any fluxes of near 90° pitch angle protons at synchronous altitude.

Data presented by Armstrong *et al.* (1969), was purported to show the exclusion of 0.82–1.9 MeV solar protons from the "ordered magnetic field of the near ($\lesssim 8\ R_E$) magnetosphere" near the equator on July 13, 1966. Krimigis (1969) expanded on this observation and stated that this apparent exclusion of 0.82 MeV protons from the geomagnetic field close to the equator showed that the radiation belts could not be directly populated via the infusion of particles of comparable energy from solar particle events. Although it is difficult, from the data presented by Armstrong *et al.*

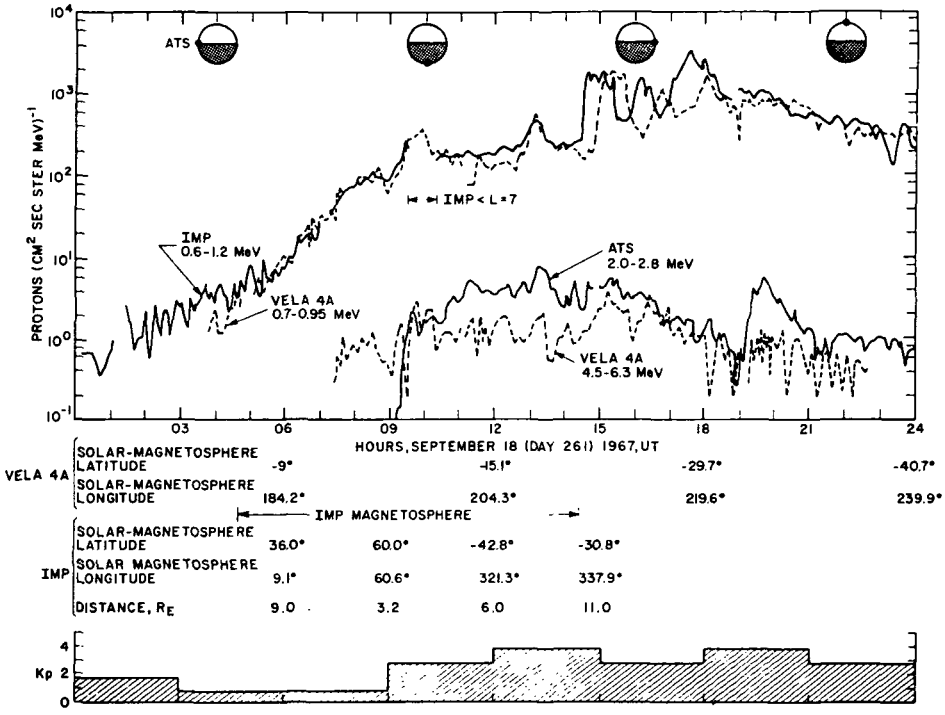


Fig. 19. Explorer 34, ATS-1 and Vela 4A magnetotail data during day 261, 1967. (From Lanzerotti *et al.*, 1970.)

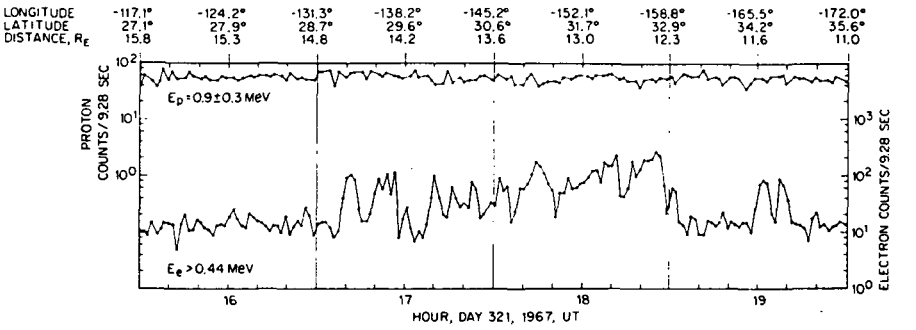


Fig. 20. Proton and electron data observed during the Explorer 34 magnetopause crossing (1700–1710 UT) on day 321, 1967. Geographic coordinates are shown above the data.

to tell when the magnetosphere boundary and trapping regions were entered, the data discussed here and presented by Lanzerotti (1968b) and Paulikas and Blake (1969) show conclusively that solar particles do frequently penetrate as deep as 6.6 $R_E$ into the magnetosphere. In fact, as seen from the data of Figure 1, the exceptions are quite infrequent. The question of populating the radiation belts by these protons is discussed briefly below.

### C. CONSEQUENCES OF SOLAR PARTICLES IN THE MAGNETOSPHERE

A recent paper by Lanzerotti *et al.* (1969b), described the observation of an occurrence of the drift mirror instability (Hasegawa, 1969) at synchronous altitude during a time period of enhanced solar fluxes inside the magnetosphere (day 177, 1967). It was suggested that substantial fluxes of 20–100 keV interplanetary protons having access to the synchronous altitude contributed to the occurrence of the instability. Figure 21, taken from their paper, shows electron and proton oscillations at synchronous altitude and electron heating during the period of occurrence of the instability. Their detailed analyses indicated that the protons and electrons oscillated out of phase and that the electrons oscillated in phase with the local ATS-1 magnetic field intensity.

The most detailed considerations of data in conjunction with Hasegawa's (1969) theoretical treatment of the drift mirror instability was an analysis of the April 18, 1965, magnetic storm observations of Brown *et al.* (1968). Lanzerotti *et al.* (1969) expressed the opinion that during this storm there was also evidence for enhanced interplanetary fluxes and that some evidence even existed for the observation of these protons at low latitudes in the magnetosphere.

There may be other significant consequences of the ready access of solar particles, not only to the equatorial regions but also in the polar and auroral regions. A recent paper by Haurwitz (1969) reported very sharp increases in AE at the time of large SSC storms when a polar cap event was in progress. She speculated that the low energy energetic storm particles that are present at the time of the SSC's are directly injected into the auroral zones via the magnetospheric tail and cause the bay activity. There were no large energetic storm particle enhancements at the times of the two sudden commencements of Figure 1. Furthermore, no large storm followed either SC, so that Haurwitz's conjectures could not be readily investigated.

One of the more interesting observations in the data of Figure 1 is that the synchronous altitude particle enhancements do not persist after the interplanetary particle source is gone. Hence, it is difficult to define or discuss a 'life-time' for these protons and $\alpha$'s in the outer zone. It was observed that during the 'quiet period', days 321–324 (Figures 3 and 11), the lowest energy protons appeared to have a diurnal distribution similar to the electrons. This could indicate that the proton loss processes were quite small. Lanzerotti (1968b) also noted a similar distribution for 2.4 MeV protons during a quiet time in June, 1967. It appears, however, that generally the disturbances in the outer magnetosphere are such as to cause continued losses of these protons so that no appreciable fluxes are trapped for any substantial length of time ($\sim$ 1 day).

The processes producing proton loss in the outer regions of the magnetosphere are unknown. The absence of a build-up of flux levels greater than the interplanetary fluxes at the ATS orbit suggests that there is a continual loss of protons back out of the magnetosphere during the period of an interplanetary enhancement. There is undoubtedly also a pitch angle scattering loss of these protons down the field lines. The lack of persistence of the synchronous altitude fluxes when the interplanetary source is gone suggests that 'back-diffusion' of the protons out of the magnetosphere is the predominant loss mechanism.

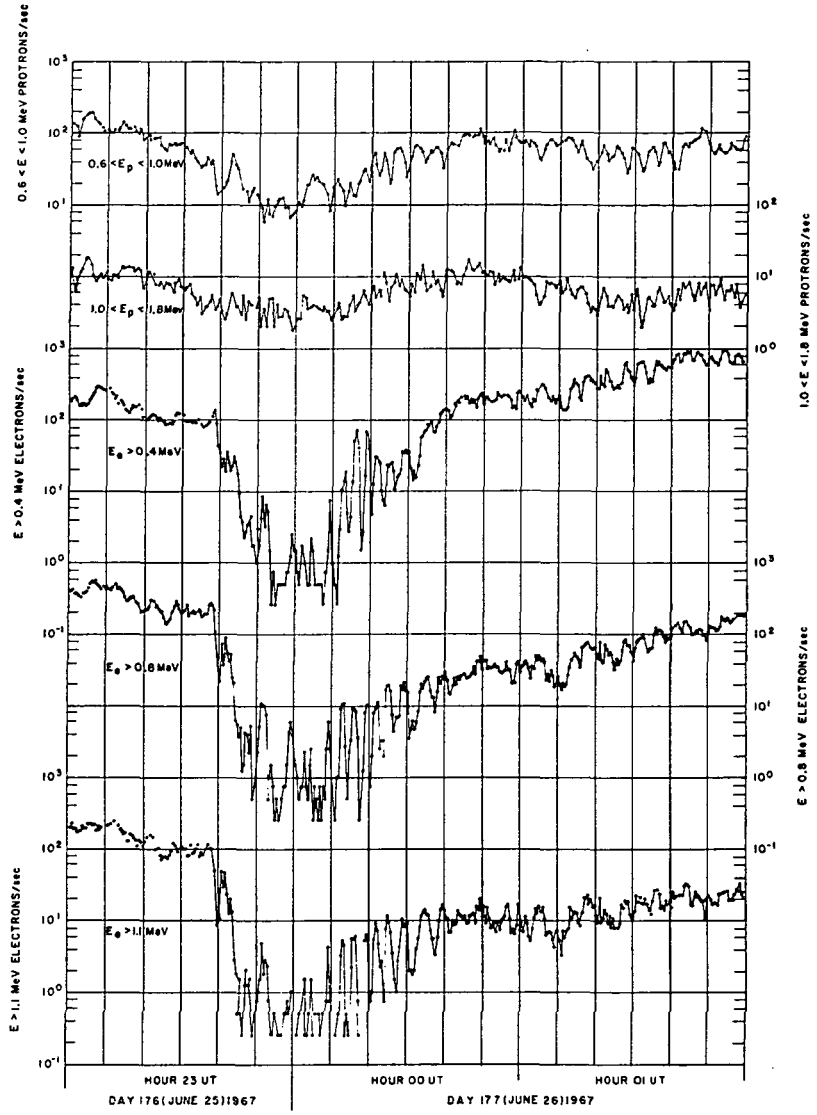


Fig. 21. ATS-1 proton and electron data showing anti-correlation of the proton and electron oscillations and simultaneous electron heating during the substorm on day 177, 1967. (From Lanzerotti *et al.*, 1969b.)

An interesting question that has not been answered yet concerns the possibility of a further diffusion of a small percentage of these solar protons deeper into the magnetosphere by the classic third-invariant violating diffusion mechanism first discussed by Kellog (1959). The population of the proton radiation belt by $L$-diffusion of protons from the magnetosphere boundary ($L=10\ R_E$) has been extensively discussed, for example, by Nakada *et al.* (1965), and Nakada and Mead (1965), and reviewed by Hess (1968). For equatorial particles, the calculational results of Nakada and Mead (1965) appear to be convincing that cross-$L$ diffusion of solar wind protons control the outer regions of the proton belt.

The possibility of partially populating the magnetosphere with these solar protons is nevertheless interesting. The most recent model of the 'inner belt' protons (Lavine and Vette, 1969) indicates an omni-directional equatorial proton flux ($E>4.0$ MeV) of $\sim 4\times 10^4$ protons$\cdot$(cm$^2$ sec)$^{-1}$ at $L=3$. Conserving the first adiabatic invariant of these equatorial particles yields a proton energy of $\sim 0.38$ MeV at $L=6.6$ (and $\sim 100$ keV at $L=10$). ($L=3$ was selected here since the extrapolation of the fluxes from the ATS-measured energy values to 0.38 MeV was not very large.)

It is quite reasonable to assume that 0.38 MeV protons had ready access to synchronous altitude during the moderate solar event of Figures 15 and 17. Hence, extrapolating the proton spectrum of Figure 17 to 0.38 MeV, assuming a uniform proton spectrum over all pitch angles, and integrating yields a flux of $\sim 6\times 10^3$ protons$\cdot$(cm$^2$ sec)$^{-1}$ for energies $>0.38$ MeV. A power-law spectrum remains a power-law with the same exponent during the $L$-drift. Thus, the proton fluxes from this event are $\sim 7$ times less than the $L=3$ population. The fluxes from one moderate event are obviously not enough to explain the entire $L=3$ population. However, with a large number of events (as in Figure 1), a portion of the quite stable inner proton belt population could be due to these solar energetic particles.

As pointed out by Brewer *et al.* (1969), the electron longitudinal dirft echoes observed by Lanzerotti *et al.* (1967), on ATS-1 are indications of magnetosphere boundary motions. These same boundary motions could cause the further inward radial diffusion of solar protons after their initial rapid entry to $L\sim 6$–7. Of course the same process should act to diffuse the $\alpha$-particles as well. The data have been searched, but no evidence for the longitudinal bunching of these protons at synchronous altitude during boundary disturbances have been observed. This negative result was also reported by Paulikas and Blake (1969).

## 6. Summary

The existence of low energy ($\sim$1–20 MeV) solar protons in the outer regions of the magnetosphere at synchronous altitude during interplanetary enhancements has been discussed and reviewed. The fluxes of the magnetosphere particles often exhibit diurnal variations, with fewer particles seen at local noon than at local midnight. The access of these particles is only weakly correlated with such indices of geomagnetic activity as AE, $K_p$, and Dst. Infrequently, large (several hour) time delays are

measured between the onset of the interplanetary and synchronous altitude enhancements. However, once access to 6.6 $R_E$ has been achieved, the magnetosphere fluxes increase rapidly to the interplanetary flux values. The access of the interplanetary particles to the magnetosphere is probably due to a rapid diffusion (scattering) of the protons across the magnetic field lines. The protons are probably incident both across the magnetopause and through the geomagnetic tail. Two observations of a plasma instability in the magnetosphere have been identified during periods of solar proton enhancements. It was speculated that a fraction of the interplanetary particles would be further diffused deeper into the magnetosphere to contribute to the trapped radiation belt population.


## Acknowledgements

I would like to thank Miss C. G. Maclennan for computational assistance. I would also like to thank Prof. P. J. Coleman and Mr. J. Barfield for use of their magnetic field data and Dr. W. L. Brown and Dr. G. A. Paulikas for numerous profitable discussions.


## References


Armstrong, T. P. and Krimigis, S. M.: 1968, *J. Geophys. Res.* **73**, 143.
Armstrong, T. P., Krimigis, S. M., and Van Allen, J. A.: 1969, *Annals IQSY* **3**, 313.
Bostrom, C. O.: 1970, this volume, p. 229.
Brewer, H. R., Schulz, M., and Eviatar, A.: 1969, *J. Geophys. Res.* **74**, 159.
Filius, R. W.: 1968, *Annals de Geophys.* **24**, 821.
Hasegawa, A.: 1969, *Phys. Fluids* **12**, 2642.
Haurwitz, M. W.: 1969, *J. Geophys. Res.* **74**, 2348.
Hess, W. N.: 1968, *The Radiation Belt and Magnetosphere*, Blaisdell Pub. Co., 213–241.
Hofmann, D. J. and Sauer, H. H.: 1968, *Space Sci. Rev.* **8**, 850.
Kellog, P. J.: 1959, *Nature* **183**, 1295.
Krimigis, S. M.: 1969, *Annals IQSY* **3**, 457.
Lanzerotti, L. J., Roberts, C. S., and Brown, W. L.: 1967, *J. Geophys. Res.* **72**, 5893.
Lanzerotti, L. J.: 1968a, *Nucl. Instr. and Methods* **61**, 99.
Lanzerotti, L. J.: 1968b, *Phys. Rev. Letters* **21**, 929.
Lanzerotti, L. J., Brown, W. L., and Roberts, C. S.: 1968, *J. Geophys. Res.* **73**, 5751.
Lanzerotti, L. J., Lie, H. P., and Miller, G. L.: 1969a, *IEEE Trans. Nucl. Sci.* **NS-16** (1), 343.
Lanzerotti, L. J., Hasegawa, A., and Maclennan, C. G.: 1969b, *J. Geophys. Res.* **74**, 5565.
Lanzerotti, L. J., Montgomery, M. D., and Singer, S.: 1970, *J. Geophys. Res.* **75**.
Lavine, J. P., and Vette, J. I.: 1969, *Models of the Trapped Radiation Environment*, Vol. 5: *Inner Belt Protons*, 15.
Leinbach, H.: 1967, *J. Geophys. Res.* **72**, 5473.
Nakada, M. P., Dungey, J. W., and Hess, W. N.: 1965, *J. Geophys. Res.* **70**, 3529.
Nakada, M. P., and Mead, G. D.: 1965, *J. Geophys. Res.* **70**, 4777.
Paulikas, G. A., Blake, J. B., Freden, S. C., and Imamoto, S. S.: 1968, *J. Geophys. Res.* **73**, 4915.
Paulikas, G. A., and Blake, J. B.: 1969, *J. Geophys. Res.* **74**, 2161.
Paulikas, G. A.: 1970, this volume, p. 193.
Roederer, J. G.: 1969, *Rev. Geophys.* **7**, 77.
Smart, D. F., Shea, M. A., and Gall, R.: 1969, *J. Geophys. Res.*, **74**.
Störmer, C.: 1955, *Polar Aurora*, Oxford University Press.
Williams, D. J., and Bostrom, C. O.: 1969, *J. Geophys. Res.* **74**, 3019.

N72-21837

# CHAPTER 6

## RAPID ACCESS OF SOLAR ELECTRONS TO THE POLAR CAPS

by

J. P. Turtle,[1] E. J. Oelbermann, Jr.,[2] J. B. Blake,[3]
L. J. Lanzerotti,[4] A. L. Vampola,[3] and G. K. Yates[1]

ABSTRACT

Simultaneous measurement of solar electrons and protons in interplanetary space and in the magnetotail were made during the onset of the 2 November 1969 solar particle event. These particle measurements, when compared with continuous trans-polar VLF measurements on three propagation paths, indicate the solar electrons have access to the magnetotail and north polar cap with a time delay $\tau$ such that $0 \lesssim \tau < 1$ min.

[1]Air Force Cambridge Research Laboratories, L. G. Hanscom Field, Bedford, Massachusetts.

[2]Ordnance Research Laboratory, Pennsylvania State University, University Park, Pennsylvania.

[3]Space Physics Laboratory, Aerospace Corporation, El Segundo, California.

[4]Bell Laboratories, Murray Hill, New Jersey.

## INTRODUCTION

The measured characteristics of the access of solar electrons to the magnetotail long have been attributed to direct coupling between the magnetotail field lines and the interplanetary field lines. Lin and Anderson (1966) observed five impulsive solar electron events within the magnetotail and compared their arrival times after the presumed originating solar flares with impulsive electron events observed outside the magnetosphere. On a statistical basis, they concluded that the delay for access to the magnetotail could be no more than 10 minutes, although it was consistent with zero. They placed an upper limit on the point of field line interconnection in the tail at ~5000 $R_E$.

*Portions of the data contained in this paper were originally presented by several of the authors individually at the COSPAR Symposium on the 2 November 1969 Solar Particle Event, Boston College, June, 1971.

[1]Air Force Cambridge Research Laboratories, L. G. Hanscom Field, Bedford, Massachusetts.

[2]Ordnance Research Laboratory, Pennsylvania State University, University Park, Pennsylvania.

[3]Space Physics Laboratory, Aerospace Corporation, El Segundo, California.

[4]Bell Laboratories, Murray Hill, New Jersey.

Van Allen (1970) observed an impulsive solar electron event on 14 August 1968 by instruments on two satellites, one outside the magnetosphere and one deep in the tail. He concluded that, since the access delay measured for the 50 keV electrons could not be more than 100 seconds, the inter-connection point could not have been further than 900 $R_E$ behind the earth. The studies of lunar shadowing of streaming solar electron fluxes in the magnetotail (Van Allen and Ness, 1969; Anderson and Lin, 1969) also indicated that the field inter-connection point was probably beyond the lunar orbit (~64 $R_E$).

Solar electrons have been measured over the polar caps and the latitude cutoffs studied (Vampola, 1969, 1971; McDiarmid and Burrows, 1970; McDiarmid et al., 1971). Detailed examination of solar electron spectra outside the magnetosphere and over the polar caps during the 12 April 1969 event indicated that uniform particle distributions were observed over both polar caps and that there was good tracking of the fluxes and spectra between the interplanetary region and both polar regions throughout the event (West and Vampola, 1971). In addition, an interplanetary field sector boundary crossing by the earth during the event did not produce any change in the polar cap fluxes. While the good tracking of the interplanetary and polar cap fluxes argue for the direct connection model, the fact that uniform, equal electron fluxes were seen at both polar caps and during a sector crossing argue against such a hypothesis unless the additional requirement is made that the interplanetary electron fluxes be isotropic. The measurements described above do not require direct connection, only rapid access.

Evidence for the occurrence of direct connection of the interplanetary field to the polar cap field, using protons as test particles, has been published by Van Allen et al., (1971). They demonstrated that intensity differences in the solar proton fluxes between the two polar caps during the solar particle event of 24 January 1969 can be related to the direction of the interplanetary field and the interplanetary particle anisotropies.

Further information on the arrival of solar particles to the polar regions could be obtained from the direct measurement of a solar event onset over the polar caps. As yet, a polar-orbiting satellite has not been properly situated during an event onset. In this report, trans-polar VLF signal changes during the onset of a solar event are compared to the arrival times of solar electrons and protons in interplanetary space and in the magnetotail. This comparison indicates that solar electrons were observed in the magnetotail and in interplanetary space at essentially the same time (within ~1 min.) as the onset of disturbance of the polar VLF paths.

## RESULTS

### (a) Interplanetary and Magnetotail Measurements

At the beginning of the 2 November 1969 event, solar particles were measured in the magnetotail and in interplanetary space by instrumentation carried on the Explorer 41 and OV5-6 (1969-46B) satellites, respectively. The OV5-6 instruments relevant to this discussion were a counter telescope sensitive to protons from 5.8 to 100 MeV and to electrons greater than 280 keV and two solar x-ray detectors. One x-ray sensor was an EON 6213 geiger tube also sensitive to electrons >45 keV and protons >700 keV; the other x-ray detector was a NaI scintillator with several channels of pulse height analysis. Of interest here is the fact that the latter sensor also monitored the omnidirectional fluxes of all protons >17 MeV. The BTL instrumentation on Explorer 41 measured spin-average proton fluxes from ~0.5 to ~20 MeV and electrons >350, >600, and >1000 keV (Lanzerotti et al., 1969). The locations of the satellites at 1100 UT, projected upon the ecliptic and noon-midnight meridian planes, are shown in an inset to Fig. 1. Explorer 41 had entered the distant magnetotail at ~0700 UT on a perigee pass which occurred at ~2230 UT. OV5-6 was almost at apogee at the onset of the solar particles at the earth.

Figure 1 indicates that the first particles from the flare were electrons (>45 keV) detected by OV5-6 at 1031:30± ~1 minute. Solar electrons ( >350 keV) were measured by Explorer 41 in the magnetotail at 1034:30 UT. Electrons >600 keV and >1000 keV were not observed by

Explorer 41 until ~1037 UT and ~1041 UT, respectively. Due to the background counts from a weak $Am^{241}$ calibration source in the OV5-6 instrument and the low sampling rate of ~once per 4 minutes, it is more difficult to determine a precise onset time for the >280 keV solar electrons in interplanetary space. However, Fig. 1 indicates that > 280 keV solar electrons were definitely seen by 1038:30 UT. Reasonable extrapolation of the enhanced fluxes measured by OV5-6 in Fig. 1 backwards in time indicates that the >280 keV solar electrons were first present in interplanetary space at ~1034±0001 UT. The onset times of the solar electrons as a function of particle energy are shown in a second inset to Fig. 1.

The proton data plotted in Fig. 1 indicate that 40-100 MeV protons were first seen in interplanetary space by OV5-6 at 1052:10 UT. Lower energy protons appeared later. The count rate of the x-ray scintillation counter, sensitive to all protons >17 MeV, did not rise above background until 1046 UT. Since this channel is also somewhat sensitive to relativistic electrons, it is not possible to say with certainty that the first protons arrived at 1046 UT; however, it can be stated definitely that no protons were present before 1046. Protons 17-20 MeV measured in the magnetotail by Explorer 41 were first observed at 1102 UT. The implications of the proton observations of OV5-6 and Explorer 41 for proton access to the magnetotail will be discussed in a future publication.

(b) Polar Cap Observations

The phase and amplitude of two trans-polar VLF paths were being monitored at Payerne, Switzerland before and during the solar particle

event: NPM (from Hawaii at 23.4 kHz) and NPG (from Seattle at 18.6 kHz). In addition, the phase of the signal from NPM was being monitored at the AFCRL Geopole Observatory at Thule, Greenland (Turtle and Oelbermann, 1971). The NPM-Thule path was in complete darkness at the time of the solar flare at 0939 UT and the ensuing solar x-ray enhancement at 0945 UT (Buckman and Lincoln, 1971). The sun was more than 16° below the horizon over the entire path length. At Payerne, Switzerland, the sun was 25° above the horizon so that the two trans-polar paths were only about 25% sunlit. In November the normal sunrise effects on the two trans-polar paths do not begin until after 1100 UT. Hence, all three paths can be considered to have been under nighttime conditions with the upper boundary of the VLF waveguide at an altitude of 85-90 km. Because the NPM - Thule path was in complete darkness, no sudden phase anomaly (SPA) at the time of the flare was detected. In addition, the two trans-polar paths showed no disturbance at this time, indicating that they were not sufficiently sunlit to be affected by solar x-rays. However, a typical SPA flare disturbance was recorded at 0946±0001 UT on the sunlit VLF path from NAA (Cutler, Maine at 17.8 kHz) to Tananarive, Malagasy (Reder and Westerlund, private communication, 1971).

The phase (in μsec) and the amplitude (in dB) measurements from the VLF paths discussed above are plotted in Fig. 2 for the period 0700-1400 UT. There clearly are no disturbances on the VLF paths from the solar flare in the interval starting at 0945 UT. The first disturbances on the VLF paths were recorded at 1032:30±30 sec when the amplitudes on both transpolar paths showed abrupt attenuation. These amplitude

effects were followed by sudden phase advances at 1034±30 sec UT on the NPM-Payerne path, at 1036±60 sec UT on the NPM-Thule path, and at 1039±30 sec UT on the NPG-Payerne path.

The VLF amplitude data for the interval 1020-1120 UT are shown on an expanded time scale in Fig. 3. Also indicated are the onset times of three of the electron channels and the earliest possible proton onset. The VLF disturbances were quite similar to those normally recorded at the onset of particle precipitation along VLF paths (e.g., Oelbermann, 1970). Protons can be ruled out as the cause of the VLF disturbances beginning after 1032 UT as they were not present before 1046 UT, at the earliest. X-rays could not have caused the VLF disturbances as lower latitude sunlit paths showed no additional disturbances at this time. In addition, the three paths (and particularly the NPM-Thule path) were not sufficiently sunlit to be affected by solar x-rays.

The VLF effects observed and illustrated in Figs. 2 and 3 are consistent with having been produced by the solar electrons detected by OV5-6 outside the magnetosphere and by Explorer 41 in the magnetotail. OV5-6 data show that electrons in the 45-300 keV range were present at 1031:30±1 min. The VLF amplitude disturbances began at 1032:30±30 sec. Both OV5-6 and Explorer 41 report electrons >300 KeV at about 1034 UT. Since 45 keV electrons produce their maximum number of ion pairs/$cm^3$ at about 90 km (Rees, 1963), electrons in the 45-300 keV range are capable of producing the observed VLF disturbances. The low counting rate and uncertain particle geometric factor of the x-ray sensor which detected the electrons with energies greater than 45 keV precludes making an

estimate of the VLF effects of the >45 keV electrons. However, such an estimate can be made for the >300 electrons. Explorer 41 measurements (Fig. 1) indicate that there were about 30±15 electrons/($cm^2$ sec ster) present in the magnetotail at 1034 UT. The number of 300 keV electrons required to produce a 1 μsec phase advance on the NPM-Thule path is about 1-5 electrons/($cm^2$ sec ster) (Zmuda, 1966; Potemra et al., 1969).

In order to produce the VLF disturbances these electrons must have been simultaneously present at D-region altitudes over the polar cap. Hence, within about one minute of their first observation, the interplanetary electrons had access to the magnetotail and to at least the northern polar cap.

An estimate of the latitude extent of the northern hemisphere electron precipitation at 1045 UT can be obtained by examining another low latitude path. The great circle path NPG-Payerne goes to 70°N geomagnetic while the path from the Omega Station at Aldra, Norway (10.2 kHz and 13.6 kHz) to Deal, N. J., goes only to 69°N geomagnetic. The NPG path was significantly disturbed at 1045 UT, while the Aldra path was not affected until about 1100 UT (Reder and Westerlund, private communication, 1971). It is evident that electrons must have been precipitating from a southern boundary of about 70° geomagnetic well up towards the pole. This observation was confirmed by measurements made aboard the polar satellite OV1-19 (1969-26C) beginning at 2130 UT on 2 November. Solar electrons were cut off at 70° or higher (depending upon local time); solar protons precipitated at substantially lower latitudes. The Aldra-New Jersey path was first affected at 1100 UT when significant fluxes of protons were beginning to be observed in the magnetotail.

## DISCUSSION

The first particles from the 2 November 1969 flare observed in interplanetary space near the earth were electrons and were recorded at ~1032 UT. These particles had access to the earth's magnetotail and northern polar cap essentially instantaneously; a maximum delay time of ~1 min for access to the tail and polar cap could be extracted from the set of particle and VLF observations. If it is assumed, as commonly is done, that the solar electrons had access to the polar regions via the tail, then a one-minute delay time would imply an access point into the tail at ~600 $R_E$ behind the earth. The observations are consistent with no delay for the northern polar cap access time implying possible direct entry of the electrons other than by entry downstream in the tail.

Interplanetary field directions near the earth are not available at the onset of the event. Neither are southern polar cap VLF propagation path data. However, polar cap electron and proton measurements beginning at ~2130 UT indicate that equal fluxes of solar electrons were observed over both northern and southern caps at that time while a large asymmetry was observed between the northern and southern polar cap porton fluxes (more protons seen in the north than in the south, Blake et al., 1970; Masley and Satterblom, 1970). The results of electron access presented here cannot argue definitively for the interconnection magnetosphere model but, taken together with the results of Blake et al., (1970) and West and Vampola (1971), they indicate that solar electrons apparently

have ready access to both polar caps independently of the interplanetary field configuration.

VLF propagation techniques provide a continuous ground-based monitor of D-region disturbances and as such can be used as a sensitive means of studying the question of the access of solar particles to high latitudes. To obtain more precise results than those presented here, interplanetary solar electron data are needed together with nighttime high latitude, trans-polar VLF paths with better time resolution.

## ACKNOWLEDGEMENTS

We would like to thank Dr. J. Rieker (Swiss Institute of Meteorology) for providing the Payerne VLF data. The work of two of the authors (J. B. Blake, A. L. Vampola) was performed under U. S. Air Force Space and Missile Systems Organization (SAMSO) Contract No. F04701-69-C-0066.

## REFERENCES


Anderson, K. A., and R. P. Lin, Observation of interplanetary field lines in the magnetotail, J. Geophys. Res., 74, 3453, 1969.

Blake, J. B., G. A. Paulikas, and A. L. Vampola, A compilation of the latitudinal profiles of solar protons and electrons over the polar caps during the event beginning 2 November 1969, EOS, Trans. Am. Geophys. Union, 51, 800, 1970.

Buchman, D. B., and J. V. Lincoln (ed.), University of Iowa Explorer 33 and 35 Data, World Data Center A Report UAG-13, May 1971.

Lanzerotti, L. J., H. P. Lie, and G. L. Miller, A solar cosmic ray particle spectrometer with on-board particle identification, IEEE Trans. Nucl. Sci., NS-16 (1), 343, 1969.

Lin, R. P., and K. A. Anderson, Evidence for connection of geomagnetic tail lines to the interplanetary field, J. Geophys. Res., 71, 4213, 1966.

Masley, A. J., and P. R. Satterblom, Observations during the 2 November 1969 solar cosmic ray event, EOS, Trans. Am. Geophys. Union, 51, 799, 1970.

McDiarmid, I. B., and J. R. Burrows, Latitude profiles of low-energy solar electrons, J. Geophys. Res., 75, 3910, 1970.

McDiarmid, I. B., J. R. Burrows, and M. D. Wilson, Structure observed in solar particle latitude profiles and its dependence on rigidity, J. Geophys. Res., 76, 227, 1971.

Oelbermann, E. J., Jr., Solar particle effects on polar cap VLF propagation, J. Franklin Inst., 290, 1970.

Potemra, T. A., A. J. Zmuda, C. R. Haave, and B. W. Shaw, VLF phase distrubances, HF absorption, and solar particle events of August 28 and September 2, 1966, J. Geophys. Res., 74, 6444, 1969.

Rees, M., Auroral Ionization and excitation by incident energetic electron, Planet. Sp. Sci., 11, 1209, 1963.

Turtle, J. P., and E. J. Oelbermann, Jr., Discussion of polar VLF and particle precipitation data for the 2 November 1969 solar particle event, Proc. COSPAR Symp. on November 1969 Solar Particle Event, to be published, 1971.

Vampola, A. L., Access of solar electrons to closed field lines, J. Geophys. Res., 76, 36, 1971.

Vampola, A. L., Energetic electrons at latitudes above the outer-zone cutoff, J. Geophys. Res., 74, 1254, 1969.

Van Allen, J. A., On the electric field in the earth's distant magnetotail, J. Geophys. Res., 75, 29, 1970.

Van Allen, J. A., J. F. Fennell, and N. F. Ness, Asymmetric access of solar protons to the earth's north and south polar caps, J. Geophys. Res., 76, 4262, 1971.

Van Allen, J. A., and N. F. Ness, Particle shadowing by the moon, J. Geophys. Res., 74, 71, 1969.

West, H. I., Jr., and A. L. Vampola, Simultaneous observation of solar flare electron spectra in interplanetary space and within the earth's magnetosphere, Phys. Rev. Letters, 26, 458, 1971.

Zmuda, A. J., Ionization enhancement from Van Allen electrons in the South Atlantic magnetic anomaly, J. Geophys. Res., 71, 1911, 1966.

## FIGURE CAPTIONS

Fig. 1. Solar flare particles measured in interplanetary space on OV5-6 and in the magnetotail on Explorer 41 during the onset of the 2 November 1969 event. Intensity vs. time curves are given for electrons and protons and the electron onset time as a function of energy. The positions of the OV5-6 and Explorer 41 spacecraft at 1100 UT on Day 306, 1969 are shown. Gaps in the lines connecting points are due to missing data.

Fig. 2. Real time VLF phase and amplitude records with disturbance and particle onset times, 2 November 1969.

Fig. 3. Expanded VLF amplitude records from Switzerland with particle onset times from OV5-6 and Explorer 41 data. The sharp break in the VLF curves at ~1032:30 UT indicates the onset of the VLF attenuation, 2 November 1969.

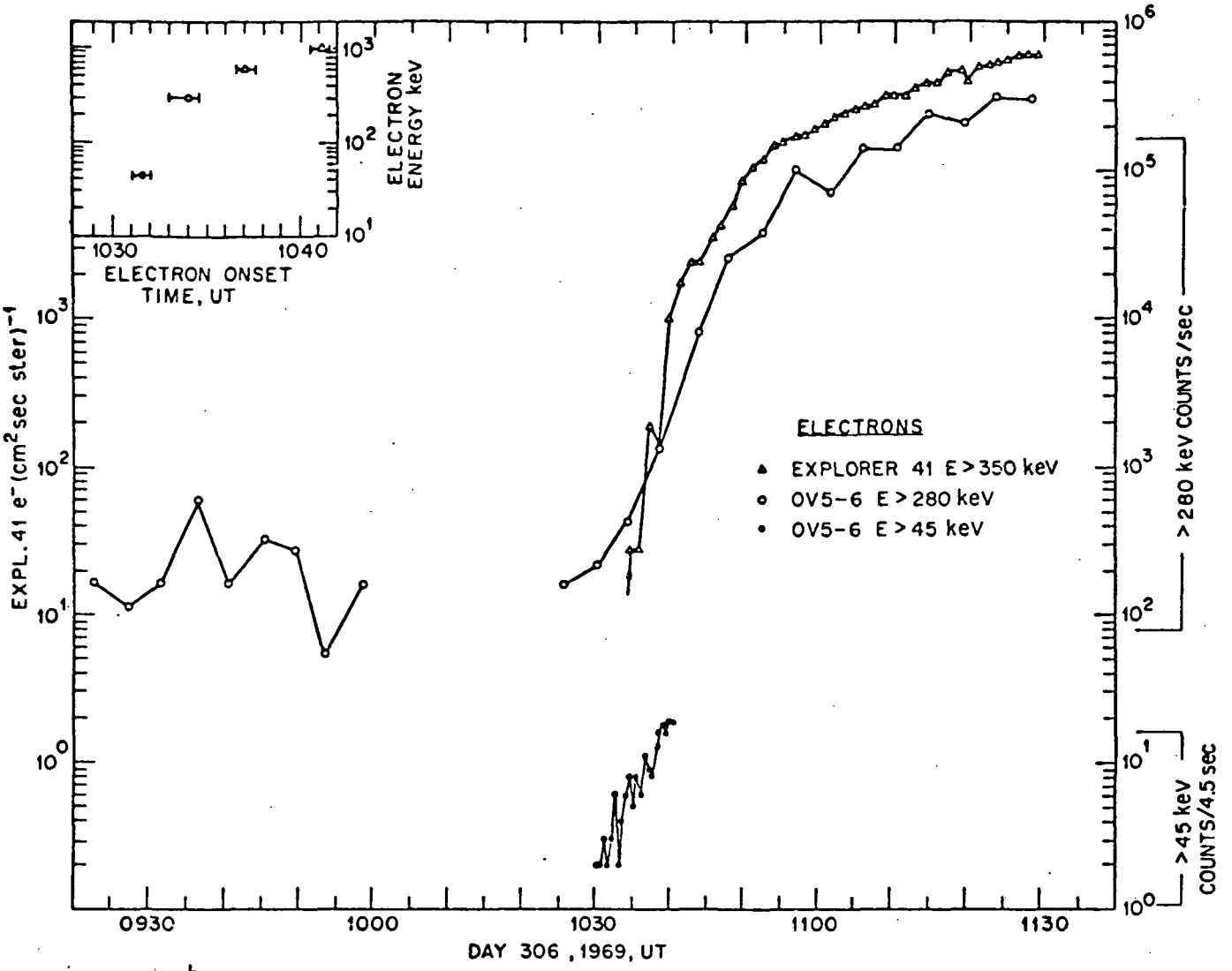
ELECTRON ONSET TIME, UT
1030
1040
ELECTRON ENERGY keV
EXPL. 41 e⁻ (cm² sec ster)⁻¹
ELECTRONS
EXPLORER 41 E > 350 keV
OV5-6 E > 280 keV
OV5-6 E > 45 keV
> 280 keV COUNTS/sec
> 45 keV COUNTS/4.5 sec
0930
1000
1030
1100
1130
DAY 306, 1969, UT

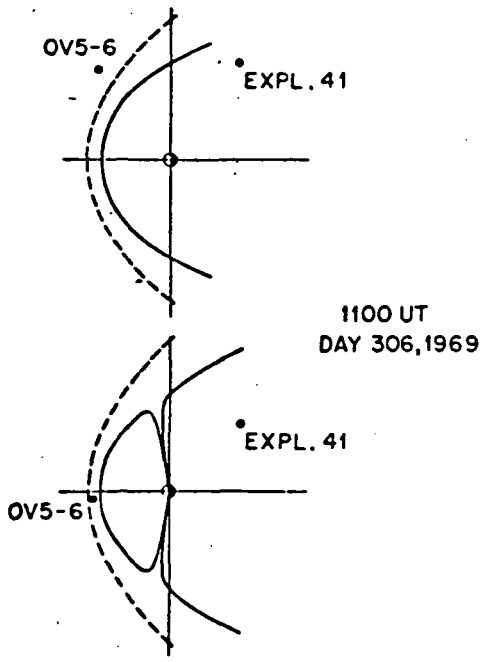
OV5-6
EXPL. 41
1100 UT
DAY 306, 1969
EXPL. 41
OV5-6

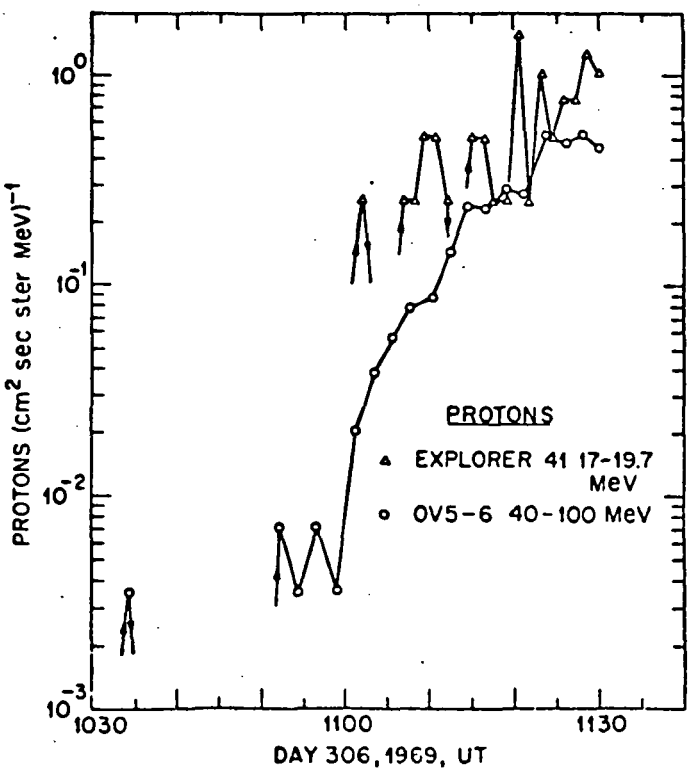
PROTONS (cm² sec ster MeV)⁻¹
PROTONS
EXPLORER 41 17-19.7 MeV
OV5-6 40-100 MeV
1030
1100
1130
DAY 306, 1969, UT

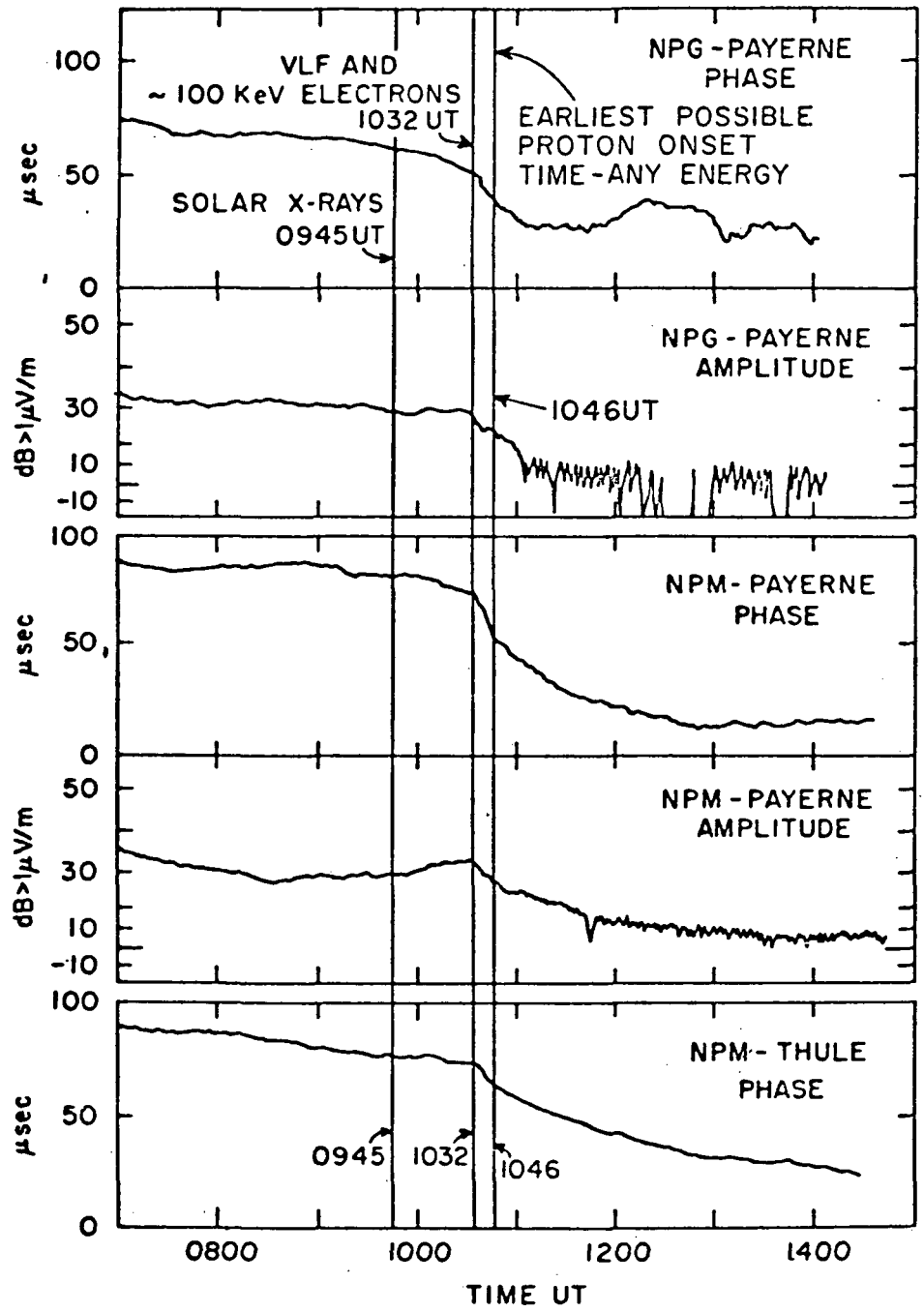
VLF AND
~ 100 KeV ELECTRONS
1032 UT
SOLAR X-RAYS
0945UT
NPG - PAYERNE
PHASE
EARLIEST POSSIBLE
PROTON ONSET
TIME - ANY ENERGY
NPG - PAYERNE
AMPLITUDE
1046UT
NPM - PAYERNE
PHASE
NPM - PAYERNE
AMPLITUDE
NPM - THULE
PHASE
0945
1032
1046
μsec
dB>1μV/m
100
50
0
30
10
-10
0800
1000
1200
1400
TIME UT

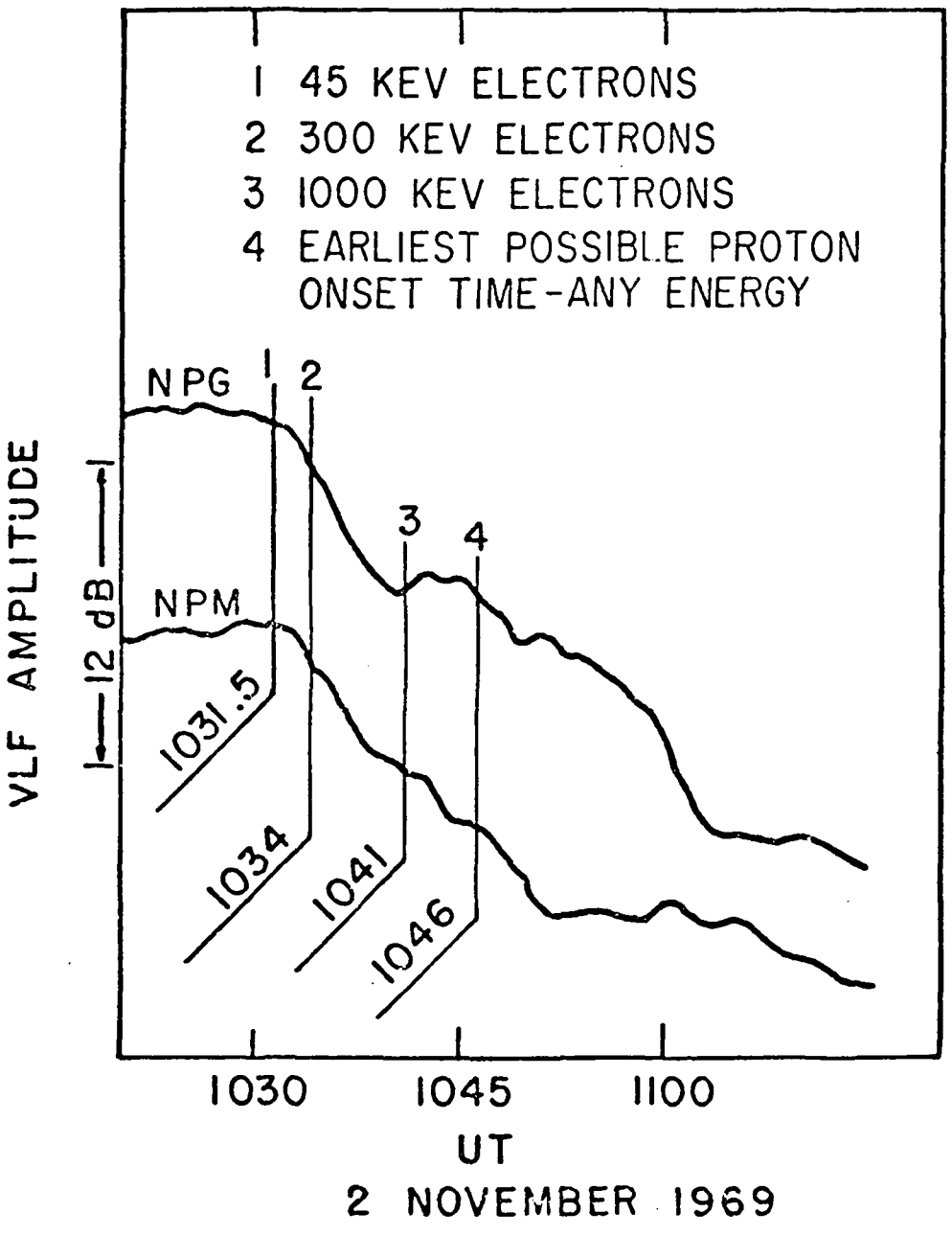
1 45 KEV ELECTRONS
2 300 KEV ELECTRONS
3 1000 KEV ELECTRONS
4 EARLIEST POSSIBLE PROTON ONSET TIME-ANY ENERGY
NPG
NPM
12 dB
VLF AMPLITUDE
1031.5
1034
1041
1046
1030
1045
1100
UT
2 NOVEMBER 1969

N72-21838

# CHAPTER 7

# Low-Energy Solar Protons and Alphas as Probes of the Interplanetary Medium: The May 28, 1967, Solar Event

L. J. LANZEROTTI

*Bell Telephone Laboratories*
*Murray Hill, New Jersey 07974*

The low-energy solar protons and alpha particles detected during the May 28 (day 148), 1967, solar flare are used as 'probes' to investigate the properties of the interplanetary medium during the course of the event. The lower energy fluxes exhibit characteristics of particle storage either at the sun or in interplanetary space. The higher energy particle fluxes exhibit 'classical' west limb flare profiles and are fit both to a simple isotropic diffusion-with-boundary model and to a radial dependent scattering center model. The diffusion coefficient model of Jokipii is used with the results of a fit to the exponential decay of the event to predict an $f^{-3}$ dependence of the power spectral density of the interplanetary magnetic field fluctuations (assuming a boundary location independent of rigidity). The ratio of particle fluxes before and after a sudden, discontinuous flux decrease (attributed to a sector boundary) is found to be $\sim R^3$ for protons and $\sim R^6$ for alphas for particles with rigidities $\lesssim$ 200 Mv. Significant velocity dispersions are discovered in three of the flux modulations during the onset stage of the event. The velocity dispersions in one of these modulations could be interpreted as due to a modulating region located ~0.03 AU from the earth. It is speculated that this region was responsible for an sc at the earth some two hours later.

## INTRODUCTION

Although many higher energy solar proton events can be described by invoking various diffusion models for the transport of these particles through interplanetary space [see, e.g., *Webber*, 1964; *Krimigis*, 1965; *Burlaga*, 1967] many events exhibit time variations that are quite complicated and are clearly not pure diffusion [see, e.g., *Bryant et al.*, 1963, 1965]. In particular, measurements of the fluxes of solar protons with energies $\gtrsim$ 0.5 Mev have shown the existence of temporal structures that are indeed very complex [*Fan et al.*, 1966*b*]. In the past, the discussions of solar particle diffusion have usually involved the correlation of a large number of high-energy observations resulting from different solar events [*Burlaga*, 1967] or the discussion of a single event for several different proton energies $\gtrsim$20–30 Mev [*Krimigis*, 1965]. No detailed studies have yet been reported on the characteristics of alpha particle propagation. Clearly, it is desirable to extend the investigations of solar particle propagation to lower energies and to study simultaneous proton and alpha observations in individual events.

The purpose of this paper is to examine the proton and alpha particle temporal development of the May 28 (day 148), 1967, west limb solar flare event as observed by the BTL experiment on the Explorer 34 (IMP F) satellite. The fluxes of higher energy particles from this flare exibit 'classical' west limb temporal profiles. However, the lower energy particle fluxes deviate appreciably from this classical behavior. The relatively high energy resolution and the unambiguous mass definition of the BTL Explorer 34 experiment permit a detailed discussion of the propagation of both protons and alphas from this flare. In addition, the fast time resolution of the experiment permits a more detailed examination of the temporal structure present in the lower energy channels.

The event, considered in its entirety, is discussed in the context of two simple particle diffusion models. The diffusion coefficient calculation of *Jokipii* [1966] is used in conjunction with the proton and alpha results to give a prediction of the frequency dependence of the power spectrum of the interplanetary field fluctuations encountered by the diffusing particles.

The rigidity dependence of proton and alpha diffusion across a corotation region boundary is investigated. The fine time structure features observed during both the onset and the decay of the event are discussed in terms of interplanetary plasma clouds or shock waves from the day 148 and earlier flares.

The day 148 3B flare (maximum intensity at 0545; class 4B at maximum) occurred in McMath plague region 8818 at heliographic latitude N28 and longitude W33. McMath region 8818 had been quite active from its first appearance on the east limb; a series of three east limb flares (27°–30°N, 25°–28°E) on May 23 produced the largest particle fluxes observed at earth (May 25) during the passage of the region [*Lanzerotti*, 1969]. The May 23 flare is believed to be the largest solar X-ray emitter yet observed [*Van Allen*, 1968] as well as one of the largest radio burst producers [*Castelli et al.*, 1968]. A detailed compilation of geophysical, solar, and some satellite measurements made during the May 23–30, 1967, period has been given by *Lindgren* [1968]. Riometer measurements made during the same time interval have been published by *Goedeke and Masley* [1969].

## Experiment

The Explorer 34 satellite, launched May 24, 1967, is a spin-stabilized (with spin axis perpendicular to the ecliptic plane) polar-orbiting satellite with an apogee of approximately 34 $R_E$. The BTL experiment consists of a four-element axially symmetric solid-state detector telescope (oriented perpendicular to the spin axis) and the associated electronics shown in block diagram in Figure 1.

The detector telescope is preceded by a defining collimator of 20° half-angle, which gives an effective geometrical solid angle of 0.37 ster. Titanium and nickel foils in front of the first detector serve as light shields and primarily determine the lower limits on the heavy particle energies that can be observed. The detector stack and collimator are housed in an aluminum shielding block that stops high-energy particles incident from the rear or sides of the telescope.

Protons and alphas up to an energy of approximately 4 Mev/nucleon are distinguished by the amount of energy deposited in the first two detectors of the telescope; heavy particle species above this energy are distinguished by the use of an on-board pulse multiplier. During each satellite telemetry sequence (10.227 sec) a particular set of coincidence requirements and pulse height and multiplier discrimination requirements is established among the pulses from the various detectors. If a particle event satisfying these conditions occurs during a 9.28-sec counting interval within the sequence period, the pulse heights from the detectors in coincidence are summed and analyzed in a five-channel

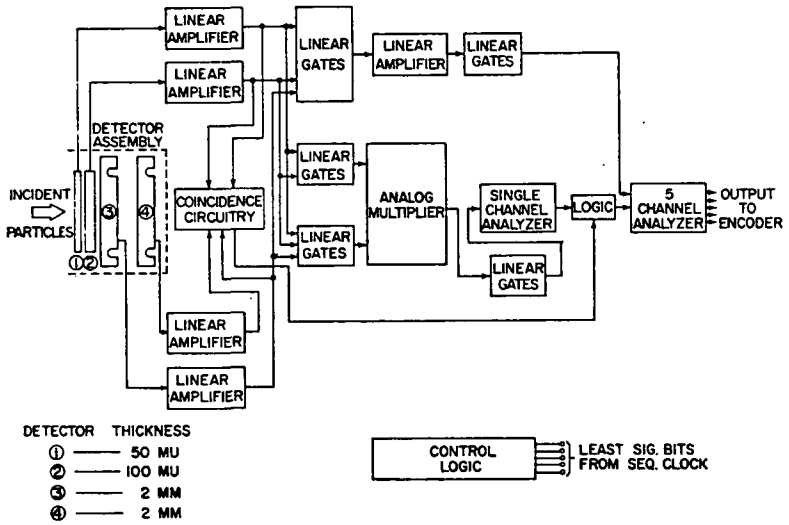


Fig. 1. Block diagram of the detector telescope and the electronics of the BTL Explorer 34 experiment.

pulse height analyzer. The digital data from the analyzer are read out at the end of each counting interval.

A list of the particle energy channels, their energy widths, and their average velocities for the particle modes discussed in this paper are given in Table 1. Further details on the experiment, its on-board particle identifier, and a discussion of the modes for counting other particle types are given in *Lanzerotti et al.* [1969]. The location of Explorer 34 with respect to the earth during the time periods discussed here are shown in perspective view in Figure 2.

## Results

The over-all characteristics of the May 28 solar particle event as observed at 1 AU can best be discussed by considering the half-hour averaged proton and alpha data obtained from the experiment and plotted in Figures 3*a*, *b*, and 4. Plotted at the bottom of each figure are the hourly neutron monitor counts from Alert (vertical cutoff = 0.00 Gv, atmospheric cutoff $\approx$ 1 Gv), the 30-MHz Shepherd Bay riometer absorption (A. J. Masley, personal communication), and *Kp*. The riometer absorption, for a falling spectrum, is most sensitive to protons in the 10–25 Mev range [*Adams and Masley*, 1966]. Both the riometer data and the higher energy proton data show the temporal characteristics of particles emitted from a west

TABLE 1

| Mode | Lower Energy, Mev | Upper Energy, Mev | Mean Velocity, AU/hr |
|---|---|---|---|
| | Protons | | |
| A1 | 0.56 | 0.60 | 0.25 |
| A2 | 0.60 | 1.18 | 0.31 |
| A3 | 1.18 | 2.45 | 0.45 |
| B3 | 2.45 | 4.3 | 0.61 |
| D1 | 4.3 | 5.0 | 0.72 |
| D2 | 5.0 | 9.4 | 0.89 |
| D3 | 9.4 | 17.3 | 1.22 |
| D4 | 17.3 | 18.9 | 1.39 |
| | Alphas | | |
| A4 | 4.05 | 6.6 | 0.38 |
| A5 | 6.6 | 8.8 | 0.47 |
| B5 | 8.8 | 11.4 | 0.54 |
| P3 | 16.3 | 24.0 | 0.74 |
| P4 | 24.0 | 45.9 | 0.99 |

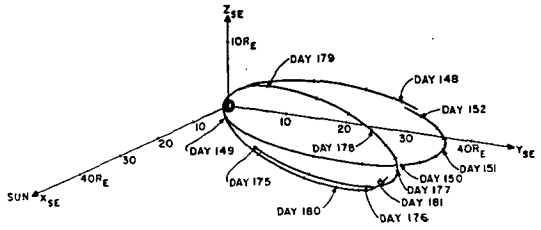


Fig. 2. Orbital locations of Explorer 34 (perspective view) during the periods of observation of the day 148, 1967, flare particles and their 27-day reappearance.

limb flare: a rapid rise to a maximum and then a steady decay (approximately exponential in this case for the particles). Owing to poorer statistics, this temporal history is more difficult to see in the alpha data.

In the lower energy proton and alpha channels the times of the peak fluxes after the particle onsets are much less well defined because of the considerable structure in the fluxes for almost half a day after the initial particle observations. In addition, rather than decaying, the protons in the lowest energy channels, Figure 3*a*, are observed to steadily increase throughout almost the entire event. After approximately the beginning of day 149 the proton spectrum becomes softer with time both because of the faster decay of the higher energy particles and because of the continued increase in the number of lower energy protons being observed.

An approximate anticorrelation between the lowest energy proton flux measurements and the Alert neutron monitor counts during the last quarter of day 148 and the first half of day 149 is observed in the data plotted in Figure 3*a*. The Alert neutron monitor rate (which is slowly recovering from a large Forbush decrease on day 145) is seen to decrease at the time of the large, low-energy proton fluxes during the latter part of day 148. During the first half of day 149, as the proton fluxes decrease, the neutron monitor rate increases sharply and then decreases again.

Both the neutron monitor rate and lowest energy proton fluxes continue to increase in intensity until approximately 0300 UT, day 150, when the proton fluxes begin to decrease. However, the neutron monitor counts continue to increase until approximately the time of the sudden commencement at 1426 UT day 150.

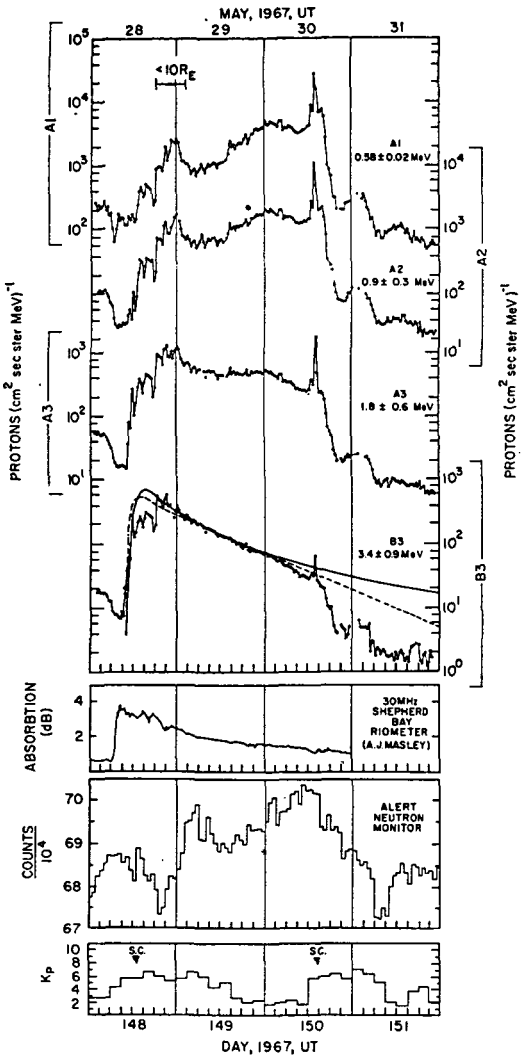


Fig. 3*a*. Half-hour averaged proton data from channels A1, A2, A3, and B3 (see Table 1) during days 148–151, 1967. The solid line and the dashed line through the B3 channel data are the fits of the radial dependent model and the diffusion-with-boundary model, respectively, to the data.

During the latter part of day 150, beginning at approximately 1700 UT, the proton and alpha fluxes are observed to decrease sharply over a time period of three to four hours. The decrease is much larger for the lowest energy particles than for the highest energy particles. During the four hours before the day 150 flux cutoff, at the approximate time of the sc and the neutron monitor count decrease, several large peaks are observed in the lowest energy channels (Figures 3*a*, *b*, and 4).

The gross temporal behavior of the Alert neutron monitor rate and the lower energy particle fluxes during the last half of day 148 and the first part of day 149 suggest that the lower energy particles from the 3B flare are

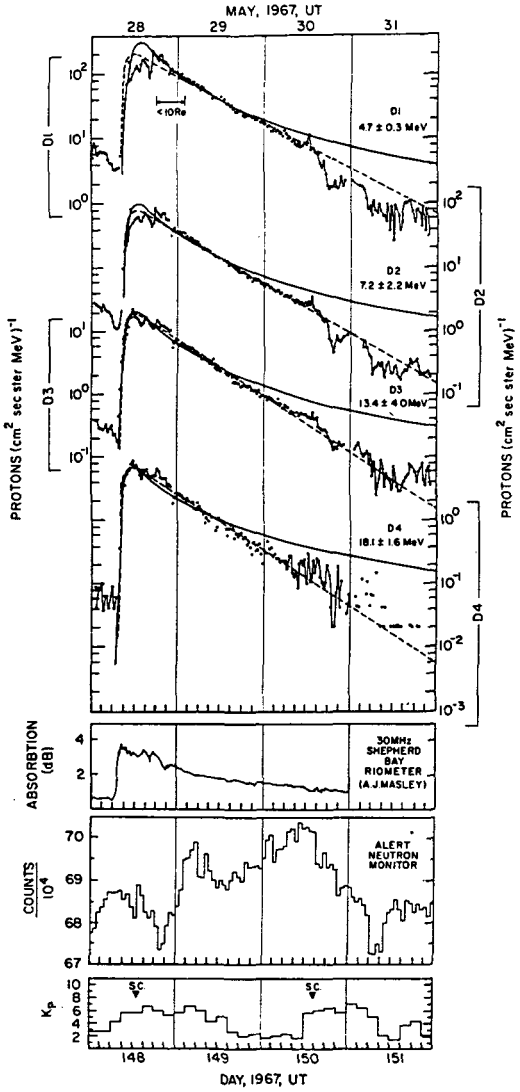


Fig. 3*b*. Half-hour averaged proton data from channels D1, D2, D3, and D4 (see Table 1) during days 148–151, 1967. The solid line and the dashed line through each set of data points are the fits of the radial dependent model and the diffusion-with-boundary model, respectively, to the data.

more easily confined behind or within an outward propagating shock or disturbance than the higher energy particles. This enhanced plasma cloud probably resulted from a flare on May 25 that occurred at approximately 1130 UT. Such enhancements of low-energy solar cosmic rays at the times of geomagnetic storms have been reported by a number of observers [e.g., *Axford and Reid*, 1962, 1963; *Bryant et al.*, 1962] and have been discussed most recently in a review by *Obayashi* [1967].

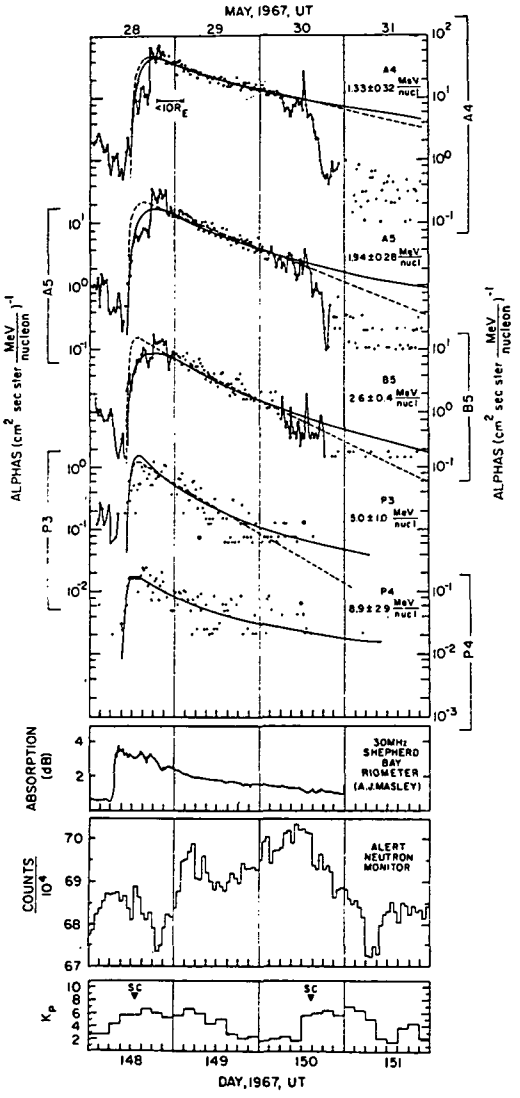


Fig. 4. Half-hour averaged alpha particle data from channels A4, A5, B5, P3, and P4 (see Table 1) during days 148–151, 1967. The solid lines and the dashed lines through each set of data points are the fits of the radial dependent model and the diffusion-with-boundary model, respectively, to the data.

Hence, during the latter half of day 148, as the interplanetary disturbance reaches the earth, it produces a sudden commencement storm and a decrease in the fluxes of very high energy galactic cosmic rays measured by the neutron monitor. The enhanced fluxes of lower energy solar particles, predominately confined behind or within the enhanced plasma cloud, is then observed.

As can be seen from Figures 3*a*, *b*, and 4, the higher energy solar particles are relatively unaffected by their passage through the interplanetary disturbance. As the disturbance passes beyond the earth, both the neutron monitor counts and the lower energy particle intensities increase. The flux of high energy galactic cosmic rays, measured by the neutron monitor, increases to a flux level greater than that observed before the day 148 decrease.

The large over-all drops in both the neutron counts and the flare particle intensities during the latter part of day 150 were probably not due solely to a plasma cloud disturbance from the day 148 flare reaching the earth. Rather, the data in Figures 3*a*, *b*, and 4 as well as the observed 27-day reappearance of the lower energy particles (as discussed more thoroughly in a following section), strongly suggest that an interplanetary magnetic field reversal moved past the earth; i.e., a solar sector boundary, inside which predominantly the lower energy protons were confined, rotated past the earth.

## Discussion

*Particle onsets.* The fast time resolution proton data measured in five representative proton channels during the onset at the earth of the solar flare-produced fluxes is shown in Figure 5. Plotted in the figure is each individual data point measured in the five channels during 0000 to 2000 UT, day 148. The modulations seen in the fluxes, particularly at the lower energies, will be discussed in detail in the next section.

By using all of the fast time resolution proton and alpha data the solar particle transit time from the day 148 maximum (0545 UT) as a function of energy/nucleon (or velocity)

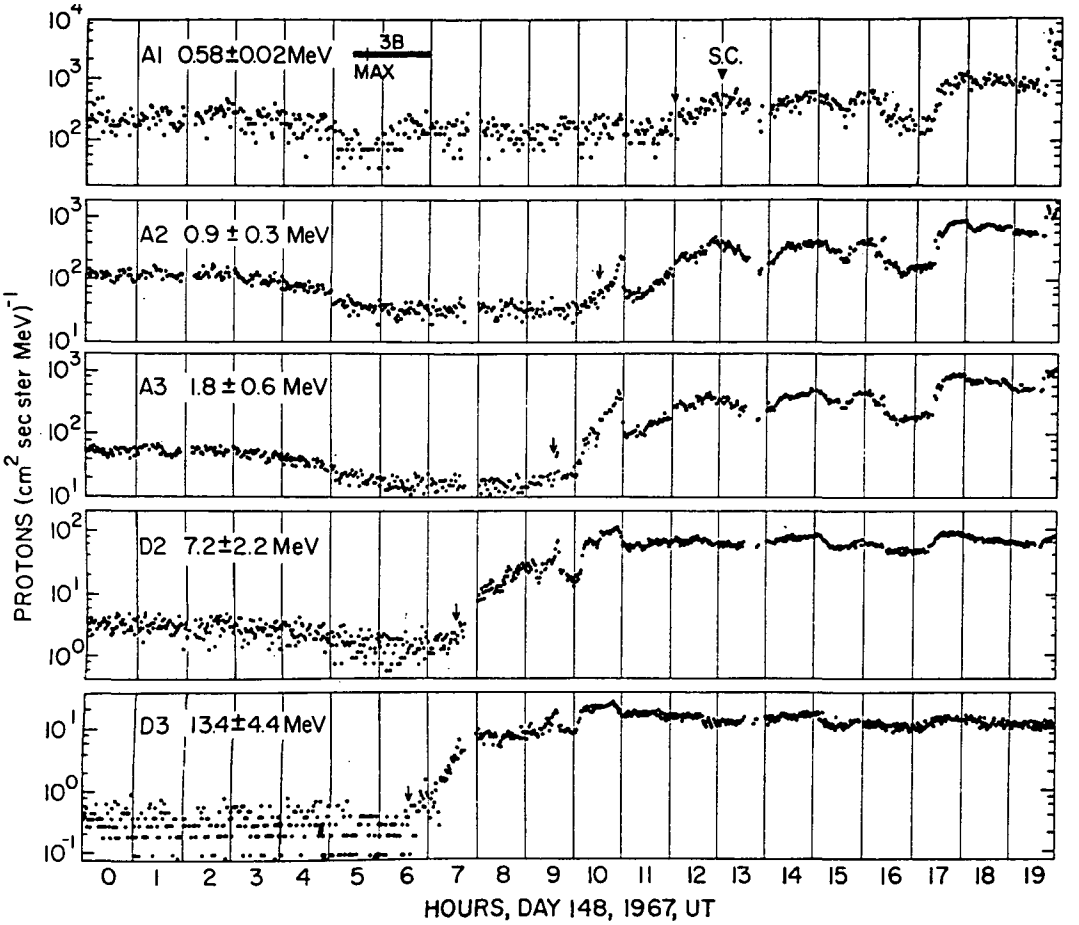


Fig. 5. Fast time resolution proton data from channels A1, A2, A3, D2, and D3 for hours 0000–2000 UT, day 148, 1967. Each data point corresponds to one 9.28-sec counting interval of the experiment. The small arrows indicate the time, $t_0$, of the first observation of the flare-enhanced fluxes. The time of observation of the 3B flare is noted at the top. The time of the maximum of the flare is denoted by the vertical line at 0545 UT.

is plotted in Figure 6. The solid lines are the predicted arrival time as a function of velocity for particles with pitch angles of 0° traveling along a spiral field trajectory for solar wind velocities of 250 km/sec and 500 km/sec and for rectilinear travel. A numerical integration of the transit time for 10-Mev particles with an initial pitch angle of 45° shows essentially no difference in the time of arrival at 1 AU of these particles and those of initial 0° pitch angle [*Winge and Coleman*, 1968]. The observed onset time of the absorption measured by the 30-MHz Shepherd Bay riometer is also shown in Figure 6 (A. J. Masley, personal communication).

The measured arrival times tend to agree better with the predictions for a 250-km/sec solar wind than for a 500-km/sec solar wind. However, solar wind velocities as small as this are only infrequently observed [*Coon*, 1968]. A mean velocity of 420 km/sec and a most probable velocity of 325 km/sec was observed in 1964–1965, near the minimum of the solar cycle [*Coon*, 1968]. During a more active part of the solar cycle in 1962, *Neugebauer and Snyder* [1966] measured a mean solar wind velocity of 504 km/sec.

These observations suggest that some type of confinement of these particles is occurring near the sun. However, due to the probably

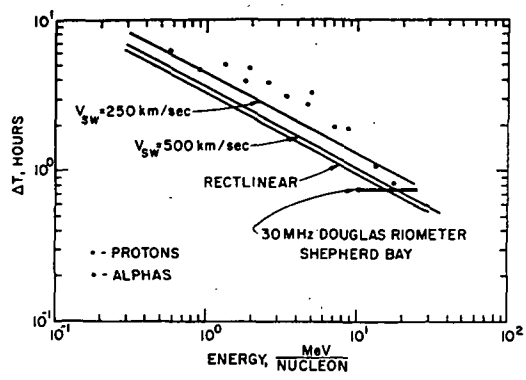


Fig. 6. Solar particle transit time from the day 148 flare maximum (0545 UT) as a function of particle energy/nucleon. The solid lines indicate, for 0° pitch-angle particles, the travel time along a spiral field trajectory for solar wind velocities of 250 km/sec and 500 km/sec and for rectilinear travel.

disturbed nature of the interplanetary medium at least until day 149, it would be exceedingly difficult at this stage of understanding to definitively unravel any confinement by an outward-propagating interplanetary disturbance (as discussed in the previous section) from a confinement closer to the sun.

*Particle modulations.* A close inspection of the fast time resolution proton data, both those channels shown in Figure 5 and those energy channels not shown, reveals that a significant velocity dispersion exists in the time of occurrence of several of the modulations during the particle flux onsets. A cross-correlation analysis was performed on a number of pairs of proton energy channels to investigate the velocity dispersion in detail. The time leads (or lags) resulting from such an analysis between energy channels D2-A2 and D3-A3 for each half-hour interval of data between 0800 and 2000 UT are shown in Figure 7.

The time lag point for the 1230–1300 UT interval in Figure 7 results from the fact that the A2 counting rate was increasing sharply while the D2 rate was decreasing slightly during the interval. Neglecting this point, Figure 7 indicates that significant velocity dispersions were observed in the modulations during parts of hour 10 and during the period 1730–1800 UT. Cross-correlation analyses showed little or no velocity dispersions during 1000–1030 UT between most pairs of proton channels. This, together with the small time values shown in Figure 8, is interpreted as due to a modulating source very close to the satellite. No dispersion was observed between channels D3-A3 between 1730 and 1800 UT because almost no modulation was measured in the D3 fluxes (Figure 5).

The large flux increases and decreases before and after hour 1100 were investigated in detail by taking the cross correlation between six different pairs of energy channels from 1040 to 1105 UT. The results, shown in Figure 8, demonstrate that there is a shift of the correlation peaks to larger lead times for larger energy differences between the paired channels. Figure 9 is a summary plot of the Figure 8 peak positions plotted as a function of the velocity difference between the average velocity of each channel of the paired channels. A possible interpretation of the slope of the line, drawn visually through the points and zero, is that the region producing the modulation is located approximately 0.03 AU from the earth at this time. Note that no disturbance is seen in the lowest, A1, energy channel (Figure 5), presumably because these energy flare particles have not yet had sufficient time to travel from the sun to the modulating region (Figure 6).

It is interesting to speculate that the disturbance that caused the sharp particle decreases at

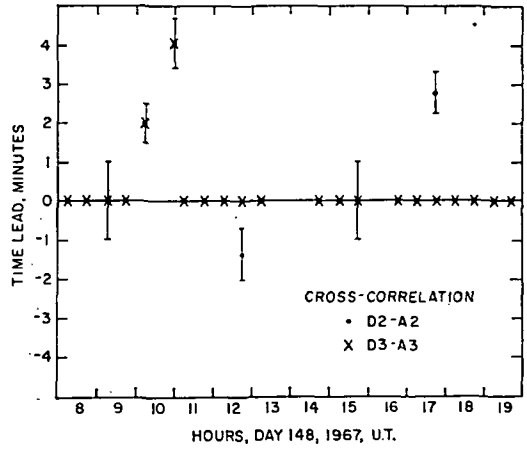


Fig. 7. Results of cross-correlation analyses on the channel pairs D2-A2 and D3-A3 for each half hour of fast time resolution data (see Figure 5) from 0800–2000 UT. The errors on all of the points lying along the abscissa are ±1 min.

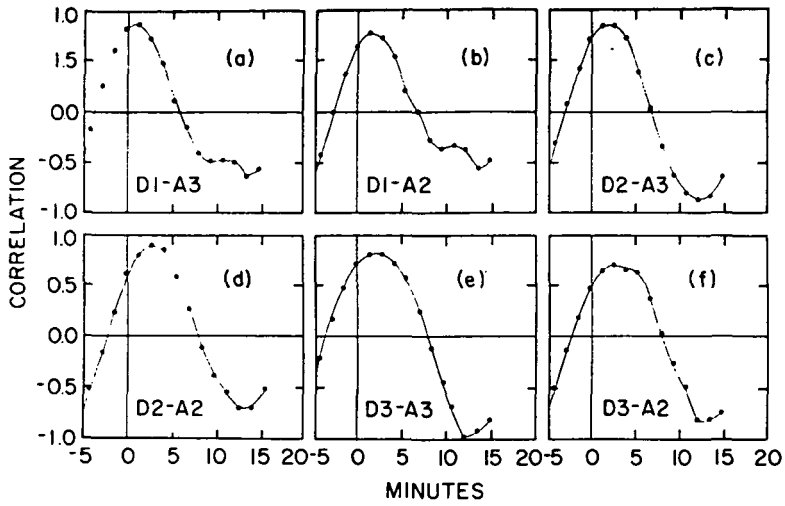


Fig. 8. Results of cross-correlation analyses on six different pairs of proton channels for the interval 1040–1105 UT.

~1050 UT is also associated with the shock that produced the sc observed on earth at 1302 UT. If this is indeed the case, then the velocity of the shock, taking its distance at 1050 UT to be ~0.03 AU would be ~500–600 km/sec. This is not an unreasonable velocity for the solar wind flow during a period of solar activity.

The interplanetary particle fluxes are not significantly perturbed at the time of the 1302 UT sc although the lower energy fluxes do tend to steadily decrease during the remainder of hour 13 (Figure 5). Hence, if the disturbance

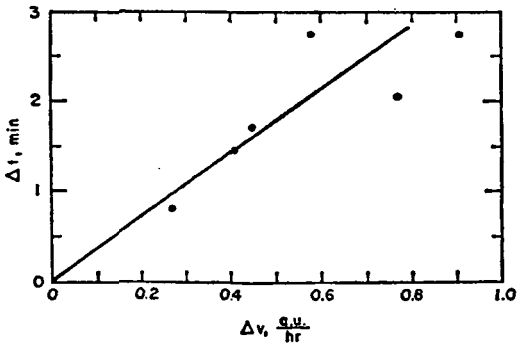


Fig. 9. The peak positions from the data of Figure 8 plotted as a function of the velocity difference between the channels (Table 1). The line is drawn visually through the points and the origin.

that perturbed the particles between 1040 and 1105 UT developed momentarily in a region of larger solar wind density or momentum flux, it may no longer have existed at the time of the sc, even though the enhanced momentum flux would still exist and produce the sc. These observations strongly suggest, therefore, that a disturbance that modulated the lower energy particle fluxes developed in the enhanced solar wind flux quite close to the earth. The shock region in which the disturbance occurred propagated at 500–600 km/sec past the earth, producing an sc at 1302 UT.

Much broader cross-correlation results, shown in Figure 10, are obtained when the modulations between 1600 and 1815 UT are investigated. Essentially no velocity dispersions are observed in the 1600–1700 UT interval, whereas very broad 'peaks' are obtained from correlations over the entire 1600–1815 UT interval. Plotted in Figure 11 are the peak positions resulting from the cross-correlation analyses of six different energy channel pairs for the 1700–1815 UT time interval (the middle correlations in Figure 10 are two examples of these). Again a line was drawn visually through the data points and zero. The slope of this line implies that the disturbance producing the modulation is ~0.12 AU from the earth.

Although there is no doubt as to the actual existence of velocity dispersions in the modula-

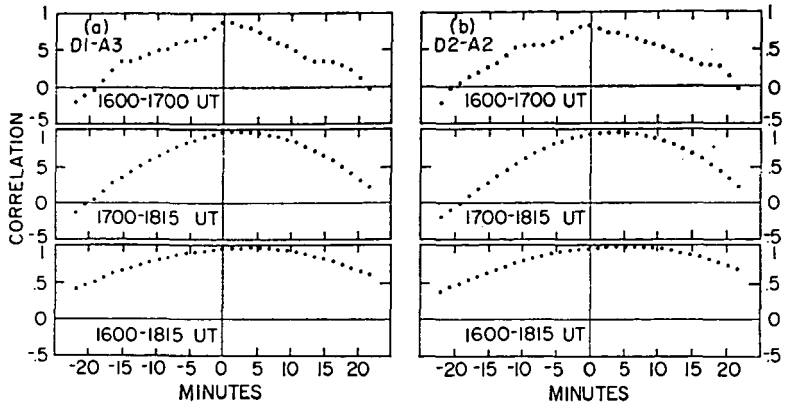


Fig. 10. Results of cross-correlation analyses on two different pairs of proton channels for the intervals 1600–1700 UT, 1700–1815 UT, and 1600–1815 UT, day 148.

tions, a completely unambiguous interpretation of these dispersions may be clouded somewhat by the proximity of Explorer 34 to the magnetopause. The satellite was ~17.5 $R_E$ from the center of the earth at the time of the large 1050 UT modulations and was ~10 $R_E$ from the center of the earth at the time of the 1700–1815 UT modulations. It is difficult to conceive of a particle-boundary interaction mechanism that could produce the type of time dispersions summarized in Figures 9 and 11. Nevertheless, the proximity of the satellite to the magnetopause must be kept in mind, particularly when the hour 1700 modulations are being considered.

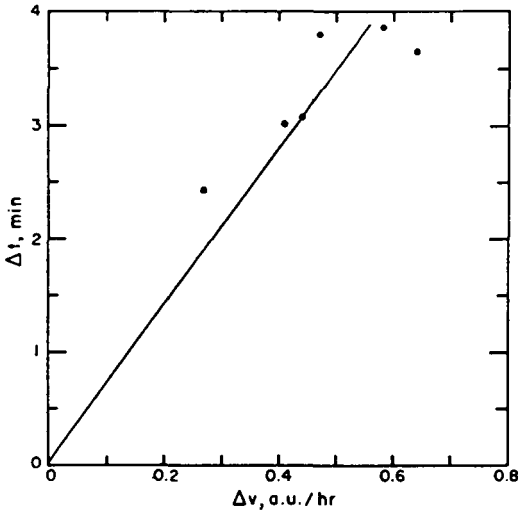


Fig. 11. The peak positions from the results of cross-correlation analyses on six different pairs of proton channels for the interval 1700–1815 UT plotted as a function of the velocity differences between the channels. The line is drawn visually through the points and the origin.

*Particle diffusion.* The rise and subsequent approximately exponential decay of the proton intensities observed in the five highest energy proton channels (Figures 3*a*, *b*) and several of the alpha channels (Figure 4) suggest that simple isotropic diffusion theory might give a useful quantitative determination of the similarities and differences of the proton and alpha particle interplanetary propagation characteristics. This simple theory was thus used to make clearer the alpha and proton fluxes temporal development and to make more striking the deviations from the simple theory, particularly at the lowest energies.

Accordingly, the half-hour average solar flare particle data of Figures 3 and 4 were fit assuming a model of isotropic diffusion into a uniform scattering medium with a boundary [*Parker*, 1963]

$$F(r, t) = \frac{2\pi N}{r_b^2 r} \sum_{n=1}^{\infty} n \sin\left(\frac{n\pi r}{r_b}\right) \cdot \exp\left(\frac{-n^2\pi^2 Dt}{r_b^2}\right) \quad (1)$$

where $r_b$ is the boundary radius and $D$ is the diffusion coefficient. This diffusion model immediately yields an exponential decay for $t \gg r_b^2/D$. The proton and alpha data in each channel were fit, varying $r_b$ and $D$, from the onset time of each channel (as determined from the fast time resolution data, Figure 5) to hour

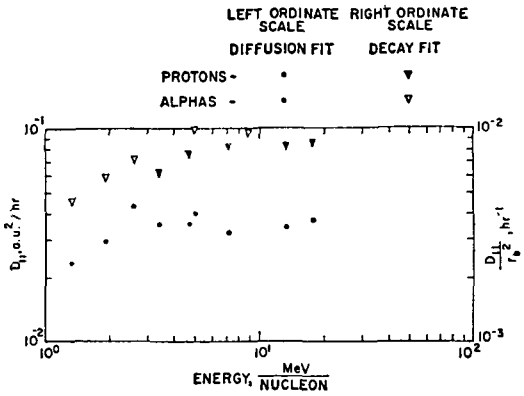


Fig. 12. Values of the diffusion coefficient, $D_{\parallel}$, and the ratio $D_{\parallel}/r_b^2$ obtained from the diffusion-with-boundary model and an exponential fit to the decay data plotted as a function of the particle energy/nucleon.

1100 day 148 and from day 149 to day 150.5. Omitted was the approximately half-day of data during the most severe modulations. The results of the diffusion with boundary fits are shown superimposed upon the data (dashed lines) in Figures 3*a*, *b*, and 4; the values of $D$ obtained from the boundary fit are shown in Figure 12. No satisfactory fit was obtained for the P4 alpha particle channel (Figure 4). The variation of the boundary distance, $r_b$, resulting from the fit of equation 1 to the data in Figures 3*a*, *b*, and 4 is shown in Figure 13.

The data from day 149.0 to day 150.5 was also fit to an exponential decay to give an independent determination of the ratio $D/r_b^2$. This ratio is also plotted in Figure 12.

A fit was also made to the data of Figures 3*a*, *b*, and 4 using a model with a radial spatial

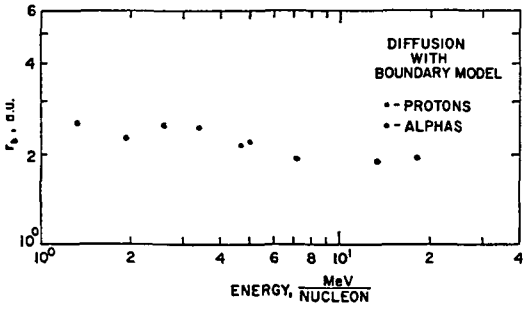


Fig. 13. Plot of the boundary distance, $r_b$, obtained from the diffusion-with-boundary model.

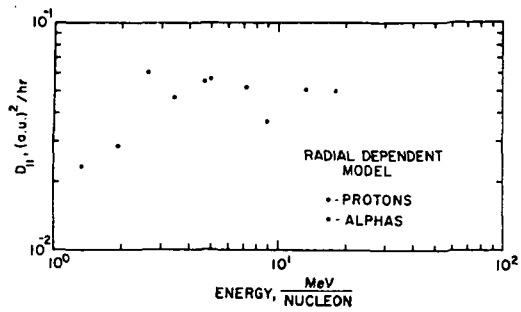


Fig. 14. Values of the diffusion coefficient, $D_{\parallel}$, resulting from fits of the radial dependent model to the data.

dependence in the diffusion coefficient [*Parker*, 1963; *Krimigis*, 1965]. That is

$$D = Qr^{\beta} \qquad (2)$$

Following *Krimigis* [1965], a fit to the data, varying $Q$ and $\beta$, was made assuming diffusion from a point source into three-dimensional space; the results of these fits are also shown superimposed upon the data of Figures 3*a*, *b*, and 4 (solid lines). The values of $D$ at the earth obtained from the fits are shown in Figure 14. The values of $\beta$ obtained from the fits are shown in Figure 15.

The diffusion coefficients for the highest energy protons from both types of fits in Figures 12 and 14 are approximately a factor of 2 lower than the results Krimigis obtained for $E_p > 40$ Mev using the radial dependent diffusion model in an analysis of the September 28, 1961, solar event [*Krimigis*, 1965].

Neither of the two models fit the data of Figures 3 and 4 particularly well during the onset of the event at the earth. This is perhaps due in large measure to the anisotropy of the particle fluxes that was observed to exist during the onset stage [*Palmeira et al.*, 1968]. Much better fits were obtained to the onset data when the time of the beginning of the event, $t_0$, was allowed to vary in addition to $D$ and $r_b$ or $Q$ and $\beta$. However, the values of $t_0$ obtained in this manner were generally unreasonable, as often $t_0$ occurred before or at approximately the same time as, the day 148 flare.

As is clear from Figure 3*b*, the decay phase of the highest energy proton data fits the diffusion-with-boundary model much better than the radial dependence model. In fact, it was

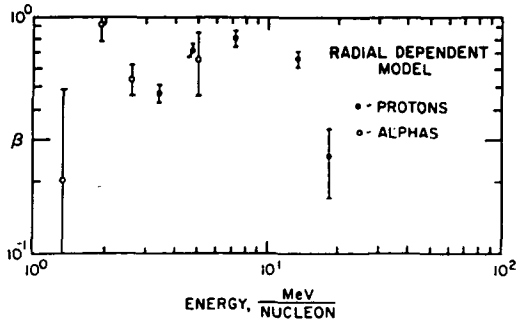


Fig. 15. Values of the diffusion coefficient radial dependence power, $\beta$, resulting from fits of the radial dependent model to the data.

essentially impossible to obtain reasonable fits of the radial dependence model to the higher energy proton data. However, for the lower energy/nucleon protons and alphas, either fit appears to be a reasonable representation of the particle flux temporal behavior.

Although the two models used here do demonstrate the over-all temporal characteristics of the particle fluxes, *McCracken et al.* [1967] and *Fisk and Axford* [1968] have pointed out that the values of the diffusion coefficients or mean free paths obtained from such models could be grossly incorrect due to persistent anisotropies in the fluxes. The anisotropic behavior of an event must be considered as well as the intensity-time variations [*Fisk and Axford*, 1968].

Since the diffusion-with-boundary model fit the data over the largest energy range, the values of $D/r_b^2$ obtained from the exponential decay fit to the data were used to further investigate the particle diffusion processes. The mean collision time, $T$, can be written as a function of $D$ as

$$T \propto D/v^2 \tag{3a}$$

or

$$T/r_b^2 \propto D/(v^2 r_b^2) \tag{3b}$$

Figure 16 contains the rigidity ($R$) dependence of $T/r_b^2$ for protons and alpha particles in interplanetary space during the event. The lines proportional to $R^{-2}$ are separated by factors of 2 and 4 to examine the dependence of the proton and alpha data on $A/Z$ or $(A/Z)^2$.

*Jokipii* [1966] has calculated a diffusion coefficient for cosmic-ray propagation in random magnetic fields. In the addendum to his paper, he has published an alternative expression for the diffusion coefficient that avoids a problem of a divergence in $D_\parallel$ if the power spectrum of the interplanetary field falls off as fast as $f^{-2}$ at large $f$. Using his expression for $D_\parallel$

$$D_\parallel = \frac{2}{9} v^2 \left[ \int_0^1 \frac{\langle (\Delta\mu)^2 \rangle}{\Delta t} \, d\mu \right]^{-1} \tag{4}$$

where $v$ is the particle velocity and the argument of the integral is the particle pitch-angle diffusion coefficient, the mean collision time, equation 3, can be written as

$$T_\parallel \propto \left[ \int_0^1 \frac{\langle (\Delta\mu)^2 \rangle}{\Delta t} \, d\mu \right]^{-1} \tag{5}$$

Using Jokipii's derived expression for the argument of equation 5 and a power spectrum $P_{xx}(f) \sim \delta/f^n$, equation 5 was integrated over $\mu$ to yield

$$T_\parallel \propto \frac{A}{Z} \frac{1}{R^{n-1}} \tag{6}$$

If the boundary distance, $r_b$, has a rigidity dependence such that $r_b \propto R^m$, then

$$\frac{T_\parallel}{r_b^2} \propto \frac{A}{Z} R^{-2m-n+1} \tag{7}$$

The proton data in Figure 16, with an approxi-

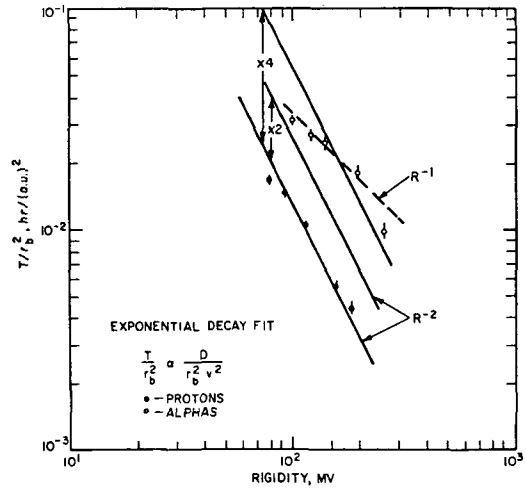


Fig. 16. Results for $T/r_b^2$ obtained from exponential fits to the decay phase of the protor and alpha temporal observations.

mately $R^{-2}$ dependency, implies that $2m + n = 3$ (interpreting the results as $T_{\parallel}/r_b^2$). If the boundary distance were essentially constant, independent of rigidity as in Figure 13, then the results in Figure 16 imply that the power spectrum of the transverse fluctuations in the interplanetary field during much of the event varied as $f^{-3}$ between the frequencies of $\sim 7 \times 10^{-4}$ to $\sim 2 \times 10^{-3}$ sec$^{-1}$ (assuming $V_w \sim 500$ km/sec and $B_0 = 5\ \gamma$). This is a more rapid falloff with $f$ than has been observed by *Coleman* [1966] on Mariner 2 ($\sim f^{-1}$) or deduced by *Nathan and Van Allen* [1968] from 1965 solar electron and proton data ($\sim f^{-2}$).

The power spectrum of the transverse field fluctuations would vary as $f^{-1}$ if $r_b \propto R$. However, there is no a priori reason to believe that an $f^{-1}$ power spectrum need exist during a solar disturbed period. It is probably to be expected that the power spectrum during a disturbed period should differ from the essentially average spectrum Coleman reported observing in 1962. In addition, as *Jokipii* [1968] has pointed out in a discussion of the Nathan and Van Allen results, a steeper frequency spectrum could also be a manifestation of the breakdown of the theory at these low rigidities.

The alpha and proton data plotted in Figure 16, particularly at the higher rigidities, would appear to be better represented by an $(A/Z)^2 = 4$ dependence rather than the $A/Z = 2$ dependence predicted by equations 6 and 7.

*Particle confinement.* Two proton channels are plotted on a fast time scale in Figure 17 to depict the particle fluxes before and after the large rate decreases on day 150. Three very distinct peaks plus several other smaller structures are seen within 4 hours of the flux decreases. Two of the peaks have a half-width of approximately 20 minutes and the other about 15 minutes. There is no dispersion between different energy channels in the time of occurrence of the peaks. Figure 18 contains the one-half hour averaged proton spectrum observed at

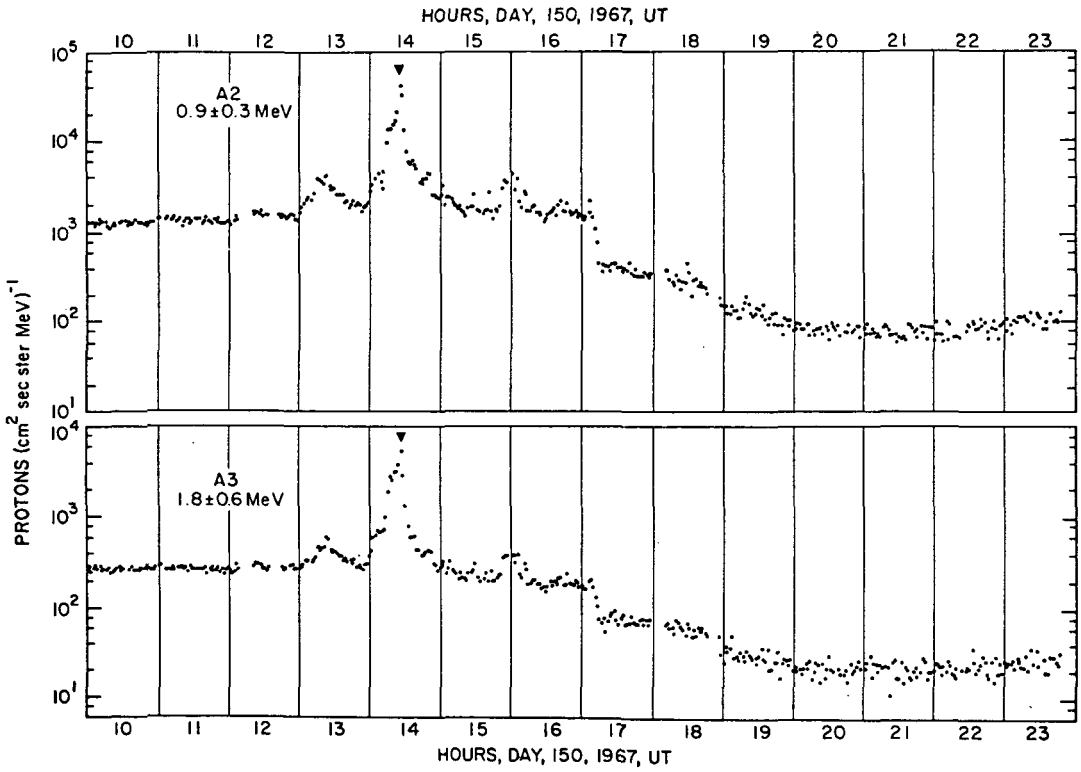


Fig. 17. Fast time resolution data for proton channels A2 and A3 during the flux peaks and cutoffs on day 150, 1967.

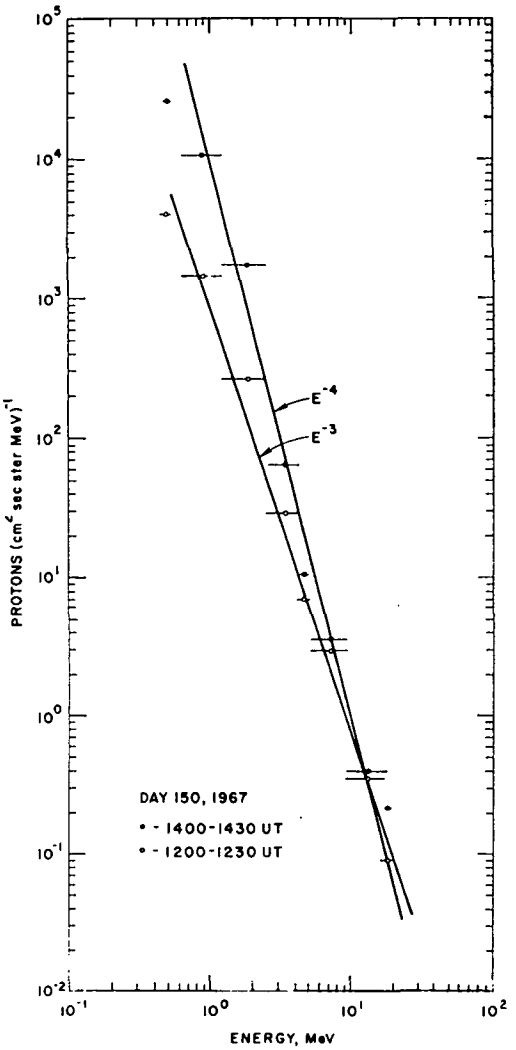


Fig. 18. Half-hour averaged proton spectra obtained at 1200–1230 UT and 1400–1430 UT, day 150.

1200 UT and at the time of the peak intensity during hour 14. The proton spectrum softened sharply from $\sim E^{-3}$ to $\sim E^{-4}$ at the time of the largest peak.

The sharp particle flux drops observed after the large flux increase on day 150 have a strong rigidity dependence (Figures 3*a*, *b*, 4, and 17). The ratio between the actual fluxes observed between 2000–2030 UT day 150 (approximately the minimum of the large drop) and the fluxes predicted by the exponential decay fit (extrapolated to 2015 UT) are plotted in Figure 19. The proton ratios have an $\sim R^3$ dependence, and the alpha particle ratios have an $\sim R^6$ dependence. Furthermore, both the proton and alpha ratios $\simeq 1$ at $R \simeq 200$ Mv.

The characteristic of the sharp flux decreases observed on day 150 was also observed at the end of the flux enhancement caused by the 27-day reappearance of the day 148 flare region. The half-hour averaged interplanetary proton data for $E_p = 1.80$ Mev, the hourly Alert neutron monitor counting rate, and $Kp$ for days 175–181, 1967, are shown in Figure 20. This interval spans a time period of 27–33 days after the day 148 flare (27-day corotational features have been described previously by, e.g., *Fan et al.* [1966, 1968] and *Bryant et al.* [1965]). The onset of the flux enhancements on day 176 was more gradual than the sharp drop in the fluxes on day 179 (characteristic of the flux drop on day 150). This observation implies that the leading edge of the corotating region was less well defined than the trailing edge.

Figures 21*a*, *b* contain half-hour average proton and alpha spectra from 1530–1600 day 149 and 1200–1230, day 177, respectively. The proton spectrum has softened appreciably from the time of observation of the diffusing flare particles to the time of observation of the corotating region. The continued large enhancement of the lowest energy proton fluxes could be due

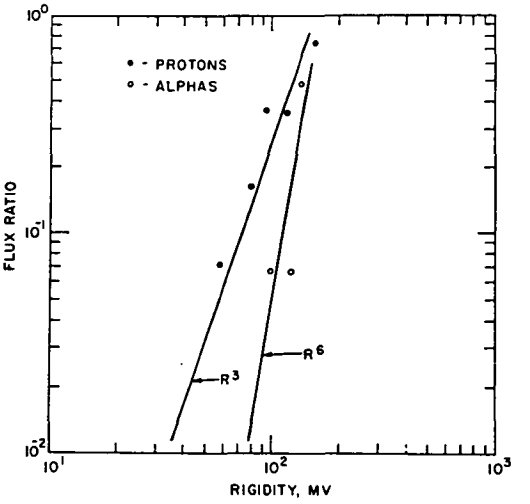


Fig. 19. Ratio of the actual fluxes observed during 2000–2030 UT, day 150, to the fluxes predicted by the decay phase of the diffusion-with-boundary model fits.

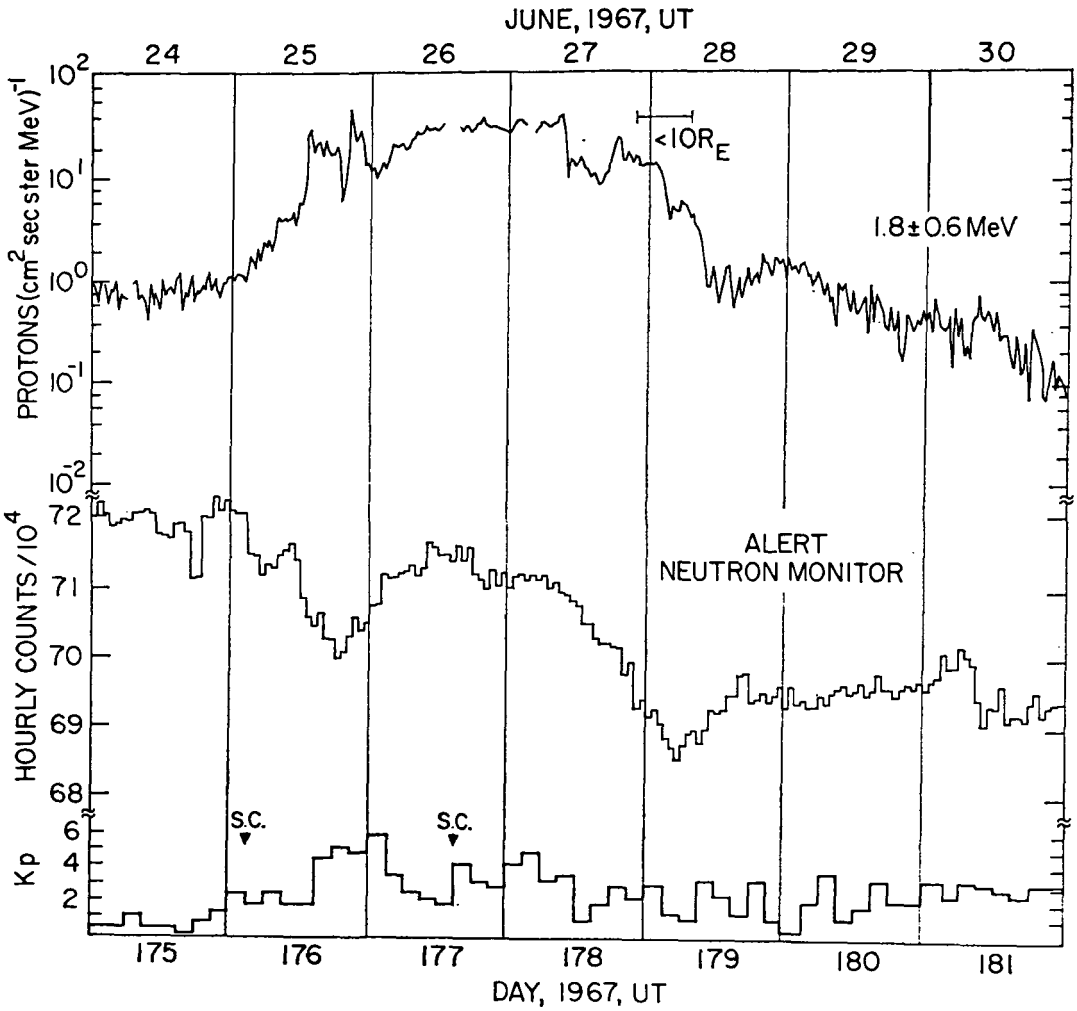


Fig. 20. Plot of the half-hour average data from the A3 proton channel for days 175–181, 1967. Also shown is the hourly count rate of the Alert neutron monitor and the 3-hour average *Kp*.

to a number of physical processes, among them (*a*) more rapid diffusion of the higher energy particles both along the field lines (Figures 12 and 14) and across the sharp flux boundary (Figure 19) and (*b*) more continued acceleration of the lower energy particles near the sun [*Fan et al.*, 1966*a*]. Continued emission of lower energy particles from an active region is also consistent with the lowest energy fluxes observed after the day 148 flare. As was noted previously, the fluxes in these energy channels deviated most severely from a classical west limb flare profile and, in fact, continued to increase during most of the event.

Although there is a strong possibility a shock from the day 148 flare was associated with the large, low-energy particle intensity peaks observed on day 150, the rigidity dependent flux decreases on day 150 were probably not caused solely by this mechanism, as has been suggested by *Lindgren* [1968]. Rather the rigidity dependence of the decreases (Figure 19), the reappearance of the sharp flux cutoffs in the 27-day corotation data (Figure 20), and the evidence that there were interplanetary field tangential discontinuities at this time on day 150 [*Arens et al.*, 1968] suggest that the day 150 flux decreases were due to the passage of an

interplanetary magnetic field structure past the earth. The rigidity dependences of proton and alpha particle transmission or diffusion across such a structure is given in Figure 19. In addition, it is not totally improbable, since the same structure was observed approximately 27 days later, that it was a magnetic field sector boundary that moved past the earth on day 150, producing the observed particle decreases and particle confinement on the eastward side of the sector boundary.

Perhaps, in addition to an association of the low-energy particle peaks with the day 148 flare plasma cloud, some of this structure could be due to the plasma cloud or shock interacting with and being reflected from, the fields comprising the sector boundary region. Both the deduced (from the occurrence of the sc) enhanced plasma density and the observed enhanced neutron monitor rates (Figures 3 and 4) before the boundary are also generally consistent with *Wilcox*'s [1968] summary of observations of enhanced particle counts at the edge of an interplanetary field sector boundary. However, the effects observed here on day 150 are greatly complicated by the existent solar flare-produced conditions.

*Jokipii and Parker* [1968], interpreting some solar active region proton data that were observed to extend over a broad (~180°) longitude spread [*Fan et al.*, 1968] suggest that the interplanetary magnetic field lines random walk at the sun, producing strong diffusion across the average magnetic field in interplanetary space. They conclude, by retaining the $P_{zz}(0)$ dependence in Jokipii's calculation of $D_\perp$ [*Jokipii*, 1966], that for protons of ~10 Mev, $D_\perp \sim D_\parallel$. From the data presented here for day 150 (Figures 3*a*, *b*, 4, and 17) and day 179 (Figure 20), the conclusion can be drawn that although low-energy solar cosmic ray particles may readily diffuse transverse to the average interplanetary magnetic field as suggested by Jokipii and Parker, nevertheless they are also apparently strongly confined by interplanetary field discontinuities or sector boundaries (Figure 19).

A very thorough correlation and analysis of interplanetary and ground-based data during

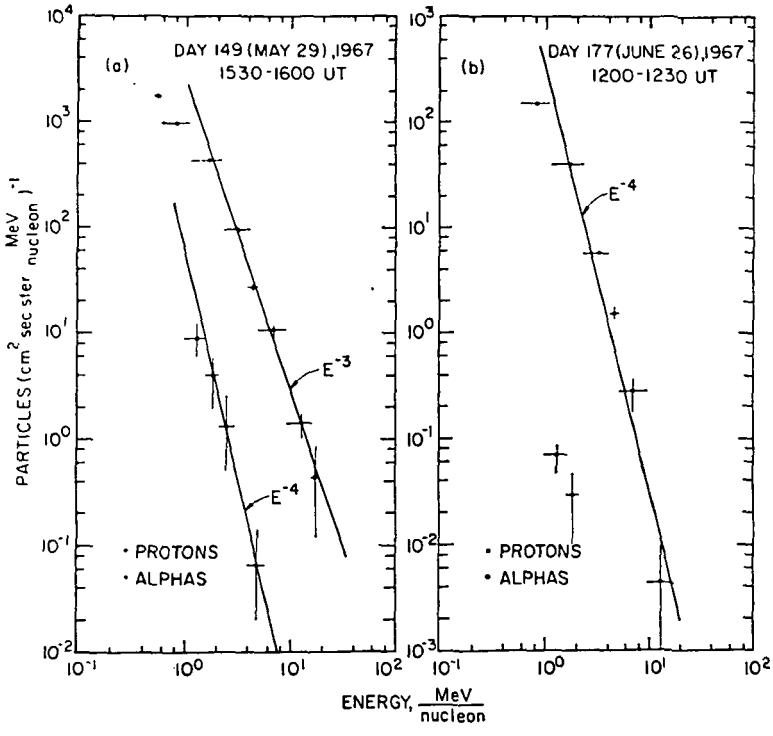


*Fig. 21. (a) Half-hour average proton and alpha spectra from 1530–1600 UT, day 149; (b)* half-hour average proton and alpha spectra from 1200–1230 UT, day 177.

the time interval after the July 7, 1966, solar flare has recently been published by *Svestka* [1968]. He concludes that solar proton storage (for protons up to ~20 Mev) occurred behind a sector boundary observed on July 8, 1966, and that particle transmission through the sector boundary was less and less likely for the lower rigidity particles ($\lesssim$100 Mv). The conclusions from the correlative study of Svestka are quite consistent with the observations and conclusions drawn from the Explorer 34 proton and alpha data observed on day 150 and day 179, 1967.

## Summary

The onset times at the earth of the lower energy solar particles were observed to deviate appreciably from the prediction of direct propagation along a spiral interplanetary field line carried by a 500 km/sec solar wind. It was suggested that this deviation was due either to storage closer to the sun or by an interplanetary plasma cloud, or both. However, the lowest energy proton channel was apparently not affected by the disturbance at ~1050 UT, day 148, that caused the 1302 UT sc at the earth. This fact implies that 0.6 Mev protons had not yet arrived at ~0.97 AU (since the disturbance was deduced to be ~0.03 AU from the earth) and therefore particle storage at the sun may have predominated in the determination of the particle arrival time. It must be emphasized, however, that the probable disturbed condition of the interplanetary medium <1 AU during day 148 makes an unambiguous determination of storage mechanisms impossible.

Significant velocity dispersions were discovered in the flux modulations during the onset at the earth of the flare-produced particles. Cross-correlation of pairs of different energy channels were performed at two different times. The cross-correlation analysis for the latter part of hour 1000, day 148, suggested that the disturbance that caused the particle modulation was located at ~0.03 AU from the earth. By attributing the sc at the earth approximately two hours later to this disturbance, a velocity of propagation of ~500–600 km/sec was deduced for the disturbance, a velocity that is not unreasonable for the solar wind during a disturbed period. A broad, less conclusive cross correlation was obtained between pairs of energy channels for the period 1700–1815 UT, day 148. The peaks of these correlations suggested that the modulating region was located ~0.12 AU from the earth. This is believed to be the first time such time dispersions in modulating phenomena have been observed in interplanetary space.

The half-hour averaged solar proton and alpha particle data resulting from the day 148 solar flare were fit with an exponential decay, an isotropic diffusion-with-boundary model, and a radial-dependent scattering center model. Using the $R^{-2}$ dependence of $T/r_b^2$ resulting from the exponential decay fit, together with Jokipii's diffusion coefficient model, a power spectral density varying as $f^{-3}$ was deduced for the fluctuations in the interplanetary field (assuming the boundary distance, $r_b$, had no rigidity dependence). The Jokipii model predicts an $(A/Z)$ dependence for the relaxation time, $T$. The data from the exponential decay fit suggested that an $(A/Z)^2$ dependence would be a better representation of the results.

Proton and alpha transmission across an interplanetary magnetic structure (perhaps a sector boundary) was observed to be strongly rigidity dependent. For particles with $R \sim$ 33–200 Mv, the proton transmission was observed to be $\sim R^2$ and the alpha transmission $\sim R^6$. Above $R \sim$ 200 Mv, both species of particles were apparently little affected by such a structure.

This analysis of a 'classical' west limb flare has shown that many qualitative and quantitative results can be obtained using the relatively high-energy resolution and the fast time resolution of the fluxes of two distinct species of different particles acting as probes in the medium. Present plans call for a continued investigation of other classic low-energy events that may perhaps exhibit different rise and decay shapes. In addition, the investigation will be extended to flares whose particle propagation characteristics are more complex; for example, it has been preliminarily noted [*Lanzerotti*, 1969] that in some of these the proton/alpha ratio often changes over the course of a few tens of minutes when an abrupt particle change is detected in interplanetary space.

*Acknowledgments.* The author would like to thank Dr. W. L. Brown for many fruitful discussions and a number of critical comments and suggestions. He also thanks Dr. M. Schulz and the

referee for a discussion of the interplanetary field power spectrum. He would like to thank Dr. A. J. Masley for supplying the riometer data. He also thanks Mr. W. A. Burnett and Miss C. G. Maclennan for their expertise in computing the cross-correlation results and the diffusion model fits to the data.

## References

Adams, G. W., and A. J. Masley, Theoretical study of cosmic noise absorption due to solar cosmic radiation, *Planetary Space Sci., 14,* 227, 1966.

Arens, J. F., D. H. Fairfield, D. J. Williams, and C. O. Bostrom, Simultaneous low energy proton and magnetic field observations from the Explorer 34 satellite, paper presented at 1968 Midwest Cosmic Ray Conference, Iowa City, March 1–2, 1968.

Axford, W. I., and G. C. Reid, Polar cap absorption and the magnetic storm of February 11, 1958, *J. Geophys. Res., 67,* 1692, 1962.

Axford, W. I., and G. C. Reid, Increases in intensity of solar cosmic rays before sudden commencements of geomagnetic storms, *J. Geophys. Res., 68,* 1793, 1963.

Bryant, D. A., T. L. Cline, U. D. Desai, and F. B. McDonald, Explorer 12 observations of solar cosmic rays and energetic storm particles after the solar flare of September 28, 1961, *J. Geophys. Res., 67,* 4983, 1962.

Bryant, D. A., T. L. Cline, U. D. Desai, and F. B. McDonald, New evidence for long-lived solar streams in interplanetary space, *Phys. Rev. Letters, 11,* 144, 1963.

Bryant, D. A., T. L. Cline, U. D. Desai, and F. B. McDonald, Studies of solar protons with Exp. 12 and 14, *Astrophys. J., 141,* 478, 1965.

Burlaga, L. F., Anisotropic diffusion of solar cosmic rays, *J. Geophys. Res., 72,* 4449, 1967.

Castelli, J. P., J. Aarons, and G. A. Michael, The great solar radio burst of May 23, 1967, *Astrophys. J., 153,* 267, 1968.

Coleman, P. J., Jr., Variations in the interplanetary magnetic field: Mariner 2, 1, Observed properties, *J. Geophys. Res., 71,* 5509, 1966.

Coon, J. H., Solar wind observations, in *Earth's Particles and Fields,* edited by B. M. McCormac, Reinhold Book Corp., New York, 1968.

Fan, C. Y., M. Pick, R. Pyle, J. A. Simpson, and D. R. Smith, Protons associated with centers of solar activity and their propagation in interplanetary magnetic field regions corotating with the sun, *J. Geophys. Res., 73,* 1555, 1968.

Fan, C. Y., G. Gloeckler, and J. A. Simpson, Protons and helium nuclei within interplanetary magnetic regions which co-rotate with the sun, *Proc. Intern. Conf. Cosmic Rays,* vol. 1, p. 109, The Physical Society, *London,* 1966*a*.

Fan, C. Y., J. E. Lamport, J. A. Simpson, and D. R. Smith, Anisotropy and fluctuations of solar proton fluxes of energies 0.6–100 Mev measured on the Pioneer 6 space probe, *J. Geophys. Res., 71,* 3289, 1966*b*.

Fisk, L. A., and W. I. Axford, Anisotropies of solar cosmic rays, University of California, San Diego, *Preprint IPAPS 68/69-268,* November 1968.

Goedeke, A. D., and A. J. Masley, The 23 and 28 May 1967 solar cosmic ray events, to be published in *Space Res., 8,* 1969.

Jokipii, J. R., Cosmic-ray propagation, 1, Charged particles in a random magnetic field, *Astrophys. J., 146,* 480, 1966.

Jokipii, J. R., Discussion of paper by K. V. S. K. Nathan and J. A. Van Allen, 'Diffusion of solar cosmic rays and the power spectrum of the interplanetary magnetic field,' *J. Geophys. Res., 73,* 6864, 1968.

Jokipii, J. R., and E. N. Parker, Stochastic aspects of magnetic field lines of force with application to cosmic ray propagation, *EFI Preprint 68-35,* University of Chicago, May 1968.

Krimigis, S. M., Interplanetary diffusion model for the time behavior of intensity in a solar cosmic ray event, *J. Geophys. Res., 70,* 2943, 1965.

Lanzerotti, L. J., Solar protons and alphas from the May 23, 1967, solar flares, *World Data Center A—Upper Atmosphere Geophysics Reports UAG-5,* February, 1969.

Lanzerotti, L. J., H. P. Lie, and G. L. Miller, A satellite solar cosmic ray spectrometer with on-board particle identification, *IEEE Trans. Nucl. Sci., NS-16,* February 1969.

Lindgren, S. T., The solar particle events of May 23 and May 28, 1967, *Solar Phys., 5,* 382, 1968.

McCracken, K. G., U. R. Rao, and R. P. Bukata, Cosmic ray propagation processes, 1, A study of the cosmic ray flare effect, *J. Geophys. Res., 72,* 4293, 1967.

Nathan, K. V. S. K., and J. A. Van Allen, Diffusion of solar cosmic rays and the power spectrum of the interplanetary field, *J. Geophys. Res., 73,* 163, 1968.

Neugebauer, M., and C. W. Snyder, Mariner 2 observations of the solar wind, 1, Average properties, *J. Geophys. Res., 71,* 4469, 1966.

Obayashi, T., The interaction of the solar wind with the geomagnetic field during disturbed conditions, in *Solar-Terrestrial Physics,* Academic Press, London, 1967.

Palmeira, R. A. R., F. R. Allum, K. G. McCracken, and U. R. Rao, Anisotropy measurements of low energy solar cosmic rays, paper presented at 1968 Midwest Cosmic Ray Conference, Iowa City, March 1–2, 1968.

Parker, E. N., *Interplanetary Dynamical Processes,* Interscience Publisher, New York, 1963.

Svestka, Z., Effects associated with the sector boundary crossing on July 8, 1966, *Solar Phys., 4,* 361, 1968.

Van Allen, J. A., Solar X-ray flares on May 23, 1967, *Astrophys. J., 152,* L85, 1968.

Webber, W. R., A review of solar cosmic ray events, in *AAS-NASA Symp. Physics of Solar Flares, NASA-SP-50,* edited by W. N. Hess, p. 215, U.S. Government Printing Office, Washington, D.C., 1964.

Wilcox, J. M., The interplanetary magnetic field, solar origin and terrestrial effects, *Space Sci. Rev., 8,* 258, 1968.

Winge, C. R., Jr., and P. J. Coleman, Jr., The motion of charged particles in a spiral field, *J. Geophys. Res., 73,* 165, 1968.

# CHAPTER 8

## DISCUSSION OF PAPER, 'A COMPARISON OF ENERGETIC STORM PROTONS TO HALO PROTONS'

L. J. LANZEROTTI
*Bell Telephone Laboratories, Murray Hill, N. J., U.S.A.*

In a recent paper Kahler (1969) presented solar particle data for time periods spanning a number of different storm sudden commencement (SSC) events as seen on the earth. In addition to arguing that the energetic storm particles and solar proton 'halo' particles had similar origins, he presented a model for the origin and propagation of energetic storm particles and halo protons. This note makes use of newly published low energy solar particle data from an experiment on Explorer 34 for two of the May 1967 events discussed by Kahler. (Data from the earlier 1967 and the 1966 events discussed by Kahler were not available since Explorer 34 was launched on May 24, 1967.) These data suggest for these two events, that although the energetic storm particles were originally particles emitted from the sun, other processes were subsequently operative on these particles in their travel to the earth (Parker, 1965; Rao *et al.*, 1967). These solar-originated particles were 'accelerated' or 'confined' in interplanetary disturbances, becoming 'energetic storm particles', so that they cannot be uniquely identified as 'halo'-type particles as Kahler does.

The half-hour averaged proton data in Figure 1, taken from Lanzerotti (1969a), were measured in four of the proton channels in the Bell Laboratories experiment on Explorer 34. These proton data at the lower energies have a radically different temporal appearance around the time of the May 24 SC than do the data from a similar time period in Figure 1 of Kahler. The proton fluxes between the two SSC's *do not* have the characteristic halo structure (Lin *et al.*, 1968) as Kahler maintains. Furthermore, the first SSC (May 24) occurs near the *peak* of a large enhancement in the lower energy proton fluxes (the energetic storm particles) and not merely during a rise in the fluxes as shown by the data of Kahler and required by his propagation model.

A recent analysis of the solar alpha to solar proton flux ratios during this event suggested that the solar particle fluxes *following* the May 24 SSC were due to a series of three east limb flares on May 23 while the solar particles observed *prior to and during* the May 24 SSC were due to a large flare on May 21 (Lanzerotti and Robbins, 1969). If this 'source effect' in the particle fluxes did exist on May 24, then there should indeed be no halo effects seen between the two SSC's as the data in Figure 1 show.

The low energy solar proton data during the May 30, 1967, SSC published by Lanzerotti (1969b) is also quite different than the data contained in Figure 3 of Kahler for the same event. No energetic particle enhancement is seen in Kahler's data at the time of the SSC whereas Lanzerotti has shown a narrow spike in the

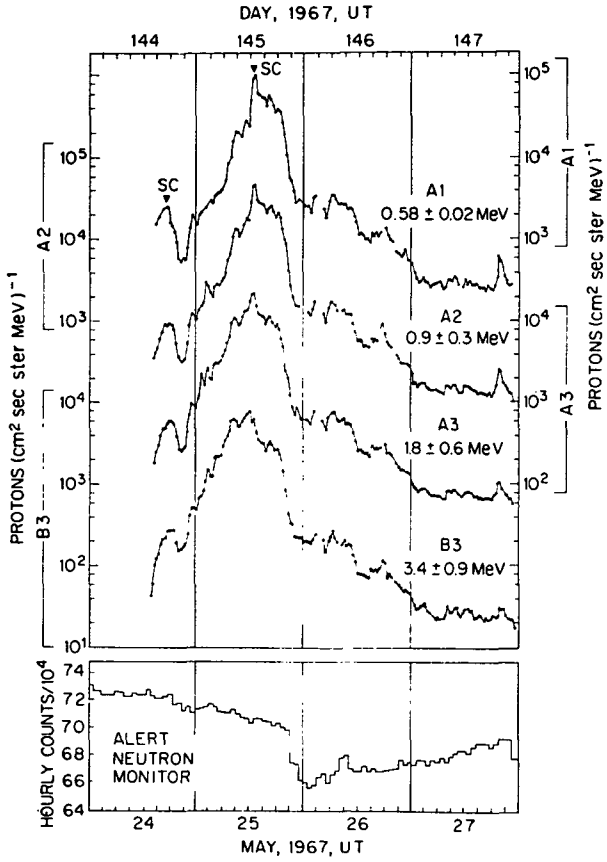


Fig. 1. Solar proton fluxes measured in four proton detection channels during May 24–26, 1967. At the bottom of the figure is plotted the Alert neutron monitor hourly counting rate.

fluxes that is as much as four times as intense (at $E_p \sim 600$ keV) as any of the fluxes measured prior to the energetic particle enhancement. Although proton fluxes that had a 'halo'-like appearance preceded the energetic particle spike in Lanzerotti's lowest energy data by several hours, nevertheless the flux values in the intensity spike were much larger than the halo fluxes. Furthermore, the energetic particle enhancement spike was also seen with diminishing intensities in higher energy fluxes that had a 'diffusive' temporal appearance (rather than a 'halo' appearance) for a day and one-half prior to the SSC (Lanzerotti, 1969b).

In summary, it is believed that the data discussed above show that two of the

events described by Kahler do not fit his contention that energetic storm particles and 'halo' particles have 'similar origins' except, of course, that both sets of particles originally eminated from the sun. Although this author believes there are interplanetary processes operative on these solar particles to produce the energetic storm particles the understanding of these processes is still at a rudimentary stage.

## References


Kahler, S. W.: 1969, *Solar Phys.* **8**, 166.
Lanzerotti, L. J.: 1969a, *World Data Center A, Report UAG-5*, 56.
Lanzerotti, L. J.: 1969b, *J. Geophys. Res.* **74**, 2851.
Lanzerotti, L. J. and Robbins, M. F.: 1969, *Solar Phys.* **10**, 212.
Lin, R. P., Kahler, S. W., and Roelof, E. C.: 1968, *Solar Phys.* **4**, 55.
Parker, E. N.: 1965, *Phys. Rev. Letters* **14**, 55.
Rao, U. R., McCracken, K. G., and Bukata, R. P.: 1967, *J. Geophys. Res.* **72**, 4325.

# CHAPTER 9

## SOLAR FLARE ALPHA TO PROTON RATIO CHANGES FOLLOWING INTERPLANETARY DISTURBANCES

L. J. LANZEROTTI and M. F. ROBBINS
*Bell Telephone Laboratories, Murray Hill, N.J., U.S.A.*

**Abstract.** A discussion is presented on the half hour averaged low energy solar alpha to solar proton flux ratios observed following the three large solar flares of May 23, 1967. One of the large changes observed in the particle ratios (following a sudden commencement (SC) storm observed on the earth) is interpreted as due to a source effect. The second large change, again observed following an SC, is observed in the equal velocity and equal rigidity ratios and not in the equal energy/charge ratios. This observation suggests that electric fields in an interplanetary disturbance may be the cause of the modulations.

This note presents a discussion on the detailed temporal behavior of the low energy (2.5–8.0 MeV/nucleon) alpha to proton ratios observed at 1 AU by an experiment on the Explorer 34 satellite after the series of three east limb solar flares (plague region 8818; 27°–30°N, 25°–28°E) on May 23, 1967. The first detailed temporal study of the alpha to proton ratio during a solar event was published by Biswas and Fichtel (1963) using rocket flight particle data $>30$ MeV/nucleon obtained during November 12–18, 1960. They reported that, in addition to the fact that the alpha to proton ratio varied greatly from event to event, the ratio varied by as much as a factor of 5 during the November event. Fichtel and McDonald (1967) have stated that a part of these variations are presumably due to 'propagation effects'. Armstrong *et al.* (1969) published the first low energy/nucleon (0.5–4.0 MeV/nucleon) proton to alpha ratio results using three hour average data obtained during the July, 1966, solar flare event.

Alpha to proton ratio data are presented in this note for particles compared as to equal velocities (equal energy/nucleon), equal rigidities (equal kinetic energy), and equal energy/charge. The data show that: (1) the alpha to proton ratios during this solar event vary greatly in magnitude and temporal characteristics according to the energy frame of reference in which the data are plotted; (2) two of the largest changes in the alpha to proton ratios for particles of equal energies and rigidities occur after interplanetary disturbances resulting in sudden commencement (SC) storms as seen on the earth; and (3) no significant changes are observed in the equal energy per charge ratios at the time of the second SC. These observations suggest that: (1) the ratio changes following the first SC may be due to a source effect, and (2) the equal velocity and equal rigidity ratio changes following the second SC may perhaps be due to interplanetary electric fields modulating the particle fluxes.

The Explorer 34 satellite was launched into a highly eccentric polar orbit at approximately 1420 UT May 24, during the onset of the solar flare particle observations at the

earth. Explorer 34 is a spin stabilized (with spin axis perpendicular to the ecliptic plane) satellite with an apogee of approximately 34 $R_E$. The Bell Laboratories experiment consists of a four element solid state detector telescope oriented perpendicular to the spin axis. The half angle of the detector telescope defining collimator is 20°; the flux measured by the experiment is the spin averaged flux of particles in the ecliptic plane. Protons and alphas up to an energy of approximately 4 MeV/nucleon are distinguished by the energy deposited in the first two detectors of the telescope and subsequently measured in a five channel pulse height analyzer. Particle species above this energy are distinguished by the use of an on-board pulse multiplier (Lanzerotti *et al.*, 1969).

A number of published articles have dealt with the particle, X-ray, and radio emissions from this series of flares (Castelli *et al.*, 1968; Smith and Webber, 1968; Van Allen, 1968; Goedeke and Masley, 1969; Lincoln, 1969). Lanzerotti (1969) has reported detailed half hour averaged proton and alpha particle flux observations made during the event by the experiment on Explorer 34. Plots of the particle fluxes in three proton and two alpha energy channels during May 24–27, 1967 (taken from the report) appear as Figures 1a and 1b, together with the Alert neutron monitor counting rate. As is evident from the data in this figure, the alpha and proton energy channels of the experiment do not have the same energy widths, nor do they have the same central energy values. A simple power law was only indicative of the particle flux spectral dependence during the event (Lanzerotti, 1969).

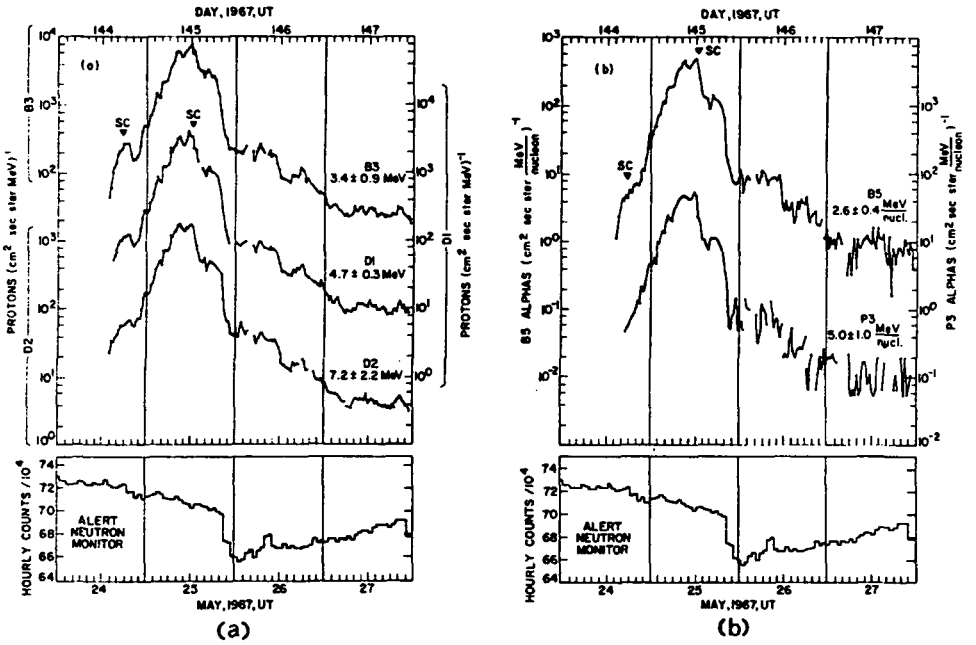


Fig. 1. (a) Proton fluxes in three energy channels for May 24–27, 1967. – (b) Alpha particle fluxes in two energy channels for May 24–27, 1967.

In order to study the temporal variations of the alpha to proton ratios for a common set of velocities for the two particles the following procedure was adopted. The alpha and proton differential flux values at the given velocities were determined by linear interpolations between adjacent log (velocity) values of the half-hour averaged proton and alpha log (flux) values. Figure 2 contains six sets of equal velocity alpha to proton ratios using these interpolated fluxes.

Approximately two hours after the May 24 sudden commencement, the ratios for the lowest velocities increase. These initial increases correspond in time to the larger decreases in the lower energy proton fluxes and no similar decreases in the alpha fluxes following the appearance of energetic storm particles around the SC (Figure 1; Lanzerotti, 1969). The enhancement of the alpha to proton ratios following the SC can be noted in all of the MeV/nucleon time plots of Figure 2, although the magnitude of the increase diminishes at the highest velocities. At ~0800 UT a decrease is ob-

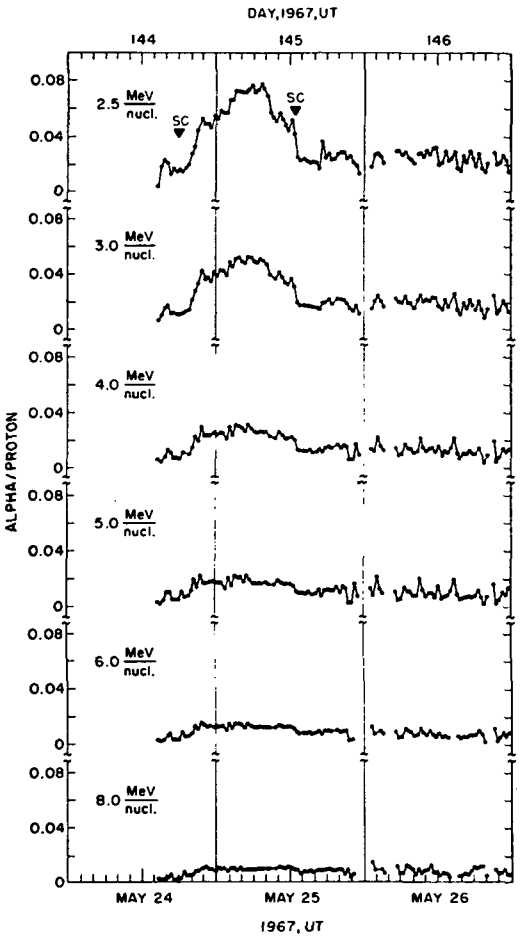


Fig. 2. Alpha to proton ratios for six different equal energy/nucleon (velocity) values, May 24–26, 1967. The errors in the flux ratios due to statistical uncertainties are ~ 10–15%.

served in the three lowest velocity data plots. Another decrease, observed to some degree in all of the energy/nucleon ratios, occurs at the time of the May 25 SC. The alpha to proton ratios remain fairly steady during the remainder of the time period except for small decreases and the subsequent recoveries at the time of the large May 25 Forbush decrease at ~2000–2100 UT (Figure 1).

The alpha to proton ratios for particles of equal energy (rigidity) are plotted in Figure 3. (These ratios were also obtained using the half-hour averaged alpha and proton fluxes differential in energy as discussed above.) Again the ratios tend to increase following the May 24 SC. However, in these ratio comparisons, the largest increases are observed for the highest rigidity particles rather than the lowest velocity particles as in Figure 2. The ratios continue a general increase during the first half of

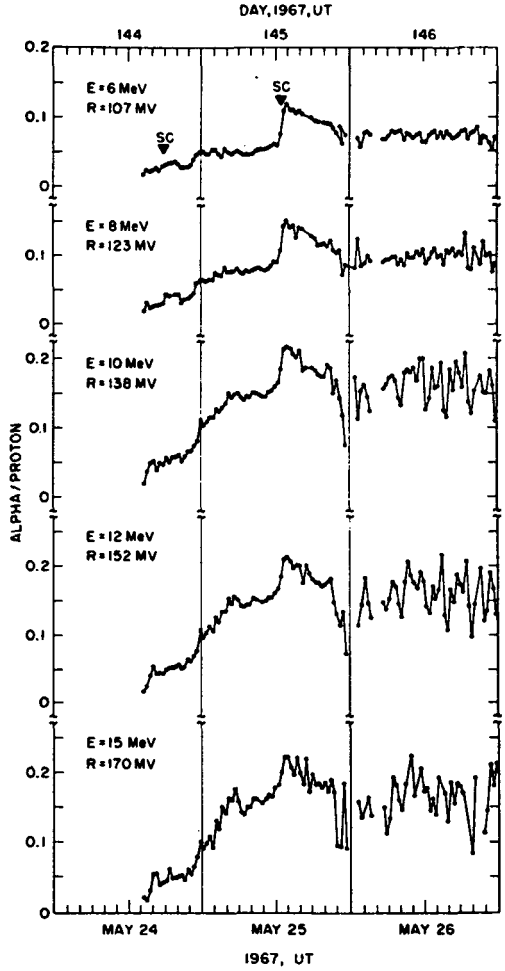


Fig. 3. Alpha to proton ratios for five different equal energy (rigidity) values, May 24–26, 1967. The errors in the flux ratios due to statistical uncertainties are ~ 10–15% for days 144 and 145. The statistical uncertainties on day 146 are ~ 30–40%.

May 25. At the time of the May 25 SC, there is a sudden increase in the ratios observed in all of the energy channels. Although the magnitude of the increase is approximately the same in all of the energy channels ($\Delta[\alpha/p] \sim 0.05$), the percentage increase in the lowest energy channel is the largest ($\sim 100\%$). After the May 25 SC the enhanced alpha to proton ratios decrease only slightly until large decreases are observed in the ratios at the higher rigidities at approximately the time of the large Forbush decrease (Figure 1). After recovery from these decreases, the ratios remain fairly steady during the remainder of May 26.

The alpha to proton ratios for particles compared as to equal energy/charge are plotted in Figure 4. (These ratios again were obtained using the half-hour averaged particle fluxes differential in energy/charge as discussed earlier.) Following the May 24 SC the ratios again increased. Both the magnitude of the increases and the values of the ratios after the increases are nearly the same for all energy/charge ratios. These

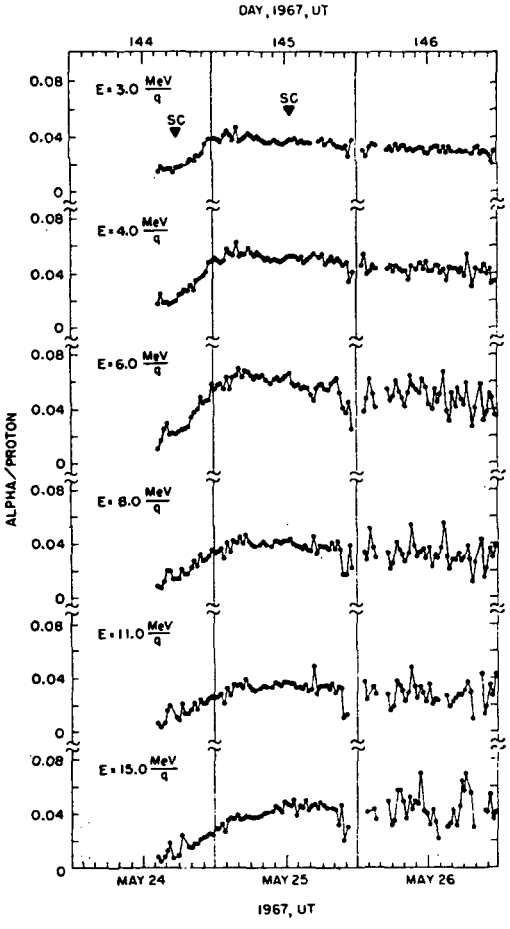


Fig. 4. Alpha to proton ratios for six different equal energy/charge values, May 24–26, 1967. The errors in the flux ratios due to statistical uncertainties are $\sim 10$–$15\%$ for days 144 and 145. The statistical uncertainties for the several highest energy/charge ratios on day 146 are $\sim 25$–$30\%$.

observations are in distinct contrast to the rigidity and velocity dependent ratio increases and ratio magnitudes observed for the data in Figures 2 and 3. Moreover, although all of the equal energy/charge ratios decrease slowly during May 25–26, no significant modulation is observed at the time of the May 25 SC. Ratio decreases and recoveries are again observed at the time of the Forbush decrease.

The alpha to proton ratios as a function of energy/nucleon and total particle energy are plotted in Figures 5a and 5b, respectively, for five different hourly flux

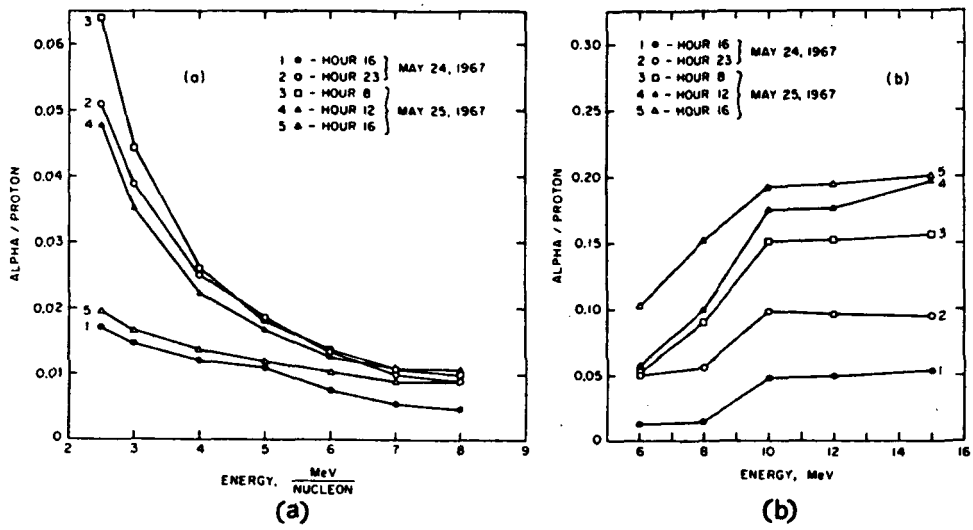


Fig. 5. (a) Hourly average alpha to proton ratios as a function of energy/nucleon for five different hours, May 24–25, 1967. – (b) Hourly average alpha to proton ratios as a function of energy for five different hours, May 24–25, 1967.

averages during the event. These plots are to emphasize the results obtained from Figures 2 and 3: the alpha to proton ratios during this solar event vary greatly in temporal characteristics and magnitudes according to whether the data is expressed in terms of rigidity or velocity. However, after the approximately equal increases following the May 24 SC, the equal energy/charge ratios remained approximately constant, with equal magnitudes, for all the energy/charge data.

Since post-May 24 SC increases are observed in all of the alpha to proton ratios for particles compared as to equal velocity, equal rigidity, and equal energy/charge, it is tempting to interpret these increases as due to a source difference in the production of energetic alphas and protons. This is an even more tempting interpretation if the disturbance producing the May 24 SC is attributed to the extreme east limb solar event at ~1900 UT on May 21 (plague region 8818; Castelli *et al.*, 1968). If this were indeed the case, then the low energy particle population prior to the May 24 SC (largely unmeasured by Explorer 34) might be due predominately to the May 21 solar event, whereas the particle population after the May 24 SC might be due predominately to the May 23 flares.

The lack of modulation in the equal/energy charge ratios together with the large modulations in the equal velocity and rigidity ratios at the time of the May 25 flux decreases and SC suggest that the particle modulating mechanism in the interplanetary disturbance may be electric fields. The approximately constant and equal ratios (energy/charge) during May 25–26 suggest that electric fields may have played an important role in the initial acceleration and/or the interplanetary propagation of these particles.

Until the present measurements, no continuous temporal observations of the alpha to proton ratios at a number of different energies had been made during any solar event. In addition, the rocket and satellite data on solar proton and alpha observations had been discussed only for particles compared as to equal energy/nucleon or equal rigidity (see, e.g., Biswas and Fichtel, 1965). It is clear from the above discussions that changes observed in the alpha to proton ratios may not be due solely to propagation effects and that in order to unravel the source and propagation effects the particle fluxes should also be compared as to equal energy/charge. By using these three methods of comparison it may be possible to eliminate propagation effects and then study only the source changes for a number of different flares.

Large enhancements of alpha particles and a corresponding increase in the equal rigidity alpha to proton ratios, may well be a common occurrence in interplanetary disturbances. Similar enhancements in the ratio may commonly exist for energies as low as the solar wind particles. An observation of an enhanced alpha to proton ratio in the solar wind was reported by Gosling *et al.* (1967), during the main phase of a large 1965 geomagnetic storm. In addition, Ogilvie *et al.* (1968), observed a seven fold increase in the solar wind alpha to proton ratio approximately five hours following the May 30, 1968, SC.

**Acknowledgement**

We thank Dr. W. L. Brown for a number of stimulating discussions and a careful reading of this manuscript.

**References**

Armstrong, T. P., Krimigis, S. M., and Van Allen, J. A.: 1969, *Annals of the IQSY* **3**, 313.
Biswas, S. and Fichtel, C. E.: 1963, *Astrophys. J.* **139**, 941.
Biswas, S. and Fichtel, C. E.: 1965, *Space Sci. Rev.* **4**, 709.
Castelli, J. P., Aarons, J., and Michael, G. A.: 1968, *Astrophys. J.* **153**, 267.
Fichtel, C. E. and McDonald, F. B.: 1967, *Annual Rev. Astron. Astrophys.* **5**, 351.
Goedeke, A. D. and Masley, A. J.: 1969, in *Solar Flares and Space Research* (ed. by C. de Jager and Z. Švestka), North Holland Publ. Co., Amsterdam, p. 284.
Gosling, J. T., Asbridge, J. R., Bame, S. J., Hundhausen, A. J., and Strong, I. B.: 1967, *J. Geophys. Res.* **72**, 1913.
Lanzerotti, L. J.: 1969, *World Data Center A*, Report UAG-5, p. 56.
Lanzerotti, L. J., Lie, H. P., and Miller, G. L.: 1969, *IEEE Trans. Nucl. Sci.* **NS-16**, No. 1, 343.
Lincoln, J. V. (ed.): 1969, *World Data Center A*, Report UAG-5.
Ogilvie, K. W., Burlaga, L. F., and Wilkerson, T. D.: 1968, *J. Geophys. Res.* **73**, 6809.
Smith, R. W. and Webber, N. J.: 1968, *J. Atmospheric Terrest. Phys.* **30**, 169.
Van Allen, J. A.: 1968, *Astrophys. J.* **152**, L85.

CHAPTER 10

N72-21841

# RELATIVE IMPORTANCE OF SOLAR ELECTRONS, PROTONS, AND ALPHAS IN THE NOVEMBER 1969 PCA EVENT

by

L. J. Lanzerotti and C. G. Maclennan
Bell Laboratories
Murray Hill, New Jersey, U.S.A.

## ABSTRACT

The fluxes of electrons ($E > 0.35$, $> 0.6$, and $> 1.1$ MeV), protons (0.47-19.7 MeV in ten differential channels), and alpha particles (1.0-21.4 MeV/nucleon in six differential channels) produced by the 2 November 1969 west limb flare were measured in interplanetary space by a semiconductor particle telescope on the Explorer 41 satellite. Intense fluxes of electrons arrive at the earth ~1 hour after the flare and prior to the arrival of the higher energy protons. Calculations indicate that these electrons produce approximately fifty percent of the intense (~14 dB) riometer absorption observed near the beginning of the event. The calculated electron and proton total riometer absorption agrees well throughout most of the event with that measured at 30 MHz at McMurdo, Antarctica. The alpha-to-proton ratios are presented for several different values of particle energy-per-nucleon. These ratios are quite low and indicate that the alphas were relatively insignificant contributors to the ionization of the PCA event.

---

COSPAR Symposium on November 1969 Solar Particle Event, 16-18 June, 1971

## INTRODUCTION

Beginning with the ionospheric effects observed during the great solar cosmic ray event of 23 February 1956 (Bailey, 1957), polar cap absorption events (PCA events) have been studied extensively in recent years both as distinct ionospheric phenomena and as diagnostic tools for solar-magnetospheric processes (see, e.g., reviews by Reid, 1970a,b). In recent years, with the advent of satellite measurements with good time-resolution and spectral information on the solar proton fluxes, satisfactory agreement has frequently been achieved in calculating the expected excess riometer cosmic noise absorption due to the stopping of these solar protons in the high-latitude terrestrial atmosphere (Potemra et al., 1967, 1969, 1970; Potemra and Lanzerotti, 1971).

Although alpha particles and electrons are also constituents of the solar flare-produced cosmic rays, quantitative examination of their relative contributions to the PCA ionization has not previously been reported (Reid, 1970b). Hakura (1967) originally suggested that electrons

may play a role in the initial stages of a PCA event. Masley and Goedeke (1969) qualitatively attributed a part of the absorption during the July 1966 event to solar electrons. This paper demonstrates quantitatively that intense fluxes of high energy solar electrons incident on the polar ionosphere contributed approximately fifty percent of riometer abosrption in the southern polar cap for the first several hours of the 2 November 1969 PCA event. In contrast, it is concluded that alpha particles contributed only a few percent to the total absorption measured in the southern polar cap.

In this paper, a discussion is first presented of the solar particle fluxes measured during the PCA event. The data are then used to compute the expected riometer absorption due to the assumed incidence of these particles on the polar ionosphere. This predicted absorption is then compared with actual absorption measurements made during the event at McMurdo, Antarctica.

The solar particle data used in this study were obtained by the Bell Laboratories particle telescope on the Explorer 41 (IMP-G) spacecraft. The details of the solid state telescope and associated electronics, which consist of coincidence circuitry and a particle identifier to separate protons, alpha particles, and electrons, have been described previously (Lanzerotti, et al., 1969). The 30 MHz riometer data was obtained by the McDonnell-Douglas observatory at

McMurdo (79°S, 294.9°E geomagnetic; L ~32). These observations have been reported by Masley et al. (1970).

## OBSERVATIONS

### Solar Particle Fluxes

The fluxes of solar protons, alpha particles, and electrons measured on Explorer 41 during the November 1969 PCA event are presented in Fig. 1. Figure 1a contains a plot of the one-half hour average fluxes in eight of the ten differential energy channels of the experiment. These protons were apparently produced by a solar flare behind the west limb of the sun (Thomas, 1970; Masley et al., 1970). The lower energy proton fluxes increase slowly to a peak intensity which does not occur until approximately one day after the initial particle onsets. In contrast, the higher energy protons increase more rapidly to a peak intensity (the exact time and intensity of which is somewhat uncertain due to a perigee pass of the satellite). The proton decay at the lower energies is approximately exponential; the decay appears more like a power-law in time at the higher energies.

Plotted in Fig. 1b are the one-half hour average alpha particle fluxes measured in the six differential alpha channels of the experiment. The overall temporal appearance of the alpha fluxes resembles that of the proton fluxes in Fig. 1a. The lower energy fluxes increase more slowly to a peak intensity and have an approximately exponential decay. At higher energies, the peak intensities are reached within several hours of the first particle observations. The high energy alpha fluxes decay with a power-law time dependence.

The one-half hour averaged electron fluxes measured in three integral channels are plotted in Fig. 1c. The temporal profiles of the electron fluxes resemble those of the highest energy alphas and protons. The electron fluxes increase rapidly to a peak intensity soon after the first particles are observed and then exhibit a predominantly power-law decay in time. The electron fluxes were quite intense during the onset of the event with $\sim 10^4$ electrons $(cm^2 \text{ sec ster})^{-1}$ of energy > 350 keV measured at the peak of the event.

Particle Onsets

During the onset of the solar particle event, the IMP-G satellite was approaching the perigee of its orbit. The satellite entered the high latitude magnetosphere at ~0700 UT 2 November and remained within the magnetosphere until ~1300 UT on 3 November (D. H. Fairfield, private communication). The period when the satellite was within 10 earth radii (10 $R_E$) of the center of the earth is indicated on Figs. 1a-c by the heavy bars. At 1100 UT on 2 November (shortly after the particle onsets), the satellite was located ~18 $R_E$ from the earth at a solar-magnetosphere latitude of ~45° and longitude of ~125°. Hence, during the solar particle onset, the satellite was entering perigee ~35° behind the dawn meridian at high latitudes in the northern hemisphere.

Although the solar flare that produced the PCA event occurred behind the west limb and thus could not be optically classified, its onset time could nevertheless be estimated from optical, radio, and X-ray measurements (Thomas, 1970; Castelli, 1970). Evidence of the flare was first observed on November 2 optically at 0943 UT and in the 10 cm band at 0944 UT (Thomas, 1970). An X-ray burst was reported by Vela 3 beginning at 0934 UT (Thomas, 1970).

The solar particle enhancements at 1 a.u. occurred quite late after the flare with the first electrons not observed on Explorer 41 until ~1037 UT. The energetic protons began arriving even later. These time relationships are seen in Fig. 2 where high time resolution counting rates in two of the integral electron channels, and two of the differential proton channels are plotted for 0900-1400 UT on 2 November. Each data point represents a 9.28 second spin-averaged counting rate. An electron channel sample is made approximately once each 1.2 mins. The higher energy proton channel plotted in Fig. 2 is sampled as frequently as the electron channel. The lower energy proton channel is sampled once every ~5 mins.

The slow proton onsets measured by Explorer 41 at the beginning of the event, and the proton velocity dispersions seen in Fig. 2 could be due to proton delays in entering the distant magnetosphere from interplanetary space. Such delays would be compatible with the Vela satellite measurements of solar particles made in the magnetotail by Montgomery and

Singer (1969). In addition, there is evidence that the interplanetary proton fluxes increased more rapidly in intensity than did the proton fluxes measured by Explorer 41 (J. B. Blake, private communication).

In contrast to the proton measurements, the sharp onset profile of the electron fluxes suggest rapid access of these solar particles to the satellite location. Such a rapid access would be compatible with the observations of lower energy electrons (> 40 keV) rapidly entering the magnetotail (Lin and Anderson, 1966). The importance of these proton and electron measurements for studying solar particle access to the magnetosphere will be discussed in a future paper.

The relativistic electrons measured by Explorer 41 arrived essentially at the time of the first reported observations of riometer absorption between 1045-1055 at McMurdo (Masley et al., 1970) and at 1048 UT at both Thule (the magnetic pole) and Godhaven ($L \sim 20.5$) (Cormier, 1970). Excess cosmic noise absorption was observed to begin somewhat later, ~1100 UT, in the auroral zone at Churchill ($L \sim 8.6$; Cormier, 1970). It is clear from the quoted riometer onsets that the solar electrons played a major role in producing significant enhancements of polar cap ionization during the onset of the PCA event.

Alpha-to-Proton Ratios

The half-hour averaged alpha particle-to-proton ratios for four different values of equal particle energy

per nucleon are plotted in Fig. 3. Initially, the ratios are largest at the lowest energies. For example, at the beginning of 3 November, the ratio is ~0.13 for 2 MeV/nucleon particles and ~0.04 for 12 MeV/nucleon particles. Late in the event the ratios for all energies are approximately the same, equal to about 2% of the proton fluxes.

The alpha-to-proton fluxes plotted in Fig. 3 exhibit a distinctly different temporal structure than the same ratios measured following the west-limb flare of 18 November 1968 (Lanzerotti, 1970). This is due to the fact that, unlike the 1968 event, the solar cosmic rays from the 1969 event apparently propagated to the earth unaccompanied by a flare-produced shock wave. Such a shock disturbance apparently affects differently the propagation characteristics of alphas and protons of equal energy per nucleon. This effect was first noted by Lanzerotti and Robbins (1969) and Lanzerotti and Graedel (1970) and is currently being studied further.

The daily-averaged alpha-to-proton ratio measured during November 2-5 are plotted in Fig. 4 as a function of particle energy per nucleon. This figure clearly shows the relative enhancement of alphas at low energies early in the event. During the last two days plotted, the alpha-to-proton ratio is ~0.02 at all energies measured.

Particle Spectra

Half-hour average proton, alpha particle, and electron spectra are plotted in Fig. 5 for three different

periods during the PCA event. On November 3 and 4 both the proton and the alpha particle spectra had approximately power-law spectral dependences, particularly at the higher energies. However, the spectra of November 2 indicate a positive energy slope (in the case of the alphas) and definite evidence of a spectral turnover with a peak at ~7.5 MeV (in the case of protons). A turnover in both the alpha particle and proton spectra is observed until ~1100 UT November 3.

The gradual change with time of the proton spectra and the peak in intensity during November 3 is shown in Fig. 6 where six one-half hour average spectra are plotted. Another unusual aspect of these proton spectra is that not only is a peak (which shifts to lower energies in time) observed, but the spectra also turns upward at the lowest energy measured. (This increase in the proton spectra at ~500 keV has also been observed in the solar particles measured over the polar caps during this event; J. B. Blake, private communication). These spectra are currently being studied in terms of particle access to the magnetosphere as well as propagation mechanisms at the sun and in interplanetary space.

The three-point electron spectra measured by Explorer 41 during the event could be well represented by an exponential spectral representation

$$J(>E) = J_o(E_o)\exp(-E/E_o)(\text{cm}^2 \text{ sec ster})^{-1} \qquad (1)$$

over the energy range measured (c.f. Fig. 5). The spectra were quite hard early in the event ($E_o \sim 0.5$ MeV) and softened during the later days of the event ($E_o \sim 0.3$ MeV). For the riometer calculations considered in the following section, it was assumed that exponential electron spectra such as those of Fig. 5 could be extrapolated to zero energy.

Solar electrons of relativistic energies ($\gtrsim 1$ MeV) have been commonly represented quite well by power law spectral shapes (Cline and McDonald, 1968; Simnett, 1971). However, when electron fluxes from some events have been plotted for particle energies $\lesssim 1$ MeV, the spectra appear to change slope and have less steep energy dependencies (Simnett, 1971). Hence, the measured electron spectra in this event may be more like exponential distributions than power law distributions at the lower energies.

## CALCULATED RIOMETER RESPONSE

### Electrons

It was assumed that the measured solar electrons had unimpeded access to the earth's polar regions. From the work of Vampola (1971) and West and Vampola (1971) it would seem that this is a valid assumption, at least for solar electrons of energies as low as ~70 keV (the lowest energies measured and reported to date).

The expected riometer absorption due to these electrons was then determined from the daytime vertical-incidence 30 MHz absorption calculation results presented by Bailey (1968). Bailey calculated the expected absorption for auroral electrons assuming exponential energy spectra for the precipitating particles. As such, he presented results for relatively soft electron spectra ($E_o \leq 150$ keV). However, since his results showed that the absorption A(dB) could be given by

$$A(dB) = B\sqrt{J(>E_{min})} \qquad (2)$$

where B is a proportionality factor dependent upon $E_{min}$, it is possible to extend Bailey's work to the hard spectrum solar electrons discussed here.

The proportionality factor B for electrons in Eq. (2) can be obtained from Bailey's absorption calculation results which are plotted as a function of incident particle flux (for values of $E_o$ = 20, 40, 60, 100 and 150 keV). The

relationship between the particle flux required to produce 0.1 dB absorption and the e-folding spectral energy $E_o$ was determined from Bailey's results to be given by a power-law expression

$$J(.1\ \mathrm{dB}, E_o) \sim 1.5 \cdot 10^7 E_o^{-2.8} \qquad (3)$$

where $J(.1\ \mathrm{dB}, E_o)$ has dimensions of electrons $(\mathrm{cm}^2\ \mathrm{sec\ ster})^{-1}$ and $E_o$ is in keV. Using this relationship, the expected riometer absorption in Eq. (2) can be written as

$$A(\mathrm{dB}) = \sqrt{\frac{0.01\ J_o}{J(.1\ \mathrm{dB}, E_o)}} \qquad (4)$$

where $J_o$ is the measured electron flux extrapolated to E = 0 and

$$B(E > 0) = 2.6 \cdot 10^{-5} E_o^{1.4}\ \mathrm{db}(\mathrm{cm}^2\ \mathrm{sec\ ster})^{\frac{1}{2}} .$$

The values of $E_o$ and $J_o$ were determined from the measured half-hour averaged electron spectra during the first five hours of the event. After that time, the hourly-averaged spectra were used. The estimates of the expected riometer absorption using Eqs. (3) and (4) and the measured (extrapolated) values of $E_o$ $(J_o)$ were multiplied by 1.6 in order to obtain the approximate absorption that would be observed by a broad-beam riometer such as that at McMurdo

(Bailey, 1968). These results are plotted as open circles in Fig. 7a.

The calculations show that the measured integral electron fluxes are expected to produce significant absorption (~1 dB) during the period 1030-1100 UT. The calculated solar electron-produced absorption increases to a peak value of ~10 dB between 1230-1300 UT and then decreases during the remainder of the event.

Protons and Alphas

As indicated in the introduction, good agreement has been achieved recently between the observed riometer absorption and that calculated due to solar protons using magnetoionic theory and an appropriate ionosphere model (Potemra et al., 1967, 1969, 1970). In addition, in the past a number of workers have investigated an empirical relationship of the form of Eq. (2) between the measured solar proton fluxes and the measured absorption (Fichtel et al., 1963; Van Allen et al., 1964; Juday and Adams, 1969; Reid, 1969, 1970a). Potemra and Lanzerotti (1971) were able to determine the proportionality factor B in Eq. (2) for seven values of $E_{min}$ (5, 10, 15, 20, 25, 30, and 50 MeV). They found Eq. (2) to give an excellent fit to the data for all values of $E_{min}$ and concluded that this was due to the fact that the proton spectrum did not change appreciably during the event they analyzed.

Potemra (1971) has recently calculated, using the results of Potemra et al. (1967, 1969), the proportionality

factor B as a function of $\gamma$, the power-dependence in the proton differential spectrum when expressed as a power-law in energy

$$\frac{dJ(E)}{dE} \propto E^{-\gamma}. \tag{5}$$

He found that for a power-law proton spectrum, B was essentially independent of spectral shape (independent of $\gamma$) for $E_{min} \sim 7$ MeV. He found that

$$A(dB) = 0.083\sqrt{2\pi J(E > 7\ MeV)} \tag{6}$$

The relationship in Eq. (6) was used to calculate the expected riometer absorption due to the solar protons measured by Explorer 41 incident on the polar ionosphere. As in the case of the electrons, it was assumed that these solar protons had free access to the polar caps. This is not always true, of course, as frequently substantial asymmetries between north and south polar fluxes and the interplanetary fluxes are observed during an event (see, e.g., recent reviews by Bostrom, 1970, and Paulikas et al., 1970).

The differential proton fluxes from the Bell Laboratories Explorer 41 experiment were used together with the integral fluxes of protons > 30 MeV and > 60 MeV measured by the monitoring experiment on the same satellite

(Solar-Geophysical Data, 1970) to give proton spectra from 0.5 to 60 MeV. The hourly average integral proton spectra for protons > 7 MeV were computed from these spectra. These computed integral spectra were used together with Eq. (6) to give the expected riometer absorption due to the protons. These values of the absorption are plotted as solid points in Fig. 7a.

It is seen from Fig. 7a that electrons produce more absorption than the protons until hour 17 on 2 November. After that time, the protons are the dominant producers of the excess ionosphere ionization for the remainder of the event.

Equal fluxes of alpha particles and protons of the same energy per nucleon will produce the same amount of excess ionosphere absorption (e.g., Adams and Masley, 1966). From the data of Figs. 3 and 4, it is clear that the integral alpha intensities for alphas of energy > 7 MeV/nucleon are only a few percent of the proton intensities during this event. Hence, the alphas contributed less than 1 dB to the total absorption at the beginning of the event and substantially less later.

Total Absorption

The sum of the calculated electron and proton riometer absorption for the November 1969 event (Fig. 7a) are plotted in Fig. 7b together with the absorption measured at McMurdo. The most striking result in Fig. 7b, of course,

is the fact that the peak absorption observed near the beginning of the event can only be accounted for by including the substantial fluxes of solar electrons. Substantial deviation (~1-4 dB) between the calculated and the observed absorption is seen after the peak for the remainder of 2 November. However, for the duration of the event, beginning ~0600 on 3 November, the general agreement between the calculations and the observations is satisfactory with the calculated total absorption being somewhat higher than the observed absorption.

## DISCUSSION

The most significant result of this study is the conclusion that intense fluxes of solar electrons incident on the polar ionosphere early in the event provided approximately one-half the total measured polar cap absorption during the first few hours of the event. The electrons appear to have contributed a finite amount of ionization for producing the measured polar cap absorption throughout the event.

It should be stressed that the calculated electron absorption in this paper was determined from the work of Bailey (1968) rather than by use of an empirical relationship between the measured absorption and electron precipitation such as has been derived by Jelly et al. (1964), Parthasarathy et al. (1966), or Hakura (1969). This was done because the empirical relationships in these references were obtained for electrons of energy > 40 keV without reference to their spectral e-folding energies $E_o$. Bailey (1968) finds a strong energy dependence to the proportionality constant B (Eq. 2), with B approaching unity for fluxes > 40 keV and $E_o \sim 300$ keV (in contrast to an empirical $B \sim 10^{-3}$ for $E_o \sim$ 10-100 keV as determined by Jelly et al., 1964; Parthasarathy et al., 1966 and Hakura, 1969). All of the high-energy electron spectra measured during this event had values of $E_o \gtrsim 250$ keV.

From the measured alpha flux-to-proton flux ratios, it was concluded that the solar alpha particles never

contributed more than a few percent to the total measured absorption. This conclusion would hold for other PCA events where alpha particle fluxes have been reported in detail (e.g., Lanzerotti and Robbins, 1969; Lanzerotti, 1970).

The expected absorption was not calculated from solar fluxes measured directly over the polar caps station. Hence, it is reasonable that perfect agreement was not achieved between the calculated and observed values. A large discrepancy between the calculated and the measured absorption was obtained for about one-half day after the peak of the event. This is not understood and could be due to one or more of the factors discussed below.

a) The discrepancy was observed during part of the period when a peak was observed in the proton spectra. Hence, the discrepancy could be due to the use of Eq. (6) (derived for pure power-law spectra) for computing the proton absorption during this time. To investigate this possibility, the absorption was computed from the integral proton intensities with $E_{min}$ = 10 MeV and 15 MeV. Above both of these $E_{min}$ values the spectra were essentially power-law dependent in energy. The values of the Eq. (2) proportionality constant B were obtained from Potemra (1971) for each value of $\gamma$ and $E_{min}$. The proton absorption values obtained in this way were essentially the same as those plotted in Fig. 7a.

b) Another possibility for the discrepancy could arise from an invalidity of the extrapolation of the electron spectra to zero energy. This extrapolation could also cause

the smaller deviations between the calculated and observed absorption during the period from 1200 UT 3 November to 6 November. There is no way to definitely decide this question without detailed electron spectral measurements at lower energies.

c) A substantial part of the excess calculated absorption occurs during the perigee pass of the satellite when the satellite is $\lesssim$ 10 $R_E$ from the center of the earth and probably close to, or within, the radiation belts. The magnetosphere would tend to shield the satellite from the solar fluxes and thus cause the calculated proton absorption to be too low. However, a portion of the electron fluxes measured near perigee could be due to the radiation belts and thus cause too large a calculated electron absorption. This latter possibility, although quite attractive as an explanation for the excess calculated absorption, is impossible to definitely confirm. All that can be concluded is that both the solar electron rates outside the magnetosphere and the electron rates during the perigee pass on 2 November are comparable to trapped magnetosphere electron rates measured during non-solar event perigee passes.

d) A final possibility for the discrepancy could be due to changes in the accessibility of the solar electrons and/or protons to the south polar region. In particular, the fluxes of polar cap protons are frequently observed to be less than those measured in interplanetary space (e.g.,

Bostrom, 1970; Paulikas et al., 1970). If this were the case in this event, then the proton absorption calculated and plotted in Fig. 7a would be too large. There is evidence, from a polar-orbiting satellite, of easier access of the lower energy protons to the north polar region later in 2 November (J. B. Blake, private communication). Such an asymmetry might contribute to the discrepancy observed.

In conclusion, it should be stressed that it is not possible to ignore the importance of hard-spectra solar electrons for producing significant early PCA riometer absorption following some solar fluxes. It would be of great value to study other PCA events that have occurred when the sun-earth propagation path was such that the electrons arrived appreciably prior to the protons. In addition to studying which flares produce copious fluxes of relativistic electrons, future investigations should consider the solar longitude of the parent flare to determine which longitudes tend to give rise to the greatest time differences between the arrival of the electrons and protons.

## ACKNOWLEDGMENTS

We would like to thank J. B. Blake and A. L. Vampola (Aerospace Corporation), J. B. Reagan (Lockheed Research Labs), and T. A. Potemra (Applied Physics Laboratory) for profitable

discussions of various aspects of this event and T. E. Graedel (Bell Labs) for comments on the manuscript.

## REFERENCES


Adams, G. W., and A. J. Masley, Theoretical study of cosmic noise absorption due to solar cosmic radiation, Planet. Space Sci., 14, 277, 1966.

Bailey, D. K., Disturbances in the lower ionosphere observed at VHF following the solar flare of 23 February 1956 with particular reference to auroral zone absorption, J. Geophys. Res., 62, 431, 1957.

Bailey, D. K., Some quantitative aspects of electron precipitation in and near the auroral zone, Rev. Geophys., 6, 289, 1968.

Bostrom, C. O., Entry of low energy solar protons into the magnetosphere, Intercorrelated Satellite Observations Related to Solar Events, ed. V. Manno and D. E. Page (D. Reidel, Holland), 229, 1970.

Castelli, J. P., Microwave burst spectra and PCA's, Proc. Meeting on Operation PCA 69, AFCRL-70-0625, pg. 19, October 1970.

Cline, T. L. and F. B. McDonald, Relativistic electrons from solar flares, Solar Phys., 5, 507, 1968.

Cormier, R. J., Riometer observations during PCA's, Proc. meeting on Operation PCA 69, AFCRL-70-0625, pg. 21, October 1970.

Fichtel, C. E., D. E. Guss, and K. W. Ogilvie, Solar Proton Manual, ed. F. B. McDonald, NASA Report, NASA-TRR-169, 1963.

Hakura, Y., Entry of solar cosmic rays into the polar cap atmosphere, J. Geophys. Res., 72, 1461, 1967.

Hakura, Y., The polar cap absorption on 7-10 July 1966, Annals IQSY, 3, 337, 1969.

Jelly, D. H., I. B. McDiarmid and J. R. Burrows, Correlation between intensities of auroral absorption and precipitated electrons, Canadian J. Physics, 42, 2411, 1964.

Juday, R. D. and G. W. Adams, Riometer measurements, solar proton intensities and radiation dose rates, Planet. Space Sci., 17, 1313, 1969.

Lanzerotti, L. J., Protons, alpha particles, and electrons resulting from the 18 November 1968 solar flare, World Data Center A, Report UAG-9, 34, April 1970.

Lanzerotti, L. J., and T. E. Graedel, Observations of solar electron, proton and alpha particle propagation, Bull. Am. Phys. Soc., 15, 610, 1970.

Lanzerotti, L. J., H. P. Lie, and G. L. Miller, A satellite solar cosmic ray spectrometer with on-board particle identification, I.E.E.E. Trans. Nucl. Sci., NS-16(1), 343, 1969.

Lanzerotti, L. J., and M. F. Robbins, Solar flare alpha to proton ratio changes following interplanetary disturbances, Solar Phys., 10, 212, 1969.

Lin, R. P., and K. A. Anderson, Evidence for connection of geomagnetic tail lines to the interplanetary field, J. Geophys. Res., 71, 4213, 1966.

Masley, A. J., and A. D. Goedeke, The 7 July 1966 solar cosmic-ray event, Annal IQSY, 3, 353, 1969.

Masley, A. J., J. W. McDonough, and P. R. Satterblom, Solar cosmic-ray observations during 1969, Antarctic J. of the U.S., 5, 172, 1970.

Montgomery, M. D. and S. Singer, Penetration of solar energetic protons into the magnetotail, J. Geophys. Res., 74, 2869, 1969.

Parthasarathy, R., F. T. Berkey, and D. Venkatesan, Auroral zone electron flux and its relation to broadbeam radiowave absorption, Planet Space Science, 14, 65, 1966.

Paulikas, G. A., J. B. Blake, and A. L. Vampola, Solar particle observations over the polar caps, Intercorrelated Satellite Observations Related to Solar Events, ed. V. Manno and D. E. Page (D. Reidel, Holland), 193, 1970.

Potemra, T. A., The empirical connection of riometer absorption to solar protons during PCA events, submitted to J. Geophys. Res., 1971.

Potemra, T. A., and L. J. Lanzerotti, Equatorial and precipitating solar protons in the magnetosphere, 2. Riometer observations, J. Geophys. Res., 76, 1971.

Potemra, T. A., A. J. Zmuda, B. W. Shaw, and C. R. Haave, VLF phase disturbances, HF absorption, and solar protons in the PCA events of 1967, Radio Science, 5, 1137, 1970.

Potemra, T. A., A. J. Zmuda, C. R. Haave, and B. W. Shaw, VLF phase disturbances, HF absorption, and solar protons in the events of August 28 and September 2, 1966, J. Geophys. Res., 74, 6444, 1969.

Potemra, T. A., A. J. Zmuda, C. R. Haave, and B. W. Shaw, VLF phase perturbations produced by solar protons in the event of February 5, 1965, J. Geophys. Res., 72, 6077, 1967.

Reid, G. C., Associate detachment in the mesosphere and the diurnal variation of polar cap absorption, Planet. Space Sci., 17, 731, 1969.

Reid, G. A., Current problems in polar cap absorption, Intercorrelated Satellite Observations Related to Solar Events, ed. V. Manno and D. E. Page (D. Reidel, Holland), 319, 1970a.

Reid, G. A., The energetic particle environment of the polar caps, J. Franklin Inst., 290, 197, 1970b.

Simnett, G. M., Relativistic electrons from the sun observed by IMP-4, Inst. of Geophys. and Planetary Phys. Report, Univ. of California, Riverside, April, 1971.

Solar-Geophysical Data, U. S. Dept. Commerce, Boulder, Colorado, Number 309, Part II, May 1970.

Thomas, C. J., History and characteristics of the active solar region that caused the proton event of 2 November 1969, Proc. Meeting on Operation PCA 69, AFCRL-70-0625, pg 15, October 1970.

Vampola, A., Access of solar electrons to closed field lines, J. Geophys. Res., 76, 36, 1971

Van Allen, J. A., W. C. Lin, and H. Leinbach, On the relationship between absolute cosmic ray intensity and riometer absorption, J. Geophys. Res., 69, 4481, 1964.

West, H. I., Jr., and A. L. Vampola, Simultaneous observations of solar flare electron spectra in interplanetary space and within the earth's magnetosphere, Phys. Rev. Letters, 26, 458, 1971.

## FIGURE CAPTIONS

Fig. 1a One-half hour average proton fluxes measured on Explorer 41 during the 2 November 1969 solar event. The heavy lines on November 2-3 and 6 indicate the intervals when the satellite was within 10 $R_E$ of the earth.

Fig. 1b One-half hour average alpha particle fluxes measured on Explorer 41 during the 2 November 1969 solar event. The heavy lines on November 2-3 and 6 indicate the intervals when the satellite was within 10 $R_E$ of the earth.

Fig. 1c One-half hour average electron fluxes measured on Explorer 41 during the 2 November 1969 solar event. The heavy lines on November 2-3 and 6 indicate the intervals when the satellite was within 10 $R_E$ of the earth.

Fig. 2 Particle onsets at the beginning of the event as measured in two electron and two proton channels. The data points in the two electron channels and the higher energy proton channel represent 9.28 sec averages taken approximately once a minute; the lower energy proton points are 9.28 sec averages taken once each five minutes.

Fig. 3 One-half hour alpha flux-to-proton flux ratios for the 2 November 1969 solar event.

Fig. 4 Daily-average alpha flux-to-proton flux ratios as a function of particle energy per nucleon.

Fig. 5 One-half hour average alpha, proton, and electron spectra measured between 1230-1300 UT on November 2, 3, and 4.

Fig. 6 Six one-half hour proton spectra measured during the first half of 3 November showing the slow disappearance of the peak in the proton spectra.

Fig. 7a Riometer absorption calculated from the proton and electron fluxes measured by Explorer 41 during the 2 November event.

Fig. 7b Total calculated proton- and electron-produced riometer absorption (from 7a) and the absorption observed at McMurdo during the event. The heavy lines indicate the period when the satellite was within 10 $R_E$ of the earth.

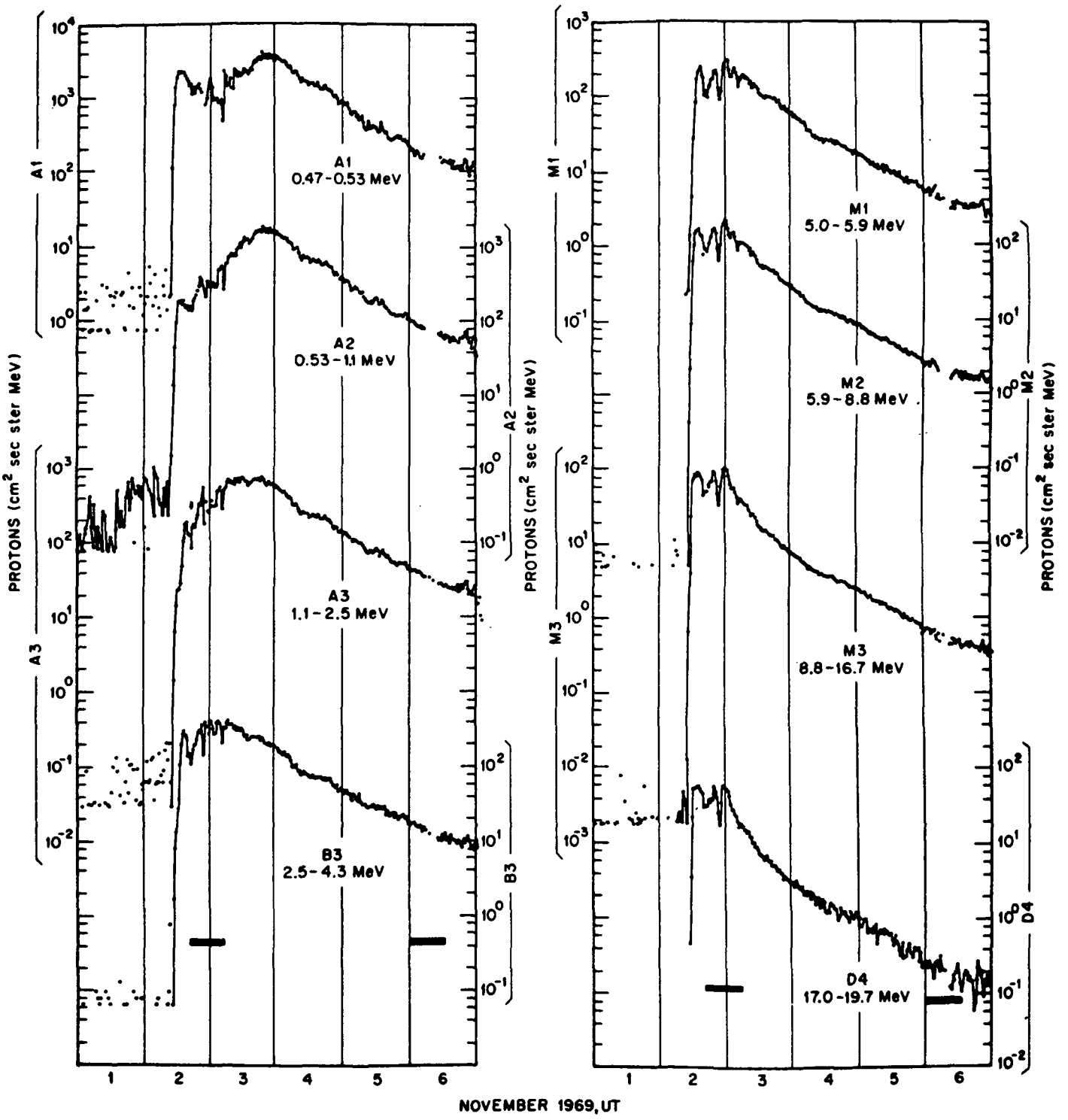
A1
0.47-0.53 MeV
A2
0.53-1.1 MeV
A3
1.1-2.5 MeV
B3
2.5-4.3 MeV
M1
5.0-5.9 MeV
M2
5.9-8.8 MeV
M3
8.8-16.7 MeV
D4
17.0-19.7 MeV
PROTONS (cm² sec ster MeV)
NOVEMBER 1969, UT

Figure 1a

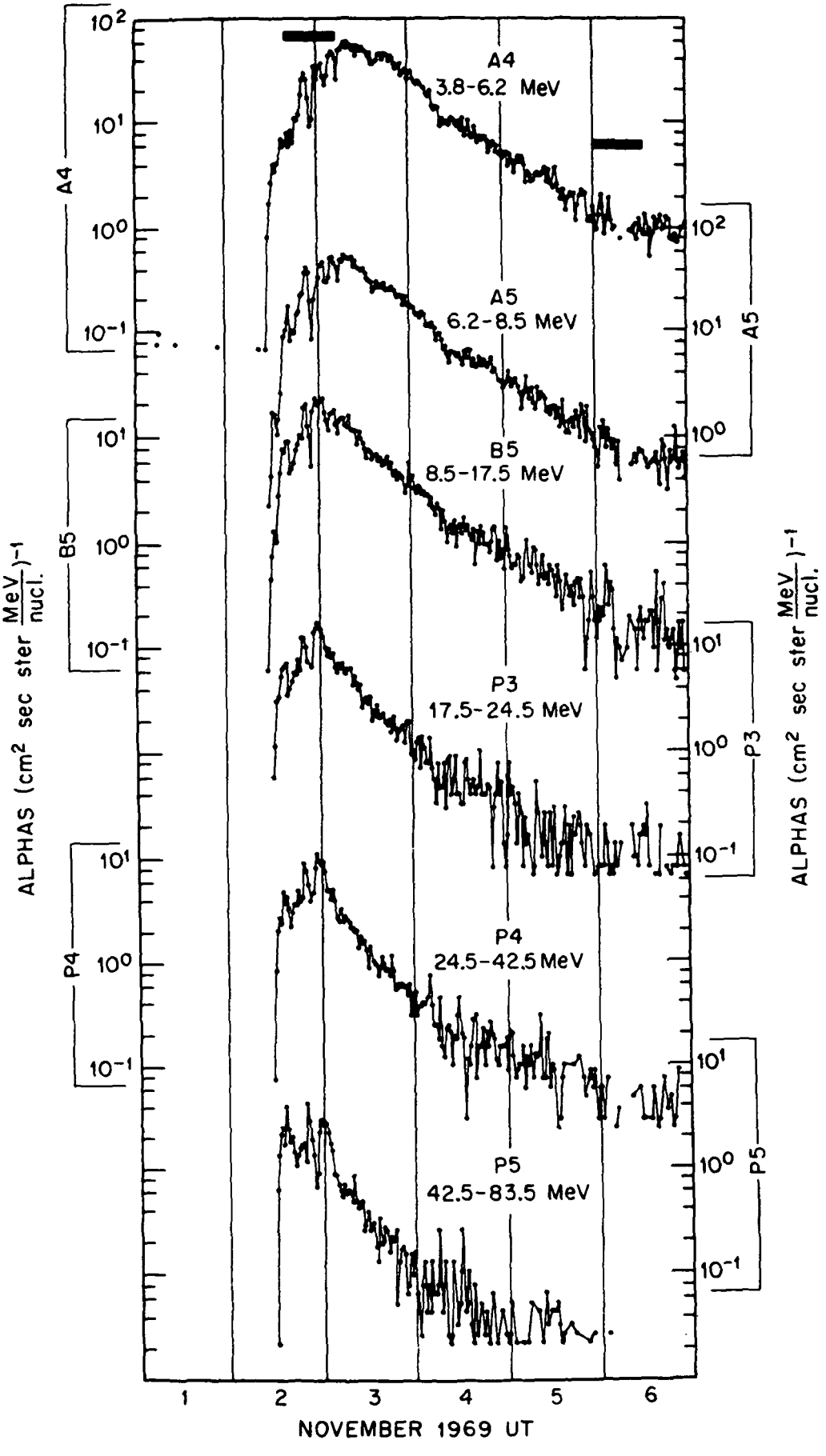
A4
3.8-6.2 MeV
A5
6.2-8.5 MeV
B5
8.5-17.5 MeV
P3
17.5-24.5 MeV
P4
24.5-42.5 MeV
P5
42.5-83.5 MeV
ALPHAS (cm² sec ster MeV/nucl.)⁻¹
NOVEMBER 1969 UT
1
2
3
4
5
6

Figure 1b

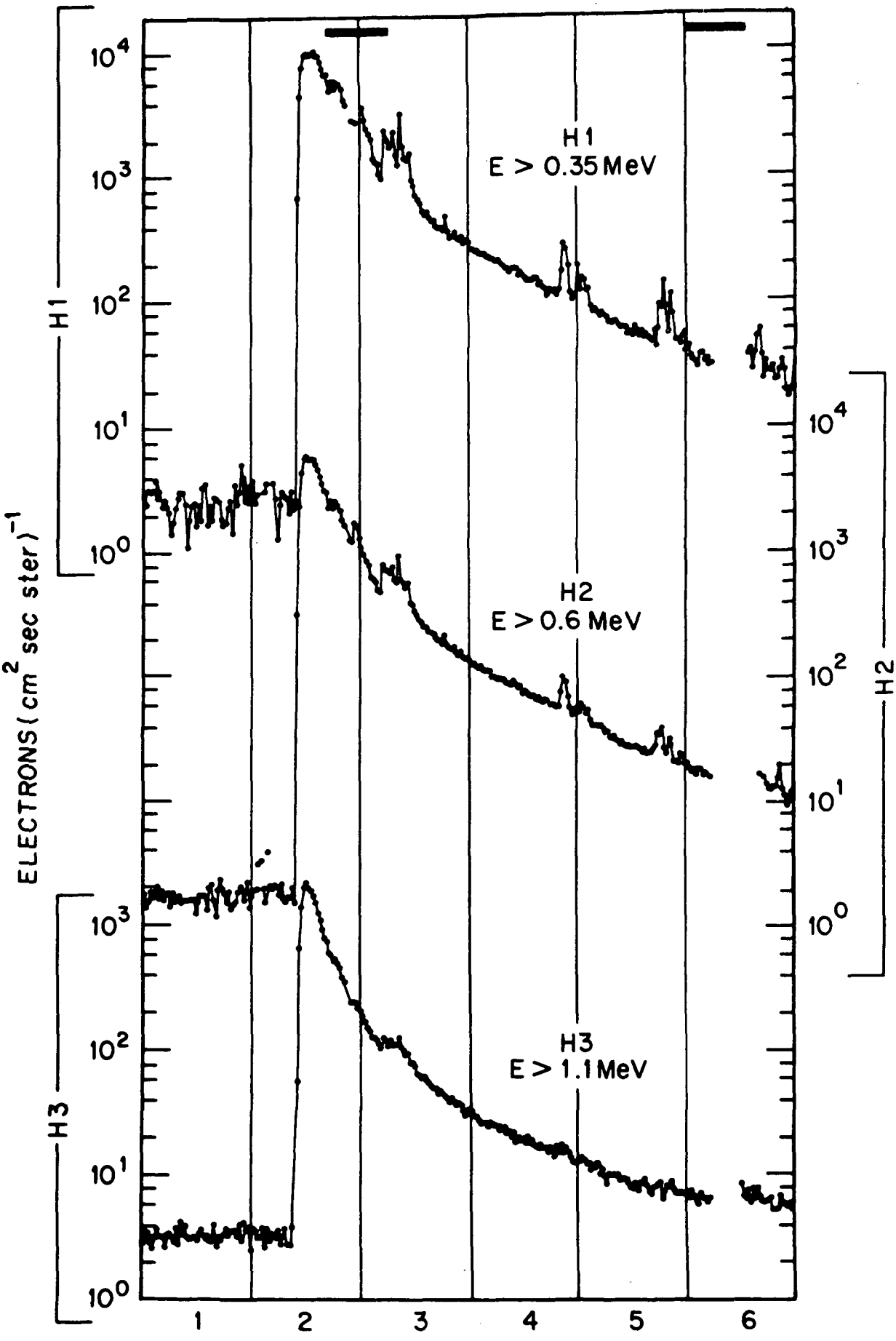
H1
E > 0.35 MeV
H2
E > 0.6 MeV
H3
E > 1.1 MeV
ELECTRONS (cm² sec ster)⁻¹
H1
H2
H3
10⁴
10³
10²
10¹
10⁰
1
2
3
4
5
6
NOVEMBER 1969 UT

Figure 1c

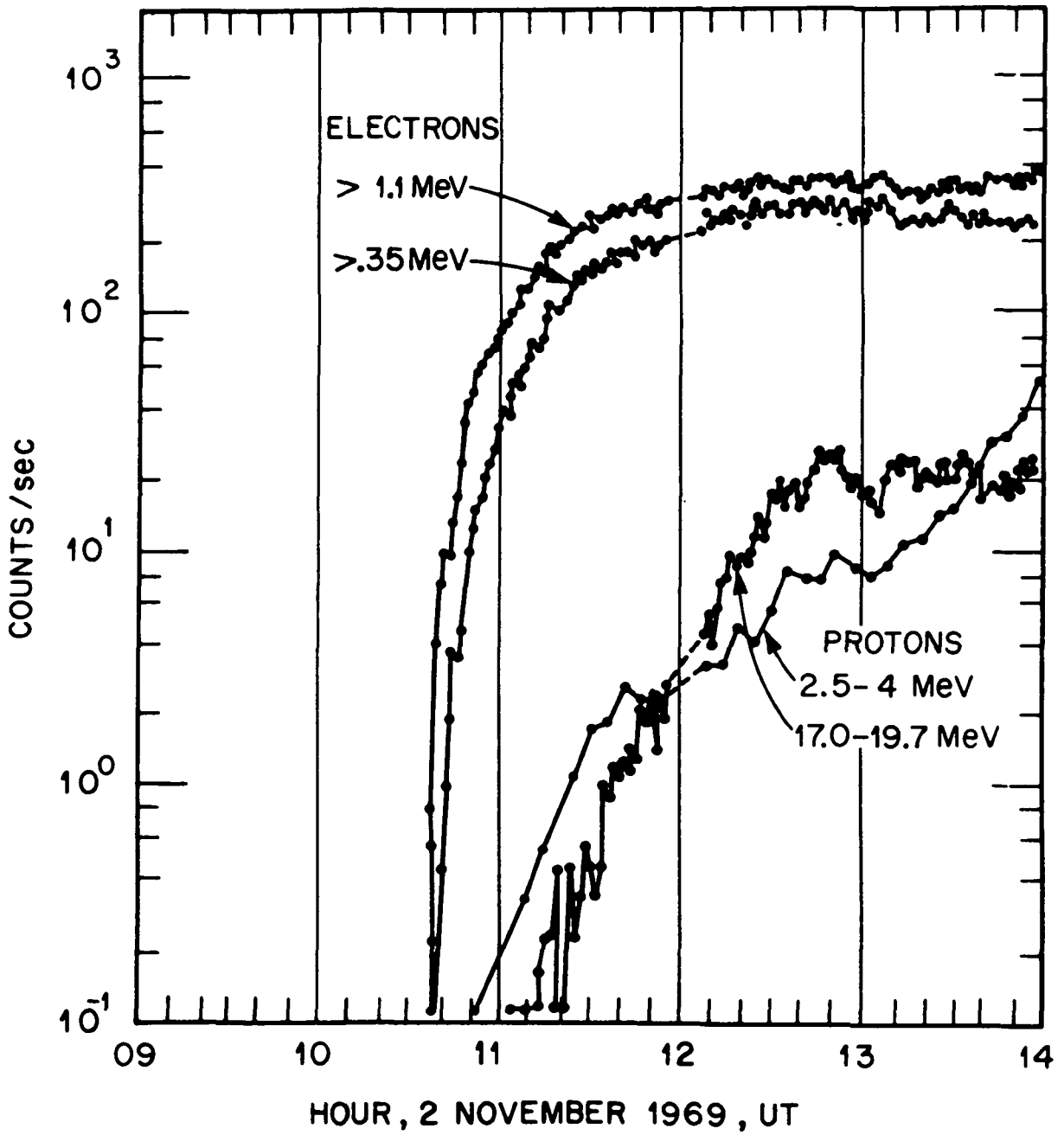
ELECTRONS
> 1.1 MeV
>.35 MeV
PROTONS
2.5-4 MeV
17.0-19.7 MeV
COUNTS/sec
HOUR, 2 NOVEMBER 1969, UT

Figure 2

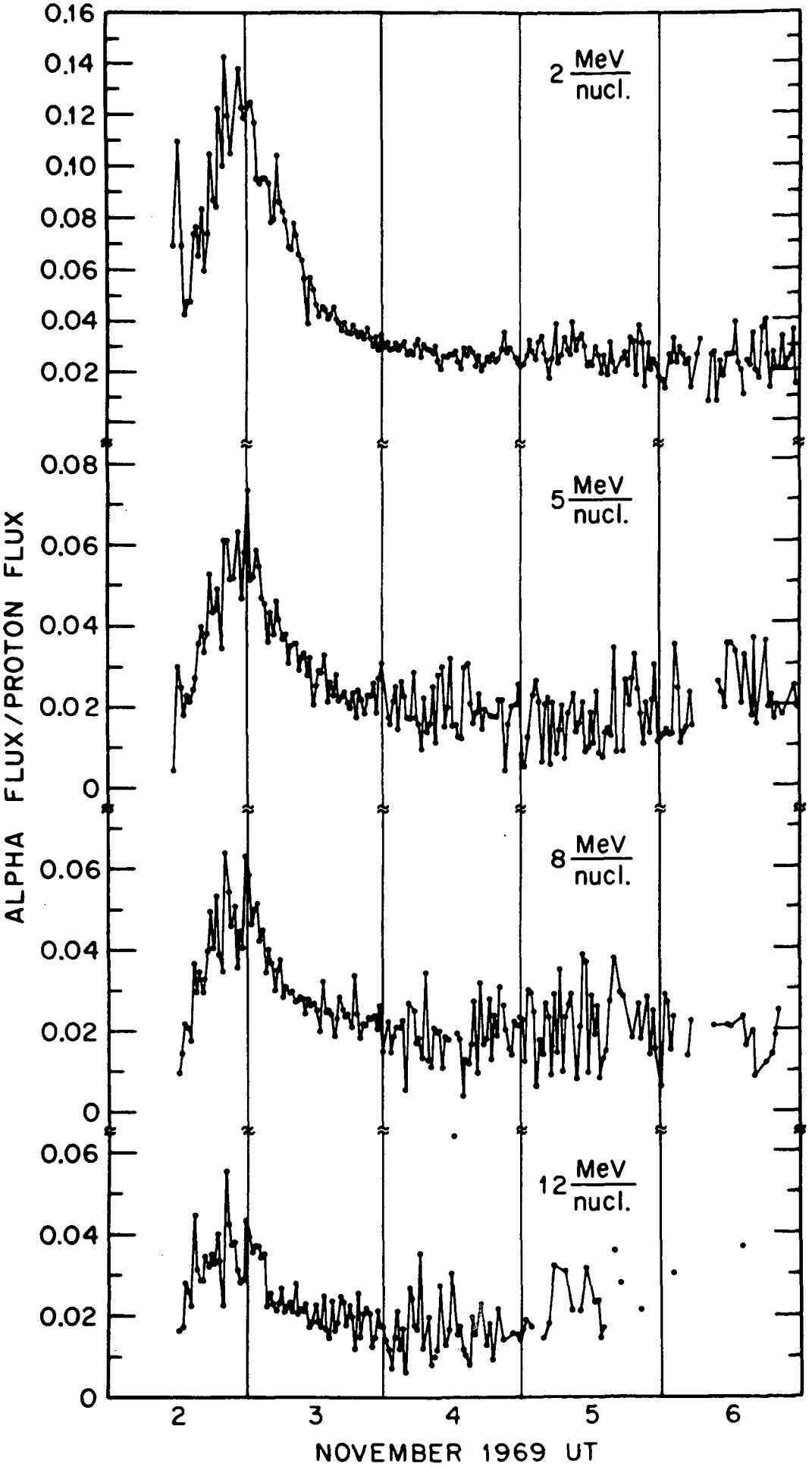
0.16
0.14
0.12
0.10
0.08
0.06
0.04
0.02
2 MeV/nucl.
0.08
0.06
0.04
0.02
0
5 MeV/nucl.
0.06
0.04
0.02
0
8 MeV/nucl.
0.06
0.04
0.02
0
12 MeV/nucl.
ALPHA FLUX/PROTON FLUX
2
3
4
5
6
NOVEMBER 1969 UT

Figure 3

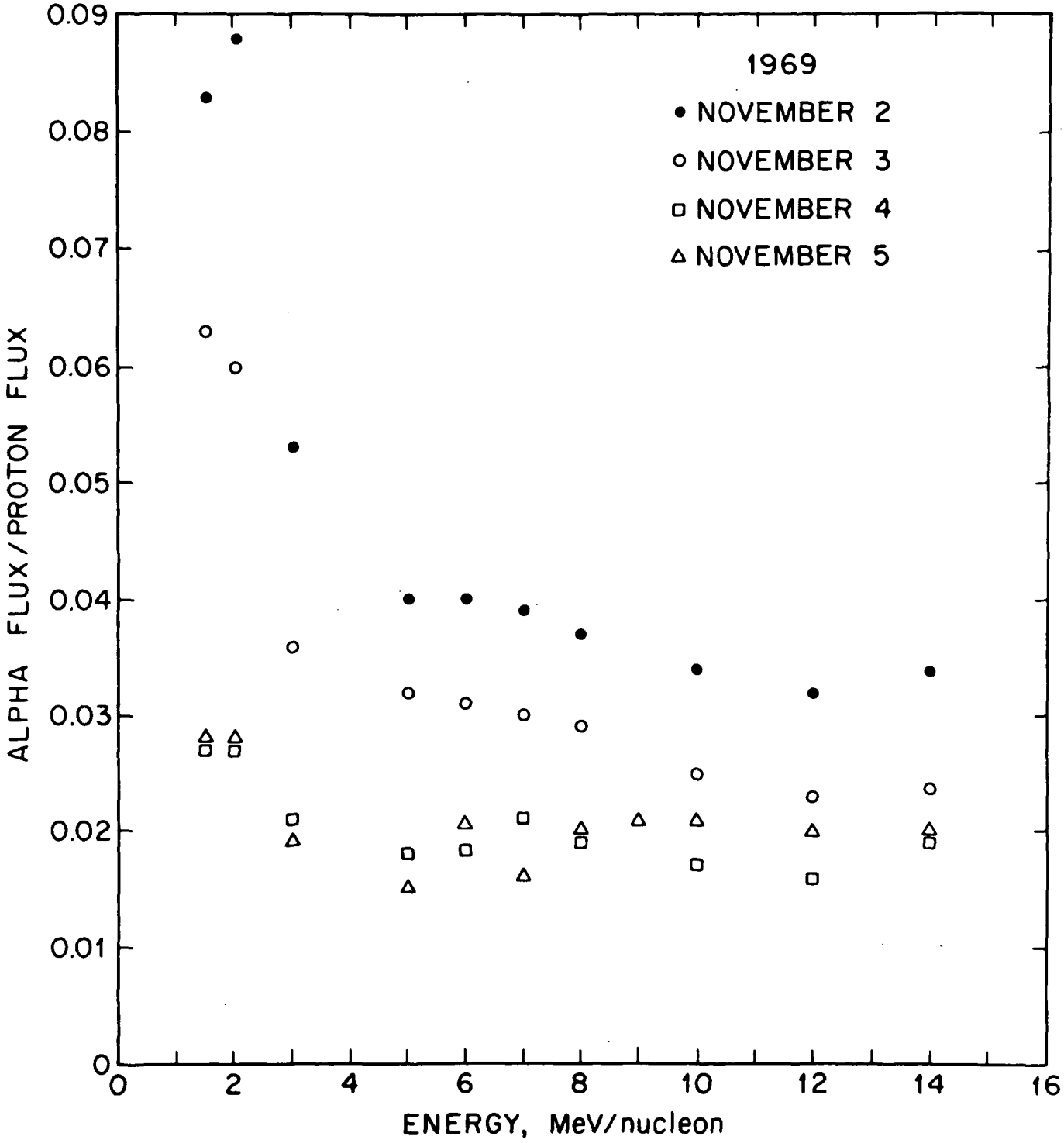
1969
• NOVEMBER 2
o NOVEMBER 3
□ NOVEMBER 4
△ NOVEMBER 5
ALPHA FLUX/PROTON FLUX
ENERGY, MeV/nucleon
0.09
0.08
0.07
0.06
0.05
0.04
0.03
0.02
0.01
0
0
2
4
6
8
10
12
14
16

Figure 4

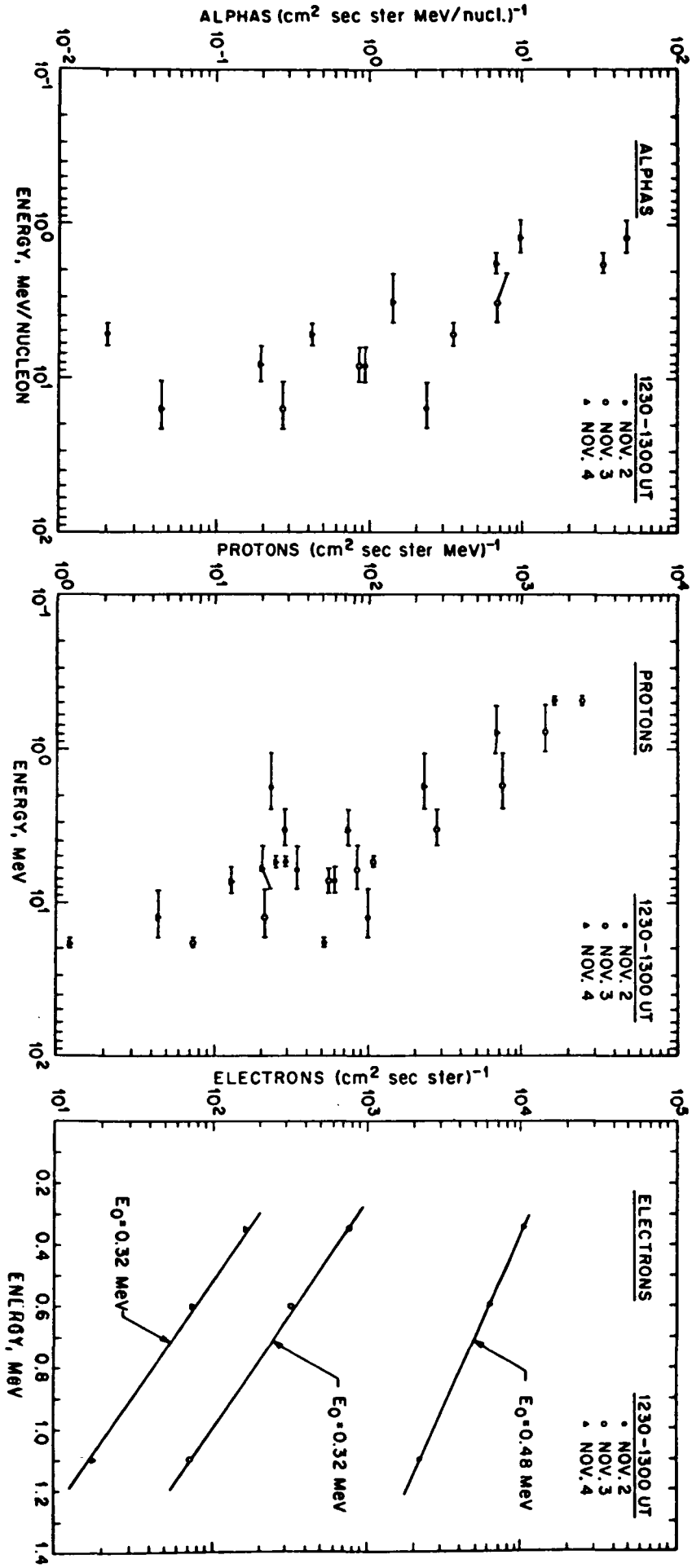
ALPHAS (cm² sec ster MeV/nucl.)⁻¹
ENERGY, MeV/NUCLEON
ALPHAS
1230–1300 UT
• NOV. 2
○ NOV. 3
▲ NOV. 4
PROTONS (cm² sec ster MeV)⁻¹
ENERGY, MeV
PROTONS
1230–1300 UT
• NOV. 2
○ NOV. 3
▲ NOV. 4
ELECTRONS (cm² sec ster)⁻¹
ENERGY, MeV
ELECTRONS
1230–1300 UT
• NOV. 2
○ NOV. 3
▲ NOV. 4
E₀=0.32 MeV
E₀=0.32 MeV
E₀=0.48 MeV

Figure 5

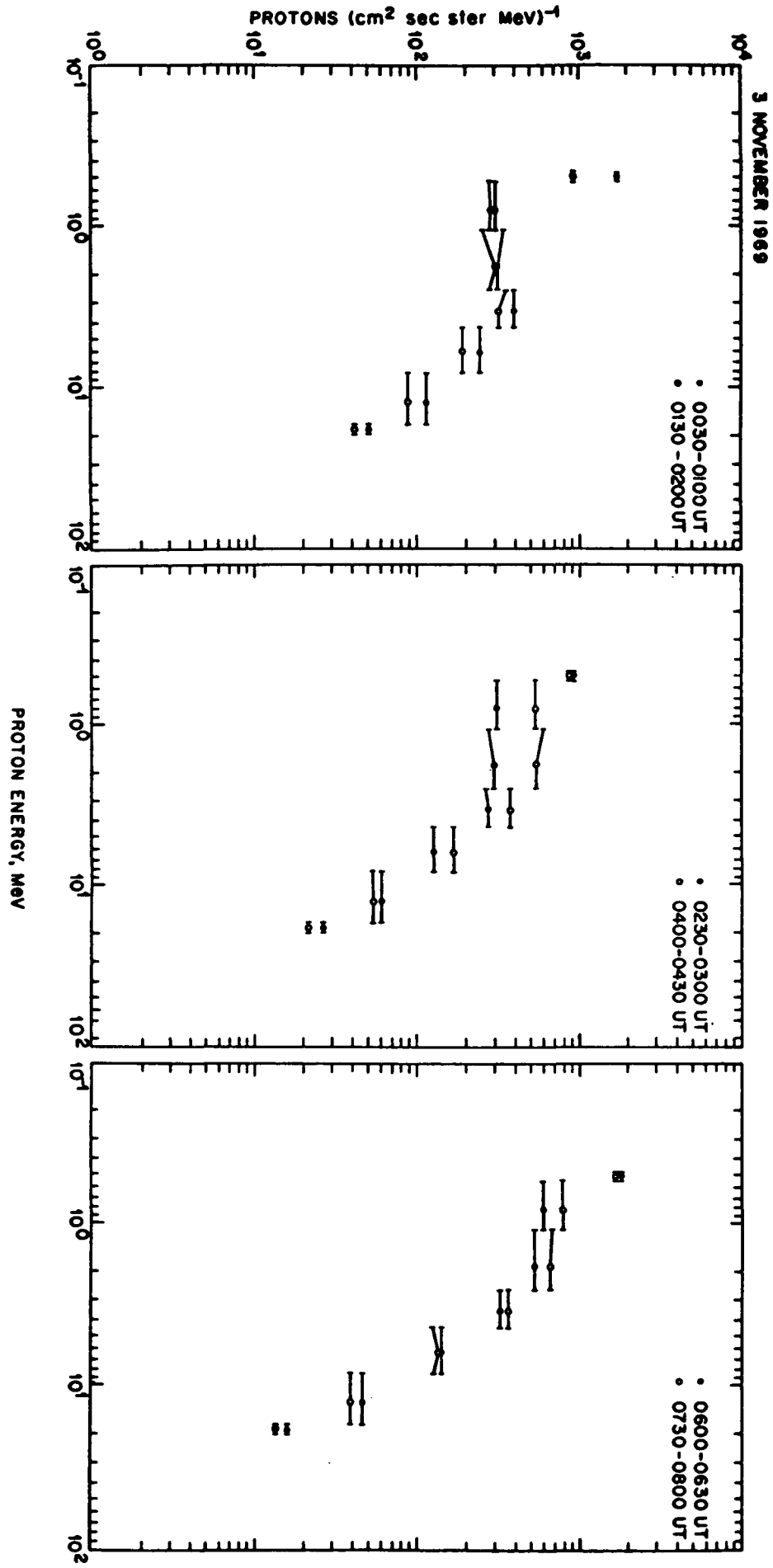
PROTONS (cm² sec ster MeV)⁻¹
3 NOVEMBER 1969
PROTON ENERGY, MeV
• 0030-0100 UT
• 0130-0200 UT
• 0230-0300 UT
• 0400-0430 UT
• 0600-0630 UT
• 0730-0800 UT

Figure 6

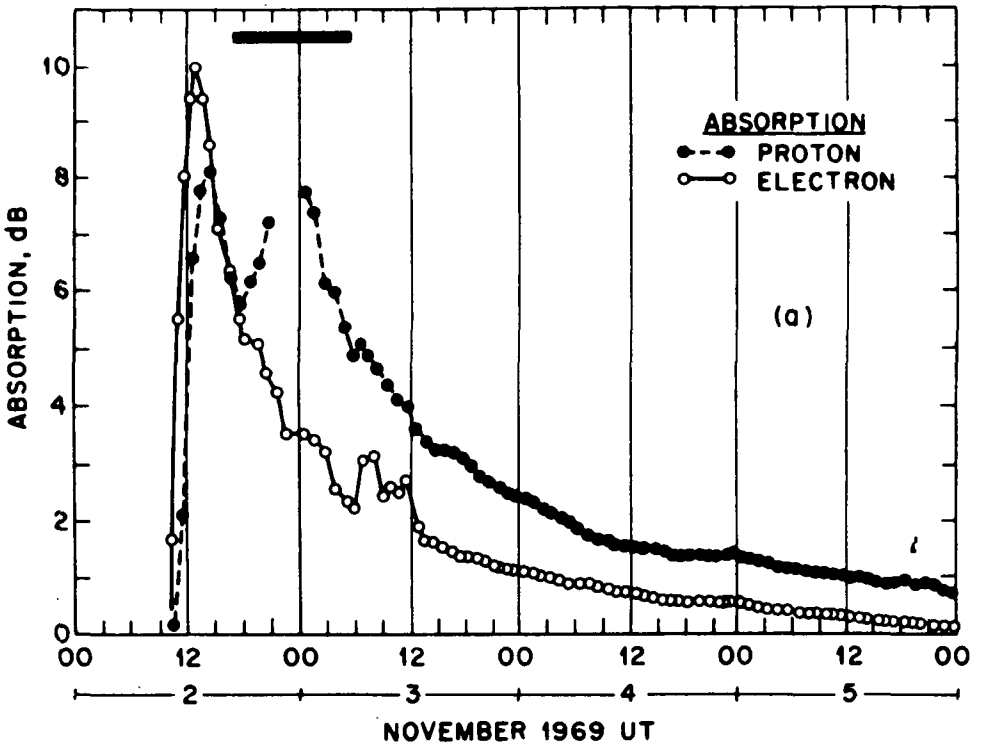
ABSORPTION
PROTON
ELECTRON
(a)
ABSORPTION, dB
0
2
4
6
8
10
00
12
00
12
00
12
00
12
00
2
3
4
5
NOVEMBER 1969 UT

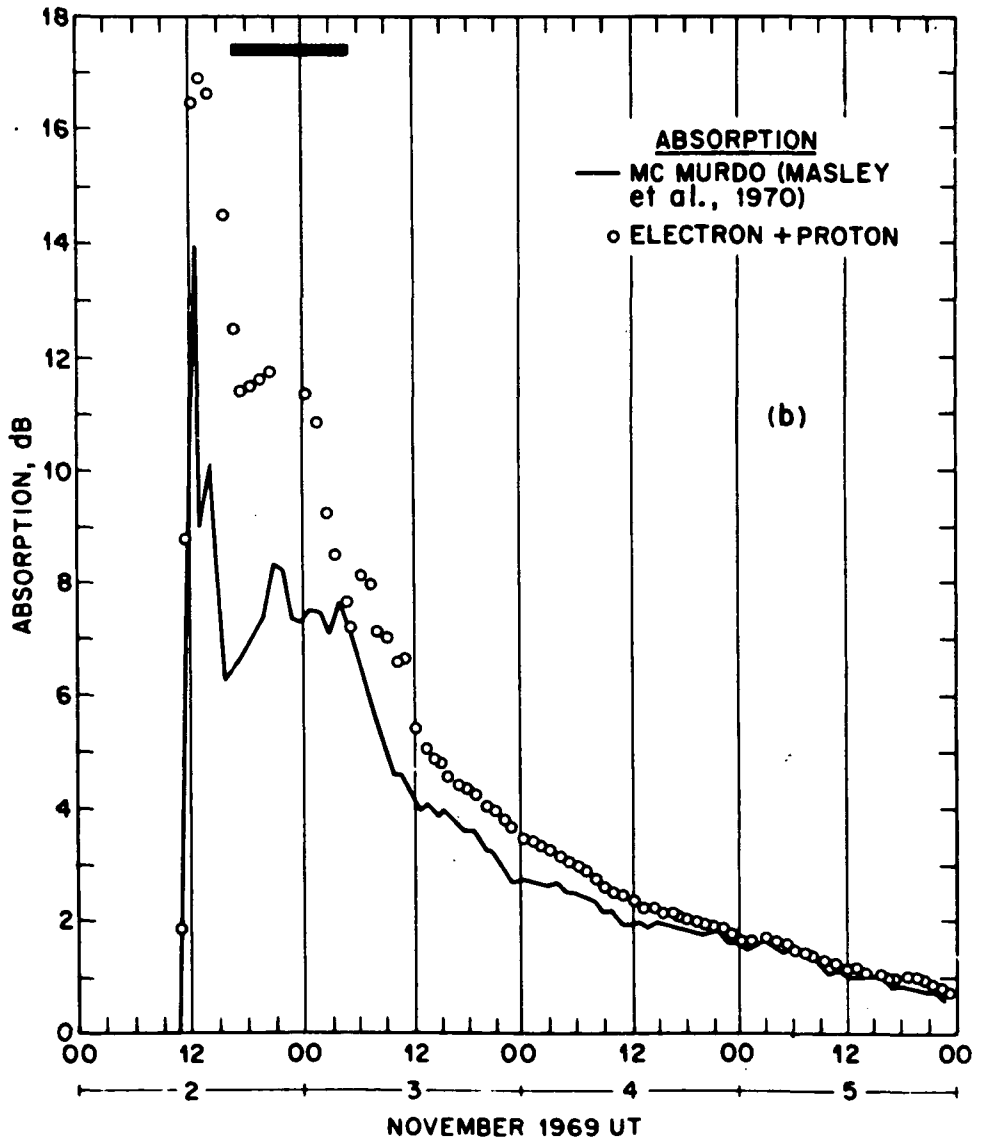
ABSORPTION
MC MURDO (MASLEY et al., 1970)
ELECTRON + PROTON
(b)
ABSORPTION, dB
0
2
4
6
8
10
12
14
16
18
00
12
00
12
00
12
00
12
00
2
3
4
5
NOVEMBER 1969 UT

Figure 7

N72-21842

# CHAPTER 11

"Solar Protons and Alphas from the May 23, 1967 Solar Flares"

by

L. J. Lanzerotti
Bell Telephone Laboratories, Incorporated
Murray Hill, New Jersey

## Introduction

The low energy protons and alpha particles emitted during a series of three east limb solar flares (McMath plage region 8818; 27-30N, 25-28E) on May 23, 1967, were measured in interplanetary space by the Bell Telephone Laboratories experiment on board the earth orbiting Explorer 34 (IMP F) satellite. This report describes the time history of the solar particle observations made by the BTL experiment and discusses the particle fluxes and spectra associated with the storm sudden commencements and the onset of the large Forbush decrease observed on the earth. A number of observations of, and details concerning, this series of flares have previously been published and they will not be reviewed in this report (Castelli, et al., 1968; Masley and Goedeke, 1968; Smith and Webber, 1968; Van Allen, 1968).

The Explorer 34 satellite was launched into a highly eccentric polar orbit at approximately 1420 UT May 24, during the onset of the solar flare particle observations at the earth. Explorer 34 is a spin stabilized (with spin axis perpendicular to the ecliptic plane) satellite with an apogee of approximately 34 $R_E$. The BTL experiment consists of a four element solid state telescope oriented perpendicular to the spin axis. The half angle of the detector telescope defining collimator is 20°; the flux measured by the experiment is the spin averaged flux of particles in the ecliptic plane. Protons and alphas up to an energy of approximately 4 MeV/nucleon are distinguished by the energy deposited in the first two detectors of the telescope and subsequently measured in a five channel analyzer. Particle species above this energy are distinguished by the use of an on-board pulse multiplier (Lanzerotti, et al., 1969). The location of Explorer 34 in its first orbit during the solar event is shown in Fig. 1.

## Observations

The half-hour averaged solar proton fluxes measured in eight energy channels during May 24-27, 1967, are shown in Fig. 2. The half-hour averaged solar alpha particle fluxes measured in five energy channels for the same time interval are shown in Fig. 3. Plotted at the bottom of each figure is the super neutron monitor counting rate from Alert and the spectral index, n, for the alpha and proton observations. The spectral index was obtained for each species of particle by least squares fitting a power law dependence on the energy/nucleon to the half-hour averaged flux measurements.

The temporal behavior of the solar proton fluxes in the approximately 10-25 MeV energy range prior to the launch of Explorer 34 can be inferred from the riometer measurements published previously by Masley and Goedeke (1968). From this riometer data and the data in Figs. 2 and 3 it is observed that, after the occurrence of the flares in the 1800-1900 UT interval of May 23, the solar particle fluxes observed at the orbit of the earth began increasing slowly, typical of an east limb flare, until they reached their peak measured values near 1200 UT on May 25.

The proton spectral index in Fig. 2 indicates that during the onset stage of the event, except for the several hour interval around the time of the sudden commencement (sc) at 1726 UT May 24, the spectrum was harder than during the remainder of the event. The alpha spectral index of Fig. 3 also suggests this behavior, although to a lesser extent. For a given energy/nucleon, the ratio of the proton flux at approximately the time of the May 24 sc to the proton flux at ~2100 UT May 24 is larger than the corresponding alpha flux ratio. However, the same flux ratios are found to be approximately similar when the 1.3 MeV/nucleon (5.2 MeV) alpha and 4.7 MeV proton channels are compared.

These observations imply that there is a rigidity dependence rather than a velocity dependence to the particle storage or trapping mechanisms behind or in the plasma cloud and shock wave associated with the May 24 sc. The trapping of low energy solar cosmic rays in an expanding plasma cloud has recently been discussed in a review by Obayashi (1967). [The plasma cloud and shock wave associated with the May 24 sc were perhaps due to the solar event that produced the large complex radio burst at 1922 UT on May 21 (Castelli, et al., 1968)].

The propagation characteristics of the low energy proton and alpha particle diffusion from the east limb flare region through interplanetary space to the earth also appears to be more dependent upon particle rigidity than upon particle velocity. That is, particles with a higher rigidity are observed at the earth first. This is demonstrated in Fig. 4 where the alpha/proton ratio is plotted for alphas and protons of approximately equal energy/nucleon (velocity). After the May 24 sc and until approximately 0800 UT on May 25, the alpha flux increased more rapidly than the proton flux. However, after 0800 UT, the ratio dropped slightly due to an increased proton flux.

The rigidity dependence of the particle propagation during the onset stage of the event is further demonstrated by the data in Fig. 5. Plotted in this figure is the time history of the alpha/proton ratio for 5.3 MeV alphas and 4.7 MeV protons (approximately equal rigidities). Note that the ratio in Fig. 5 is taken between fluxes expressed as $(cm^2 \text{ sec ster MeV})^{-1}$ for both the protons and the alphas. The alpha/proton ratio is approximately constant during the period of the May 24 sc, increases by approximately fifty percent prior to May 25, and then remains quite constant as both particle fluxes increase uniformly during the first half of May 25, prior to the 1235 UT sudden commencement. The constancy of the alpha/proton ratio for equal rigidity particles during the May 25 flux increases is in marked contrast to the more rapid alpha particle increases when equal velocity particles were compared in Fig. 4.

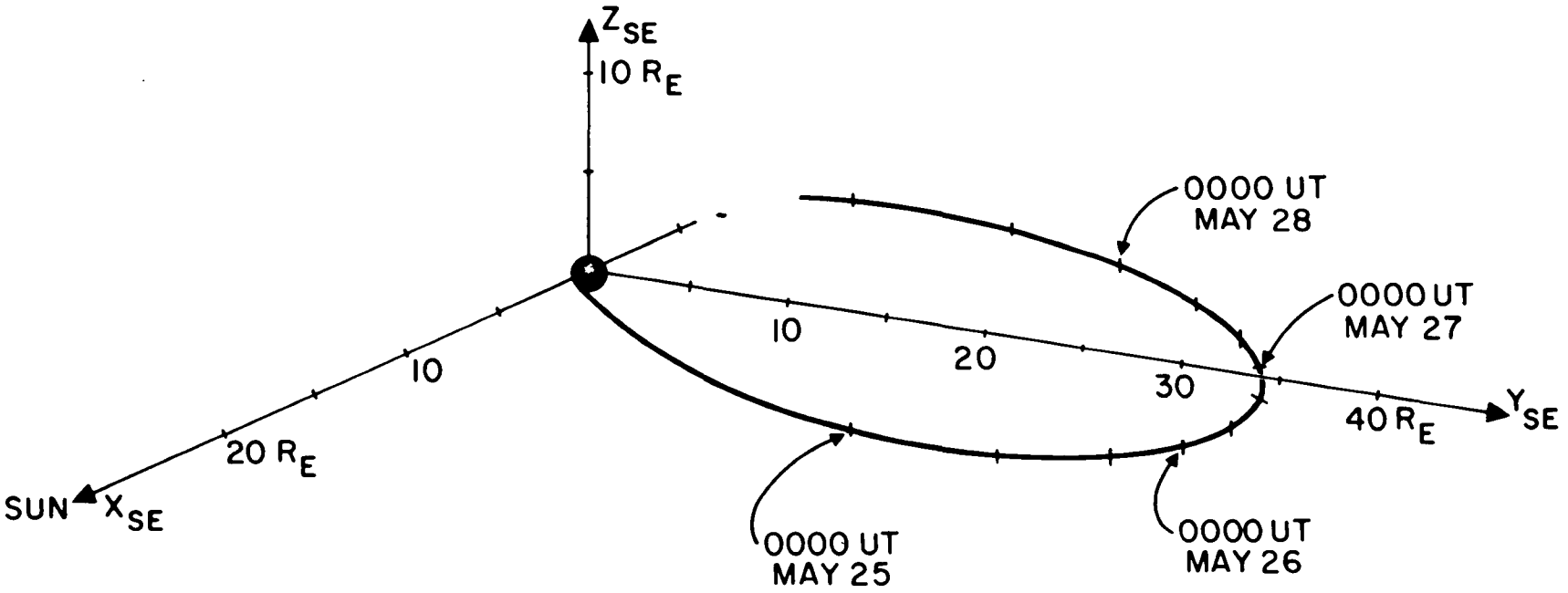


Fig. 1. Perspective view of the Explorer 34 satellite in solar-ecliptic coordinates during the period from launch to May 28, 1967.

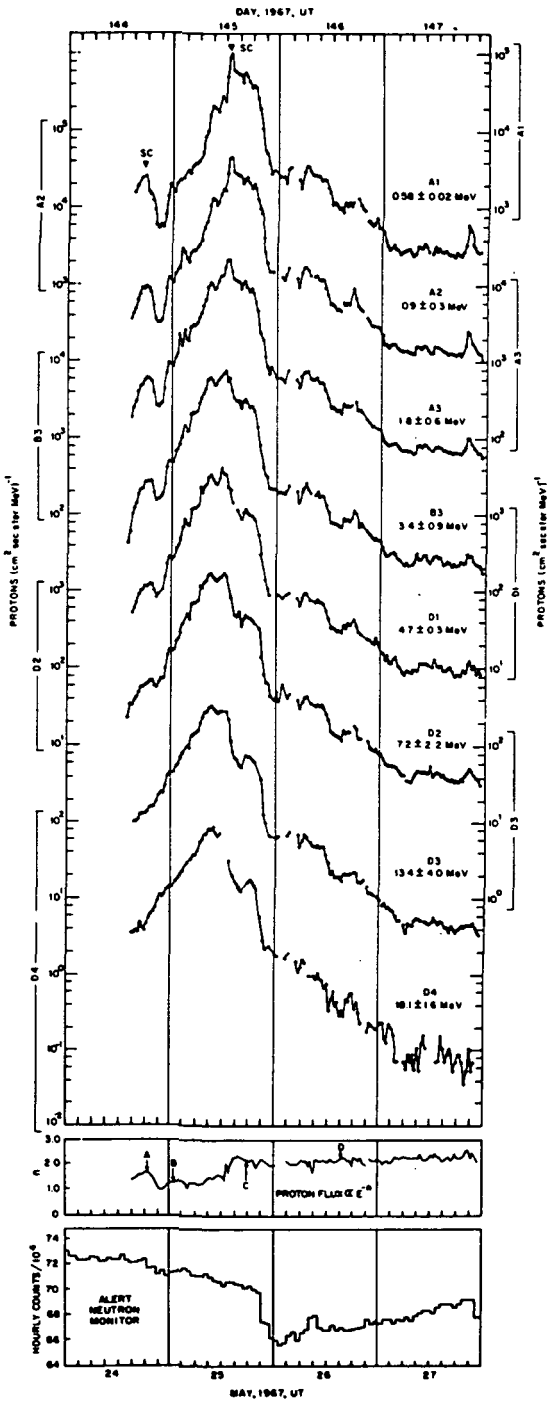


Fig. 2. Solar proton fluxes during May 24-27, 1967. Plotted at the bottom of the figure are the proton spectral index, n, and the Alert neutron monitor counting rate.

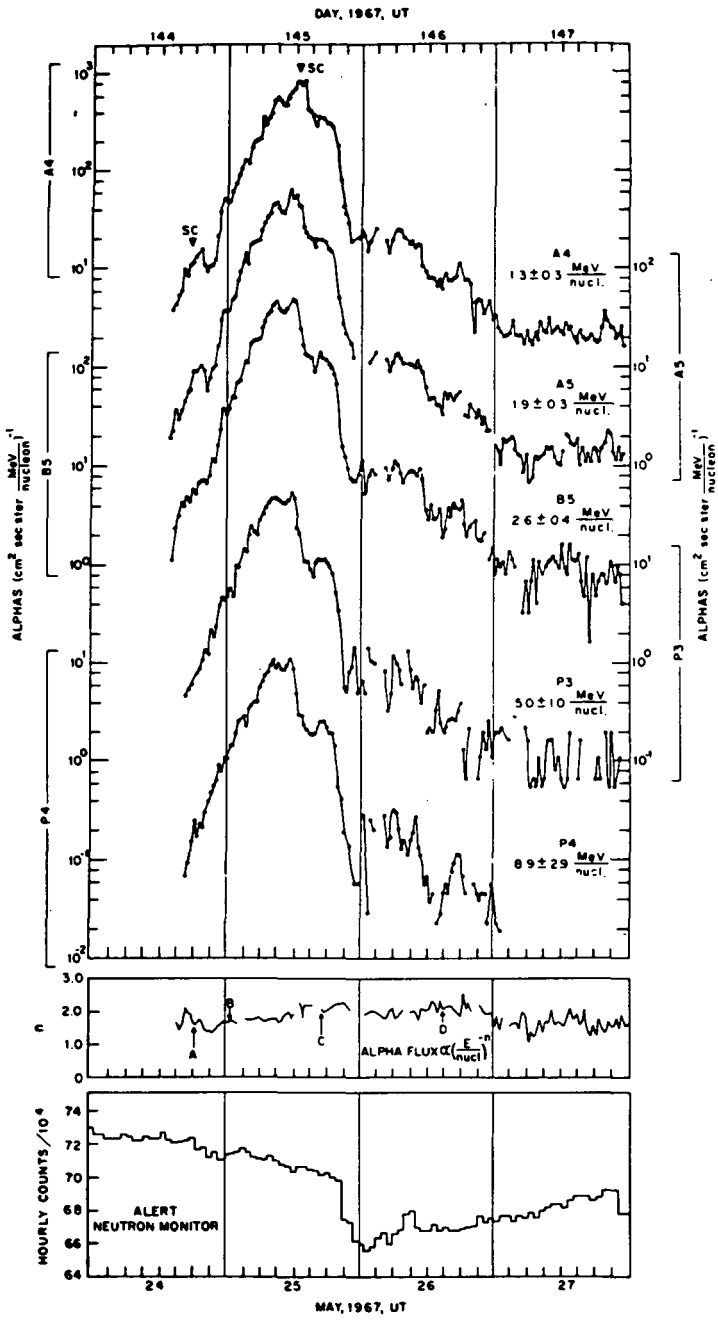


Fig. 3. Solar alpha particle fluxes during May 24-27, 1967. Plotted at the bottom of the figure are the alpha spectral index, n, and the Alert neutron monitor counting rate.

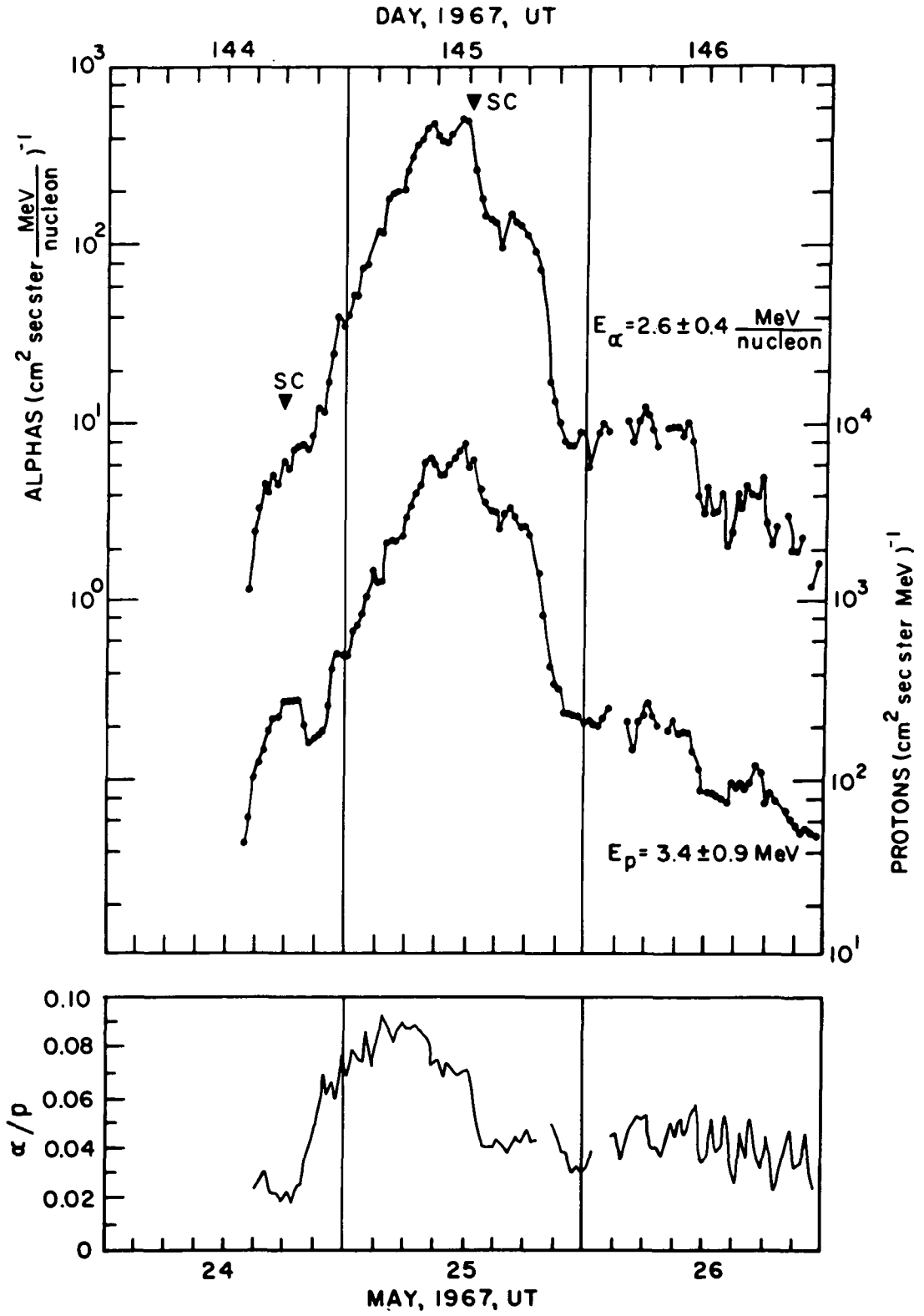


Fig. 4. Alpha particle and proton data and the alpha/proton ratio for approximately equal velocity particles.

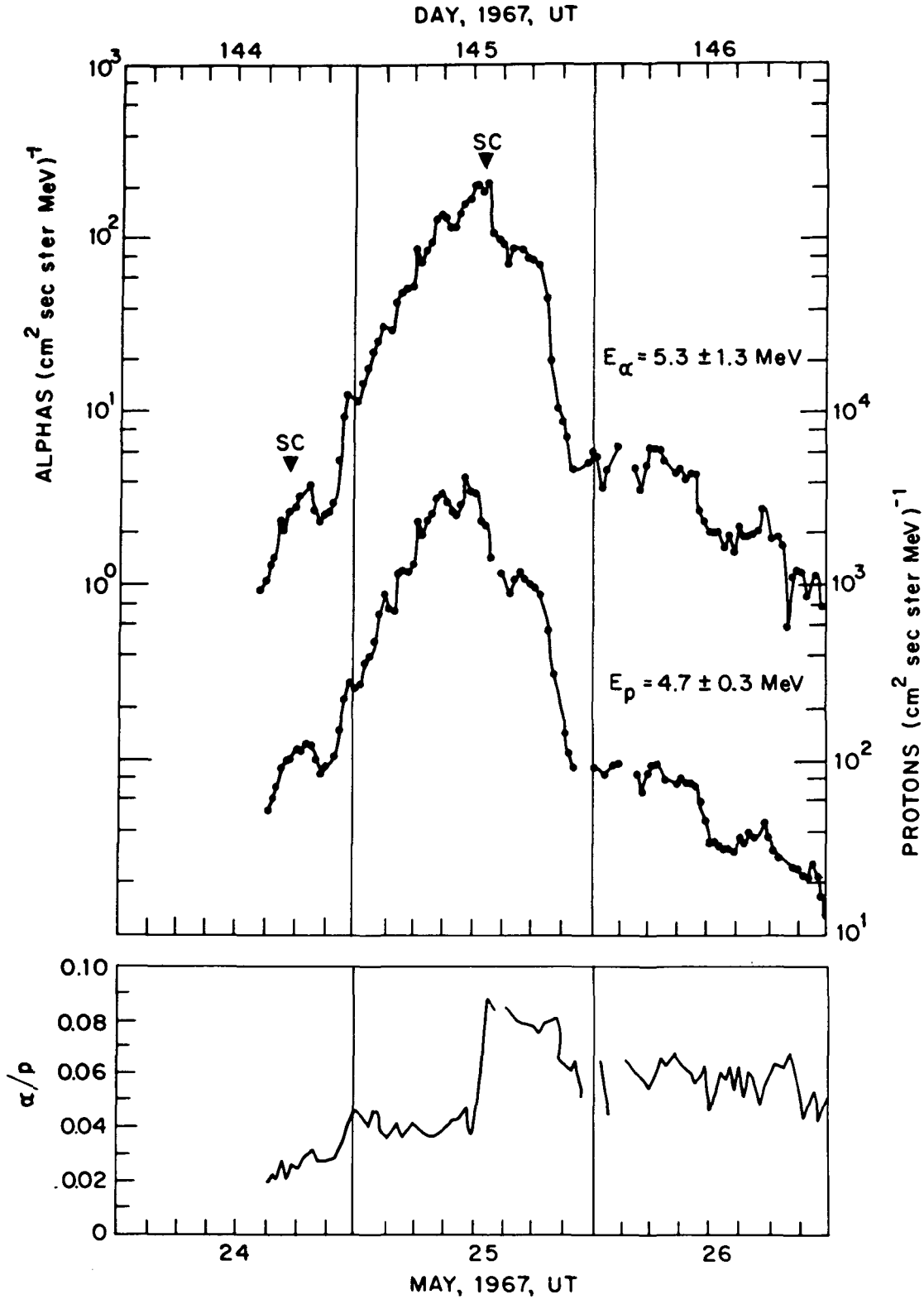


Fig. 5. Alpha particle and proton data and the alpha/proton ratio for approximately equal rigidity particles. The ratio is taken between particle fluxes expressed as $(cm^2 \text{ sec ster MeV})^{-1}$.

The two major proton and alpha particle flux decreases subsequent to the May 25 sc were quite dissimilar with respect to the rigidity dependence of the decreases. Both flux decreases were observed essentially simultaneously in all energy channels, however. Figure 6 contains the ratios of the half-hour averaged proton and alpha fluxes at 1600-1630 UT to the fluxes at 1230-1300 UT plotted as a function of rigidity. The same flux ratios as a function of rigidity for the large decreases beginning at ∿1900 UT are plotted in Fig. 7.

The initial flux decreases after the May 25 sc (Fig. 6) have a strong rigidity dependence, the decreases being observed primarily in the higher energy channels. These decreases are reflected in the softening of both the proton and alpha spectra after the sc as indicated by the spectral indices in Figs. 2 and 3. No large changes in the Alert neutron monitor rate were observed simultaneously with these flux decreases.

As the data plotted in Fig. 7 indicates, the percentages of the flux decreases, beginning at ∿1900 UT, are approximately the same for all rigidities and species of particles. Correspondingly, no significant changes in the spectra of either the protons or alphas are observed subsequent to the decreases (Figs. 2 and 3). Approximately one to two hours after the beginning of the solar particle decreases, the Alert neutron monitor rate decreased ∿4% and eventually decreased a total of ∿7% by the beginning of May 26.

The May 25 sc is probably the resultant of an interplanetary shock generated by the May 23 flares. However, the very high energy galactic cosmic rays measured by the Alert neutron monitor were not strongly modulated by the enhanced plasma clouds presumably accompanying and following the shock until ∿8 hours after the occurrence of the sc. The initial strong galactic cosmic ray modulation also occurred ∿5 hours after the higher energy solar proton and alpha particles had already once decreased significantly.

As has been seen, the solar particle flux decreases, their rigidity dependencies, and the subsequent galactic cosmic ray flux modulations after the May 25 sc are quite complex. A complete understanding of the fluxes' temporal developments will require a detailed correlation of other interplanetary and geophysical observations made during this time interval with the proton and alpha particle measurements presented in this report.

Solar flare proton and alpha spectra for four time intervals (denoted A-D in Figs. 2 and 3) during the event are shown in Figs. 8 and 9. It can easily be seen that each spectrum does not obey a single simple power law over the entire energy range. Therefore the spectral indices in Figs. 2 and 3 are only roughly indicative of the hardness or softness of the spectra.

Spectra A in Fig. 8 were observed during the flux enhancements coincident with the May 24 sc. Spectra B in Fig. 8 were observed during the flux increases prior to the May 25 sc and show distinct "bending-over" of the spectra at lower energies. Spectra C, plotted in Fig. 9, show the soft spectra observed near the time of the May 25 sc. Data on May 26, during a period after the large flux decreases, are shown as Spectra D in Fig. 9.

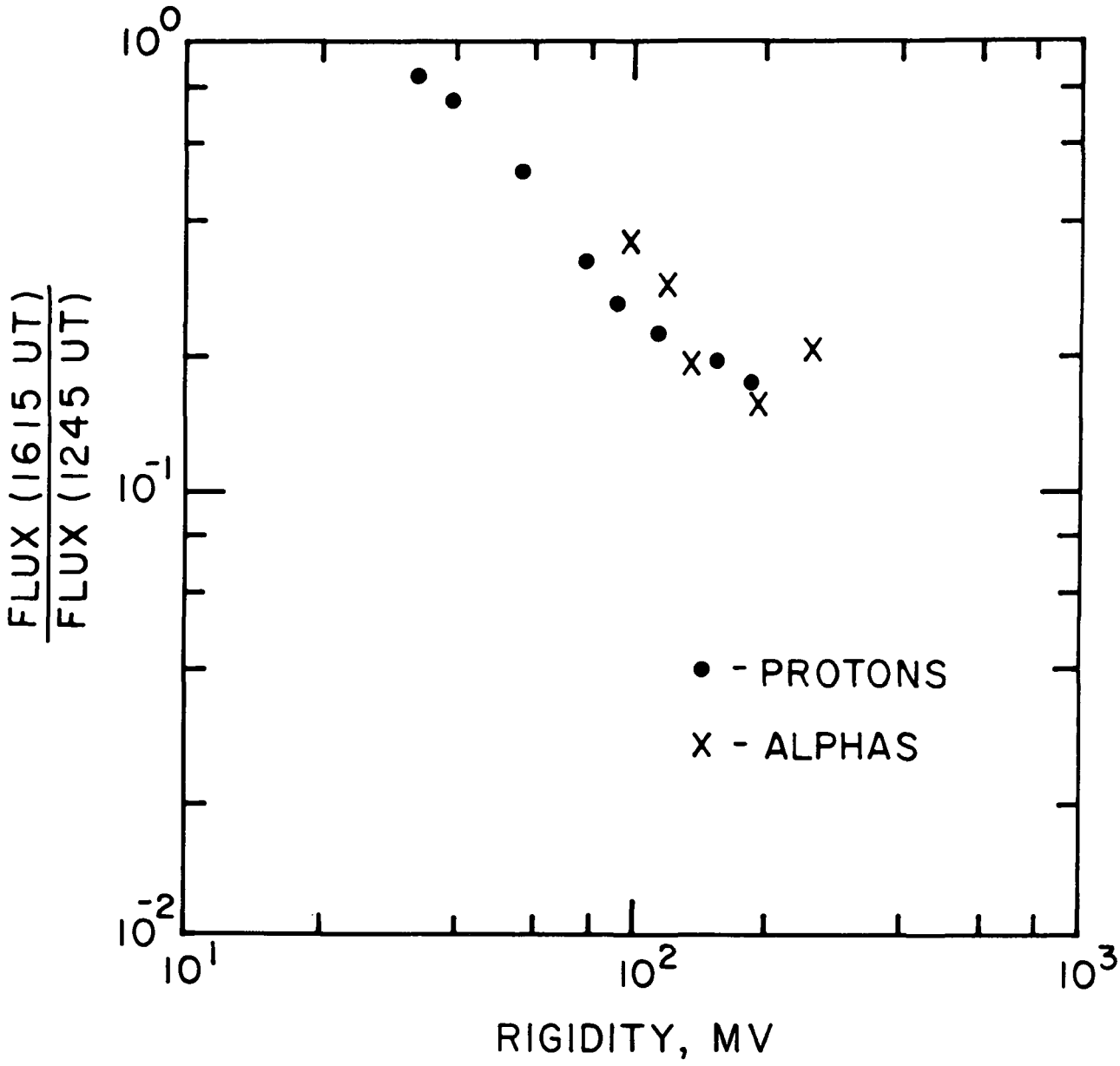


Fig. 6. The percentage proton and alpha particle flux decreases from 1230 UT to 1630 UT May 25 as a function of particle rigidity.

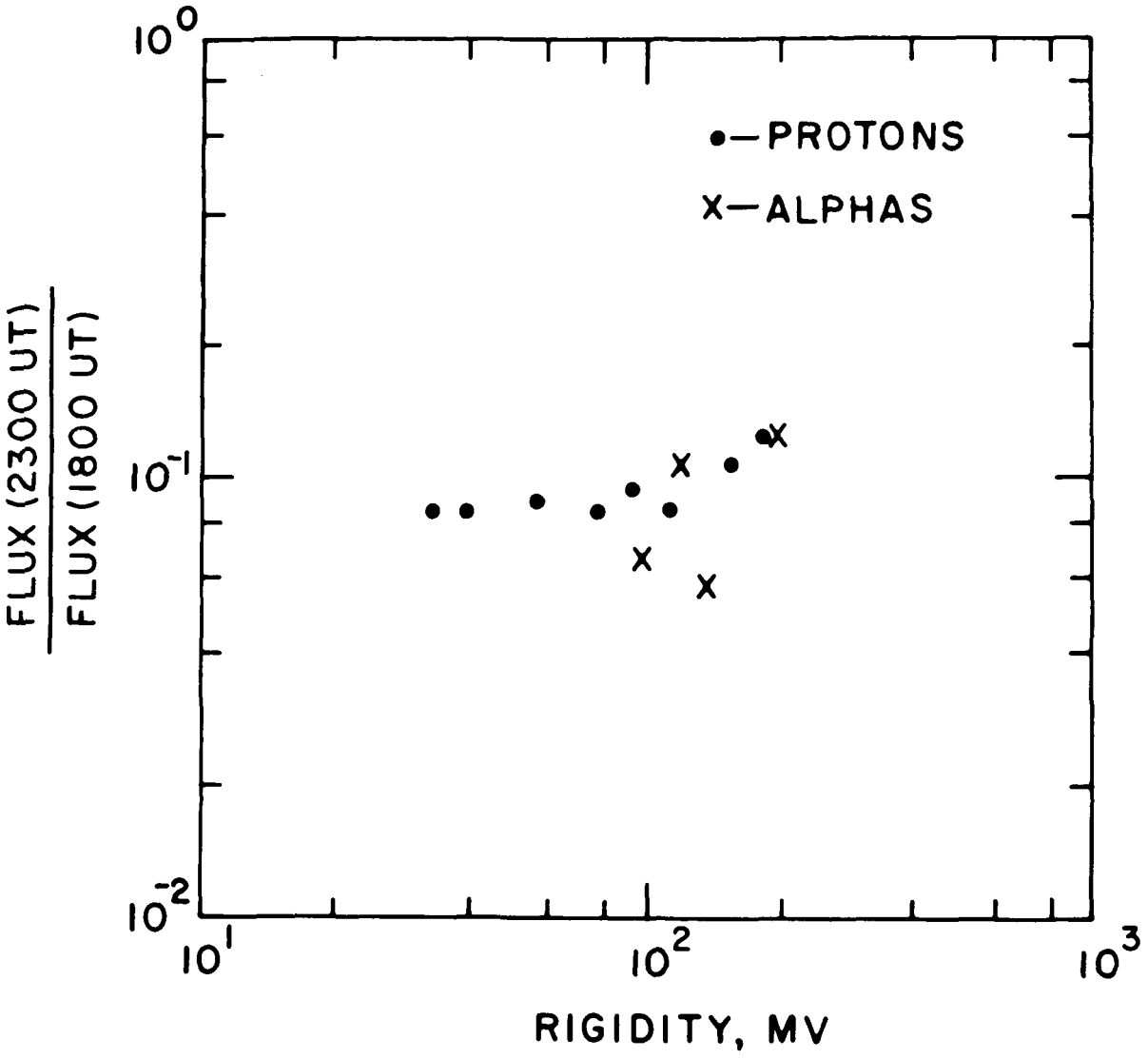


Fig. 7. The percentage proton and alpha particle flux decreases from 1800 UT to 2300 UT May 25 as a function of particle rigidity.

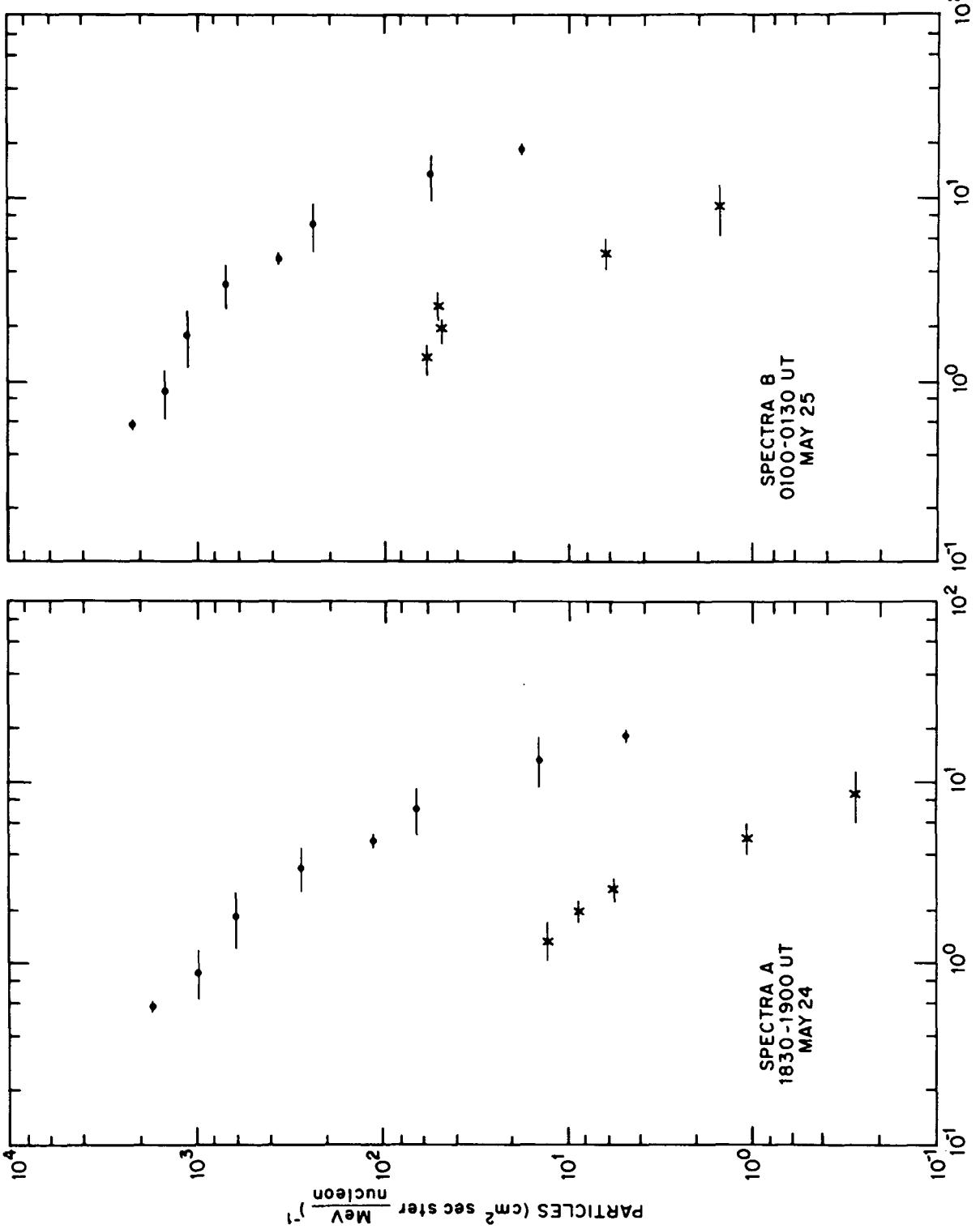


Fig. 8. Proton and alpha particle spectra during May 24 and May 25. Solid points are protons; crosses are alphas.

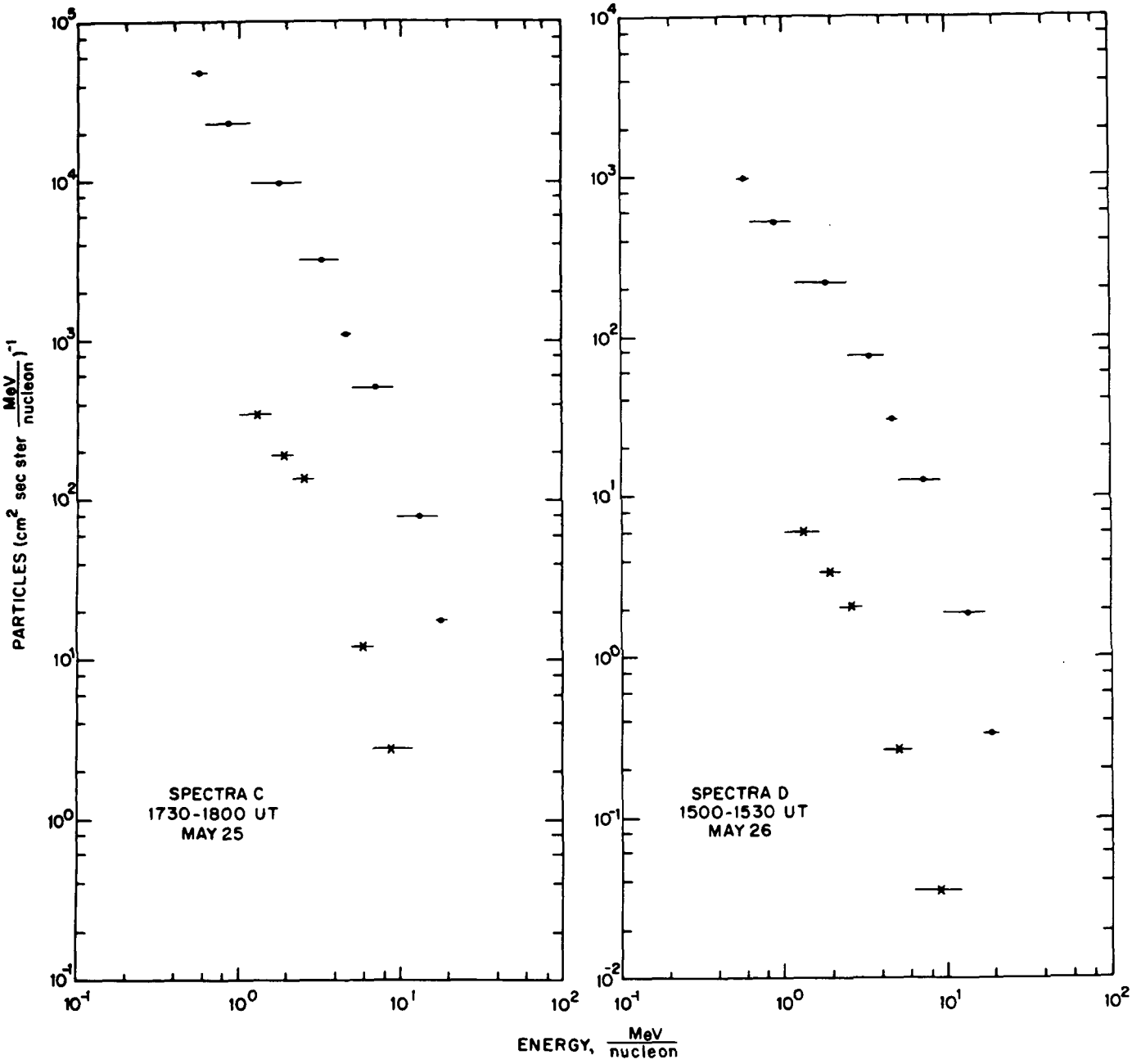


Fig. 9. Proton and alpha particle spectra during May 25 and May 26. Solid points are protons; crosses are alphas.

Summary

The observations of low energy solar particles from the east limb flares of May 23, 1967, have been discussed. A distinct softening of the solar flare proton and alpha particle spectra was observed at the times of the May 24 and May 25 sudden commencements. The particle confinement within or behind the shock that produced the May 24 sc was observed to be rigidity dependent rather than velocity dependent. The particle propagation prior to the May 25 sc was also observed to be rigidity dependent. The interplanetary solar particles were observed to decrease twice prior to the sharp Forbush decrease at approximately 2100 UT May 25. The percentage decreases in the first case were larger for higher rigidity particles. In the second case, approximately one to two hours prior to the Forbush decrease, the percentage decreases were approximately independent of particle rigidity. The alpha to proton ratio, for the same rigidity particles, varied from approximately 0.02 to 0.08 during the course of the event.

REFERENCES

Castelli, J. P., J. Aarons, and G. A. Michael, "The Great Solar Radio Burst of May 23, 1967," Astrophys. J., 153, 267, 1968.

Lanzerotti, L. J., H. P. Lie and G. L. Miller, "A Satellite Solar Cosmic Ray Spectrometer with On-Board Particle Identification," IEEE Trans. Nuc. Sci., NS-16, February, 1969.

Goedeke, A. D., and A. J. Masley, "The 23 and 28 May 1967 Solar Cosmic Ray Events," to be published in Space Research VIII, Proc. Symp. Solar Flares (North Holland Pub. Co., Amsterdam, 1969).

Obayashi, T., "The Interaction of the Solar Wind with the Geomagnetic Field During Disturbed Conditions," Solar-Terrestrial Physics (Academic Press, London, 1967).

Smith, R. W., and N. J. Webber, "The Geomagnetic Storm and Aurora of 25-26 May 1967," J. Atoms. Terr. Physics, 30, 169, 1968.

Van Allen, J. A., "Solar X-Ray Flares on May 23, 1967," Astrophys. J., 152, L85, 1968.

N72-21843

# CHAPTER 12

"Interplanetary Protons and Alphas: Days 300-313, 1968"

by

L. J. Lanzerotti and C. M. Soltis
Bell Telephone Laboratories
Murray Hill, New Jersey

## Introduction

The period in late October and early November, 1968, represented an interval of time when the interplanetary medium was quite disturbed and heavily populated with low energy solar protons. The solar flare-produced disturbances in the solar wind caused at least five large sudden commencements (SC) to be recorded in the earth during the seven days from October 26 through November 1.

The interplanetary measurements reported here were made by the Bell Laboratories experiment on the Explorer 34 (IMP F) satellite. Explorer 34 was a spin stabilized (with spin axis perpendicular to the ecliptic plane) satellite with an apogee of approximately 34 $R_E$. The BTL experiment consisted of a four element solid state telescope oriented perpendicular to the spin axis. The half angle of the detector telescope defining collimator was 20°; the flux measured by the experiment was the spin averaged flux of particles in the ecliptic plane. Protons and alphas up to an energy of approximately 4 Mev/nucleon were distinguished by the energy deposited in the first two detectors of the telescope and subsequently measured in a five channel analyzer. Particle species above this energy were distinguished by the use of an on-board pulse multiplier [Lanzerotti, Lie, and Miller, 1969].

## Interplanetary Observations - Protons

The interplanetary proton fluxes measured in four of the seven energy channels from day 300 to day 313 are plotted in Figure 1 together with the Alert neutron monitor counting rate. The time of the five sudden commencements (observed by more than 10 stations) are shown by inverted triangles on the neutron monitor plot [Solar-Geophysical Data, 1969a].

The data in Figure 1 suggest that the time interval shown could be characterized as consisting of four major solar flare enhancements. The first enhancement, beginning on October 26, extended through October 29; the second occurred almost entirely on October 30. The third enhancement, beginning on October 31, persisted for several days and decayed away until the sharp onset of the fourth on November 4. The initial two enhancements have quite soft spectra in comparison to the third enhancement.

A small cosmic ray decrease at the time of the SC on October 26 was measured by the Alert neutron monitor. The two low energy enhancements on October 29 were probably energetic storm particles associated with the interplanetary disturbances producing the SC's on October 28 and 29. The large Forbush decrease began within an hour or two of the SC on October 29. A decrease in the lowest energy solar proton fluxes was also observed at approximately the time of the SC and the beginning of the Forbush decrease.

The third interplanetary proton enhancement occurred during the large Forbush decrease and was characterized by extremely large modulations of the low energy particles. The contrast in the temporal development between the 0.56-0.60 Mev fluxes and the 1.2-2.4 Mev fluxes, for example, is quite striking. After the large energetic storm particle enhancement accompanying the SC on October 31, the proton fluxes (0.56-0.60 Mev) remained depressed for several hours while the proton fluxes (1.2-2.4 Mev) decreased in intensity for only approximately one-half hour before increasing again.

The proton flux enhancement beginning on November 4 has a temporal profile typical of a west limb flare; this is particularly true for the higher energy fluxes (Figure 1). McMath plage region 9740, on the extreme west limb of the sun, was quite active on November 4. A 1B flare (S15°, W90°) beginning at 0520 and having a maximum at 0527 [Solar-Geophysical Data, 1969b] was perhaps the source of the protons.

The time interval between the flare maximum and the initial observation of proton increases on November 4 are plotted in Figure 2 as a function of energy. Also shown in the figure are the predicted arrival times at the earth assuming the protons were injected into a 500 km/sec solar wind at the flare maximum with either a 0° or a 90° pitch angle [Winge and Coleman, 1968; C. R. Winge, Jr., private communication]. The data in the two lowest energy channels have two successive increases and, hence, a point is plotted for the beginning of each increase. The first flux increases in the two lowest energy proton channels appear to have occurred prior to the time expected if they resulted from the 0520 UT flare. Hence, it is possible that these initial increases could have been due to an earlier 1B flare that lasted from 0202 to 0334 UT [Solar-Geophysical Data, 1969b].

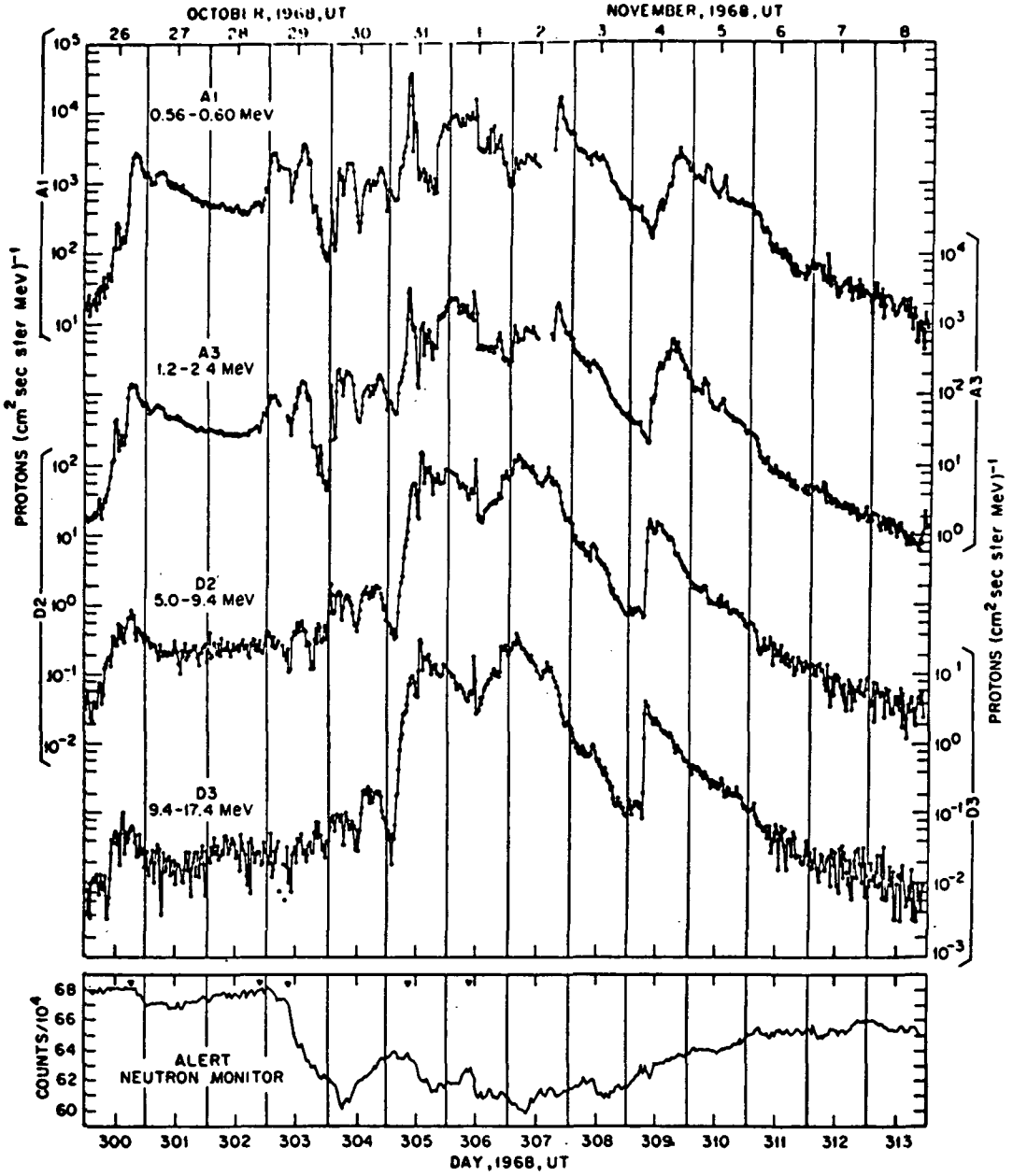


Fig. 1. Solar Proton Data from day 300 to day 314, 1968. The Alert neutron monitor counting rate is plotted at the bottom of the figure. The times of five sudden commencements are marked on the neutron monitor data.

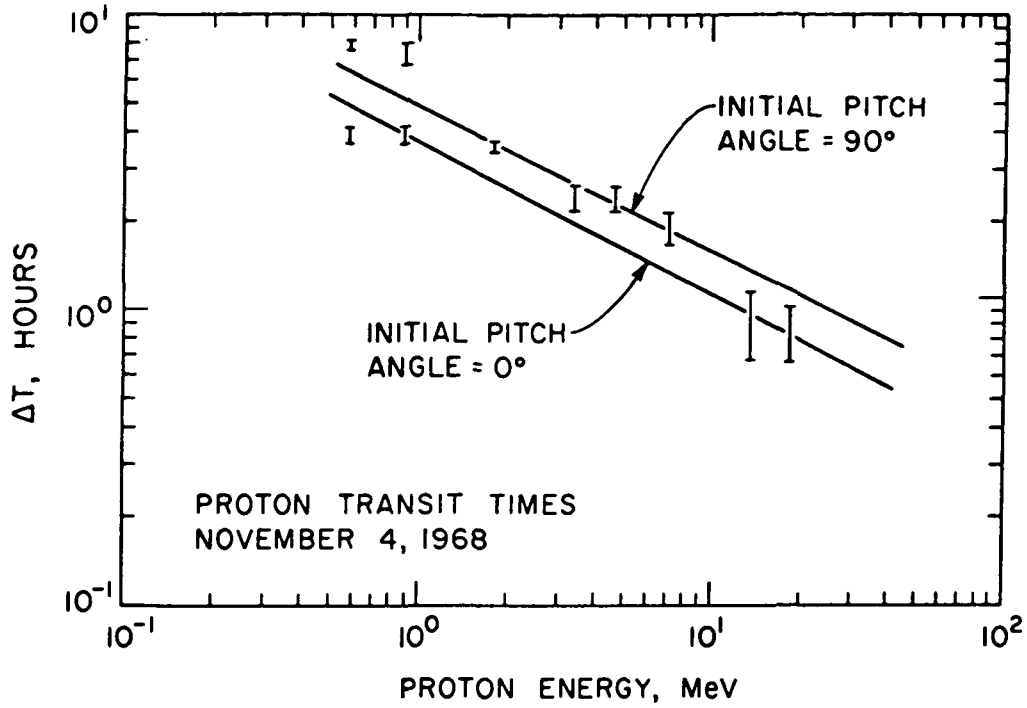


Fig. 2. Transit time for solar particle enhancements at the earth produced by a 1B flare (maximum at 0527 UT) on November 4, 1968. The two theoretical transit times for 0° and 90° initial pitch angle injections were computed by C. R. Winge, Jr.

Interplanetary Observations - Alpha Particles

Composition studies of solar cosmic rays are potentially powerful tools in unraveling source and propagation effects. The series of solar events in late October and early November were interesting in the fact that only the event commencing on October 31 contained appreciable fluxes of low energy/nucleon alpha particles. Alpha particle fluxes measured in two of the five experimental alpha channels are shown in Figure 3 for the period including the enhancement. The basic temporal history of the alpha particle fluxes during this time resembles that of the proton fluxes with the same energy/nucleon (Figure 1).

Energetic Storm Particles

Although much interesting temporal structure is seen in the data of Figure 1, there were no sharp, intense, less than one hour duration flux spikes at the time of the SC's as are sometimes seen in the low energy solar data [see, e.g., Lanzerotti, 1969]. The proton and electron counting rates measured during two time periods around the SC's on October 31 and November 1 are shown in Figures 4 and 5. Each data point corresponds to a 9.28 second counting average.

The data in Figure 4 show that a small enhancement in the lowest energy proton channel was observed approximately one minute prior to the October 31 SC at 0859 UT [Solar-Geophysical Data, 1969a]. No disturbances were seen in either the higher energy proton data or the electron data.

The data in Figure 5 show the proton and electron fluxes for the time period prior to and following the SC at 0916 UT on November 1 [Solar-Geophysical Data, 1969a]. Again the lowest energy fluxes increased in intensity prior to the SC. The higher energy proton fluxes and electron fluxes were unaffected by the interplanetary disturbance. An enhancement was observed in the proton fluxes beginning at ∿1200 UT and extending to ∿1240 UT. The flux enhancement was larger for the higher energy fluxes (as can be seen from the data in Figure 1). Almost one hour after the proton decrease at 1240, the electron fluxes increased in intensity.

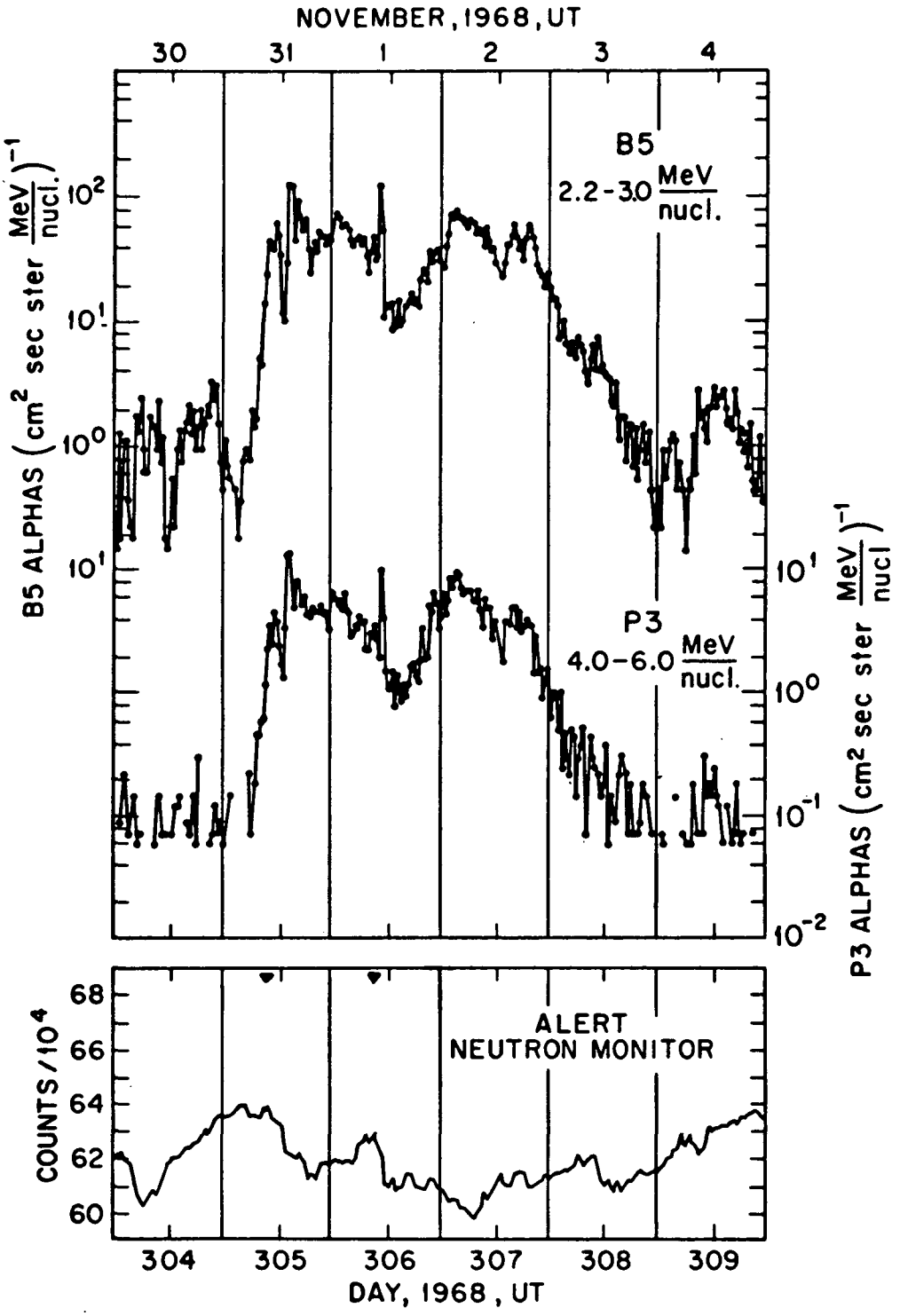


Fig. 3. Solar alpha particle fluxes during the October 31 enhancement.

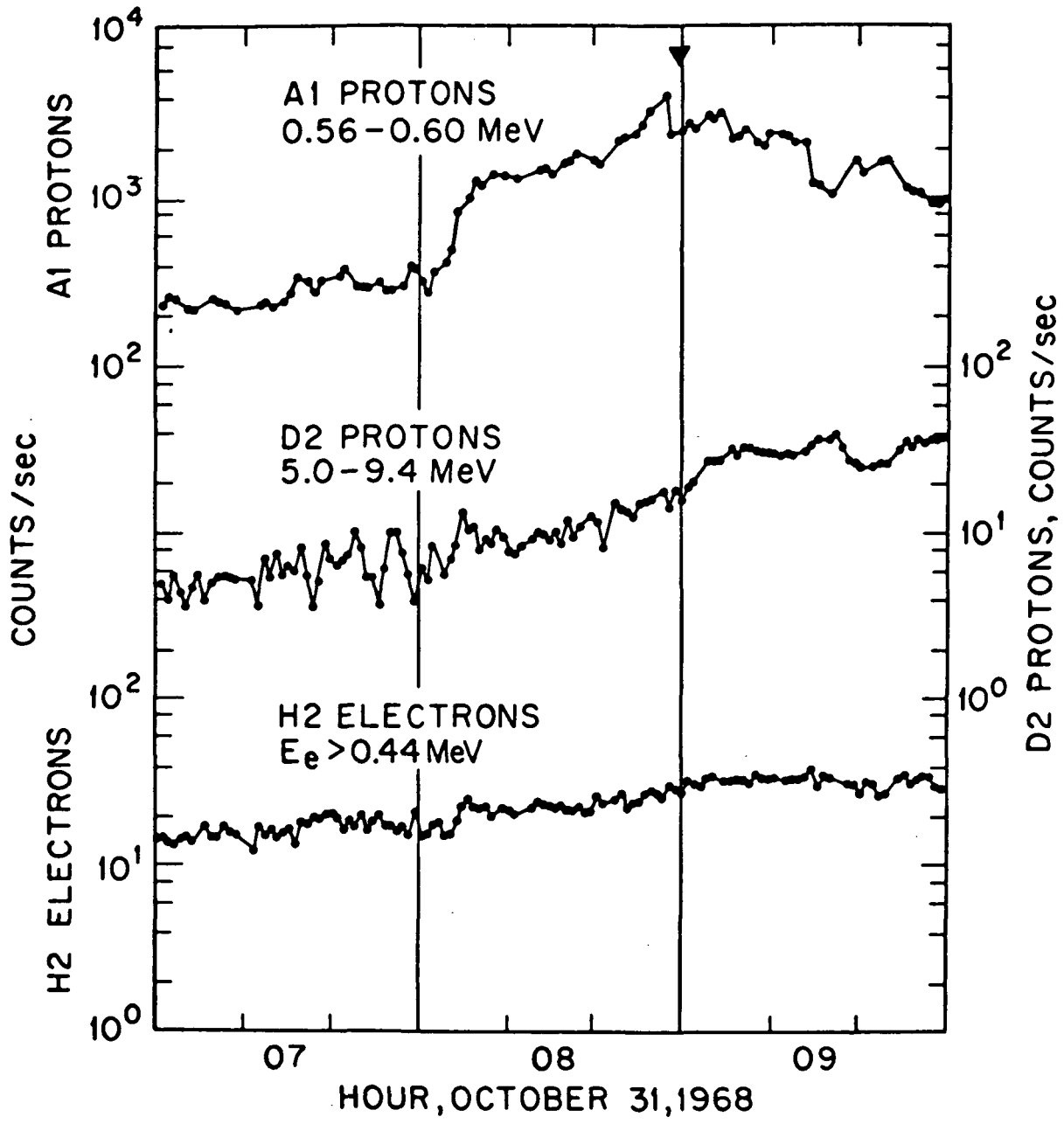


Solar particle fluxes during the time interval around the October 31 sudden commencement.

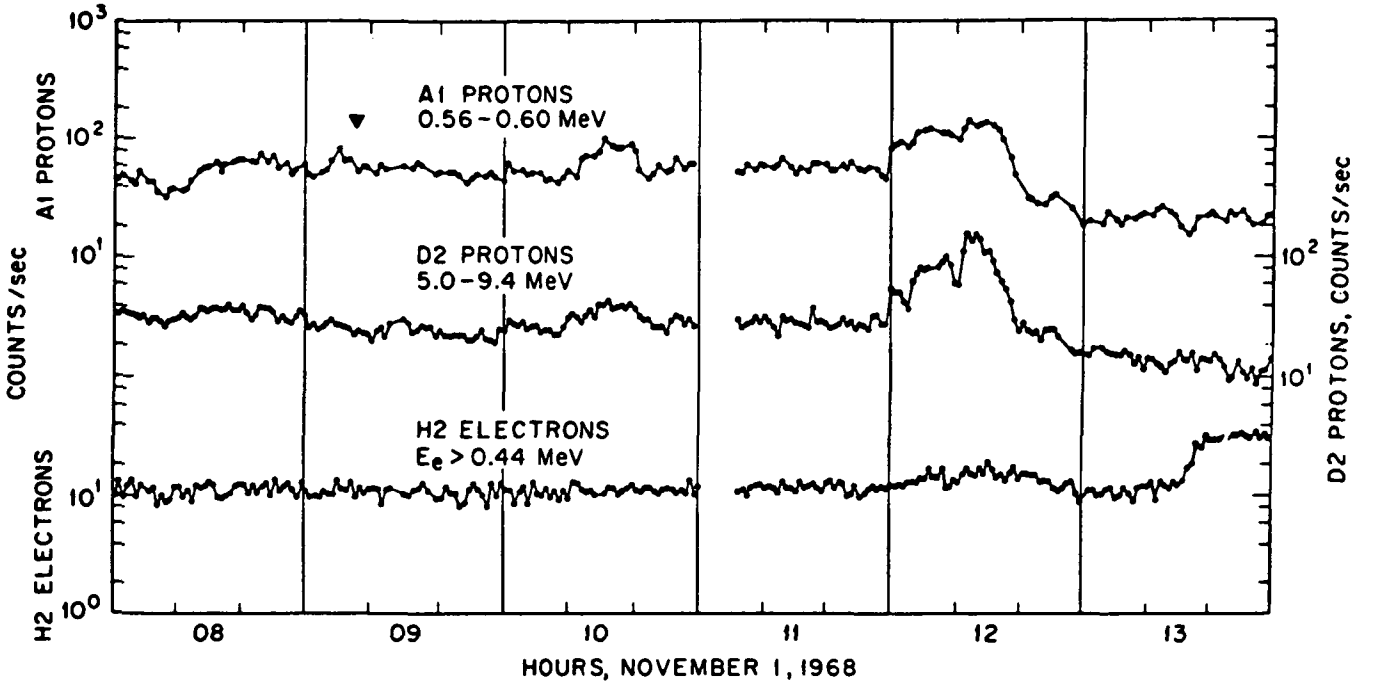


Fig. 5. Solar particle fluxes during the time interval around the November 1 sudden commencement.

## REFERENCES


| | | |
|---|---|---|
| LANZEROTTI, L. J., H. P. LIE, and G. L. MILLER | 1969 | "A Solar Cosmic Ray Particle Spectrometer with on-Board Particle Identification," IEEE Trans. Nucl. Sci., NS-16, February 1969. |
| LANZEROTTI, L. J. | 1969 | "Low Energy Solar Protons and Alphas as Probes of the Interplanetary Medium: The May 28, 1967, Solar Event," J. Geophys. Res., 74, 2851. |
| ESSA | 1969a | Solar-Geophysical Data, IER-FB-296, April 1969. |
| ESSA | 1969b | Solar-Geophysical Data, IER-FB-297, May 1969. |
| WINGE, C. R., and P. J. COLEMAN, JR. | 1968 | "The Motion of Charged Particles in a Spiral Field," J. Geophys. Res., 73, 165. |

# CHAPTER 13

N12-21844

"Protons, Alpha Particles, and Electrons Resulting from the 18 November 1968 Solar Flare"

by

L. J. Lanzerotti
Bell Telephone Laboratories
Murray Hill, New Jersey

This report presents the data on the solar proton, alpha particles, and electron fluxes measured by an instrument on the Explorer 34 (IMP F) satellite following the extreme west hemisphere (N21 W87) 1B solar flare of November 18, 1968. The Bell Telephone Laboratories instrument on Explorer 34 has been previously reported in the literature [Lanzerotti et al., 1969]. The data measurements will be described below; a more complete discussion of the observations and their implications for solar particle propagation is in preparation [Lanzerotti and Graedel, to be published].

## Proton Observations

Figure 1 contains the hourly average solar proton fluxes measured in the eight energy channels of the experiment. Plotted at the bottom of the figure are the hourly counting rates of the Alert neutron monitor. The ground level high energy particle enhancement from the flare is clearly observed. Also indicated in the neutron monitor plot is the time of the sudden commencement magnetic storm at 0904 UT on November 20.

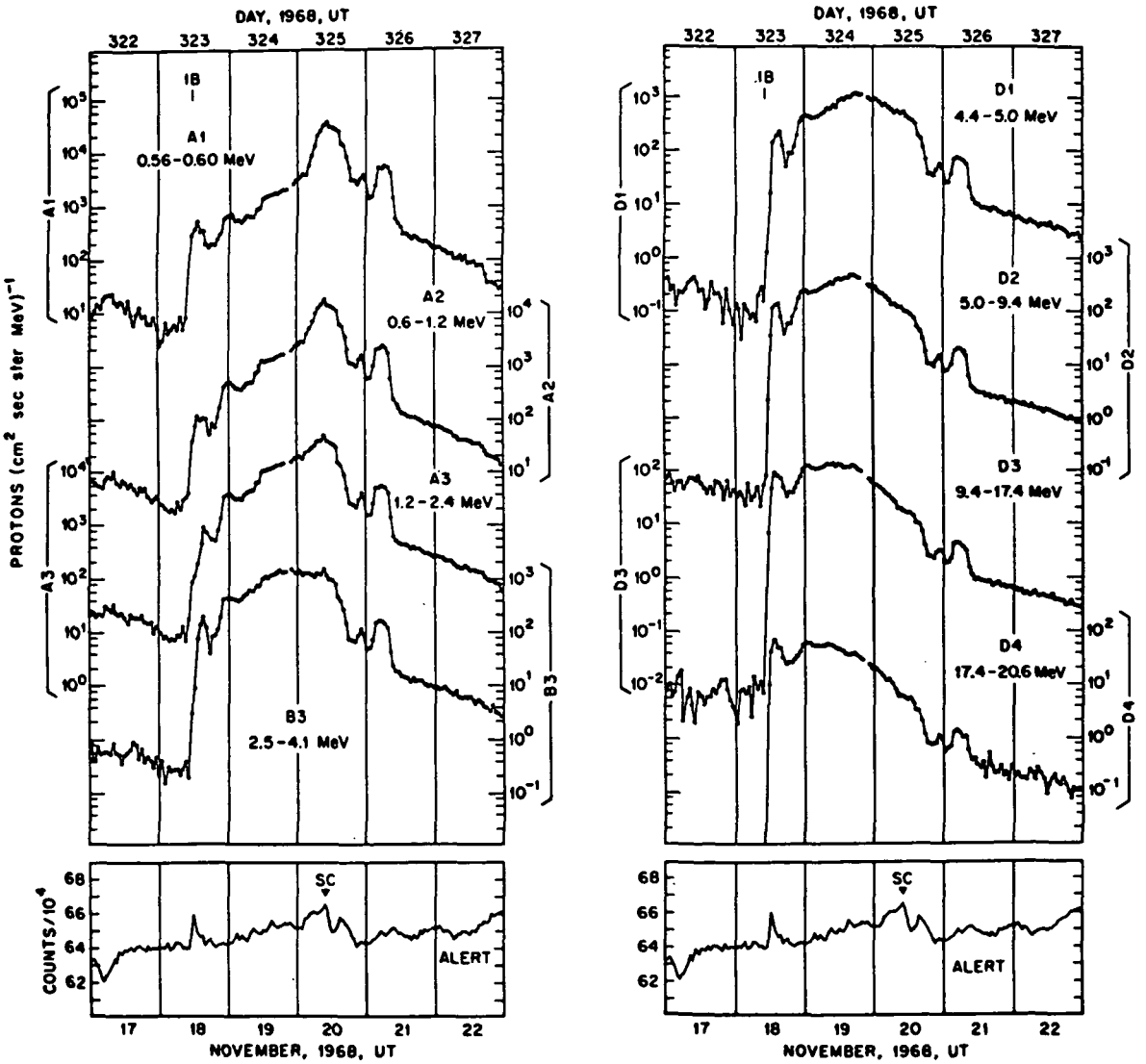


Fig. 1. Solar proton data following the 18 November 1968 solar flare. Plotted below the proton fluxes are the hourly neutron monitor rates from Alert.

The fast time resolution data (not shown) indicates that all of the proton energy channel counting rates increased at approximately the same time (±~10 minutes). The counting rates increased rapidly to a peak and then decreased to a minimum approximately seven to eight hours after the onset. The fluxes in the higher energy channels increased after the initial peak and then decreased steadily while the fluxes in the lower energy channel continued to increase steadily until the time of the sudden commencement. It is interesting to note that an initial peak in the proton fluxes after the particle onset was also observed after another extreme west hemisphere solar flare on 10 September 1961 [Bryant et al., 1965].

After the sudden commencement the fluxes in all proton channels decreased. Two subsequent enhancements were seen prior to a rather steady, exponential decay of the fluxes. The time constant of this decay, beginning at approximately 1200 UT on November 21, was approximately independent of proton energy [Lanzerotti and Graedel, to be published].

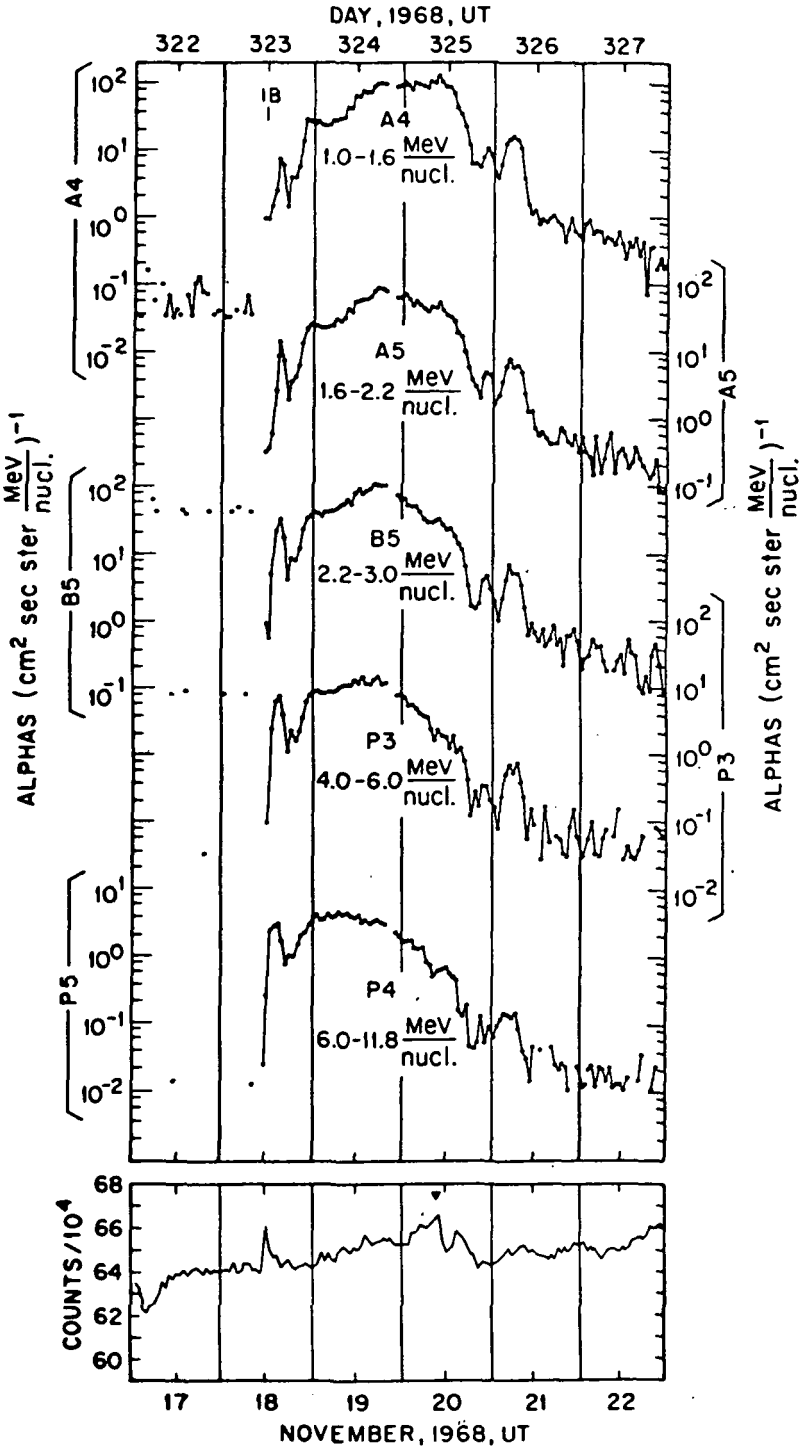


Fig. 2. Alpha particle data following the 18 November 1968 solar flare.

Alpha Particle Observations

The hourly average alpha particle fluxes measured following the 18 November flare are plotted in the Figure 2. The onset times of the alpha particles were also approximately energy independent and equal to the proton onset times. With the major exception that the initial particle peak following the onset appears narrower for the alphas than for the protons, the general flux-time profiles for the alphas and the protons are similar. The approximately exponential decay times beginning on 21 November were approximately energy independent and equal to the proton decay times [Lanzerotti and Graedel, to be published].

The alpha to proton ratios for particles compared as to equal energy (equal rigidity), equal energy per charge ($E_\alpha = 2E_p$) and equal energy per nucleon are plotted in Figure 3. For protons and alphas of equal energy, the alpha to proton ratios increase steadily to the time of the sudden commencement. Following two subsequent enhancements of the ratios, corresponding to the two flux enhancements observed in all energy channels on November 20 and 21, the equal energy ratios remained approximately constant, indicative of the energy-independent decay times beginning on 21 November.

The constant energy per nucleon alpha to proton ratios ($v_\alpha = v_p$) decreased steadily from the flux peaks following the particle onsets to the time of the sudden commencement. After an initial enhancement in the ratios following the particle onsets, the constant energy per charge alpha to proton ratios were essentially constant during the entire period when the particles were observed at the earth.

The alpha to proton ratio data of Figure 3 suggests that the initial enhanced spike of particle fluxes following the particle onsets at the earth was enriched with alpha particles from the flare. Following this enhancement, however, the three sets of alpha to proton ratios had time behaviors quite similar to those observed following the east hemisphere solar event of 23 May 1967 [Lanzerotti and Robbins, 1969]. These similarities and their implications for solar particle propagation are included in a paper in preparation [Lanzerotti and Graedel, to be published].

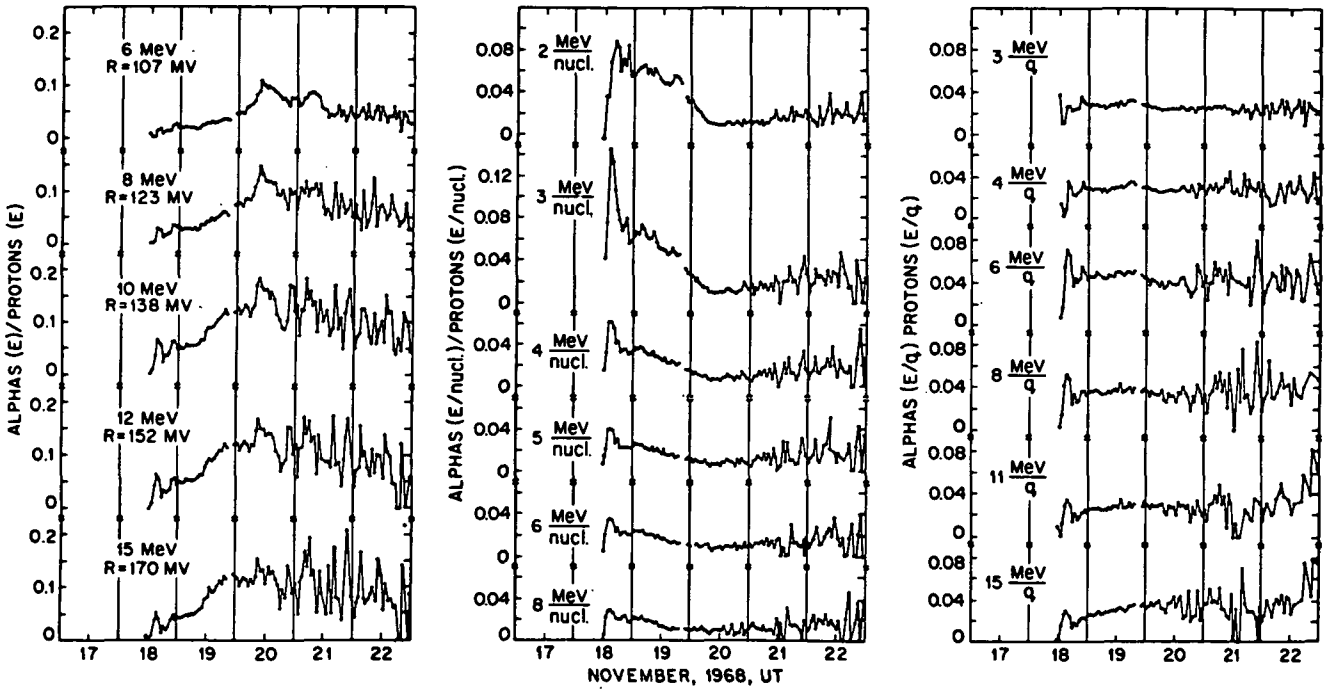


Fig. 3. Alpha to proton ratios plotted as a function of equal particle energy, equal particle energy per nucleon and equal particle energy per charge.

Electron Observations

The electron counting rates measured in three energy channels are plotted in Figure 4. The background counts in each channel are equal to the rates measured during November 17. After subtracting the backgrounds the integral electron fluxes in terms of electrons $(cm^2\ sec\ ster)^{-1}$ can be obtained approximately by multiplying the H1 rates by 57, the H2 rates by 7.2, and the H3 rates by 7.2.

The electron rate onset times on November 18 were energy independent and approximately equal to the proton and alpha particle onset times. The initial sharp enhancement after the electron onsets was seen in all of the electron channels. The electron decay times beginning on November 21 were approximately energy independent and nearly equal to the proton and alpha decay times.

Energetic Storm Particles

The four lowest energy proton channels and the lowest energy alpha particle channel all show approximately steady increases of the particle fluxes up to the time of the sudden commencement (Figures 1 and 2). In particular, the two lowest energy proton channels show flux peaks of several hours duration around the time of the sudden commencement. These energetic storm particle enhancements have often been discussed previously [Axford and Reid, 1963; Rao et al., 1967].

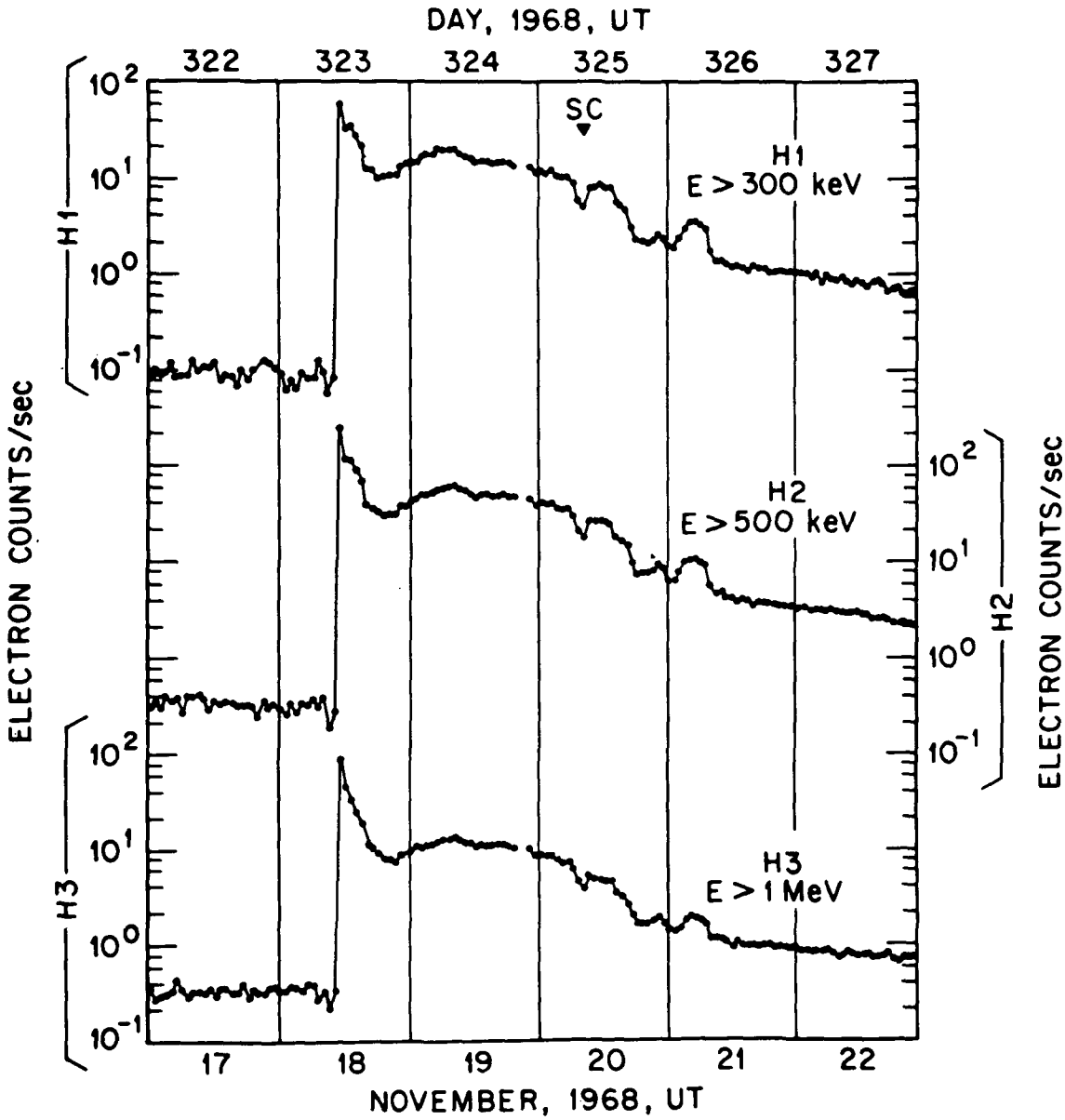


Fig. 4. Electron counting rates measured following the 18 November 1968 solar flare.

Plotted in Figure 5 is each 9.28 second average proton flux measured in five proton energy channels for a three hour interval around the sudden commencement. Clearly observed in the two lowest energy proton fluxes is a sharp, approximately one minute wide peak at the time of the sudden commencement. This peak is not observed in the higher energy fluxes. Immediately following the sudden commencement, a decrease of the proton fluxes is observed in all proton energy channels.

Although a similar narrow enhancement at the time of the sudden commencement was observed in the lowest energy alpha channel, no enhancement was observed in the electron fluxes. The data of Figure 4 indicates clearly that the electron fluxes appear to decrease prior to the sudden commencement and then to increase in intensity after the interplanetary disturbance has passed.

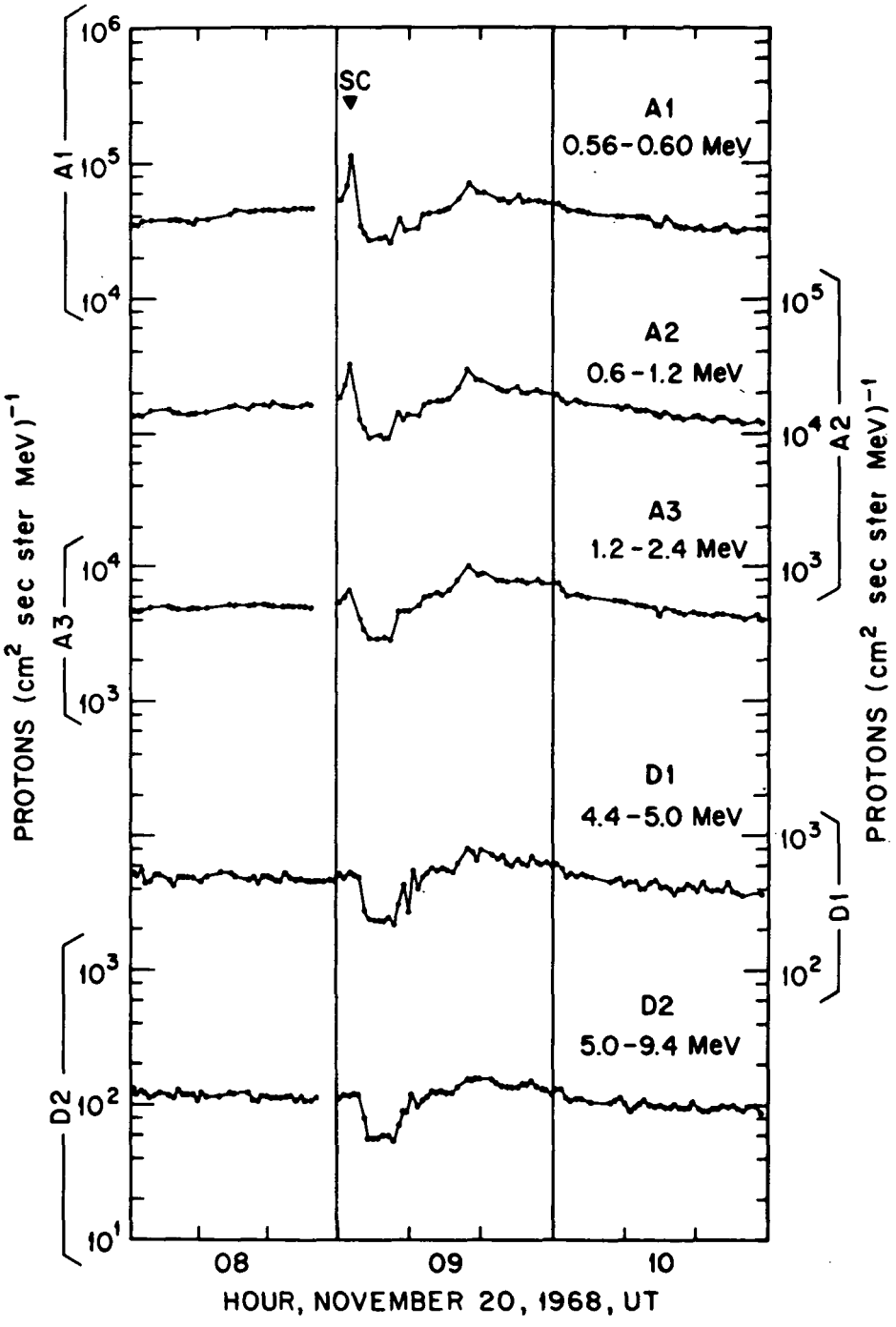


Fig. 5. High time resolution proton data measured during the time of the sudden commencement at 0904 UT, 20 November. Each data point corresponds to a 9.28 second counting average.

Acknowledgements

I thank T. E. Graedel for discussions of the data and C. M. Soltis for computational assistance. The Alert neutron monitor data was kindly supplied by World Data Center A, Upper Atmosphere Geophysics, Boulder, Colorado.

REFERENCES

AXFORD, W. I. and G. C. REID 1963 J. Geophys. Res., 68, 1793.

BRYANT, D. A., T. L. CLINE, U. D. DESAI, and F. B. MC DONALD 1965 Astrophys. J., 141, 478.

LANZEROTTI, L. J. and T. E. GRAEDEL To be published.

LANZEROTTI, L. J., H. P. LIE, and G. L. MILLER 1969 IEEE Trans. Nucl. Sci., NS-16(1), 343.

LANZEROTTI, L. J. and M. F. ROBBINS 1969 Solar Phys., 10, 212.

RAO, U. R., K. G. MC CRACKEN, and R. P. BUKATA 1967 J. Geophys. Res., 72, 4325.

# CHAPTER 14

## Brief Reports

### Interplanetary-Particle Associations with Type III Solar Bursts

T. E. GRAEDEL

*Bell Telephone Laboratories, Whippany, New Jersey 07981*

L. J. LANZEROTTI

*Bell Telephone Laboratories, Murray Hill, New Jersey 07974*

Interplanetary proton ($E \sim 0.6$ and $E \sim 1.2$ Mev) and electron ($E > 40$ kev; $E > 300$ kev) data from May 28 to November 30, 1967, are used to study the association of particle data with solar radio-burst data in the dekametric band from Ogo 3 and with data reported in Solar Geophysical Data and the I.A.U. Quarterly Bulletin. By using reasonable particle- and radio-burst association criteria, it is concluded that the observed associations during this time period do not support the common belief that interplanetary-particle observations confirm the association of electrons with type III radio bursts.

Beams of electrons moving at several tenths of the speed of light have long been invoked as the causative mechanism for type III solar bursts [*Wild et al.*, 1964; *Kundu*, 1965; *Takakura*, 1967]. With the advent of charged-particle detectors aboard interplanetary satellites, it has become possible to attempt to associate type III bursts with charged-particle fluxes observed at 1 AU. Electrons having the energies deemed appropriate (~45 kev; $\beta \equiv (v/c) = 0.35$) have indeed appeared to show an association with type III radio bursts.

Previous associations of type III bursts with interplanetary particles have involved the intermediate step of first associating the particles with a given flare. This task is complicated by uncertainties in modes of particle propagation and diffusion in interplanetary space. Some propagation models also propose particle storage regions to explain the data [e.g., *Lin and Anderson*, 1967; *Simnett et al.*, 1969]. Such a feature would further complicate the association process.

Although the difficulties involved with associating particles with a given flare have been recognized to some degree by various authors [e.g., *McCracken et al.*, 1967; *Lin*, 1970*a*], the associations between flares and particle observations have continued to be made [e.g., *McCracken et al.*, 1967; *Masley and Goedeke*, 1968; *Fan et al.*, 1968; *Lin and Anderson*, 1967; *Lin*, 1970*a*]. These associations generally show a wide range of particle transit times from the chosen flare. For example, an association of solar protons ($E \gtrsim 5$ Mev) has been made with flares occurring over a time interval of 22 min to 2½ hours ('west longitude events') and of 'a few hours' to 24 hours ('east longitude events') prior to the particle event [*Masley and Goedeke*, 1968]. Associations of solar electrons ($E \geq 40$ kev) have been made with flares occurring over a time interval of 1.5 to 83 min prior to the event [*Lin and Anderson*, 1967]. Apart from particle arrival variability arising owing to flare location on the sun, the wide range of transit times is partly due to the tendency of experimenters to associate particle events with the largest flare possible, even though other less important flares may produce less extreme values for a propagation time. These types of associations might be suspect in view of the fact that recent surveys [e.g., *Smart and Shea*, 1970] indicate that little or no correlation exists between flare importance and the resulting particle flux near the earth.

The association of a radio-burst event with a given particle event usually has been made by using flare-associated data like that cited above

[e.g., *Svestka*, 1969]. Since the occurrence of flares accompanied by type III radio bursts is very high (indeed, sometimes it may be quasi-continuous) [*Fainberg and Stone*, 1970*a*], the association of particle events with flares automatically produces an association with type III bursts.

This report bypasses the flare-association step and attempts to associate particle events directly with reported radio bursts by using a stated time-correlation interval. This procedure inherently recognizes that type III solar radio bursts often occur in conjunction with the less well-reported subflares or flares of importance 1 [*Graedel*, 1970].

## Particle Associations with Type III Bursts

The solar-particle data considered in this report consist of electron ($E > 0.3$ Mev, $\beta = 0.77$) and proton ($0.56 \leq E \leq 0.6$ Mev, $\beta \sim 0.025$; $0.6 < E < 1.2$ Mev, $\beta \sim 0.04$) information from an experiment on the Explorer 34 satellite [*Lanzerotti et al.*, 1969]. Solar radio-burst data in the dekametric band reported in Solar Geophysical Data [*U.S. Department of Commerce*, 1968] and the *I.A.U Quarterly Bulletin on Solar Activity* [1968] are used to establish possible radio-burst associations with the particle data. Radio-burst information from Ogo 3 within the frequency band 4–2 MHz [*Haddock and Graedel*, 1970] is used to obtain more complete solar radio-data coverage during the period from May 28 to September 30, 1967. (Satellite observations of radio bursts are the only ones available from ~0700–1300 UT.) Finally, association criteria for radio bursts are used with published solar-electron data ($E > 40$ kev) [*Lin*, 1970*a*] to further study associations of particles and type III bursts.

Two association criteria are used to devise the results for protons: (*a*) a proton event must begin $4 \pm 1$ hours after a type III burst, or (*b*) a proton event must occur 5–8 hours after a type III burst. The association criterion for electrons is that the event must follow a type III burst by ½ hour. (The first proton criterion and the electron criterion are derived from Archemedes' spiral travel time for particles of the energy involved; the second proton criterion allows for moderate interplanetary diffusion and the resulting time delay.) Association with any one piece of radio datum constitutes a positive result.

The proton and higher-energy electron events from May 28 to November 30, 1967, are listed in Tables 1 and 2. Their association with solar radio-burst data is indicated in the appropriate criteria columns. For the three sources of radio-burst data, the 'Obs.' columns in the tables indicate whether or not observations were being made.

Approximately 222 type III solar radio bursts were recorded in all frequency bands during the interval July 28 to August 4, 1967 [*U.S. Department of Commerce*, 1968]. This is an average of well over 1 type III burst per hour of observing time. These bursts have been attributed to the large active region 8905 by *Lin* [1970*a*, *b*, *c*]. In the following discussion, the particle-burst associations during the passage of region 8905 will be treated separately, because of the large probability of associating any interplanetary particles with occurrences in such a region.

A study of the associations in Tables 1 and 2 indicates the following:

1. *Protons.* Twenty-six of the twenty-seven proton events had corresponding solar radio coverage. Seventeen of the twenty-six events (65%) had type III solar radio-burst associations, if the criteria established were used. If the three events (July 29 and August 1 and 3) that perhaps were produced by the solar active region with McMath plage number 8905 are excluded, then 14 of 23 events (61%) had type III burst associations.

2. *Electrons.* Eleven of the eleven electron events (>300 kev) had corresponding solar radio coverage. Two of the eleven events (18%) had type III solar radio-burst associations, if the criteria established were used. If the two events (July 30 and August 3) that perhaps were produced by the McMath plage region 8905 are excluded, then 1 of the 9 events (11%) had type III burst associations.

An example of the results stated above is illustrated in Figure 1, which demonstrates the association situation for the period July 21–27, between electrons, protons, and the Ogo 3 burst data. The solar radio bursts of July 23 and 24 show definite association (if the criteria set above are used) with the increase in proton flux during the last half of July 24, whereas

TABLE 1. Association of Explorer 34 Proton Events with Type III Dekametric Solar Radio Bursts

| DATE, 1967 | START OF PROTON EVENT | MAX. OF PROTON EVENT | PEAK FLUX* | OGO 3 | | | | SOLAR-GEOPHYSICAL DATA | | | | I.A.U. QUARTERLY BULLETIN | | | |
|---|---|---|---|---|---|---|---|---|---|---|---|---|---|---|---|
| | | | | OBS. | 4±1 HR. ASSOC. | 5-8 HR. ASSOC. | NO ASSOC. | OBS. | 4±1 HR. ASSOC. | 5-8 HR. ASSOC. | NO ASSOC. | OBS. | 4±1 HR. ASSOC. | 5-8 HR. ASSOC. | NO ASSOC. |
| 5/28 | 1000 | 0500, 5/30 | 4880 | X | | | X | X | | | X | X | | | X |
| 6/3 | 1330 | 1600, 6/5 | 1960 | X | | | X | | | | | | | | |
| 6/24 | 1900 | 1400, 6/20 | 820 | X | | | X | X | X | X | | X | X | X | |
| 7/11 | 1700 | 2200 | 290 | X | | | | X | | | X | X | | | X |
| 7/24 | 0000 | 2100, 7/25 | 24 | X | X | | | X | X | X | | X | X | X | |
| 7/29 | 2100 | 1500, 7/30 | 49 | | | | | X | X | X | | X | X | X | |
| 8/1 | 1100 | 0700, 8/2 | 65 | X | | | X | X | | X | | X | | X | |
| 8/3 | 1630 | 0600, 8/4 | 110 | X | | | X | X | X | | | X | X | | |
| 8/9 | 1700 | 0500, 8/11 | 19,600 | | | | | X | X | | | X | | | X |
| 8/15 | 2030 | 1000, 8/16 | 65 | | | | | X | X | | | X | X | | |
| 8/24 | 0100 | 0200, 8/25 | 49 | | | | | X | | | X | X | | | X |
| 9/18 | 0000 | 1200, | 4880 | | | | | X | X | | | X | X | | |
| 9/26 | 1000 | | | | | | | X | | X | | X | | X | |
| 9/27 | 0700 | 0700 | 33 | | | | | X | X | X | | X | X | X | |
| 10/3 | 0330 | 0700, 10/4 | 1.4 | | | | | X | X | X | | X | X | X | |
| 10/8 | 0300 | 1730 | 10 | | | | | X | | X | | X | | X | |
| 10/20 | 0100 | 1230 | 1.6 | | | | | X | | | X | X | | | X |
| 10/27 | 0700 | 1300 | 73 | | | | | X | X | X | | X | X | X | |
| 10/29 | 0700 | 1500 | 340 | | | | | X | | X | | X | | X | |
| 10/30 | 0300 | 0530, 10/31 | 540 | | | | | X | X | X | | X | X | X | |
| 11/2 | 1100 | 0230, 11/3 | 170 | | | | | X | | | X | X | | | X |
| 11/4 | 1730 | 0730, 11/5 | 28 | | | | | | | | | X | | | X |
| 11/10 | 1930 | 2130 | 4 | | | | | X | | | X | X | | | X |
| 11/13 | 0330 | 1100 | 46 | | | | | X | | X | | X | | | X |
| 11/15 | 1600 | 0100, 11/16 | 160 | | | | | | | | | | | | |
| 11/23 | 2315 | 1200, 11/24 | 11 | | | | | X | | | X | X | | | X |
| 11/27 | 0830 | 1400, 11/28 | 400 | | | | | X | X | X | | X | X | X | |

*PROTONS $(cm^2\ sec\ ster\ MeV)^{-1}$

TABLE 2. Association of Explorer 34 Electron Events with Type III Dekametric Solar Radio Bursts

| DATE, 1967 | START OF ELECTRON EVENT | MAX OF ELECTRON EVENT | PEAK FLUX* | OGO 3 | | | SOLAR-GEOPHYSICAL DATA | | | I.A.U. QUARTERLY BULLETIN | | |
|---|---|---|---|---|---|---|---|---|---|---|---|---|
| | | | | OBS. | 0-1/2 HR. ASSOC. | NO ASSOC. | OBS. | 0-1/2 HR. ASSOC. | NO ASSOC. | OBS. | 0-1/2 HR. ASSOC. | NO ASSOC. |
| 5/28 | 0610 | | 1140 | | | | X | | X | X | | X |
| 6/3 | 0630 | 1000 | 170 | X | | X | X | | X | X | | X |
| 6/6 | 0620 | 1400 | 1140 | X | | X | | | | | | |
| 7/5 | 0900 | 1000 | 11 | X | | X | | | | | | |
| 7/30 | 0500 | 0800 | 47 | | | | X | X | | X | X | |
| 8/3 | 0930 | 1100 | 46 | X | | X | | | | | | |
| 10/30 | 0030 | 0700 | 14 | | | | X | | X | X | | X |
| 11/2 | 1015 | 1730 | 29 | | | | | | | X | | X |
| 11/4 | 1215 | 1300 | 12 | | | | | | | X | | X |
| 11/10 | 1930 | 2000 | 12 | | | | X | X | | X | X | |
| 11/13 | 0330 | 1230 | 320 | | | | X | | X | X | | X |

*ELECTRONS $(cm^2\ sec\ ster)^{-1}$

the electron channel shows only the radiation belt enhancement during the satellite perigee pass. The >40-kev electron data [*Lin*, 1970*a*] and the >45-kev electron data [*Van Allen and Krimigis*, 1968] for this time period were similarly uneventful.

At least as surprising as the apparent association in Figure 1 of the type III bursts with protons rather than with electrons is the frequent absence of particle events during periods of high radio activity, or vice versa. Figure 2 illustrates the observed electron flux for the period of May 29 to June 10, 1967. Several large radio bursts left no corresponding particle signature (May 29, 30, and June 2), whereas two large particle events (June 3, 6) were not reflected in the Ogo 3 radio-burst observations. These two particle events (and no others) were also observed by *Lin* [1970*a*] for >40-kev electrons; he is similarly unable to associate the events with electron flares or radio bursts.

The Ogo 3 radiometer has a flux detection lower limit of $1 \times 10^{-17}$ watt $cm^{-2}$ $Hz^{-1}$, which has been shown to correspond roughly to 2+ on the radio-burst importance scale used in Solar Geophysical Data [*Haddock and Graedel*, 1970]. The radio bursts indicated in Figures 1 and 2 are thus biased toward bursts of higher energy, which presumably are also those which would produce the highest particle fluxes. The nondetection of particles for the times illustrated are typical examples of the apparently anomalous behavior of the radio-burst–particle associations.

During the same period studied above, *Lin* [1970*a*] reported 35 electron events (>40 kev). These events are listed in Table 3, except that the 14 events apparently resulting from

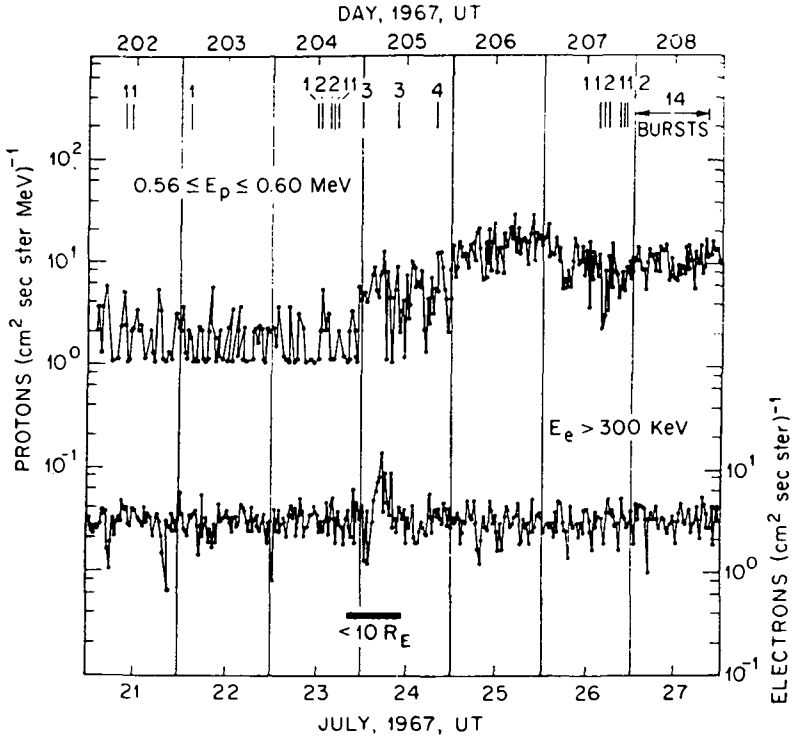


Fig. 1. The association of Explorer 34 proton and electron half-hourly averaged data with Ogo 3 type III solar radio bursts, July 21–27, 1967. The onset time and burst importance [*Haddock and Graedel*, 1970] is indicated at the top of the figure. The radio bursts are well-correlated with optical flares from McMath plage regions 8905 and 8907. Flare longitudes are approximately 70°E on July 23, 55°E on July 24, and between 30°E and 00°E on July 26–27.

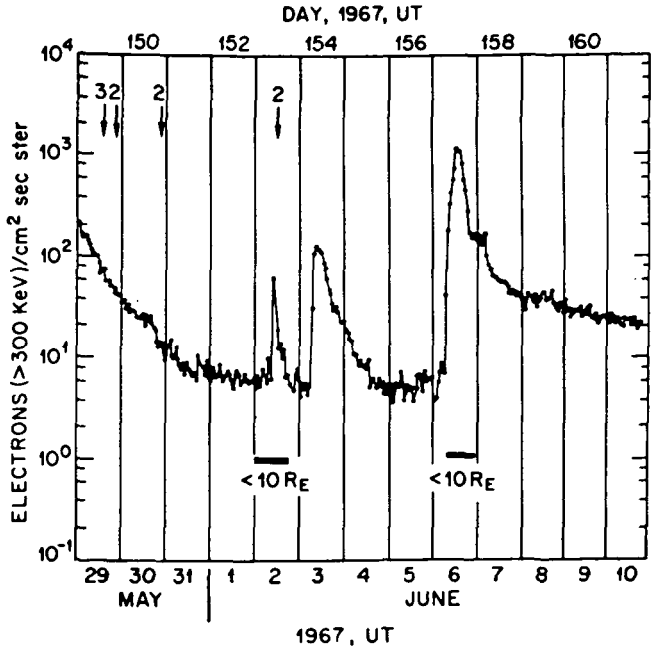


Fig. 2. The association of Explorer 34 hourly averaged electron data with Ogo 3 type III solar radio bursts, May 29 to June 10, 1967. The small event on June 2 occurred entirely during perigee passage of the spacecraft and is judged to be unrelated to solar electrons. The Ogo 3 radio bursts illustrated have been correlated with McMath plage region 8818, which was centered at approximately 45°W on May 29.

McMath plage 8905 are lumped together. Thirty-three of the thirty-five events occurred during periods of solar radio coverage. Eighteen of the thirty-three events (55%) had type III solar radio-burst associations, if criteria of an event occurring either ½ or 1 hour before the reported event onset were used. If the fourteen events resulting from McMath region 8905 are excluded, then only four of the remaining nineteen events (21%) had type III burst associations.

## Discussion

The results presented in Tables 1–3 indicate that both low-energy proton (~600 kev) and low-energy electron (~40 kev) interplanetary observations from June to November 1967 can be associated with type III radio bursts by using reasonable criteria for burst-particle associations. This finding is perhaps not surprising since type III radio bursts (as well as low-energy solar electrons and protons) are quite common occurrences. The higher-energy electrons ($E > 300$ kev) do not seem to be well associated with type III bursts. It may be that the production mechanism for these higher-energy electrons is more closely related to the mechanism for producing the relativistic electrons discussed by *Cline and McDonald* [1968] than to the mechanism for producing the lower-energy (~40 kev) electrons (although *Lin* [1970*a*] suggests the possibility of similar behavior for the >40 and >300 kev electrons). The belief that interplanetary electron observations firmly support the electron and type III burst associations [e.g., *Svestka*, 1969; *Lin*, 1970*a*] must be regarded as unproven.

The appropriateness of utilizing a given specific set of particle data for type III burst-source studies is difficult to assess. Interferometer measurements by *Wild et al.* [1959] indicate that type III sources are in rapid motion through the corona with velocities ranging from ~0.2 to ~0.8 $c$, which are much too fast for excitation by the low-energy protons used for the associations in Table 1, of course. However, it must be stressed that one aspect of particle excitation of plasma oscillations that has not

been investigated in any detail is the manner in which the energy spectra of the particles might be expected to change with time as a result of energy lost to the plasma. Present estimates of the energy in a particle stream [*Takakura*, 1967] and the energy radiated in the radio spectrum [*Maxwell et al.*, 1964] suggest that spectral changes should be insignificant. This conclusion, however, is strongly dependent on the efficiency of the plasma wave generation, a quantity that has not been determined. A recent model study of the intensity profiles of type III bursts [*Graedel*, 1970*b*], utilizing the assumption of electron excitation, has, in fact, concluded that the peak of the electron energy spectrum moves from $v \sim 0.5\ c$ to $v \sim 0.3\ c$ as the beam propagates outward from the sun. This result is consistent with observations over a wide range of frequencies [*Kundu*, 1965; *Fainberg and Stone*, 1970*b*]. The implication is that this spectral change is due to selective energy loss by the higher-velocity electrons. Extensive theoretical work in this area, including proton as well as electron beams, is obviously needed.

In conclusion, the data considered here do not lend credence to the common belief that the interplanetary-particle data confirm the association of electrons with type III radio bursts. The theoretical suggestions of *Kaplan and Tsytovich* [1968], *Friedman and Hamberger* [1969], and *Smith* [1970*a*, *b*] that proton beams may produce type III bursts should not be ignored on the basis of the present state of interplanetary-particle associations with radio bursts. A disturbing result arising from the

TABLE 3. Association of >40-kev Electron Events [*Lin*, 1970*a*] with Type III Dekametric Solar Radio Bursts

| DATE, 1967 | ONSET | OGO 3 | | | | SOLAR-GEOPHYSICAL DATA | | | | I.A.U. QUARTERLY BULLETIN | | | |
|---|---|---|---|---|---|---|---|---|---|---|---|---|---|
| | | OBS. | 0-1/2 HR. ASSOC. | 0-1 HR. ASSOC. | NO. ASSOC. | OBS. | 0-1/2 HR. ASSOC. | 0-1 HR. ASSOC. | NO ASSOC. | OBS. | 0-1/2 HR. ASSOC. | 0-1 HR. ASSOC. | NO ASSOC. |
| 5/28 | 0608 | | | | | X | | | X | X | | | X |
| 6/3 | 0623 | X | | | X | | | | | | | | |
| 6/6 | 0600 | X | | | X | | | | | | | | |
| 7/5 | 0803 | X | | | X | | | | | | | | |
| 7/28-8/4 | | (14 ELECTRON EVENTS ASSOCIATED WITH TYPE III SOLAR RADIO BURSTS) | | | | | | | | | | | |
| 9/11 | 1347 | | | | | X | | | X | X | | | X |
| 9/18 | 0415-0550 | | | | | X | | | X | X | | | X |
| 10/4 | 0847 | | | | | | | | | X | | | X |
| 10/7 | 0215-0240 | | | | | X | X | X | | X | X | X | |
| 10/7 | 1702 | | | | | X | X | X | | X | X | X | |
| 10/26 | 0004-0014 | | | | | X | | | X | X | | | X |
| 10/26 | 0640 | | | | | X | X | X | | X | X | X | |
| 10/27 | 1135 | | | | | | | | | X | | | X |
| 10/30 | 2336 10/29-0024 10/30 | | | | | X | X | X | | X | X | X | |
| 11/2 | 1017 | | | | | | | | | X | | | X |
| 11/4 | 1215 | | | | | | | | | X | | | X |
| 11/7 | 2247 | | | | | X | | | X | X | | | X |
| 11/11 | 0224-0235 | | | | | X | | | X | X | | | X |
| 11/30 | 0500-0540 | | | | | X | | | X | X | | | X |
| 11/30 | 0830-0857 | | | | | | | | | X | | | X |

above considerations is that it may be very difficult to definitively use much of the near-earth low-energy interplanetary-particle data to obtain significant information about characteristics of the solar-source region.

## References


Cline, T. L., and F. B. McDonald, Relativistic electrons from solar flares, *Solar Phys., 6,* 507, 1968.

Fainberg, J., and R. G. Stone, Type III solar radio burst storms observed at low frequencies, 1, Storm morphology, *Solar Phys., 15,* 224, 1970*a*.

Fainberg, J., and R. G. Stone, Type III solar radio burst storms observed at low frequencies, 2, Average exciter speed, *Solar Phys., 15,* 433, 1970*b*.

Fan, C. Y., M. Pick, R. Pyle, J. A. Simpson, and J. R. Smith, Protons associated with centers of solar activity and their propagation in interplanetary magnetic-field regions corotating with the sun, *J. Geophys. Res., 73,* 1555, 1968.

Friedman, M., and S. M. Hamberger, On a possible proton origin for type III continuum radiation from a solar flare, *Solar Phys., 8,* 398, 1969.

Graedel, T. E., The association of solar optical flares with type III solar bursts of 4 to 2 MHz observed by Ogo 3, *Astrophys. J., 160,* 301, 1970.

Graedel, T. E., A parametric study of the time profiles of type III solar radio bursts, *Planet. Space Sci.,* in press, 1971.

Haddock, F. T., and T. E. Graedel, Dynamic spectra of type III solar bursts from 4 to 2 MHz observed by Ogo 3, *Astrophys. J., 160,* 293, 1970.

*I.A.U. Quarterly Bulletin on Solar Activity,* nos. 158, 159, and 160, Eidgen. Sternwarte, Zurich, 1968.

Kaplan, S. A., and V. N. Tsytovich, Radio emission from beams of fast particles under cosmic conditions, *Sov. Astron.-AJ,* Engl. Transl., *11,* 956, 1968.

Kundu, M. R., *Solar Radio Astronomy,* John Wiley, New York, 1965.

Lanzerotti, L. J., H. P. Lie, and G. L. Miller, A satellite solar cosmic ray spectrometer with onboard particle identification, *IEEE Trans. Nucl. Sci., NS-16,* 343, 1969.

Lin, R. P., The emission and propagation of ~40-kev solar flare electrons, 1, The relationship of ~40-kev electrons to energetic proton and relativistic electron emission by the sun, *Solar Phys., 12,* 266, 1970*a*.

Lin, R. P., The emission and propagation of ~40-kev solar flare electrons, 2, The electron emission structure of large active regions, *Solar Phys., 15,* 473, 1970*b*.

Lin, R. P., Observations of scatter-free propagation of ~40-kev solar electrons in the interplanetary medium, *J. Geophys. Res., 75,* 2583, 1970*c*.

Lin, R. P., and K. A. Anderson, Electrons >40 kev and protons >500 kev of solar origin, *Solar Phys., 1,* 446, 1967.

Masley, A. J., and A. D. Goedeke, The 1966–67 increase in solar cosmic ray activity, *Can. J. Phys., 46,* S766, 1968.

Maxwell, A., R. J. Defouw, and P. Cummings, Radio evidence for solar corpuscular emission, *Planet. Space Sci., 12,* 435, 1964.

McCracken, K. G., U. R. Rao, and R. P. Bukata, Cosmic-ray propagation processes, 1, A study of the cosmic-ray flare effect, *J. Geophys. Res., 72,* 4293, 1967.

Simnett, G. M., T. L. Cline, S. S. Holt, and F. B. McDonald, Delayed appearance of relativistic electrons five days after a solar flare, paper MO-33 presented at 11th International Conference on Cosmic Rays, Budapest, 1969.

Smart, D. F., and M. A. Shea, The prediction of solar proton intensities expected after the occurrence of a solar flare (abstract), *Eos Trans. AGU, 51,* 410, 1970.

Smith, D. F., Towards a theory for type III solar radio bursts, 1, Nature of the exciting agency, *Solar Phys., 15,* 202, 1970*a*.

Smith, D. F., Type III solar radio bursts, *Advan. Astron. Astrophys., 7,* 147 1970*b*.

Svestka, Z., Comment on the note by Friedman and Hamberger, *Solar Phys., 8,* 400, 1969.

Takakura, T., Theory of solar bursts, *Solar Phys., 1,* 304, 1967.

U.S. Department of Commerce, *Solar Geophysical Data,* edited by J. Virginia Lincoln, IER-FB 277, 278, 279, 280, 281, NOAA, Boulder, Colo., 1968.

Van Allen, J. A., and S. M. Krimigis, paper presented at 1968 Mid-West Cosmic Ray Conference, Univ. of Iowa, Iowa City, February, 1968.

Wild, J. P., K. V. Sheridan, and A. A. Neylan, An investigation of the speed of the solar disturbances responsible for type III radio bursts, *Aust. J. Phys., 12,* 369, 1959.

Wild, J. P., S. F. Smerd, and A. A. Weiss, Solar bursts, *Ann. Rev. Astro. Astrophys., 1,* 1964.

N72-21846

# CHAPTER 15

## ENHANCED ABUNDANCES OF LOW ENERGY HEAVY ELEMENTS IN SOLAR COSMIC RAYS

L. J. Lanzerotti and C. G. Maclennan
Bell Telephone Laboratories
Murray Hill, New Jersey 07974

and

T. E. Graedel
Bell Telephone Laboratories
Whippany, New Jersey 07981

Measurements of solar cosmic ray O/He, Si/He, and Fe/He ratios during the onset phase of the 25 January 1971 flare event indicate a substantial (20-40 times) enhancement of the ratios above the solar photospheric abundances. It is suggested that preferential acceleration of the heavy elements within the solar flare region is the most likely cause of the increased abundances.

This letter reports the results of an analysis of low energy ($\sim$0.5-3 MeV/nucl.) solar flare proton and alpha particle spectra during the onset stage of the 25 January 1971 solar event (1B flare at N19 W50 at $\sim$2300 UT on 24 January). These data, together with recently reported O, Si, and Fe fluxes obtained from a rocket measurement during the flare, indicate that the ratios of the heavy element fluxes to the

alpha fluxes were ~20-40 times larger than expected on the basis of the solar photospheric abundances. These results from a single flare event confirm the detection of an enhanced solar flare Fe/He ratio which was reported from an analysis of the two year exposure of the Surveyor-3 TV camera filter to solar cosmic rays (Price et al., 1970). In addition, these results indicate that the Fe/He ratios at low energies may vary from event to event and are the first evidence that the solar flare O/He and Si/He ratios are also enhanced above the photospheric values. The degree of enhancement for the O/He and Si/He ratios is approximately one-half the amount of the Fe/He ratios in the particle energy range of 1.5-3.5 MeV/nucleon. These low energy solar cosmic ray results are strikingly different from those obtained for higher energy particles for which it has been established that the solar particle compositions and photospheric compositions are essentially identical. (Price et al., 1971; Durgaprasad et al., 1968; Biswas and Fichtel, 1965; Bertsch et al., 1969; 1972). A recent paper reports enhancements relative to solar abundances of the Si/O up to $(Cr\text{-}C_o)/O$ ratios in the energy range 14-61 MeV/nucleon (Mogro-Campero and Simpson, 1972).

The proton and alpha particle fluxes were measured by a four-element solid state detector telescope (half-angle ~20°) flown on the IMP 5 satellite. Using particle energy loss characteristics and pulse height analysis, protons, alphas,

and electrons were separately detected and energy analyzed. The Bell Laboratories telescope sampled the spin-averaged particle fluxes in the ecliptic plane approximately once each minute (Lanzerotti et al., 1969). During 25-26 January 1971 the IMP 5 satellite was in the magnetotail at a geocentric distance of ~30 earth radii ($R_E$); it was approximately along the earth-sun line with a solar-magnetospheric latitude of ~0°. The O, Si, and Fe measurements were obtained by particle track-counting procedures from a stack of Lexan and cellulose triacetate sheets flown on a rocket launched at 1519 UT on 25 January 1971 from Ft. Churchill (68.7°N, 322.8°E geomagnetic) (Price and Sullivan, 1971).

The satellite-measured proton (1.1-1.5 MeV) and alpha particle (1.5-2.1 MeV/nucl.) one-half-hour averaged profiles measured during the first three days of the particle event are shown in Fig. 1. Using the proton and alpha particle energy spectral measurements, the alpha to proton ($\alpha/p$) ratios for these first days of the event were computed and are plotted at the bottom of Fig. 1. The arrows on the figure indicate the time of the rocket flight. The rocket payload obtained a "snapshot" view of the flare particle composition during the onset phase of the event when the $\alpha/p$ ratios were enhanced relative to the ratios measured later in the event.

The O, Si, and Fe spectra obtained between 1520 and 1524 UT on 25 January and reported by Price and Sullivan

are plotted in Fig. 2, together with the proton and alpha particle spectra measured on IMP 5 during the same time period. Over the limited energy ranges shown, the alpha and proton spectra appear to be somewhat harder than the heavy element spectra. This spectral presentation implicitly assumes that the particle fluxes over Ft. Churchill are directly comparable with those measured in the magnetotail at $\sim 30\ R_E$. No direct supporting evidence for this assumption can be offered. We note, however, that direct measurements during other particle events have shown the alpha and proton fluxes in the magnetotail to be comparable with those in interplanetary space (Montgomery and Singer, 1969; Lanzerotti, et al., 1970), and that solar particle fluxes observed in the region of the auroral zone have also been measured to be comparable with interplanetary values (e.g., Van Allen, et al., 1971; Lanzerotti, 1972). We therefore feel that Fig. 2 probably constitutes a reasonable representation of the interplanetary particle population.

The low energy solar cosmic ray compositions obtained by linear interpolation and extrapolation from the spectral measurements of Fig. 2 are tabulated relative to He in Table I. Also tabulated, for comparison purposes, are the higher energy ($E \gtrsim 25$ MeV/nucl) solar cosmic ray abundances (Bertsch et al., 1969; 1972) as well as recent values of the photospheric abundances (Hange and Engvold, 1970; Withbroe, 1971a). The composition ratios measured here for 1.5-3.5 MeV/nucleon

particles are ~20 (for O and Si) to ~40 (for Fe) times higher than the photospheric values and higher-energy solar cosmic ray ratios. The Fe/He ratio is also somewhat higher than that inferred from the two-year integrated Surveyor results (Price et al., 1971). Within the uncertainties of the measurements, these O/He, Si/He, and Fe/He ratios appear to decrease slightly with increasing energy (as noted above, this is also apparent from the spectra of Fig. 2). This ratio decrease is consistent with the report of the Surveyor results that the Fe/He ratios appear to approach the energetic solar cosmic ray ratios at ~25-30 MeV/nucleon. Some evidence, consistent with the O/He ratio reported here, has been reported recently for an enhancement of the $Z > 3$ to helium ratio for ~300 keV/nucleon particles (Armstrong and Krimigis, 1971).

It does not seem likely that the low energy cosmic ray and photospheric abundance differences reported herein can be source-related; i.e., that they result from differences in elemental abundances between flaring and non-flaring regions. Flare optical spectra typically indicate enhanced temperatures within the emitting region, but no evidence for abundance differences has yet been found (Withbroe, 1971b). A recent comparison of photospheric and coronal abundances has indicated that no strong evidence exists for abundance differences between these two levels of the solar atmosphere

(Withbroe, 1971a). It seems reasonable, therefore, to ask if acceleration or propagation effects would explain the anomalous abundance ratios.

Little information or theory exists on possible flare acceleration mechanisms. The commonly discussed Fermi mechanism would not appear to be a cause of the preferential acceleration of heavy elements to helium since the rate of acceleration would be the same for equal velocity particles of the same mass-to-charge (M/Z) ratio. The abundance observations of low energy (<200 MeV/nucleon) $Z \geq 2$ galactic cosmic rays have recently been shown to have some systematic dependence upon the first ionization potential of the individual elements (Havnes, 1971). Such a suggestion might also well apply to the heavy solar cosmic rays discussed here, where the emission of He could be envisioned as suppressed. Such a suppression of the low energy He, together with the more "normal" heavy element/He ratios measured at the higher energies, would probably require a two-stage flare acceleration process with the first stage due to an electromagnetic ionization and acceleration process. The second stage might be a process such as the Fermi mechanism.

The enhancement of low energy iron to helium has been related to a possible preferential emission of heavy

elements from flare sites due to incompletely stripped nuclei at the low energies. Price et al. (1971) suggested that the effective charge Z* of the ionized particle could be given by the expression $Z^*/Z = [1 - \exp(-130\ \beta/Z^{2/3})]$ where $\beta = v/c$. Using the values of $\beta(\simeq 0.06\text{-}0.09)$ corresponding to the particle energies discussed here, it is easily seen that the low energy abundance ratios listed in Table I are not consistent with this suggestion.

Generally, low energy solar cosmic ray particles measured during the first day or so of an event exhibit an anisotropy direction approximately along the direction of the mean interplanetary field suggesting a predominantly diffusive propagation for the solar source (McCracken et al., 1971). If such a circumstance describes the propagation during 25 January, then it is difficult to see how interplanetary propagation effects would give rise to the heavy element/He ratio differences relative to the photospheric ratios observed for the equal M/Z (equal rigidities) He and heavy nuclei measured on this day.

In summary, the results presented here confirm the anomalously high Fe/He abundance in solar cosmic rays ($\sim$1-4 MeV/nucleon) relative to the photospheric abundances.

In addition, we find similar enhancements for the O/He and Si/He ratios. Such enhancements could result from the flare acceleration process. Measurements of other low energy heavy ion solar cosmic ray abundances during a large fraction of a solar cosmic ray event would be highly desirable in further exploring and understanding solar flare phenomena.

We thank Drs. P. B. Price and J. D. Sullivan for discussing their data with us.

TABLE I

ABUNDANCE DETERMINATIONS BY VARIOUS TECHNIQUES

| | H | He | O | Si | Fe |
|---|---|---|---|---|---|
| This paper | | | | | |
| a) 1.5 MeV/nucl. | 9.7 | 1 | .15 | .012 | .018 |
| b) 2.5 MeV/nucl. | 11 | 1 | .13 | .0083 | .016 |
| c) 3.5 MeV/nucl. | 17 | 1 | .11 | .006 | .014 |
| Photosphere[1,2] | 10 | 1 | .0068 | .00035 | .00025 |
| Solar Cosmic Rays[3] | - | 1 | .01 | .00028 | .0001 |

[1]Hange and Engvold (1970).

[2]Withbroe (1971a).

[3]Bertsch et al. (1969; 1972).

## References


Armstrong, T. P., and Krimigis, S. M. 1971, J. Geophys. Res., 76, 4230.

Bertsch, D. L., Fichtel, C. E., and Reames, D. V. 1969, Ap. J. (Letters), 157, L53.

_____. 1972, Ap. J. (in press).

Biswas, S., and Fichtel, C. E. 1965, Space Sci. Rev., 4, 709.

Durgaprasad, N., Fichtel, C. E., Guss, D. E., and Reames, D. V. 1968, Ap. J., 154, 307.

Hange, O., and Engvold, O. 1970, Inst. of Theor. Astrophys. Report No. 31, Blindern, Oslo, Norway.

Havnes, O. 1971, Nature, 229, 548.

Lanzerotti, L. J., Lie, H. P., and Miller, G. L. 1969, IEEE Trans. Nuc. Sci., NS-16 (1), 343.

Lanzerotti, L. J. 1972, Rev. Geophys. Space Phys., 10, (in press).

Lanzerotti, L. J., Montgomery, M. D., and Singer, S. 1970, J. Geophys. Res., 75, 3724.

McCracken, K. G., Rao, U. R., Bukata, R. P., and Keath, E. P. 1971, Solar Phys., 18, 100.

Mogro-Campero, A., and Simpson, J. A. 1972, Ap. J. (Letters), 171, L5.

Montgomery, M. D., and Singer, S. 1969, J. Geophys. Res., 74, 2869.

Price, P. B., Hutcheon, I., Cowsik, R., and Barber, D. J. 1971, Phys. Rev. Letters, 26, 916.

Price, P. B., and Sullivan, J. D. 1971, Paper SOL-9, International Cosmic Ray Conference, Hobart, Tasmania.

Van Allen, J. A., Fennell, J. F., and Ness, N. F. 1971, J. Geophys. Res., 76, 4262.

Withbroe, G. L. 1971a, U.S. Dept. Commerce, NBS Spec. Report Pub. No. 353, 121.

_____. 1971b, private communication.

## FIGURE CAPTIONS

Fig. 1. One-half hour averaged solar flare protons and alpha particles, together with the 2.5 MeV/nucleon alpha-to-proton ratios measured on IMP 5 during the 25 January 1971 event. The arrows indicate the time of the heavy element measurement.

Fig. 2. Solar cosmic ray spectra measured by satellite and rocket experiments at 1520-1524 UT 25 January 1971.

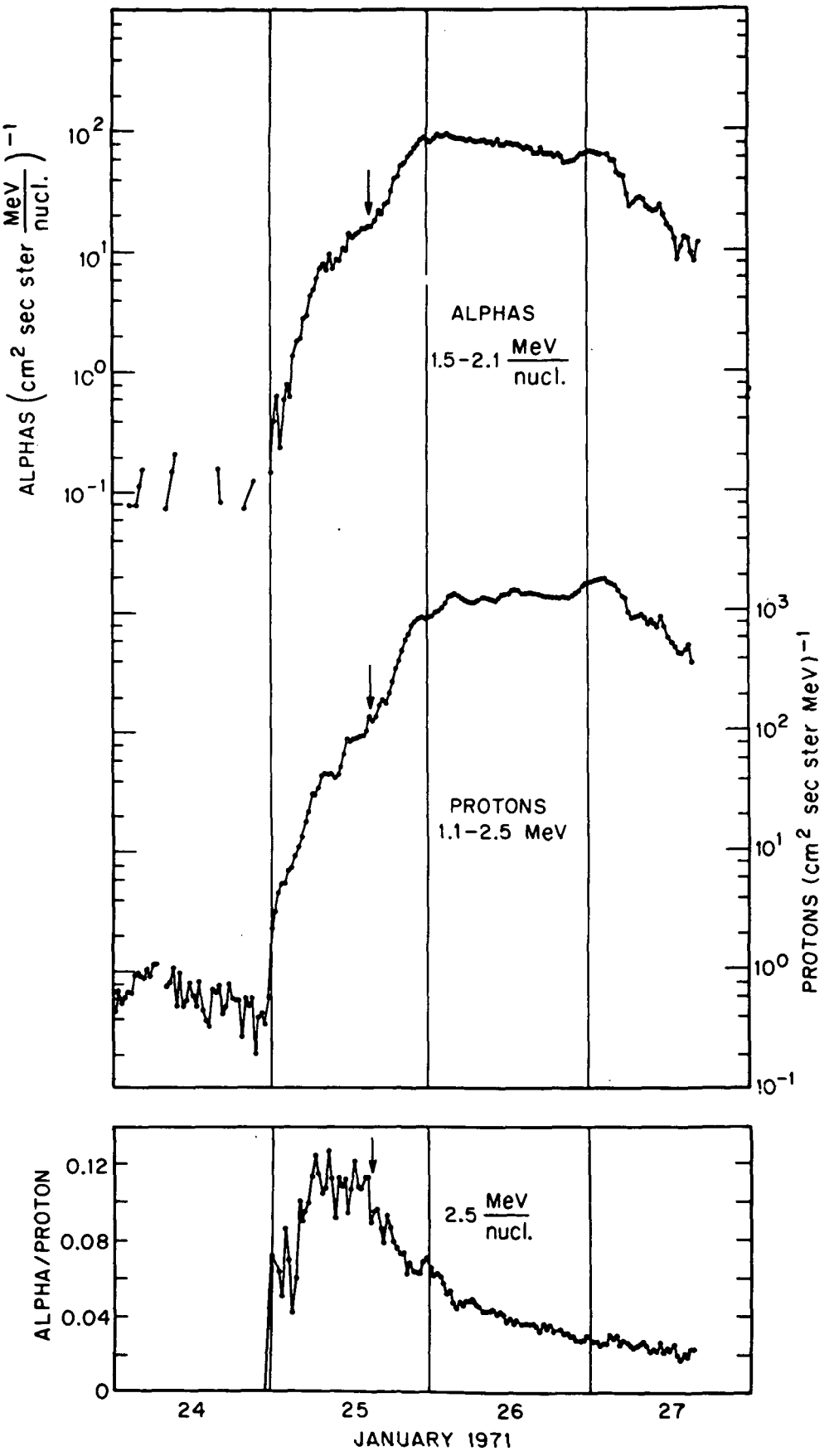
ALPHAS (cm² sec ster MeV/nucl.)⁻¹
10²
10¹
10⁰
10⁻¹
ALPHAS
1.5-2.1 MeV/nucl.
PROTONS
1.1-2.5 MeV
10³
10²
10¹
10⁰
10⁻¹
PROTONS (cm² sec ster MeV)⁻¹
ALPHA/PROTON
0.12
0.08
0.04
0
2.5 MeV/nucl.
24
25
26
27
JANUARY 1971

FIGURE 1

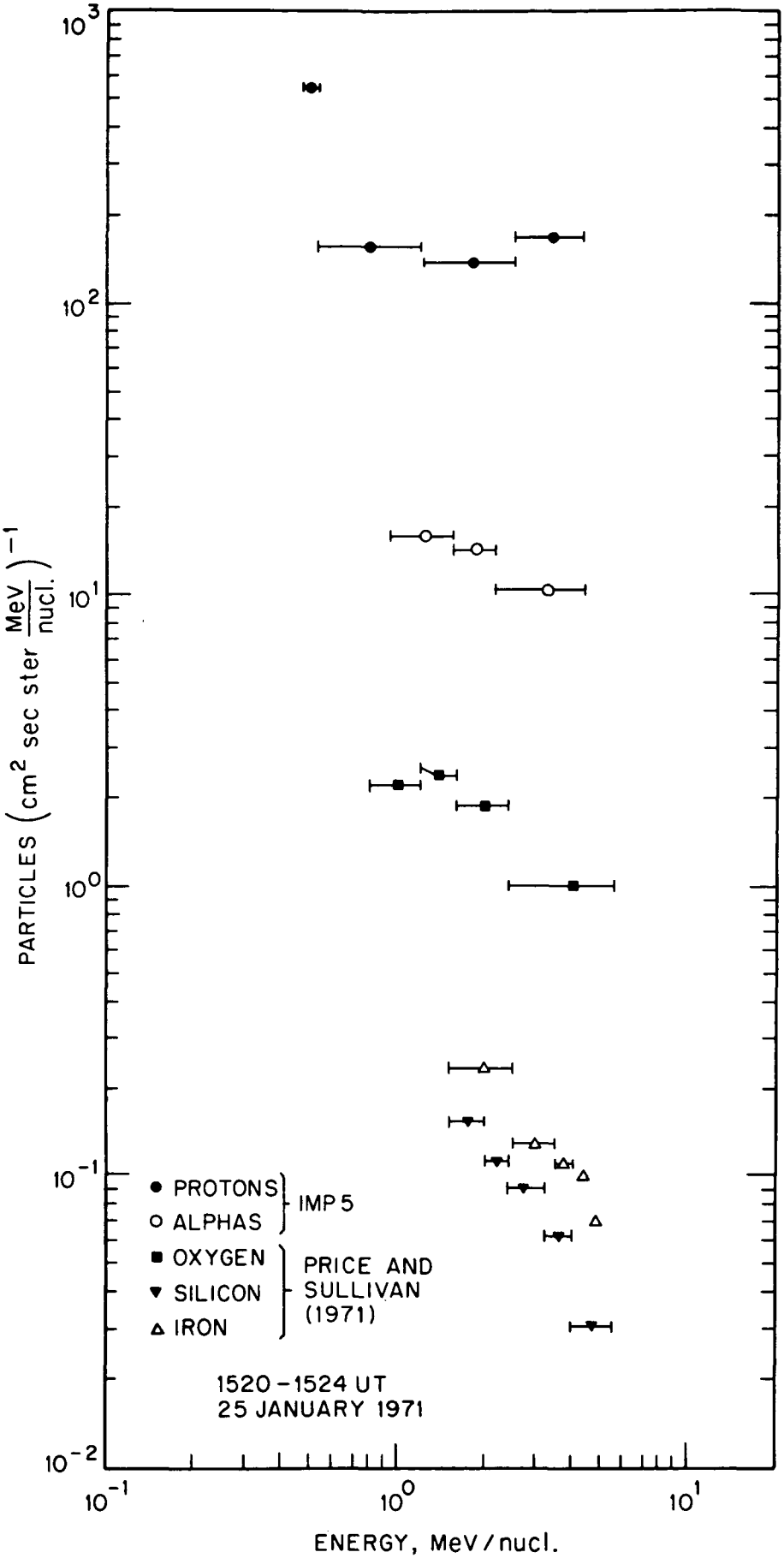
PARTICLES $\left(\text{cm}^2\ \text{sec ster}\ \frac{\text{MeV}}{\text{nucl.}}\right)^{-1}$
$10^3$
$10^2$
$10^1$
$10^0$
$10^{-1}$
$10^{-2}$
$10^{-1}$
$10^0$
$10^1$
ENERGY, MeV/nucl.
PROTONS
ALPHAS
IMP 5
OXYGEN
SILICON
IRON
PRICE AND SULLIVAN (1971)
1520 – 1524 UT
25 JANUARY 1971

FIGURE 2

N72-21847

# CHAPTER 16

## Solar Proton Radiation Damage of Solar Cells at Synchronous Altitudes

L. J. LANZEROTTI*
*Bell Telephone Laboratories, Murray Hill, N. J.*

THE synchronous altitude radiation environment is of great interest for the design of solar cell power sources for the large number of spacecraft (experimental, communication, meteorological, manned, and military) that will be flown at this altitude in the future. The purpose of this Note is to point out that recent experimental measurements of low-energy ($E$ = 1.0–20 Mev/nucleon) solar protons and alpha particles at the synchronous orbit show that the fluxes and spectra of these particles are in general quite similar to the solar particle observations made simultaneously in interplanetary space.[1] There are usually only very short time delays before the interplanetary particles are detected inside the magnetosphere at synchronous altitudes.

Although the mechanisms responsible for the rapid appearance of these particles into the outer magnetosphere is not

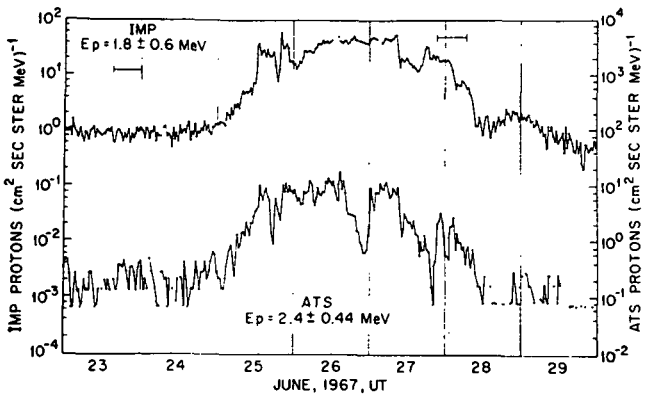


**Fig. 1 The simultaneous interplanetary and synchronous altitude half-hour averaged solar proton environment as measured in one proton detection channel on each of the ATS-1 and Explorer 34 satellites in June 1967. The horizontal bars indicate the periods when the Explorer 34 satellite was within the outer magnetosphere. ATS-1 local time (LT) is equal to universal time (UT) minus 10 hr.**

yet understood, the mere presence at synchronous altitude of a moderate flux of 1-Mev protons for several days can be the dominate damage mechanism for unshielded solar cells. These particle observations also explain the abnormal damage to unshielded solar cells discovered by the solar cell experiment on ATS-1.[2]

The comparison of the interplanetary and synchronous altitude protons and alphas in Ref. 1 was made during two moderate solar particle enhancements and a relatively long period of steady interplanetary intensities. It was concluded that whenever there were solar particles present in interplanetary space, these particles were seen at synchronous altitude; the synchronous altitude proton fluxes did not persist after the interplanetary enhancement was gone. During certain periods when the earth's geomagnetic activity was low a diurnal variation was also noted in the fluxes, with more protons seen on the night side of the earth than on the day side.[1,3,4]

Figure 1, adapted from Ref. 1, shows the half-hour averaged interplanetary and synchronous altitude proton fluxes for the time period around the flux enhancement of June 25–28, 1967. These data were obtained from Bell Laboratories particle experiments flown on the synchronous orbit ATS-1 and the interplanetary orbit Explorer 34 satellites. This moderate enhancement has been identified as probably due to the 27-day recurrence of the disturbed solar region which produced the large flares of May 21–23 and May 28, 1967.[1] Figure 1 shows very graphically that the solar particle fluxes inside and outside the magnetosphere have quite similar temporal appearance and magnitudes.

A comparison of the interplanetary and magnetosphere fluxes and spectra for a half-hour interval on June 26 is shown in Fig. 2a. In Fig. 2b is plotted the spectra observed during another solar particle enhancement in August 1967.[1] The fluxes of this Auguest event, which persisted at these magnitudes for more than one day, were approximately ten times the intensities of the June enhancement. These two enhancements, selected from the data of the past two years, are certainly not the largest solar events observed during this time period. Rather, these enhancements were selected to show the significance of even moderate solar fluxes at synchronous altitudes for radiation damage considerations.

The proton spectrum plotted in Fig. 2a was used to establish the bulk damage effects in a 1 Ω-cm n-on-p type solar cell. The effects of the alpha particles were neglected. It was assumed that the cell had infinite shielding on its rear contact. The proton equivalent 1 Mev electron flux curves given in Ref. 5 for the bulk damage effects were used.

A typical day side integral electron spectrum as observed at synchronous altitude[6] [$F(E_e > E) = 10^3 E^{-3}$ electrons cm$^{-2}$ sec$^{-1}$ sterad$^{-1}$] was used in comparing the damage due to the normal electron environment and the damage due to the low-energy solar protons. The synchronous altitude electron spectrum has diurnal as well as shorter-term changes,[6,7] but the spectrum used here is a good, conservative estimate of the electron environment for assessing maximum damage. The appropriate electron bulk damage curves, also contained in Ref. 5, were used.

The results of these damage calculations for June 26 are shown in Table 1 for the case of no solar cell shielding and for cases of shield thicknesses of 0.05 gm/cm$^2$ (~7.5 mil quartz) and 0.1 gm/cm$^2$ (~15 mil quartz). It is quite clear from the

**Table 1 Solar cell radiation damage**

| Particle | Bulk equivalent 1 Mev electrons, (cm² day)⁻¹ No shielding | 0.05 gm/cm² shielding | 0.1 gm/cm² shielding |
|---|---|---|---|
| Protons ($E$ >1.0 Mev) | $1.9 \times 10^{12}$ | $3.4 \times 10^{9}$ | $8.2 \times 10^{8}$ |
| Electrons ($E$ >0.5 Mev) | $1.5 \times 10^{10}$ | $1.4 \times 10^{10}$ | $1.2 \times 10^{10}$ |

Received June 30, 1969. The author thanks W. L. Brown for a discussion of these results.

* Member of Technical Staff.

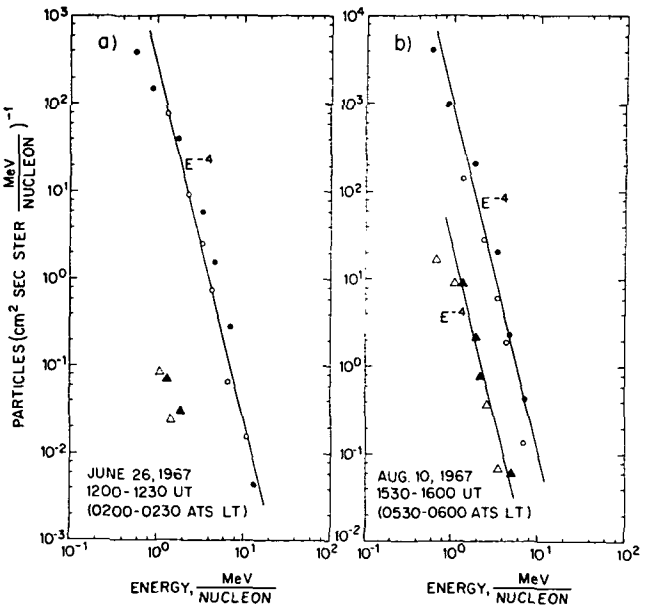


**Fig. 2 Interplanetary (solid points) and synchronous altitude (open points) particle fluxes for two solar particle enhancements in 1967. Circles correspond to protons; triangles correspond to alpha particles.**

results of Table 1 that an unshielded solar cell during a low-intensity solar enhancement like that of June 26, will suffer damage at a rate $\sim 10^2$ times the damage rate produced by the normal electron environment at synchronous altitude. However, the proton and electron damage rates would be approximately equal with an $\sim 0.03$ gm/cm$^2$ front shield; with a shield thickness of 0.05 gm/cm$^2$ the proton damage rate would be four times less than the electron damage rate. It is interesting, however, that the proton bulk damage rate to 7 mil shielded cells during the August 1967 event would be a factor of $\sim 2$ more than the electron damage rate and that therefore a large solar flare event (having the same or smaller power law dependence) could cause substantial damage to the satellite solar cells.

A degradation larger than expected was observed in the experimental solar cells in the damage experiment on ATS-1.[2] It was reported that, unexpectedly, a shield thickness of 6 mils offered greater power protection than either thinner (1 mil) or thicker (15, 30, and 60 mil) shielding. Although the thicker shielding result has not been satisfactorily explained,[2] it is likely that it is due to a decrease in the light transmission as the shield thickness is increased. It was also reported that the unshielded cells appeared to degrade by a series of steps, approximately in correlation with solar events.[2]

The results contained here in Table 1 are completely consistent with this last reported experimental observation. Since very many low-intensity, low-energy solar enhancements with soft spectra (as on June 26) have been measured at synchronous altitude, it is clear that a solar cell shield of $\sim 7$ mil thickness will largely eliminate the damage from such enhancements. With this thickness shield, only the protons from very high intensity, harder spectra solar flare events will dominate the electron environment in producing radiation damage effects in such shielded solar cells.

### References


[1] Lanzerotti, L. J., "Penetration of Solar Protons and Alphas to the Geomagnetic Equator," *Physical Review Letters*, Vol. 21, No. 13, Sept. 23, 1968, pp. 929–933.

[2] Waddel, R. C., "Solar Cell Radiation Damage on Synchronous Satellite ATS-1," X-710-68-408, Oct. 1968, NASA.

[3] Roberts, C. S. et al., "Synchronous Altitude Observation of Energetic Protons during the Solar Proton Event of January 28, 1967," *Transactions of the American Geophysical Union*, Vol. 49, No. 1, March 1968, p. 275.

[4] Paulikas, G. A. and Blake, J. B., "Penetration of Solar Protons to Synchronous Altitude," *Journal of Geophysical Research*, Vol. 74, No. 9, May 1969, pp. 2161–2168.

[5] Rosenzweig, W., "Space Radiation Effects in Silicon Devices," *IEEE Transactions on Nuclear Science*, Vol. NS-12, No. 5, Oct. 1965, pp. 18–29.

[6] Lanzerotti, L. J., Roberts, C. S., and Brown, W. L., "Temporal Variations in the Electron Flux at Synchronous Altitudes," *Journal of Geophysical Research*, Vol. 72, No. 23, Dec. 1967, pp. 5893–5902.

[7] Paulikas, G. A. et al., "Observations of Energetic Electrons at Synchronous Altitude, 1. General Features and Diurnal Variations," *Journal of Geophysical Research*, Vol. 73, No. 15, Aug. 1968, pp. 4915–4926.

N72-21848

# CHAPTER 17

## SOLAR FLARE PARTICLE RADIATION*

by

L. J. Lanzerotti
Bell Telephone Laboratories
Murray Hill, New Jersey 07974

## ABSTRACT

A review of the solar flare particle time dependence, composition, spectra, and propagation characteristics as observed at the earth is presented in this paper. Representative examples of ground and spacecraft observations of flare protons, alphas, and electrons are discussed. Differences in the time dependences of these particle fluxes after a flare as a function of particle energy and flare location are indicated. At very low energies (~1-10 MeV), the effects of convection by the solar wind apparently produce an approximately energy-independent decay time for post-flare particle fluxes that exhibit a diffusive temporal profile. Effects of solar flare particles at the earth in producing polar cap riometer absorption and in producing spacecraft solar cell damage at the synchronous altitude are also briefly outlined.

*Review presented at the National Symposium on Natural and Manmade Radiation in Space, 1-4 March 1971.

## I. INTRODUCTION

The sun is a source of copious fluxes of charged particles which escape into interplanetary space. These particles range in energy from the few keV solar wind particles to the several hundreds of MeV particles produced by the larger solar flare. There is even growing evidence that the sun may be a nearly continual emitter of low energy (several tens of keV) protons. This review is limited in that it concerns itself essentially entirely with the characteristics of the solar particles accelerated by solar flares and subsequently observed near the orbit of the earth.

The number of solar flares and the fluxes of energetic ($\gtrsim$ 20 MeV) solar particles observed at the earth varies in a manner similar to that of the sunspot number during the eleven-year solar cycle. This is illustrated by the data of Fig. 1 where the smoothed sunspot numbers for cycles of 19 and 20 are plotted as a function of time. Also shown are histograms of the yearly integrated proton intensities for protons $\gtrsim$ 30 MeV for both solar cycles (A. J. Masley, private communication). These particle fluxes are obtained

from riometer measurements of solar proton-produced PCA events in the polar-cap regions. The solar particle fluxes peaked in total intensity a year or more after the sunspot maximum during cycle 19. It remains to be seen if this same phenomenon holds during the current cycle.

This review discusses in order solar particle intensity-time profiles, the composition and spectra of solar flare events, and the propagation of solar particles in interplanetary space. The last section, dealing with the effects of solar particles at the earth, discusses riometer observations of polar cap cosmic noise absorption events and the production of solar cell damage at synchronous altitudes by solar protons.

## II. INTENSITY-TIME PROFILES

### Detectability Limits

The first observation of energetic particles due to solar production were the sea-level measurements of Lange and Forbush (1942), and Forbush (1946). Using shielded ionization chambers built to observe galactic cosmic rays, large enhancements in the chamber counting rates on 28 February 1942 ($\sim$1 day prior to a large magnetic storm), on 7 March 1942, and 25 August 1946 were observed. The development of the cosmic ray neutron monitor in the late 1940's and the super neutron monitor in the late 1950's and early 1960's have enabled many more solar particle increases to

be observed on the ground. The neutron multiplicity monitor (Nobles et al., 1967) enables particle spectral information to be obtained from a single station.

Other pre-spacecraft observations of solar cosmic rays were made during the IGY period by polar cap radio absorption techniques (Bailey, 1957) and by balloon measurements. The balloon observations of Anderson (1958) provided the first direct identification of solar protons.

The neutron monitor has continued to be a valuable tool for the detection of energetic solar particles. The world-wide deployment of stations provide data for studying both the direction of incidence of the primary particles as well as their energy. An example of the difference in response to an event by super neutron monitors at two different energy (or rigidity) cut-off latitudes is shown in Fig. 2 for data measured during the 28 January 1967 solar event (Bukata et al., 1969). The vertical cut-off rigidity for the Churchill station is 1.0 GV (determined essentially entirely by the atmospheric cut-off) while that of Dallas, at mid-latitudes geomagnetically, is 4.35 GV.

The time-intensity profile of the Churchill monitor response to the January 1967 event is quite typical of the classical, diffusive-like profiles recorded by high energy flare-particle detectors and will be discussed in more detail in Section V. In general in diffusive-like events, a rapid

rise to the peak particle intensity is followed by a slower, exponential or power-law decay with time.

With the advent of instrumentation flown on spacecraft, the energy sensitivity threshold for the detection of solar particles was dramatically reduced. This reduction in the lower limit of the energy of particle detectability has continued until today measurements of 300-500 keV solar protons are routinely carried out. Accompanying this decrease in the energy sensitivity of particles that can be measured was an increase in the number of solar events that were observed. Furthermore, at the lower energies measured, the time histories of the events became complex with no simple relationships often evident between events.

The data plotted in Fig. 3 illustrates the enormous differences in the description of the interplanetary particle intensities that could be made during a one-month period depending upon the energy sensitivity limits available for analysis. The data were obtained by the solar proton monitoring experiment on the Explorer 41 satellite (C. O. Bostrom, private communication). If only the higher energy channel ($E > 60$ MeV) were available for analysis, only one large event (March 27) and a small event (March 24) would have been apparent. Although the decay times are longer, both of these events had a diffusive temporal appearance similar to the neutron monitor event of Fig. 2.

As the particle energy threshold in Fig. 3 is lowered, more solar events are detected. The event beginning on March 6 (when viewed in the E > 10 MeV channel) no longer has a diffusvie shape. The solar fluxes in the 1-10 MeV channel of Fig. 3 are observed to remain above their background level throughout the entire 31-day period plotted.

Not all of the interplanetary particle enhancements result from discrete flare events. In general, flare-associated events occur in close association with solar X-ray and microwave emissions. Further, as noted above, the time-intensity profiles of flare-associated events tend to have a diffusive appearance. Three other types of particle enhancements, in addition to the flare-associated events considered in this paper, have been classified and discussed extensively in the literature. These are:

a) Particles associated with active centers: The onsets of these particles at the earth display no velocity dispersion and appear to be corotating with solar-active centers. Such enhancements have been observed to occur each solar rotation for many successive rotations (e.g., Fan et al., 1968; McDonald and Desai, 1971).

b) Recurrent events: These particle increases occasionally occur in the next solar rotation following a flare. They appear to originate from the same active region as that producing the flare (e.g., Bryant et al., 1965).

c) Energetic storm particles: Enhancements of low energy protons that appear for several hours around the time of occurrence of interplanetary shock waves (e.g., Axford and Reid, 1963; Bryant et al., 1965; Rao et al., 1967). Proton enhancements lasting for several minutes, apparently resulting from acceleration at the shock front, have been reported (e.g., Singer, 1970; Lanzerotti, 1969a; Armstrong and Krimigis, 1970; Oglivie and Arens, 1971).

Although the three solar particle enhancements listed above are important for understanding solar processes and interplanetary propagation, they will not be elaborated upon here.

Data Organization

Although the intensity-time profiles of high energy flare particles are similar in their overall diffusive appearance, absolute differences as a function of particle energy are common. Cline and McDonald (1968) have shown that the time history of the high energy proton and electron fluxes from the 7 July 1966 solar flare is dependent upon particle velocity. This is evident in Fig. 4 where the observed-time profiles for three proton and one electron channel are plotted in Fig. 4a. In Fig. 4b, the four particle flux channels have been normalized to their peak values and the abscissas have been transformed to represent the distance traveled from the flare occurrence.

Although the higher energy particle fluxes from this flare can be organized quite well by considerations of velocity-dependent travel, Lin (1970a) has shown that when electrons of energy > 45 keV from this event are included in the analysis, they show a broader curve than those in Fig. 4b. Furthermore, the E> 45 keV electrons appear to arrive earlier than the protons and electrons considered by Cline and McDonald (1968). Lin and Anderson (1967) and Lin (1970a) have interpreted this earlier arrival to low energy electron production either higher in the solar atmosphere or prior to the proton production.

## III. COMPOSITION

The most recent reviews of solar cosmic ray composition are those of Biswas and Fichtel (1965) and Fichtel (1970). They discuss in detail the several counter and emulsion measurements made on balloons and rockets beginning during the maximum of solar cycle 19. The discussion here will be limited primarily to observations of solar alpha particles and electrons. Observations of higher-Z elements will be briefly outlined.

### Solar Alpha Particles

The primary characteristic arising from the observations of solar alpha particles is that the ratio of the fluxes of solar alphas to solar protons appears to vary widely between individual events and even within a single

event. Both of these characteristics can be seen from Fig. 5 (Durgaprasad et al., 1967). Here are plotted the proton to alpha ratios for several different events as a function of particle kinetic energy.

More recently, using satellite instrumentation, the solar alpha measurements have been extended to lower energies and the time resolution during a single event has been substantially improved (Armstrong et al., 1969; Lanzerotti and Robbins, 1970). A comparison of the intensity-time profiles of solar protons and alphas from the series of flares on 21 and 23 May 1967, is shown in Fig. 6 (Lanzerotti and Robbins, 1970). The overall appearance of the intensity profiles of the two species are similar although differences do exist. In particular, the energetic storm particle enhancement at the time of the sudden commencement (SC) on May 24 is not strongly evident in the alpha fluxes.

The detailed alpha to proton ratios throughout the May 23 event are shown in Fig. 7. Large changes in the ratios are observed, particularly at the low energies, for protons and alphas when compared as to equal energy and equal energy per nucleon (equal velocity). However, the central panel of Fig. 7 indicates that after the increases in the ratios following the May 24 sudden commencement, the ratios remain constant throughout the remainder of the event for particles compared as to equal energy per charge.

Lanzerotti and Robbins (1970) have interpreted the increases in the alpha to proton ratios observed after the sudden commencement on May 24 as a source effect. They suggest that the solar particles observed prior to the SC were predominantly from flares on May 21 whereas those particles observed after the May 24 increase were from flares on May 23. They also suggested that the constancy of the ratios for equal energy per charge may indicate an important role for electric fields in low energy particle propagation and/or acceleration. Similar behavior of the alpha to proton ratios following other flare events have been noted (Lanzerotti, 1970a; Lanzerotti and Graedel; 1970).

Heavy Nuclei

Heavy solar cosmic ray nuclei ($Z \geq 3$) were first detected in nuclear emulsion stacks flown on a rocket during the 30 September 1960 event (Fichtel and Guss, 1961). The evidence gained from a number of balloon, rocket, and satellite experiments in the early 1960's indicates that the spectral forms for solar heavy nuclei and solar alpha particles are the same in any one event for particles down to ~30 MeV/nucleon (Fichtel, 1970).

A statistical study using satellite data has been made of the ratio of solar alphas to $Z \geq 3$ nuclei for a number of events in 1967-1968. The study indicates that for particles of $E > 0.5$ MeV/nucleon, the spectral behavior

observed at the higher energies continues to hold (Armstrong and Krimigis, 1971). It was found that the event-integrated alpha to heavy ratio was ~20 ± 10 for most events, a value substantially smaller than the ratio of 48 ± 8 reported by Durgaprasad et al. (1968) after the 2 September 1966 event in the 12-35 MeV/nucleon range. It is also smaller than the weighted mean of 58 ± 5 determined from six large events in 1960-1969 (Fichtel, 1970).

Solar Electrons

The first direct observation of solar electrons was made from data obtained on a balloon flight by Meyer and Vogt (1962) three days after a large flare on 20 July 1959. They detected highly relativistic electrons of energy 100-1000 MeV. Nonrelativistic electrons ($E > 45$ keV) were first measured in interplanetary space by Van Allen and Krimigis (1968) using an instrument flown on Mariner IV. Since that time, the time-intensity profiles of relativistic solar electrons (e.g., Cline and McDonald, 1968; Simnett et al., 1969) and nonrelativistic solar electrons (Anderson and Lin, 1966; Lin and Anderson, 1967; Anderson, 1969; Lin, 1970a, 1971) have been intensively studied.

The temporal characteristics of relativistic electrons following the 6 July 1966 flares are shown in relationship to the proton component in Fig. 4. It was found that for this flare the electron and proton components

could be organized in time by considerations of particle velocities alone. However, it was noted that Lin (1970a) showed that the low energy ($E > 45$ keV) electrons apparently arrived first, before the more energetic particles.

An example of a comparison of the electron intensity-time profiles for a single event is shown in Fig. 8 (Lin, 1970b, private communication; Lanzerotti, 1970a). These data, from a west limb flare, show rather similar time profiles for a wide range of electron energies. The similarities in the temporal profiles are in contrast to those observed in the case of protons (e.g., Fig. 3; see also Lanzerotti, 1970a, for proton temporal profiles measured during the same period as the electron data of Fig. 8). This could be due to a more direct propagation of electrons to the earth with less interplanetary diffusion and scattering than in the case of protons.

## IV. SPECTRA

As might be expected, solar flare particle spectra have large variations in intensities and spectral shapes both between individual events as well as within a single event. Representative proton, alpha particle, and electron solar flare particle spectra are discussed separately.

### Proton Spectra

The solar proton spectra, particularly for higher energies, generally steepen with time after the flare. That

is, as time progresses, relatively few higher energy particles as compared to the lower energies are present. The proton energy spectra measured in several of the large events during the last decade were found to fit very well a spectral representation with a rigidity dependence. This spectral shape can be expressed as (Freier and Webber, 1963)

$$\frac{dJ}{dR} = \frac{dJ_o}{dR_o} \exp\left[-R/R_o(t)\right] \qquad (1)$$

where $R = Mv/c$ is the proton regidity. It was found that this spectral representation was particularly applicable during the decay phase of an event for protons of energies $\gtrsim$ 20 MeV.

Six proton energy spectra obtained during several large events of the last solar cycle are plotted in Fig. 9. These spectra exhibit the exponential-in-rigidity spectral shape (Freier and Webber, 1963). Solar cosmic ray spectra such as those of Fig. 9 are very steep compared to the galactic cosmic ray spectra (e.g., Fichtel and McDonald, 1967).

Essentially all of the solar flare particle spectra taken during the last solar cycle were obtained by rocket or balloon-based instruments. Frequently, little o the time history of an event was obtained. Hence, relatively greater emphasis appears to have been placed on the spectra of the different events. During the present solar cycle, with

essentially continuous monitoring of an event's time profile and with the measurement of lower energy particles, less emphasis has been placed on the individual event spectra. This neglect of spectral emphasis partly arises, of course, because the spectra changes during an event, particularly for the events which do not exhitit a diffusive temporal profile at the lower energies (e.g., several of the events in Fig. 3). Hence, it is impossible to categorize an event simply with only one or two spectra. However, unlike the more energetic particles, and as will be discussed in Section V, the decay of low energy particles during events that do have a diffusive character appears to be energy independent. In this case, a single spectral shape would indeed describe much of the event's spectral form.

A single power-law in energy was fit by Lanzerotti (1969c) to the half-hour averaged proton spectra ($E_p$ = 0.58 to 18.1 MeV) measured during the event plotted in Fig. 6. He found that the spectra became significantly softer during the storm particle event on May 24 and for the next two and one-half days following the SC on May 25. At both times the exponent n changed from ~1.3 to ~2.0.

The low energy proton spectra measured by Bell Laboratories' instruments on Explorers 34 and 41 near the intensity maximum of several solar flare events in the past several years are plotted in Fig. 10. The spectra are

plotted on log-log scales to emphasize deviations from simple power-law relationships at these energies. In particular, the spectrum from the 2 November 1969 flare has a pronounced peak at E ~ 3.5 MeV which may signify particle propagation delays from the flare region (on the extreme west limb).

A study of the response of the world-wide network of neutron monitors to the 28 January 1967 event (see Fig. 2) has been made by Heristchi and Trottet (1971). They used the global distribution of neutron monitors as an energy spectrometer to determine a possible upper cutoff in the energy spectrum of the flare-produced protons from this event. They found an energy cutoff of 4.3 ± 0.5 GeV. This energy is $10^2$ - $10^3$ eV lower than that predicted by a flare acceleration model of Friedman and Hamberger (1969).

Alpha Particle Spectra

High energy (E $\gtrsim$ 30 MeV/nucleon) alpha particles were observed in a number of solar events to have spectra similar to those of the protons. Frequently, differential rigidity spectra (Eq. 1) were applicable to both particle species during an event, although the e-folding rigidity value $R_o$ might at times be different for the two species (e.g., Biswas et al., 1963; Durgaprasad et al., 1968).

Solar alpha particles were studied over a very wide energy range during the 12 November 1960 solar event. The differential alpha fluxes measured between ~31 and ~100

MeV/nucleon by several workers are presented in Fig. 11 (Biswas et al., 1962; Ney and Stein, 1962). Also shown are two high energy alpha flux measurements from the work of Yates (1964) during the same event.

The flux measurements of Yates (Fig. 11), if expressed on an exponential-in-rigidity basis, would fall considerably above what would be predicted by an extrapolation of the lower energy data (Yates, 1964). Yates' measurements were challenged by Waddington and Freier (1965) as perhaps being contaminated by the high fluxes of slow protons present during the event. The controversy appears still to be unresolved (Yates, 1965); very high energy measurements of solar alpha particles need to be made during other large events.

As noted in Section III, recent years have seen an increase in the time resolution of low energy solar alpha particle observations by satellite. Studies of the changes in the alpha spectra during a single event have become feasible, although little emphasis has been placed on this aspect of the observations. Lanzerotti (1969c) studied the power-law exponent of the alpha spectra for the May 1969 event (Fig. 6). He found that during the period between the two sudden commencements (May 24 and May 25), the alpha particle spectra were somewhat harder than that for protons; however, after the May 25 SC, both proton and alpha particle

power law exponents in Eq.(2) were ~2. The low energy alpha particle spectra measured by Bell Laboratories' instruments on Explorer 34 and Explorer 41 near the maximum of several solar events of the last several years are plotted in Fig. 12. These spectra give a representative example of low energy alpha spectral shapes and intensities.

Electron Spectra

Since the number of published observations of solar electrons is substantially less than for protons, detailed information on electron spectra is less plentiful. Lin (1970a) has compiled electron spectra from four solar events in 1967 as measured by instruments on Explorers 34 and 35. These spectra are shown in Fig. 13. Lin finds that if he fits the spectra to a power law (Eq. 2), the events in Fig. 13 have exponents $n \sim 2.3\text{-}3.5$.

## V. PROPAGATION

After acceleration, the flare-produced solar particles must escape from the active region and propagate through interplanetary space to the earth. Interplanetary space is permeated by the solar magnetic field. The nature of this field configuration was predicted by Parker (1960) to consist of spiral lines emanating from the sun. This prediction was subsequently confirmed by extensive satellite measurements (e.g., Ness et al., 1964). This spiral interplanetary magnetic field controls much of the propagation of

the flare particles. The guiding center of the solar particles tend to follow the spiral nature of the field. However, the small-scale irregularities in the field act as scattering centers and perturb, or scatter, the particles, moving them to other field lines. Extensive theoretical work (not discussed here) has been carried out in recent years in determining the solar particle diffusion coefficients due to these random scatterings (e.g., Jokipii, 1966, 1967, 1968; Rollof, 1966, 1968; Hasselmann and Wibberenz, 1968; Jokipii and Parker, 1969).

The propagation characteristics of solar particles have been reviewed recently (Fichtel and McDonald, 1967; Axford, 1970). The first considerations of a diffusion model for solar particle propagation was that of Parker (1956) and Meyer et al. (1956). The broad considerations and the development of isotropic diffusion theory for solar particles, i.e., solutions to a diffusion equation of the form

$$\frac{\partial n}{\partial t} = r^{-2} \frac{\partial}{\partial r}\left(r^2 \kappa \frac{\partial n}{\partial r}\right), \qquad (3)$$

have been due to Parker (1963). In Eq.(3), $n(r,t)$ is the mean density of solar particles with velocity $v$ and $\kappa = \frac{1}{3} v^2 \tau = \frac{1}{3} \lambda v$ is the diffusion coefficient and is, most generally, a tensor quantity (Jokipii, 1966). $\tau$ is the mean particle "collision time" for interaction with the

interplanetary magnetic irregularities and can be determined from the interplanetary field fluctuations (Jokipii and Coleman, 1968). Most commonly, solutions to Eq.(3) have assumed $\kappa = \kappa_o(T)r^{\beta}$ where T is the particle kinetic energy and $\beta$ is time-independent.

Solutions to Eq.(3) have chiefly considered two different boundary conditions. The first of these that has been used has taken $\beta = 0$ and has assumed a perfectly absorbing boundary ($n = 0$) at some $r = r_b > 1$ a.u. The solution to Eq.(3) at times $t >> r_b/\kappa_o$ after the flare yield an exponential decay for the fluxes

$$n(r,t) \sim \frac{1}{r} \sin \frac{\pi r}{r_b} \left[\frac{-\pi^2 \kappa_o t}{r_b^2}\right] \tag{4}$$

where the decay time is given as

$$\tau_D = \frac{r_b^2}{\pi^2 \kappa_o} \tag{5}$$

This solution to the model has been utilized by Bryant et al. (1962) and Hofmann and Winckler (1962) in analyzing solar particle events. They found that the absorbing "boundary" $r_b$ was at $r \sim 2$ a.u. Although the 2 a.u. boundary may indicate that the hydromagnetic waves producing the interplanetary irregularities are being damped out at this distance (Jokipii and Davis, 1969), Axford (1970) has maintained that an exponential decay of $\kappa$ with distance r will also produce the same results.

A number of solar events have been fit by Krimigis (1965) using a solution of Eq.(3) assuming a radial dependence to the diffusion coefficient (i.e., $\beta \neq 0$) and no boundary $r_b$ (Parker, 1963). This solution can be expressed as

$$n(r,t) \propto f(\kappa_o,\beta,T) \left[t^{3/(2-\beta)}\right]^{-1} \exp\left[-\frac{r^{2-\beta}}{(2-\beta)^2}\frac{1}{\kappa_o t}\right] \qquad (6)$$

A plot of $\ln[n(r,t)t^{3/(2-\beta)}]$ versus $t^{-1}$ should yield a straight line for the proper choice of $\beta(<2)$. Krimigis found that for protons in the energy range 50-500 MeV, good agreement with observations was obtained for $\beta \sim 1$ and $\lambda \sim 0.1$ a.u.

Anisotropic Diffusion

The isotropic solar particle diffusion model discussed above is not able to explain several important characteristics of the solar particles observed at the earth. One of these is the direction of the nonradial anisotropy of the particles measured at the earth. The anisotropy at the beginning of events is aligned along the spiral field direction, outward from the sun (McCracken, 1963; McCracken et al., 1967). (Later in the events the anisotropy becomes much less and the direction changes to radial or nearly so (McCracken et al., 1967; Rao et al., 1969). The second problem with isotropic models is that they cannot treat the observations that show tnat the particle fluxes arising from

flares in the eastern hemisphere of the sun tend to increase more slowly to maximum intensity than those that originate from west hemisphere flares (e.g., Fichtel and McDonald, 1967; Burlaga, 1967).

Reid (1964) has considered a solution to the east-west effect by postulating a thin diffusing shell around the sun. Particles originating from flares in the eastern hemisphere would diffuse (isotropically) across the solar surface to the spiral field lines connecting the sun to the earth and then propagate along the field lines to the earth (Fig. 14). Reid's model of diffusion across the solar surface must be combined with an interplanetary propagation model to provide a complete description of the particle event as seen at the earth. Since inclusion of the solar-surface diffusion increases the number of parameters that can be adjusted, it is likely that most diffusive-type observations could be fit with such a model. Indeed, a solar diffusing layer was one of the features included in a recent computational model for solar flare propagation (Englade, 1971).

The consideration of an anisotropic diffusion coefficient to solve the east-west problem was first made by Axford (1965). Burlaga (1967) solved the diffusion equation considering particle diffusion transverse to the spiral interplanetary field as well as along it and neglected Reid's diffusion layer around the sun. Expressed in spherical coordinates, Burlaga solved the equation

$$\frac{\partial n}{\partial t} = \frac{1}{r^2}\left[\frac{\partial}{\partial r}\left(r^2 \kappa_{\parallel} \frac{\partial n}{\partial r}\right)\right] + \frac{1}{r^2}\frac{\partial}{\partial \mu}\left[\kappa_{\perp}(1-\mu^2)\frac{\partial n}{\partial \mu}\right]$$

$$+ \frac{1}{r^2 \sin^2\theta}\frac{\partial}{\partial \varphi}\left[\kappa_{\varphi}\frac{\partial n}{\partial \varphi}\right] \qquad (7)$$

where $\mu = \cos\theta$ and $\kappa_{\parallel}$, $\kappa_{\perp}$, and $\kappa_{\varphi}$ are the components of the diffusion tensor.

Burlaga (1967) took the parallel diffusion coefficient $\kappa_{\parallel}$ to be a constant, independent of the radial position, the transverse coefficient $\kappa_{\perp}$ proportional to the square of the radial distance ($\kappa_{\perp} \propto r^2$), and an absorbing boundary at $r_b > 1$ a.u. Solving Eq.(7) with the above boundary conditions and assuming n to be independent of $\varphi$, he obtained quite satisfactory fits for a number of different flare events distributed over the solar disk. The event decay time resulting from his solution can be written as

$$\tau_D = \frac{r_b^2}{\pi^2 \kappa_{\parallel}} \qquad (8)$$

Eq.(8) is of the same form as the decay time derived for isotropic diffusion (Eq. 5) with the isotropic diffusion coefficient $\kappa_0$ replaced by $\kappa_{\parallel}$.

Two examples of Burlaga's fits to particle fluxes resulting from flares at two separate solar locations are shown in Fig. 15. The angle $\theta_o$ noted on the figure is the angle, measured from the center of the sun, between the flare

location and the location on the sun of the interplanetary field line passing through the earth. Fits of the model to both the neutron monitor observations of the 23 February 1956 event and the balloon observations of E > 80 MeV protons from the 20 July 1961 event are seen to be quite good.

Low Energy Propagation

It is clear from data such as those of Fig. 3 that at lower energies solar flare particles do not often have diffusive intensity-time profiles. Substantial modulation of these low energy particles by solar wind discontinuities, shock waves, and magnetic field sector boundaries must be occurring. Although there are events where the low energy particles exhibit diffusive-type profiles, the applicability of an anisotropic diffusion model such as Burlaga's to these observations is highly suspect (Forman, 1970). Forman has maintained that the "equilibrium" anisotropy present during the decay phase of an event (McCracken et al., 1967) and the evidence that the diffusion coefficient becomes small at low energies (Jokipii and Coleman, 1968) indicate that solar wind convection, and the resulting particle energy loss, is an important mode of low energy particle propagation. (The anisotropic diffusion model of Burlaga (as well as the isotropic models) considers convection effects to be negligible for the higher energy particles, and rightly so.) Forman (1971) cites as further evidence for the importance of

convection the fact that the reported decay times for both protons and alphas were essentially energy-independent for 1-20 MeV/nucleon particles after the 28 May 1967 flare (Lanzerotti, 1969a).

Forman (1971) has solved the Fokker-Planck equation first derived by Parker (1965) for particle transport including convection and diffusion:

$$\frac{\partial n(r,t)}{\partial t} + \nabla \cdot \left\{ V\left( n - \frac{1}{3} \frac{\partial}{\partial T} (\alpha T n) \right) - \kappa \cdot \nabla n \right\} = \frac{V}{3} \frac{\partial}{\partial r} \frac{\partial}{\partial T} (\alpha T n) \qquad (9)$$

Here V is the solar wind velocity, T is the particle kinetic energy, and $\alpha = (T+2Mc^2)/(T+Mc^2)$. The diffusion models discussed above all neglected the terms in Eq.(9) containing the solar wind velocity V. Forman obtained an analytic solution to Eq.(9) assuming that $\kappa_\perp = \kappa_1 r^2$, $\kappa_\parallel = \kappa_2 r$, and that there was a diffusing boundary at $r = r_b$. Forman's model predicts very well the equilibrium residual anisotropy during the decay phase of an event as observed by McCracken et al. (1967) as well as the magnitude (~14-18 hours) of the energy-independent decay time for both alphas and protons as observed by Lanzerotti (1969a).

From her solution to Eq.(9) Forman (1971) has shown that in the decay phase of the event

$$N(r,t) \propto f\left(\frac{r}{r_b}\right) r^{(V/2\kappa_2 - 1)} \exp\left(-t/\tau_D\right) \qquad (10)$$

where the decay time $\tau_D$ is given as

$$\tau_D = \frac{4r_b}{V} \frac{V/\kappa_2}{\left[J_{\eta,1}(V/\kappa_2)\right]^2} = \frac{4r_b}{V} g(V/\kappa_2) \quad . \tag{11}$$

In Eq.(11) $J_{\eta,1}$ is the first zero of the Bessel function of order $\eta$. Forman has found that for $r_b$ = 2.3 a.u. (a representative value determined from the model fits of Burlaga, 1967), $\tau_D$ has a broad maximum of ~15-17 hours for $\kappa_{||} = \kappa_2 r$ between $\sim 3 \cdot 10^{19}$ and $3 \cdot 10^{20} cm^2\ sec^{-1}$ (reasonable values for $\kappa_{||}$ as determined from the power spectra of the interplanetary magnetic field near the earth by Jokipii and Coleman, 1968). Forman's model has recently been applied successfully to the low energy proton observations from the 7 June 1969 event (Murray et al., 1970).

The energy-independence of the decay times for both protons and alpha particles during a diffusive-type event is shown in Fig. 16 for the 13 April 1969 event (Lanzerotti and Graedel, 1970). The intensity-time profiles of the proton fluxes in the $0.56 \leq E \leq 0.60$ MeV channel is shown as an insert in the figure. This event, probably originating from a flare behind the east limb, demonstrated a diffusive-type appearance even in the lowest energy-channel measured. This was quite unlike the 28 May 1967 diffusive event where energetic storm particles greatly enhanced the lower energy proton fluxes (Lanzerotti, 1969a). Also plotted

in Fig. 16 are the decay times for E > 10, >30, and >60 MeV protons measured by the solar particle monitoring experiment on the same satellite (Solar Geophysical Data, 1969). The decay time varied from ~28 hours at 0.58 MeV to ~19 hours at 60 MeV. Over the range 0.58 MeV to 20 MeV, the decay time decreased by only ~4 hours.

## VI. FLARE PARTICLE EFFECTS

Two consequences of solar flare particle effects are discussed below. The first of these is the effect of energetic flare particles in producing polar-cap cosmic noise absorption and the detection of this enhanced absorption by riometer techniques. The second is the effect of solar particles, penetrating into the outer magnetosphere, on satellite solar cell lifetimes.

### Riometer Absorption

The first indication of the production of enhanced ionosphere ionization by solar flare particles was the strong absorption of cosmic radio noise in the polar cap regions that Bailey (1957) correlated with the flare of 23 February 1956. Since that time, enhanced riometer absorptions in the auroral and polar cap regions during solar events have been studied as basic geophysical phenomena and as diagnostic tools for studying solar and magnetospheric processes (e.g., Bailey, 1964; Reid, 1970). Indeed, the significance of energetic storm particles was first outlined by Axford and Reid (1963) using riometer data.

Through the work of Potemra et al. (1967, 1969, 1970) good agreement has been achieved in calculating the expected riometer response from a measured incident solar flux. Potemra and his collaborators have calculated the expected total absorption A at a radio wave angular frequency $\omega$ from the formula

$$A(dB) = \int 1.16 \times 10^6 \frac{n_e}{\nu_m} C_{5/2} \left(\frac{\omega \pm \omega_H}{\nu_m}\right) dh \qquad (12)$$

obtained from the theory of Sen and Wyller (1960). In Eq.(12) $\omega_H$ is the angular gyro frequency, dh is the increment of ionization height in 10-km units, $C_{5/2}$ is an integral function, $n_e$ is the electron density and $\nu_m$ is the mean electron collision frequency. Using specific ionization rates due to G. W. Adams and Adams and Masley (1965) and $\nu_m$ and recombination coefficients deduced from the September 1966 event, Potemra et al. (1970) have predicted the observed absorption for high latitude riometer observations during a number of 1967 PCA events. Their calculations, using satellite measurements of the solar proton fluxes over the polar caps, are compared in Fig. 17 to the observed riometer day and night absorption measurements following the 28 January 1967 solar event. The agreement is quite good for both the day and night observations. (It is interesting to compare these lower energy proton observations of Fig. 17 with the neutron monitor profile for the same event in Fig. 2.)

Several authors (Van Allen et al., 1964; Juday and Adams, 1969; Reid, 1969, 1970) have used the empirical relation

$$(F)^{\frac{1}{2}} = R \times A \qquad (13)$$

to relate the integral fluxes F of protons above some energy $E_{min}$ to the riometer absorption A at a given frequency. In Eq.(13), R is a constant, dependent only upon $E_{min}$. Potemra and Lanzerotti (1971), using solar proton data from the synchronous equatorial ATS-1 satellite, deduced R as a function of $E_{min}$ from the 30 MHz riometer absorption observed at Byrd during the 28 January 1967 event. (Byrd (L ~7) is at nearly the same latitude as ATS-1 (L ~6.4) but three hours earlier in local time.) They found Eq.(13) to be an excellent fit to the data, essentially independent of the value of $E_{min}$. The values of $R(E_{min})$ they found for $E_{min}$ between 5 and 50 MeV are plotted in Fig. 18 as a function of $E_{min}$. Such R-values should be quite useful for the new solar proton event classification scheme (Shea and Smart, 1970).

Solar Cell Damage

Solar protons appear to have ready access to the outer regions of the magnetosphere other than through the polar cap regions. The solar particles at synchronour altitude are observed to have essentially the same intensities and spectra as the particles in interplanetary space for

protons as low as 1 MeV in energy (Lanzerotti, 1968, 1970b; Paulikas and Blake, 1969). These low energy protons could cause significant damage to unshielded solar cells on a synchronous satellite. It was pointed out by Lanzerotti (1969b) that the damage to unshielded cells from relatively low intensity solar events could dominate the normal synchronous altitude radiation (predominantly electrons) in producing damage. Indeed, anomalous, step-like changes in the short circuit current of unshielded cells in the ATS-1 solar cell damage experiment are observed in conjunction with solar flare events (Waddel, 1968).

An example of the solar proton damage to an unshielded solar cell on ATS-1 during the May 1967 events (Fig. 6) is shown in Fig. 19. The two lower bar graphs show the values of the short circuit current (in ma) measured each day for two 10 Ω-cm n-on-p type solar cells (R. C. Waddel, private communication). One cell was unshielded while the other had a 1 mil shield of 7740 glass. At the top are plotted the daily average of the integral half-hour average proton fluxes ($E > 2.4$ MeV) measured by the Bell Laboratories experiment on ATS-1. (No data were received on days 143, 144, and 147.)

Prior to the major interplanetary enhancement on day 145, the proton fluxes at ATS-1 were very low. The day after the large ATS-1 enhancement on day 145 the short

circuit current in the unshielded cell decreased sharply whereas only a slight decrease in the current was observed in the shielded cell.

Since a 1 mil shield will stop ~0.5 MeV protons, the data of Fig. 19 are indicative that protons with energies as low as this were producing the most significant damage. This could be due both to the penetration of 0.5 MeV solar protons to the synchronous orbit as well as to the fact that the magnetosphere boundary was pushed within the ATS-1 orbit for periods of time on days 145 and 146.

Even if shields were provided for synchronous satellite solar cells, the fluxes of low energy (0.5-3 MeV) solar protons penetrating to this altitude could still play an important role in the damage considerations. This is because in the manufacturing process the shields are often not deposited uniformly over the cell surfaces, leaving a small fraction of some cells uncovered (R. C. Waddel, private communication). Such partially unshielded cells would then be subjected to unexpected damage by the low energy protons.

ACKNOWLEDGEMENTS

I would like to thank the following individuals for generously providing data and comments for this review: Dr. C. O. Bostrom, Applied Physics Laboratory; Dr. R. P. Lin, University of California, Berkeley; Mr. A. J. Masley McDonnell-Douglass Astronautics Co.; Dr. T. A. Potemra, Applied Physics Laboratory; Dr. R. C. Waddel, NASA/GSFC.

## References


Adams, G. W., and A. J. Masley, J. Atmos. Terr. Phys., 27, 289, 1965.

Anderson, K. A., Phys. Rev. Letters, 1, 336, 1958.

Anderson, K. A., Solar Phys., 6, 111, 1969.

Anderson, K. A., and R. P. Lin, Phys. Rev. Letters, 16, 1121, 1967.

Armstrong, T. P., S. M. Krimigis, and J. A. Van Allen, Annals. IQSY, 3, 313, 1969.

Armstrong, T. P., S. M. Krimigis, and K. W. Behannon, J. Geophys. Res., 75, 5980, 1970.

Armstrong, T. P., and S. M. Krimigis, J. Geophys. Res., to be published, 1971.

Axford, W. I., Planet. Space Sci., 13, 1301, 1965.

Axford, W. I., Preprint, University of Calif., San Diego, August, 1970.

Axford, W. I., and G. C. Reid, J. Geophys. Res., 68, 1743, 1963.

Bailey, D. K., J. Geophys. Res., 62, 431, 1957.

Biswas, S., C. E. Fichtel, and D. E. Guss, Phys. Rev., 128, 2756, 1962.

Biswas, S., C. E. Fichtel, D. E. Guss, and C. J. Waddington, J. Geophys. Res., 68, 3109, 1963.

Biswas, S., and C. E. Fichtel, Ap. J., 139, 941, 1964.

Biswas, S., and C. E. Fichtel, Space Sci. Rev., 4, 709, 1965.

Bryant, D. A., T. L. Cline, U. D. Desai, and F. B. McDonald, J. Geophys. Res., 67, 4983, 1962.

Bryant, D. A., T. L. Cline, U. D. Desai, and F. B. McDonald, Ap. J., 141, 478, 1965.

Bukata, R. P., P. T. Gronstal, R. A. R. Palmeira, K. G. McCracken, and U. R. Rao, Solar Phys., 10, 198, 1969.

Burlaga, L. F., J. Geophys. Res., 72, 4449, 1967.

Cline, T. L., and F. B. McDonald, Solar Phys., 5, 507, 1968.

Durgaprasad, N., C. E. Fichtel, D. E. Guss, and D. V. Reames, NASA/GSFC Preprint X-611-67-324, July 1967.

Durgaprasad, N., C. E. Fichtel, D. E. Guss, and D. V. Reames, Ap. J., 154, 307, 1968.

Englade, R. C., J. Geophys. Res., 76, 768, 1971.

Fan, C. Y., M. Pick, R. Pyle, J. A. Simpson, and D. R. Smith, J. Geophys. Res., 73, 1555, 1968.

Fichtel, C. E., NASA/GFSC Preprint X-662-70-134, April 1970.

Fichtel, C. E., and D. E. Guss, Phys. Rev. Letters, 6, 495, 1961.

Fichtel, C. E., and F. B. McDonald, Ann. Rev. Astron. Astrophys., 5, 351, 1967.

Forbush, S. E.: Phys. Rev., 70, 771, 1946.

Forbush, S. E., and I. Lange: Terr. Mag., 47, 185, 1942.

Forman, M. A., J. Geophys. Res., 75, 3147, 1970.

Forman, M. A., J. Geophys. Res., 76, 759, 1971.

Freier, P. S., and W. R. Webber, J. Geophys. Res., 68, 1605, 1963.

Friedman, M., and S. M. Hamberger, Solar Phys., 8, 104, 1969.

Hasselmann, K., and G. Wibberenz, Zeit. für Geophysik, 34, 353, 1968.

Heristchi, Dj, and G. Trottet, Phys. Rev. Letters, 26, 197, 1971.

Hofmann, D. J., and J. R. Winckler, J. Geophys. Res., 68, 2067, 1963.

Jokipii, J. R., Ap. J., 146, 480, 1966.

Jokipii, J. R., Ap. J., 149, 405, 1967.

Jokipii, J. R., Ap. J., 152, 671, 1968.

Jokipii, J. R., and P. J. Coleman, Jr., J. Geophys. Res., 73, 5495, 1968.

Jokipii, J. R., and E. N. Parker, Ap. J., 155, 777, 1969.

Jokipii, J. R. and L. Davis, Ap. J., 156, 1101, 1969.

Juday, R. D., and G. W. Adams, Planet. Space Sci., 17, 1313, 1969.

Krimigis, S. M., J. Geophys. Res., 70, 2943, 1965.

Lanzerotti, L. J., Phys. Rev. Letters, 21, 929, 1968.

Lanzerotti, L. J., J. Geophys. Res., 74, 2851, 1969a.

Lanzerotti, L. J., J. Spacecraft and Rockets, 6, 1086, 1969b.

Lanzerotti, L. J., Report UAG-5, World Data Center A, 56, Feb. 1969c.

Lanzerotti, L. J., Report UAG-9, World Data Center A, 34, April 1970a.

Lanzerotti, L. J., Intercorrelated Satellite Obs. Related to Solar Events (D. Reidel Pub. Co., Dordrecht-Holland), pp. 205-228, 1970b.

Lanzerotti, L. J., and M. F. Robbins, Solar Phys., 10, 212, 1969.

Lanzerotti, L. J., and T. E. Graedel, Bull. Am. Phys. Soc., 15, 610, 1970.

Lin, R. P., and K. A. Anderson, Solar Phys., 1, 446, 1967.

Lin, R. P., Solar Phys., 12, 266, 1970a.

Lin, R. P., Report UAG-8, World Data Center A, 191, March 1970b.

Lin, R. P., Solar Phys., to be published, 1971.

McCracken, K. G., Solar Proton Manual, NASA Tech. Report R-169, 1963.

McCracken, K. G., U. R. Rao, and R. P. Bukata, J. Geophys. Res., 72, 4243, 1967.

McDonald, F. B., and U. D. Desai, J. Geophys. Res., 76, 808, 1971.

McDonald, F. B., V. K. Balasubrahmanyan, K. A. Brunstein, D. E. Hagge, G. H. Ludwig, and R. A. R. Palmeira, Trans. Am. Geophys. Union, 46, 124, 1965.

Meyer, P., and R. Vogt, Phys. Rev. Letters, 8, 387, 1962.

Meyer, P., E. N. Parker, and J. A. Simpson, Phys. Rev., 104, 768, 1956.

Murray, S. C., E. C. Stone, and R. E. Vogt, Trans. Am. Geophys. Union, 51, 798, 1970.

Ness, N. F., C. S. Scearce, and J. B. Seek, J. Geophys. Res., 69, 3531, 1964.

Ney, E. P., and W. A. Stein, J. Geophys. Res., 67, 2087, 1962.

Nobles, R. A., R. A. Alber, L. L. Newkirk, M. Walt, and C. J. Wolfson: Nucl. Instr. and Methods, 70, 45, 1969.

Ogilvie, K. W., and J. F. Arens, J. Geophys. Res., 76, 13 1971.

Parker, E. N., Phys. Rev., 103, 1518, 1956.

Parker, E. N., Ap. J., 132, 821, 1960.

Parker, E. N., Interplanetary Dynamical Processes (Interscience, New York), 1963.

Parker, E. N., Planet. Space Sci., 13, 9, 1965.

Paulikas, G. A., and J. B. Blake, J. Geophys. Res., 74, 2161, 1969.

Potemra, T. A., A. J. Zmuda, C. R. Haare, and B. W. Shaw, J. Geophys. Res., 72, 6077, 1967.

Potemra, T. A., A. J. Zmuda, C. R. Haare, and B. W. Shaw, J. Geophys. Res., 74, 6444, 1969.

Potemra, T. A., A. J. Zmuda, B. W. Shaw, and C. R. Haare, Radio Science, 5, 1137, 1970.

Potemra, T. A., and L. J. Lanzerotti, submitted to J. Geophys. Res., 1971.

Rao, U. R., K. G. McCracken, and R. P. Bukata, J. Geophys. Res., 72, 4325, 1967.

Rao, U. R., F. R. Allum, W. C. Bartley, R. A. R. Palmeira, J. A. Harries, and K. G. McCracken, Solar Flares and Space Research (North-Holland, Amsterdam), pp. 267-276, 1969.

Reid, G. C., J. Geophys. Res., 69, 2659, 1964.

Reid, G. C., Planet. Space Sci., 17, 731, 1969.

Reid, G. C., Intercorrelated Satellite Obs. Related to Solar Events (D. Reidel Pub. Co., Dordrecht-Holland), pp. 319-334, 1970.

Roeloff, E. C., Thesis, Univ. of California, Berkeley, 1966.

Roeloff, E. C., Can. J. Phys., 46, 5990, 1968.

Sen, H. K., and A. A. Wyller, J. Geophys. Res., 65, 3931, 1960.

Simnett, G. M., T. L. Cline, S. S. Holt, and F. B. McDonald, Paper MO-33, International Cosmic Ray Conference, Budapest, September, 1969.

Singer, S., Intercorrelated Satellite Obs. Related to Solar Events (D. Reidel Pub. Co., Dordrecht-Holland), pp. 571-582, 1970.

Smart, D. F., and M. A. Shea, Intercorrelated Satellite Obs. Related to Solar Events (D. Reidel Pub. Co., Dordrecht-Holland), pp. 102-107, 1970.

Solar-Geophysical Data, 303 Part II, 118-123, U. S. Department of Commerce, Boulder, Colorado, November, 1969.

Van Allen, J. A., and S. M. Krimigis, J. Geophys. Res., 70, 5737, 1965.

Van Allen, J. A., W. C. Lin, and H. Leinbach, J. Geophys. Res., 69, 4481, 1964.

Waddel, R. C., NASA/GSFC Preprint X-710-68-408, October 1968.

Waddington, C. J., and P. S. Freier, J. Geophys. Res., 70, 230, 1965.

Yates, G. K., J. Geophys. Res., 69, 3077, 1964.

Yates, G. K., J. Geophys. Res., 70, 232, 1965.

## FIGURE CAPTIONS

Fig. 1 Plot of the smoothed sunspot numbers for solar cycles 19 and 20 and histograms of the annual fluxes of solar protons (E > 30 MeV) for solar cycle 19 (shaded bars) and cycle 20 (dotted bars). Figure courtesy of A. J. Masley.

Fig. 2 Neutron monitor observations at Ft. Churchill and Dallas of the 28 January 1967 solar event (Bukata et. al., 1969).

Fig. 3 Solar protons measured in interplanetary space by the solar proton monitoring experiment on Explorer 41 during March 1970. At the bottom of the figure are plotted the satellite distance from the earth and the position of the satellite projected on the ecliptic plane. Data courtesy of C. O. Bostrom.

Fig. 4 (a) Profiles of the observed intensity of protons (16-38 MeV, 38-59 MeV, and 59-80 MeV) and electrons (>3 MeV) plotted versus time following the 7 July 1966 flare; (b) profiles of each particle channel relative intensity ($I/I_{max}$) plotted as a function of distance traveled ($x = vt$) where v is the mean velocity for each particle channel (Cline and McDonald, 1968).

Fig. 5 Ratio of protons to helium nuclei as a function of kinetic energy per nucleon measured at different times in several solar events. The events in which the measurements were made are: A, B - 12 November 1960

(Biswas et. al., 1962); C, D, E - 15 November 1960 (Biswas et. al., 1963); F - 3 September 1960 (Biswas and Fichtel, 1964); G - 16 March 1964 and 5 February 1965 (McDonald et. al., 1965); P - 2 September 1966 (Durgaprased et. al., 1967). (From Durgaprased et. al., 1967).

Fig. 6 Alpha particle and proton fluxes measured following the 21 and 23 May 1967 solar events. (Lanzerotti and Robbins, 1969).

Fig. 7 Alpha particle to proton flux ratios compared as to equal particle energy, equal particle energy per nucleon (equal velocities) and equal particle energy per charge (Lanzerotti and Robbins, 1969).

Fig. 8 Time variations of the solar electron fluxes measured following the west limb event on 18 November 1968. The $E > 45$ keV data are from Lin (1970b; private communication). The higher energy data are from Lanzerotti (1970a).

Fig. 9 Solar proton spectra measured in several solar events (Freier and Webber, 1963).

Fig. 10 Low energy solar proton spectra measured on Explorers 34 and 41 near the maximum of several solar events.

Fig. 11 High energy solar alpha particle fluxes measured by several observers following the 12 November 1960 solar event (from Yates, 1964).

Fig. 12 Low energy solar alpha particle spectra measured on Explorers 34 and 41 near the maximum of several solar events.

Fig. 13 Solar electron spectra measured during four events in 1967 (Lin, 1970a).

Fig. 14 Illustration depicting solar particle diffusion across the solar surface to the interplanetary flux tube linking the sun to the earth (Reid, 1964).

Fig. 15 Fit of the anisotropic diffusion-with-a-boundary solar particle propagation model to an event measured by a neutron monitor and an event measured by a balloon-based detector (from Burlaga, 1967).

Fig. 16 Proton and alpha particle decay times following the 13 April 1969 solar event. The intensity-time profile for the $0.56 \leq E \leq 0.60$ MeV proton channel is shown as an inset to the figure (Lanzerotti and Graedel, 1970).

Fig. 17 Comparison of observed day and night riometer absorption and the calculated absorptions using polar cap-average solar proton data from satellite 1963-38C during the 28 January 1967 event (Potemra et. al., 1970).

Fig. 18 Factor R empirically relating the riometer absorption to the square root of the integral proton fluxes plotted as a function of $E_{min}$, the lower energy limit on the integral fluxes. R was determined from the 28 January 1967 event (Potemra and Lanzerotti, 1971).

Fig. 19 Daily measurements of the short circuit current in an unshielded and a shielded solar cell in the solar cell damage experiment on ATS-1 (data courtesy of R. C. Waddel). Plotted at the top are the daily averages of the integral half-hour average proton fluxes ($E > 2.4$) measured on ATS-1 during the May 1967 solar events.

INTEGRATED SOLAR PROTON INTENSITY DISTRIBUTION
SUNSPOT CYCLES 19 AND 20

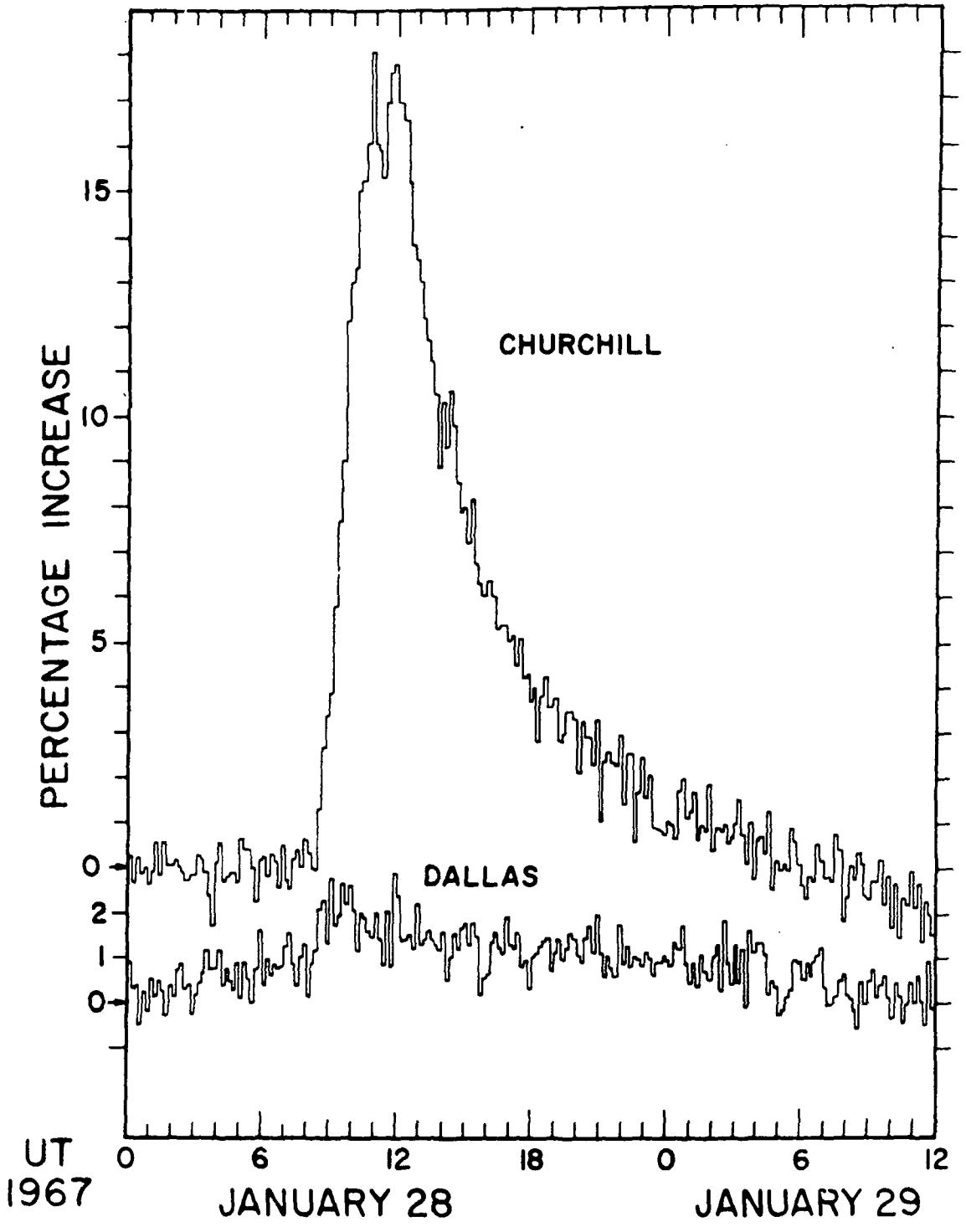
PERCENTAGE INCREASE
15
10
5
0
2
1
0
CHURCHILL
DALLAS
UT
1967
0
6
12
18
0
6
12
JANUARY 28
JANUARY 29

Figure 2

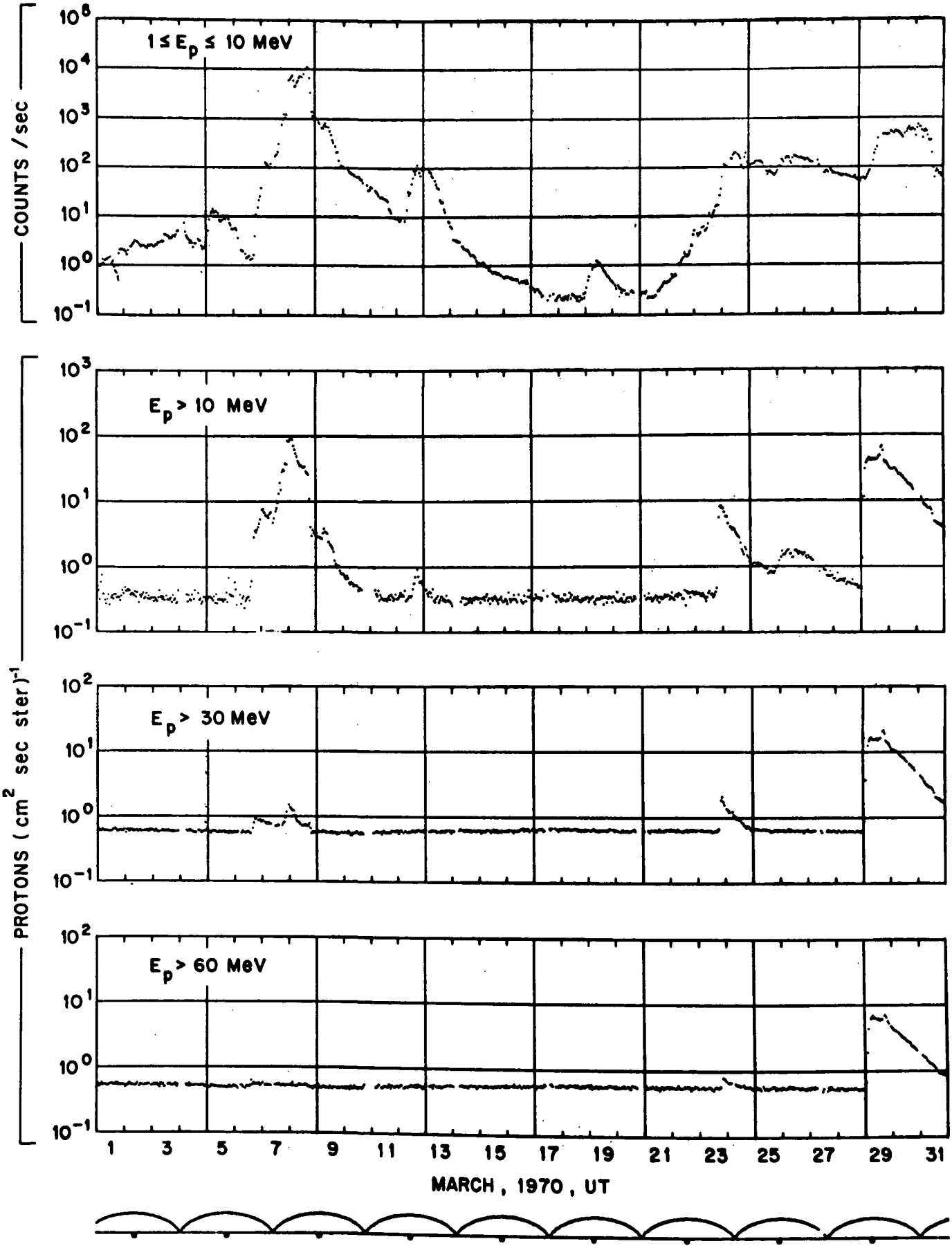
COUNTS / sec
$10^5$
$10^4$
$10^3$
$10^2$
$10^1$
$10^0$
$10^{-1}$
$1 \leq E_p \leq 10$ MeV
PROTONS ( $cm^2$ sec ster)$^{-1}$
$10^3$
$10^2$
$10^1$
$10^0$
$10^{-1}$
$E_p > 10$ MeV
$10^2$
$10^1$
$10^0$
$10^{-1}$
$E_p > 30$ MeV
$10^2$
$10^1$
$10^0$
$10^{-1}$
$E_p > 60$ MeV
1 3 5 7 9 11 13 15 17 19 21 23 25 27 29 31
MARCH , 1970 , UT

Figure 3

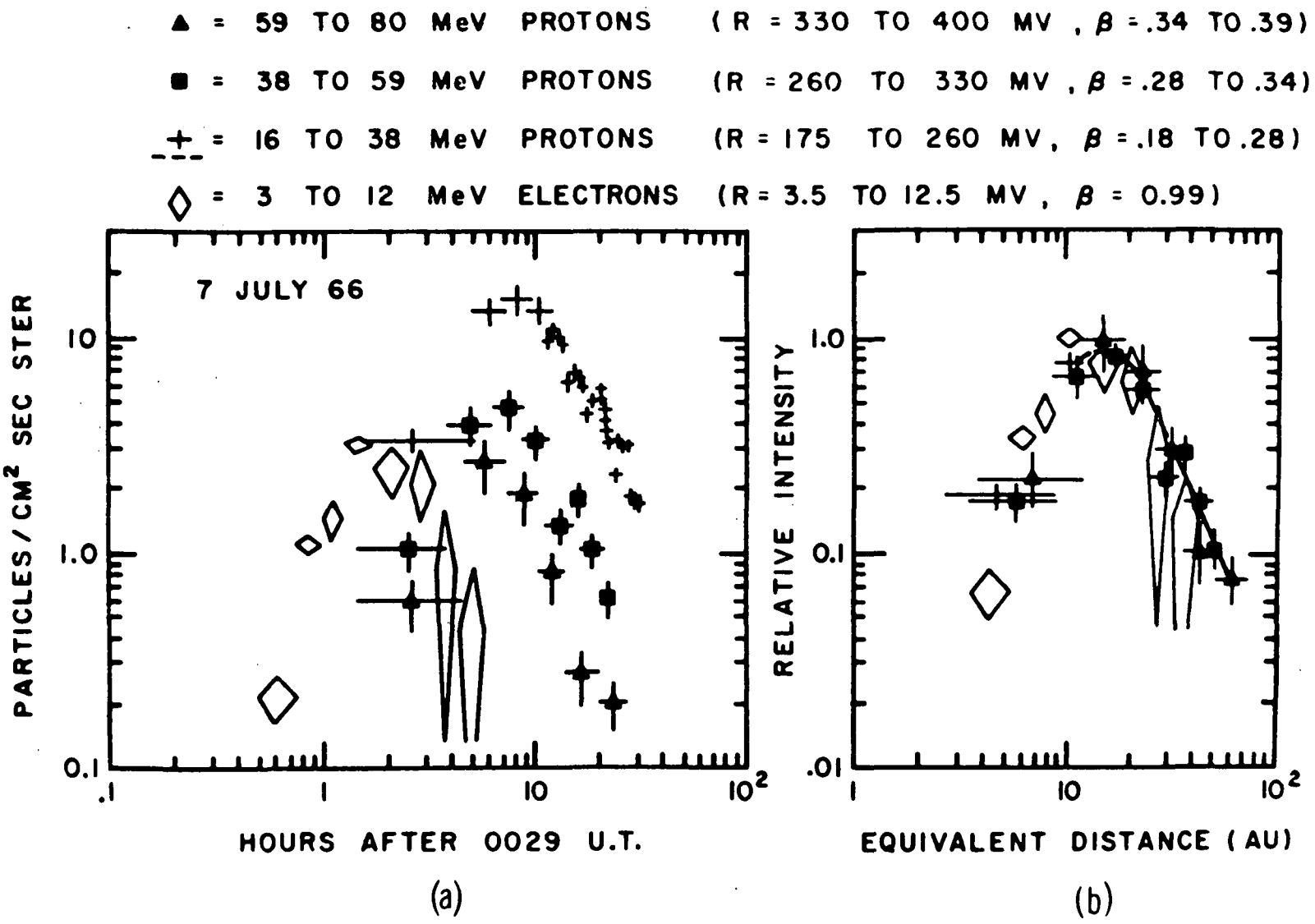
▲ = 59 TO 80 MeV PROTONS (R = 330 TO 400 MV, β = .34 TO .39)
■ = 38 TO 59 MeV PROTONS (R = 260 TO 330 MV, β = .28 TO .34)
+ = 16 TO 38 MeV PROTONS (R = 175 TO 260 MV, β = .18 TO .28)
◇ = 3 TO 12 MeV ELECTRONS (R = 3.5 TO 12.5 MV, β = 0.99)
7 JULY 66
PARTICLES / CM² SEC STER
10
1.0
0.1
.1
1
10
10²
HOURS AFTER 0029 U.T.
(a)
RELATIVE INTENSITY
1.0
0.1
.01
1
10
10²
EQUIVALENT DISTANCE (AU)
(b)

Figure 4

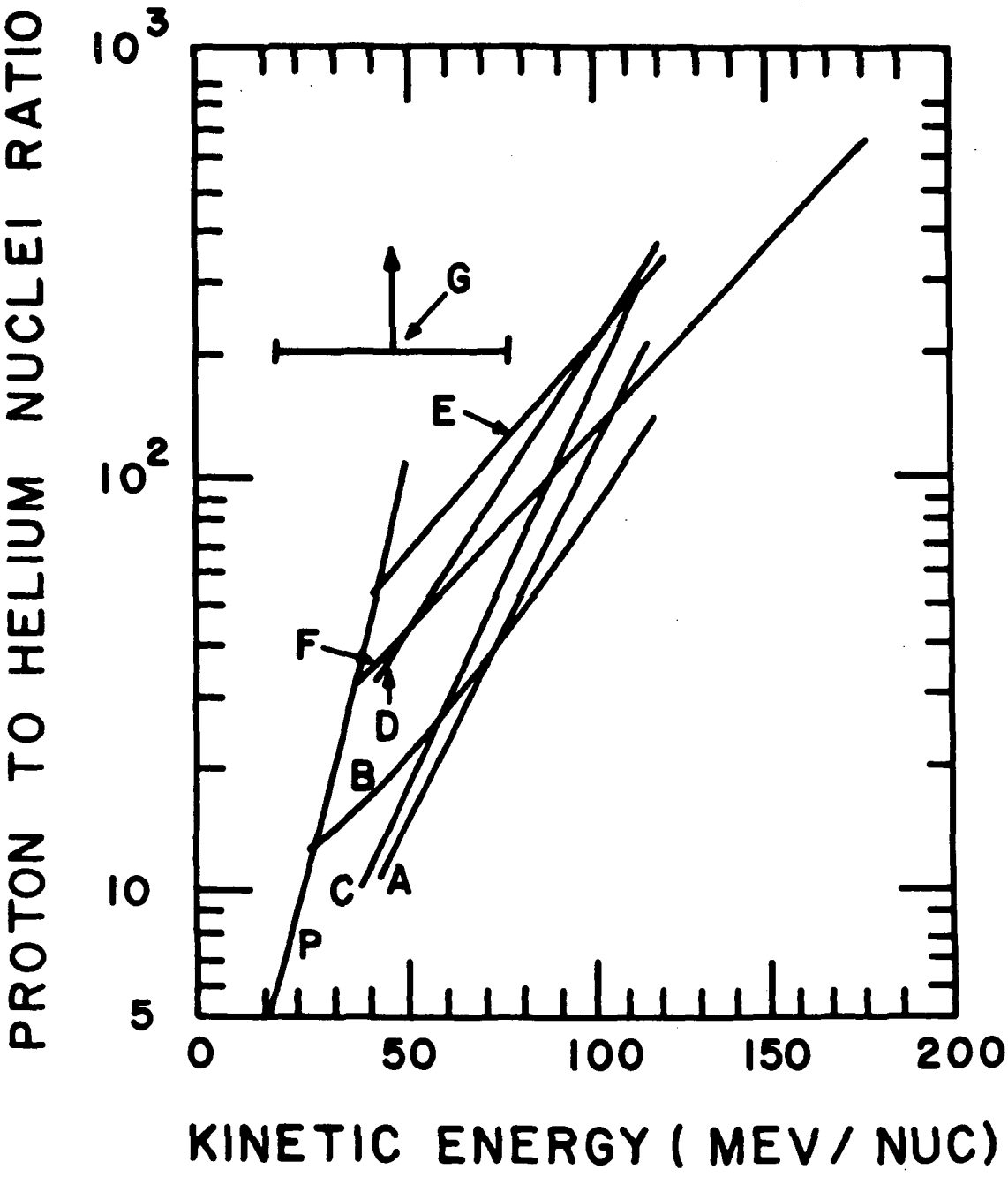
PROTON TO HELIUM NUCLEI RATIO
$10^3$
$10^2$
10
5
0
50
100
150
200
KINETIC ENERGY ( MEV / NUC)
G
E
F
D
B
C
A
P

Figure 5

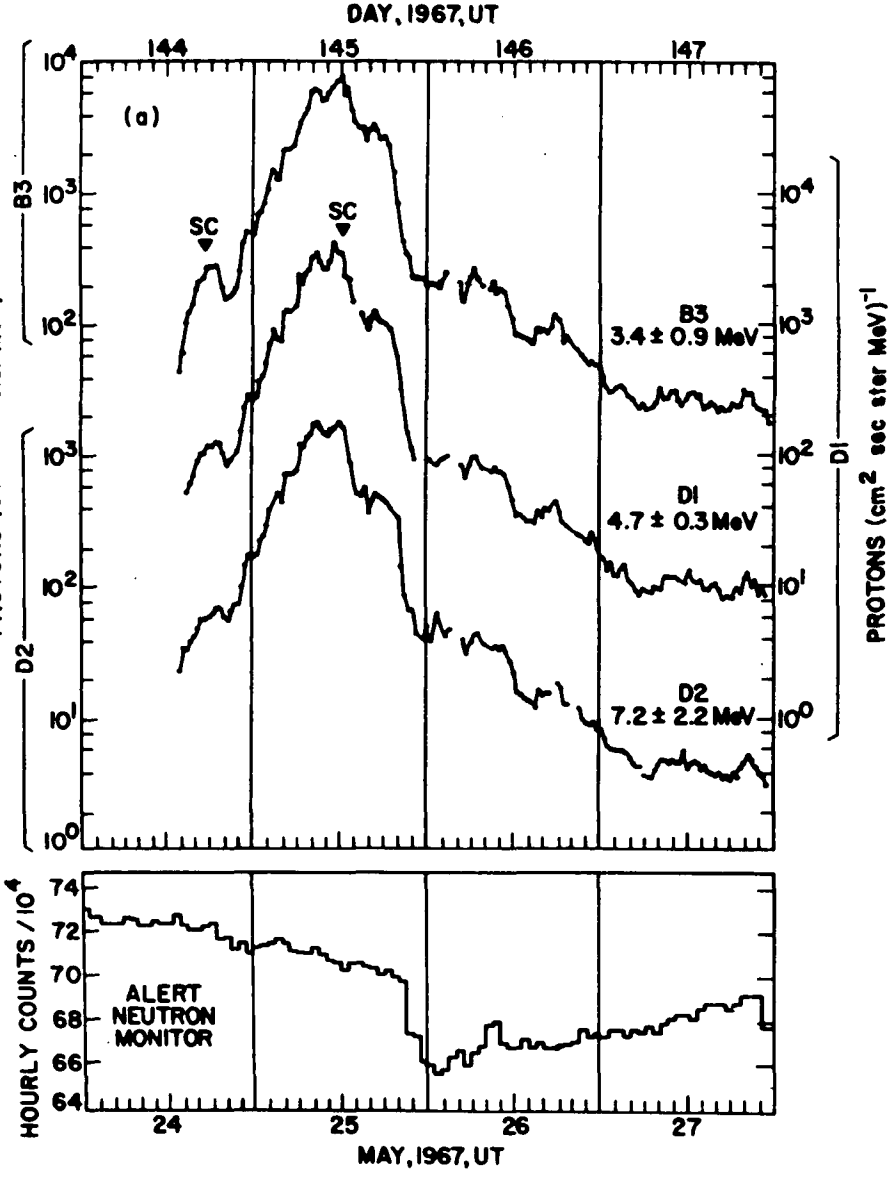
DAY, 1967, UT
144
145
146
147
(a)
SC
SC
B3
3.4 ± 0.9 MeV
D1
4.7 ± 0.3 MeV
D2
7.2 ± 2.2 MeV
PROTONS (cm² sec ster MeV)⁻¹
B3
D2
D1
PROTONS (cm² sec ster MeV)⁻¹
HOURLY COUNTS / 10⁴
ALERT
NEUTRON
MONITOR
24
25
26
27
MAY, 1967, UT

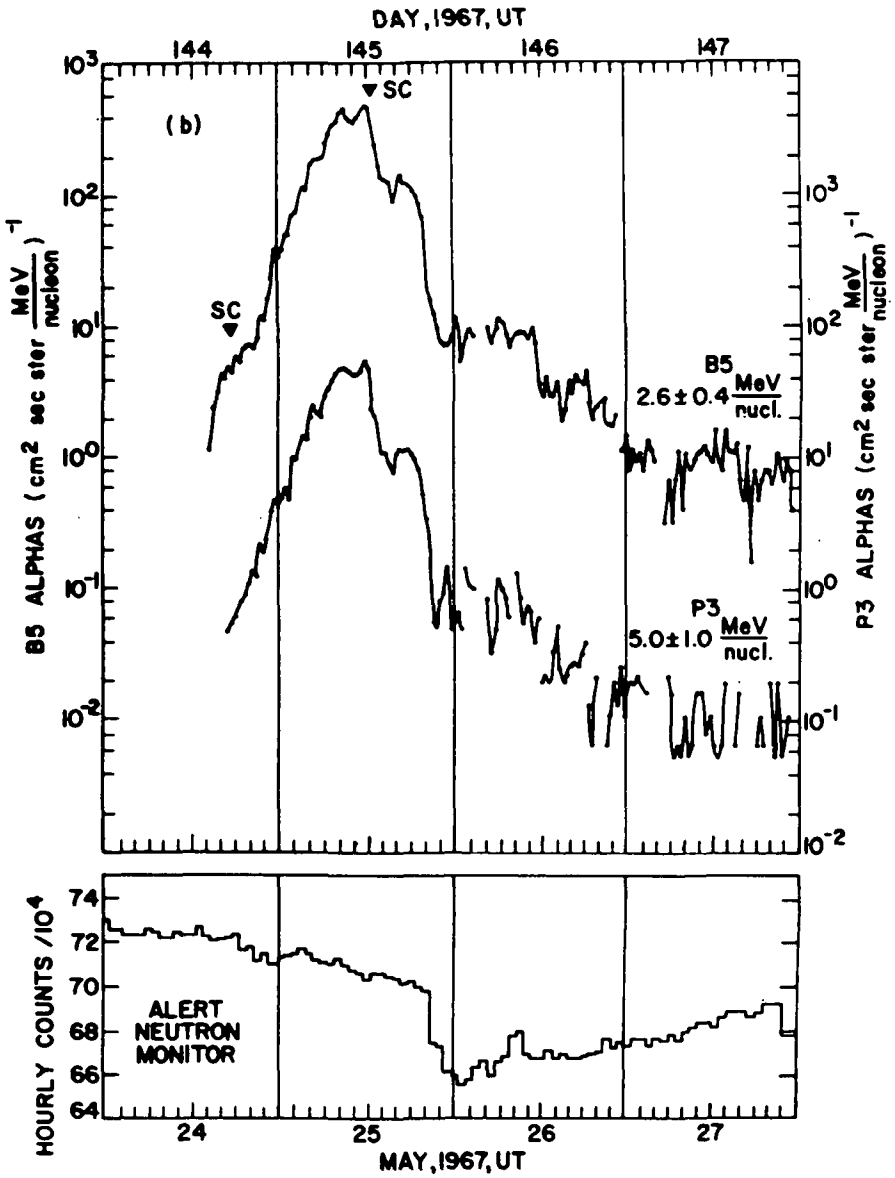
DAY, 1967, UT
144
145
146
147
(b)
SC
B5
2.6 ± 0.4 MeV/nucl.
P3
5.0 ± 1.0 MeV/nucl.
B5 ALPHAS (cm² sec ster MeV/nucleon)⁻¹
P3 ALPHAS (cm² sec ster MeV/nucleon)⁻¹
HOURLY COUNTS / 10⁴
ALERT
NEUTRON
MONITOR
24
25
26
27
MAY, 1967, UT

Figure 6

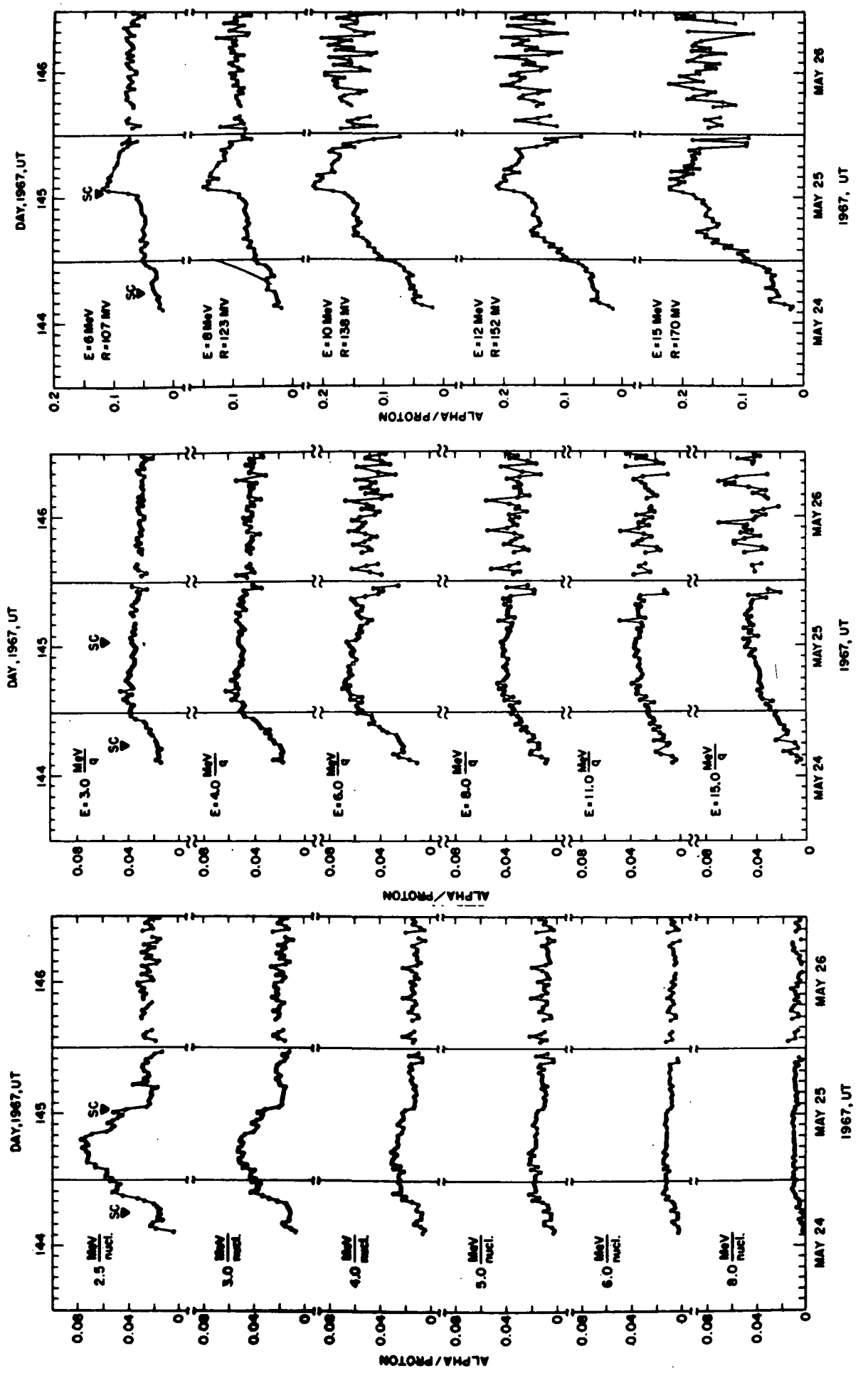
DAY, 1967, UT
144
145
146
SC
MAY 24
MAY 25
MAY 26
1967, UT
ALPHA/PROTON
E = 6 MeV R = 107 MV
E = 8 MeV R = 123 MV
E = 10 MeV R = 138 MV
E = 12 MeV R = 152 MV
E = 15 MeV R = 170 MV
E = 3.0 MeV/q
E = 4.0 MeV/q
E = 6.0 MeV/q
E = 8.0 MeV/q
E = 11.0 MeV/q
E = 15.0 MeV/q
2.5 MeV/nucl.
3.0 MeV/nucl.
4.0 MeV/nucl.
5.0 MeV/nucl.
6.0 MeV/nucl.
8.0 MeV/nucl.

Figure 7

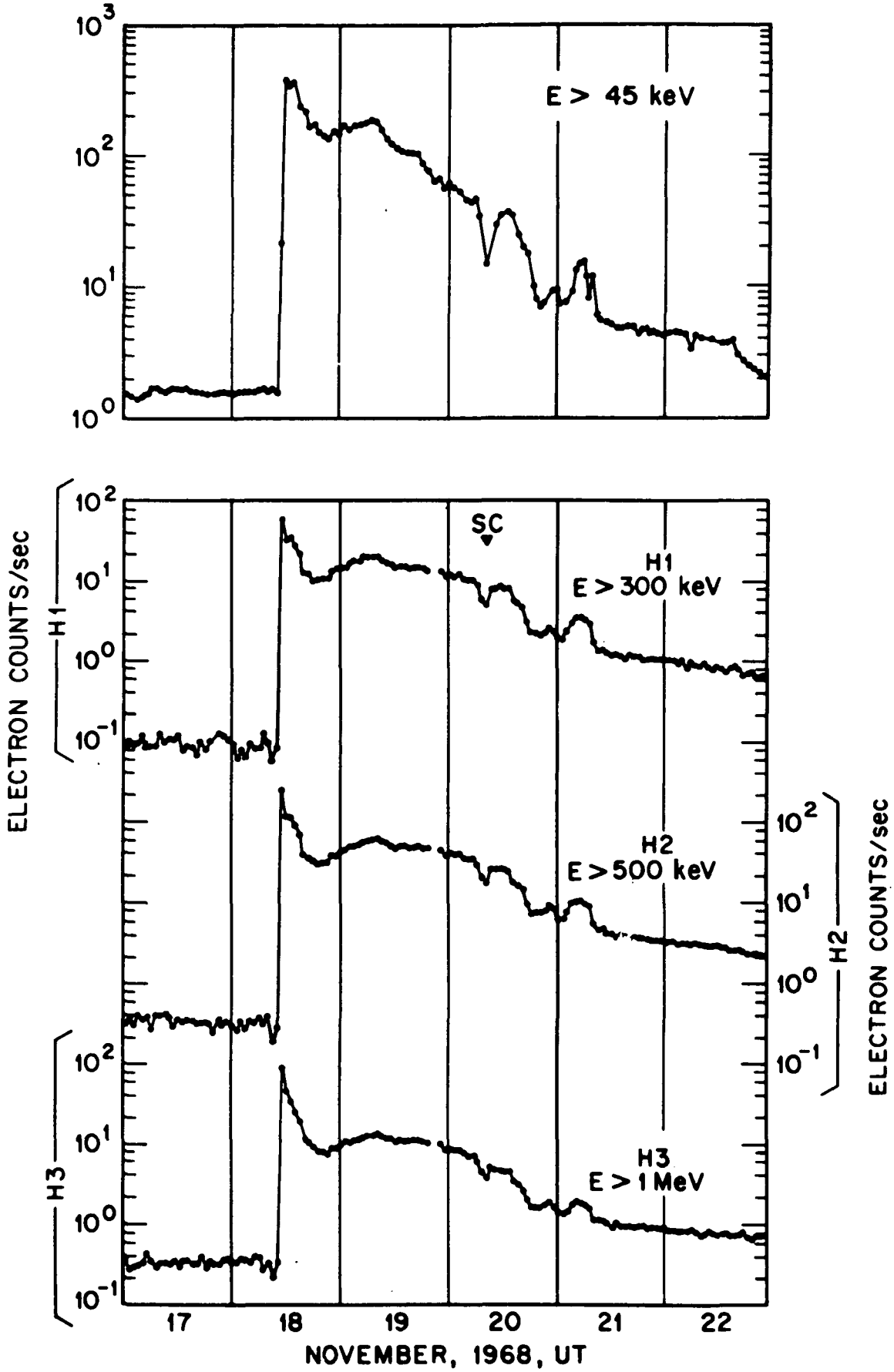
E > 45 keV
SC
H1
E > 300 keV
H2
E > 500 keV
H3
E > 1 MeV
ELECTRON COUNTS/sec
H1
H2
H3
ELECTRON COUNTS/sec
17
18
19
20
21
22
NOVEMBER, 1968, UT

Figure 8

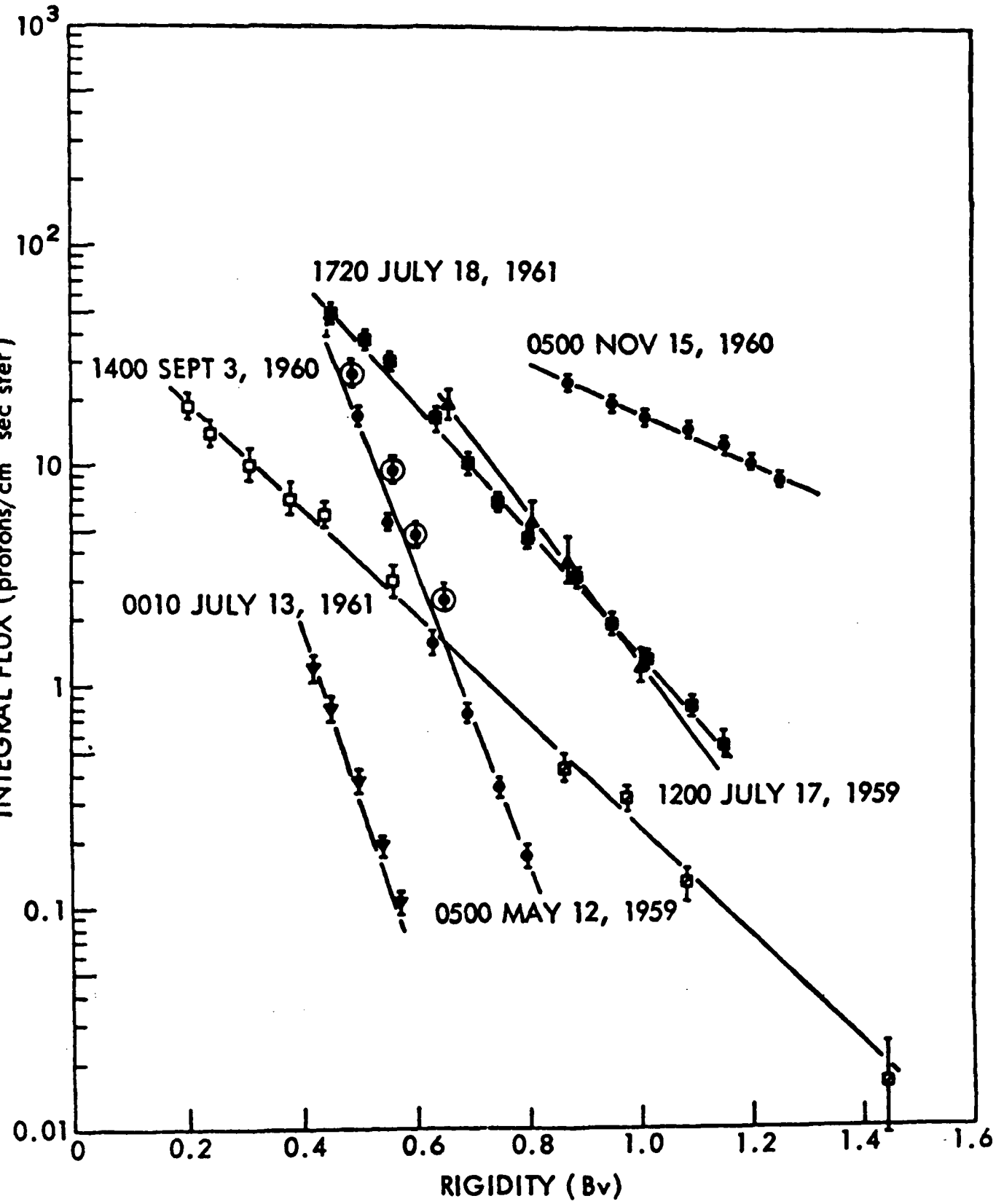
INTEGRAL FLUX (protons/cm² sec ster)
RIGIDITY (Bv)
1720 JULY 18, 1961
0500 NOV 15, 1960
1400 SEPT 3, 1960
0010 JULY 13, 1961
1200 JULY 17, 1959
0500 MAY 12, 1959

Figure 9

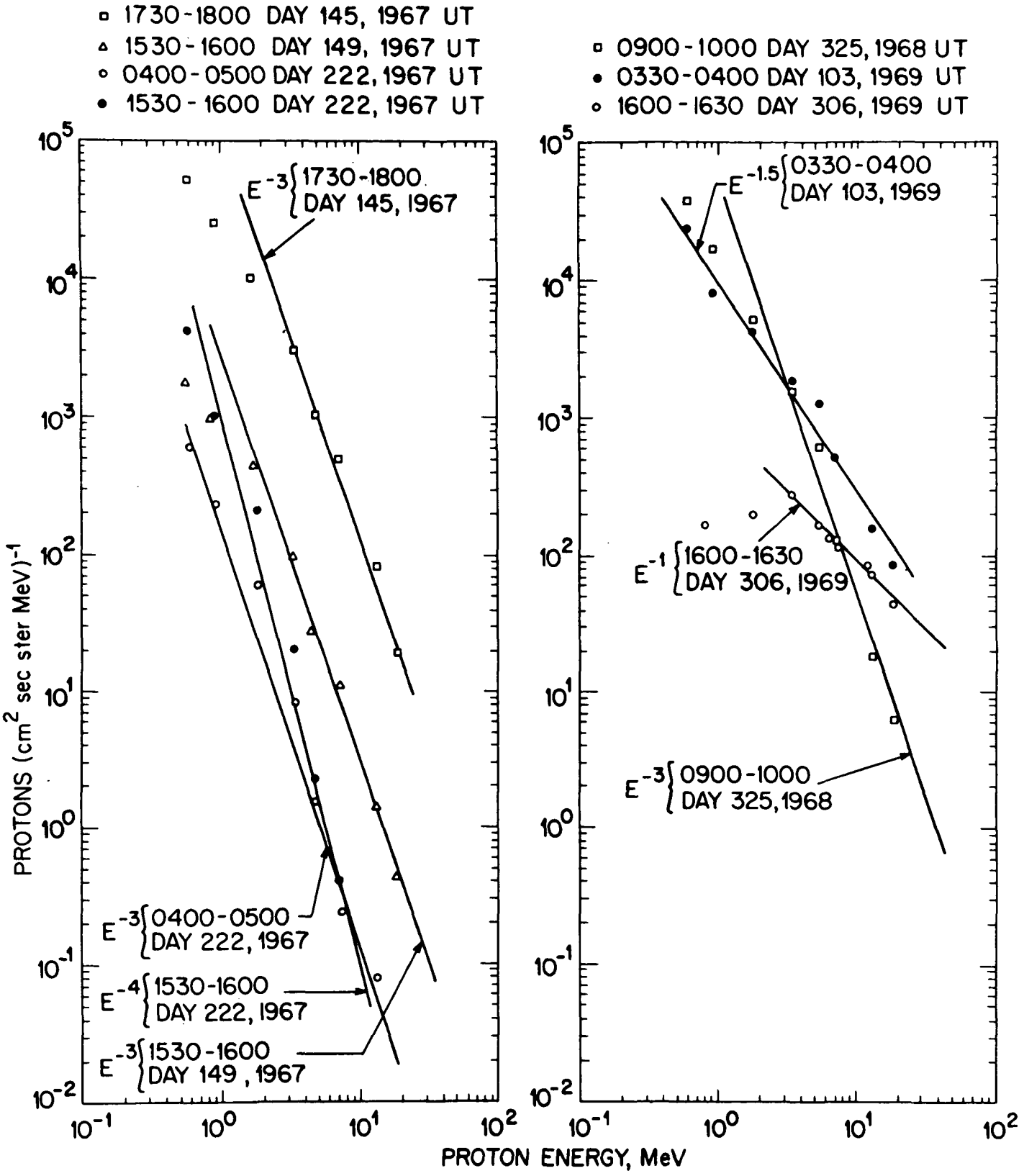
1730-1800 DAY 145, 1967 UT
1530-1600 DAY 149, 1967 UT
0400-0500 DAY 222, 1967 UT
1530-1600 DAY 222, 1967 UT
0900-1000 DAY 325, 1968 UT
0330-0400 DAY 103, 1969 UT
1600-1630 DAY 306, 1969 UT
E^-3 {1730-1800 DAY 145, 1967
E^-3 {0400-0500 DAY 222, 1967
E^-4 {1530-1600 DAY 222, 1967
E^-3 {1530-1600 DAY 149, 1967
E^-1.5 {0330-0400 DAY 103, 1969
E^-1 {1600-1630 DAY 306, 1969
E^-3 {0900-1000 DAY 325, 1968
PROTONS (cm^2 sec ster MeV)^-1
PROTON ENERGY, MeV

Figure 10

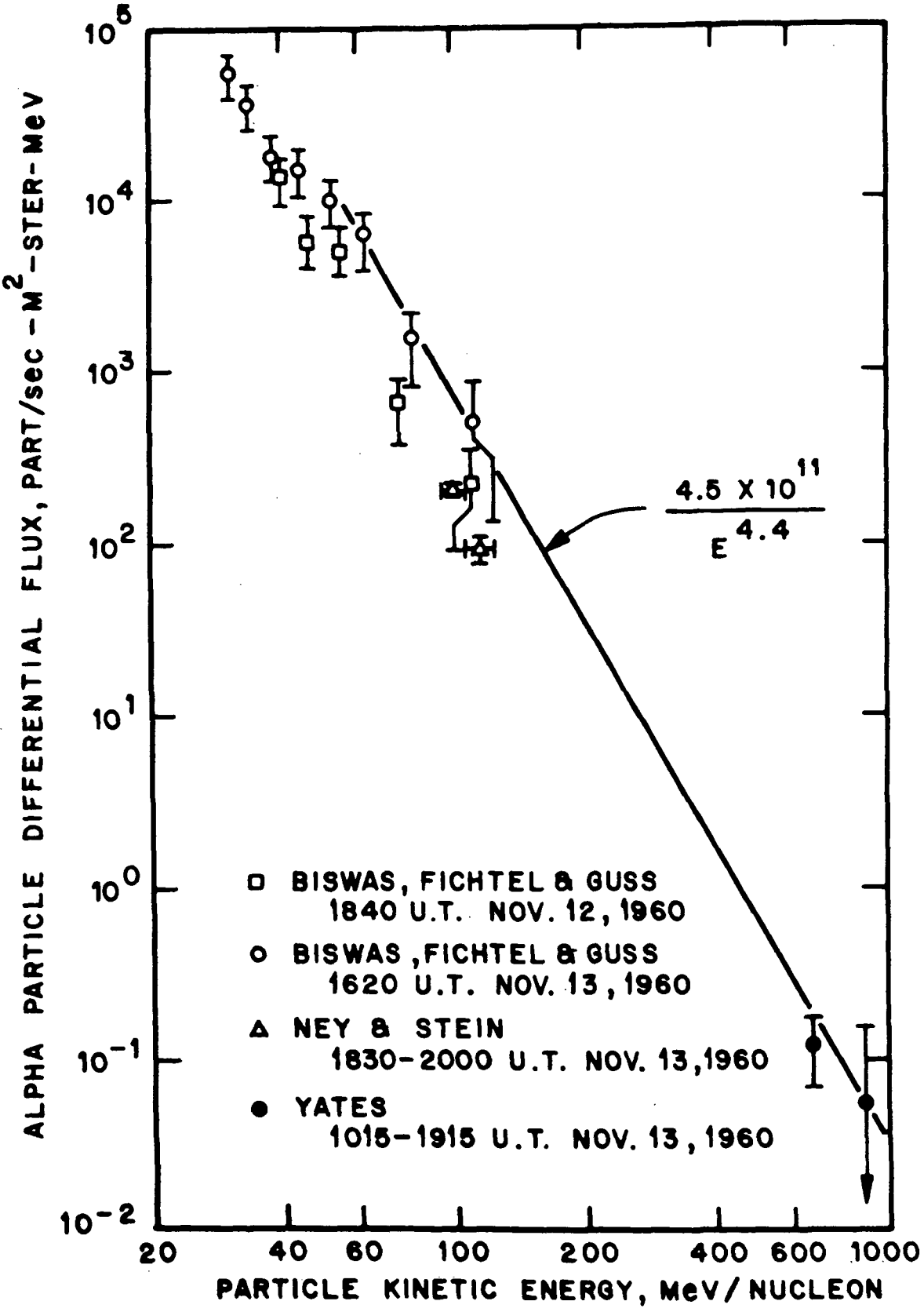
ALPHA PARTICLE DIFFERENTIAL FLUX, PART/sec - M$^2$ - STER - MeV
$10^5$
$10^4$
$10^3$
$10^2$
$10^1$
$10^0$
$10^{-1}$
$10^{-2}$
$\frac{4.5 \times 10^{11}}{E^{4.4}}$
BISWAS, FICHTEL & GUSS
1840 U.T. NOV. 12, 1960
BISWAS, FICHTEL & GUSS
1620 U.T. NOV. 13, 1960
NEY & STEIN
1830-2000 U.T. NOV. 13, 1960
YATES
1015-1915 U.T. NOV. 13, 1960
20
40
60
100
200
400
600
1000
PARTICLE KINETIC ENERGY, MeV/NUCLEON

Figure 11

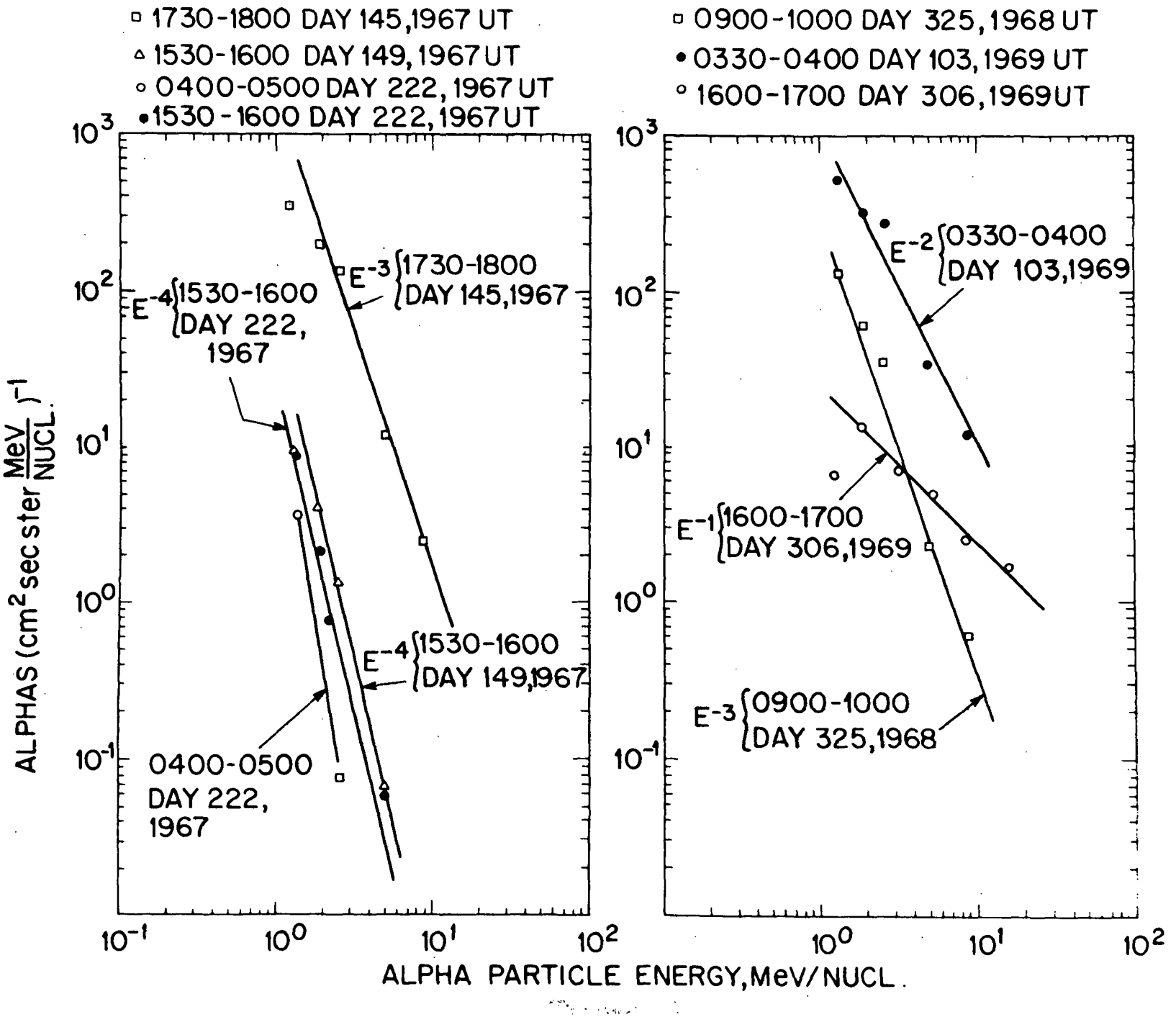
1730-1800 DAY 145,1967 UT
1530-1600 DAY 149,1967 UT
0400-0500 DAY 222,1967 UT
1530-1600 DAY 222,1967 UT
0900-1000 DAY 325,1968 UT
0330-0400 DAY 103,1969 UT
1600-1700 DAY 306,1969 UT
ALPHAS (cm² sec ster MeV/NUCL.)⁻¹
ALPHA PARTICLE ENERGY, MeV/NUCL.
E⁻⁴ {1530-1600 DAY 222, 1967
E⁻³ {1730-1800 DAY 145,1967
E⁻⁴ {1530-1600 DAY 149,1967
0400-0500 DAY 222, 1967
E⁻² {0330-0400 DAY 103,1969
E⁻¹ {1600-1700 DAY 306,1969
E⁻³ {0900-1000 DAY 325,1968

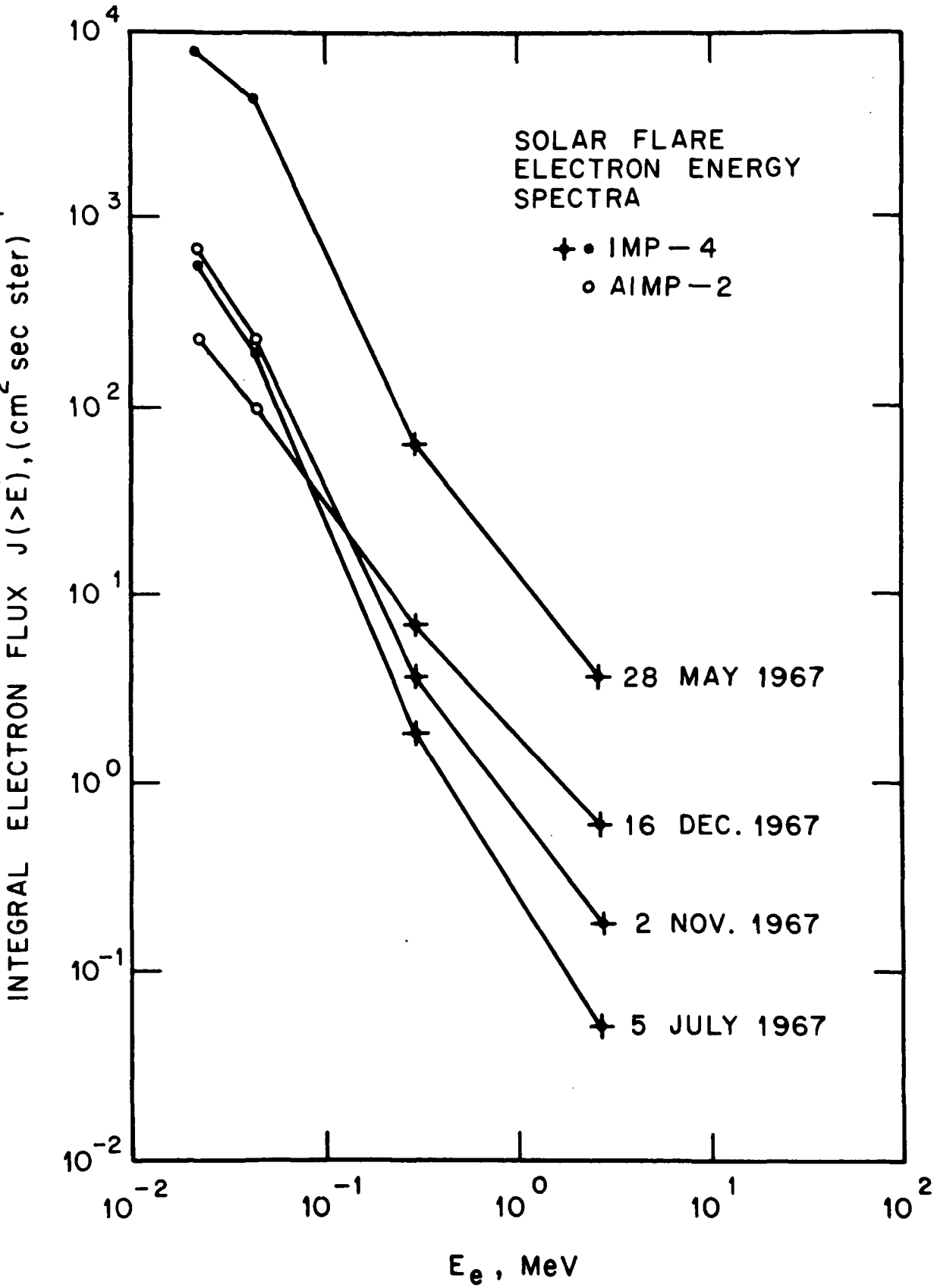
SOLAR FLARE
ELECTRON ENERGY
SPECTRA
IMP – 4
AIMP – 2
28 MAY 1967
16 DEC. 1967
2 NOV. 1967
5 JULY 1967
INTEGRAL ELECTRON FLUX J(>E), (cm² sec ster)⁻¹
E_e , MeV
10⁴
10³
10²
10¹
10⁰
10⁻¹
10⁻²
10⁻²
10⁻¹
10⁰
10¹
10²

Figure 13

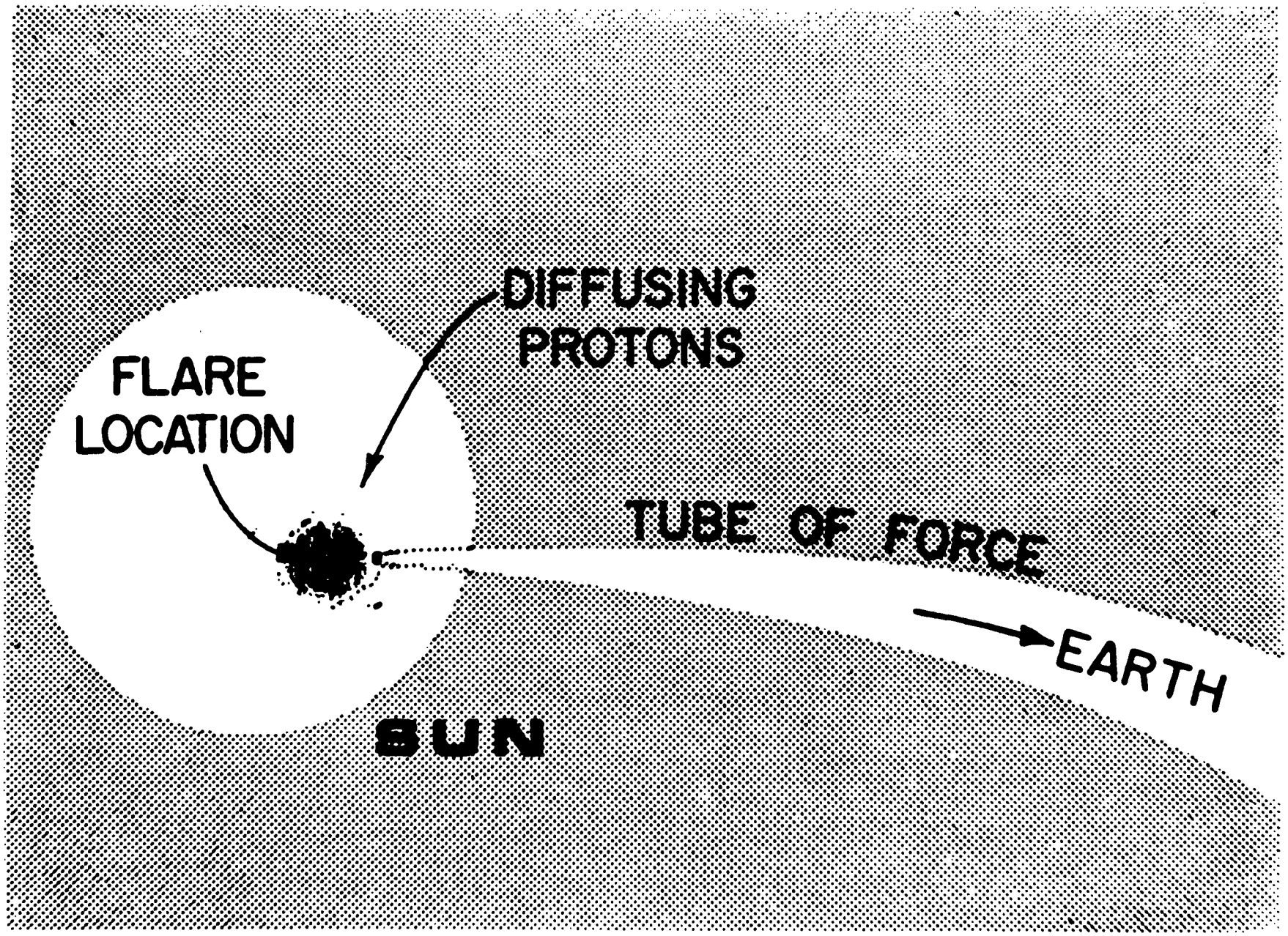


Figure 14

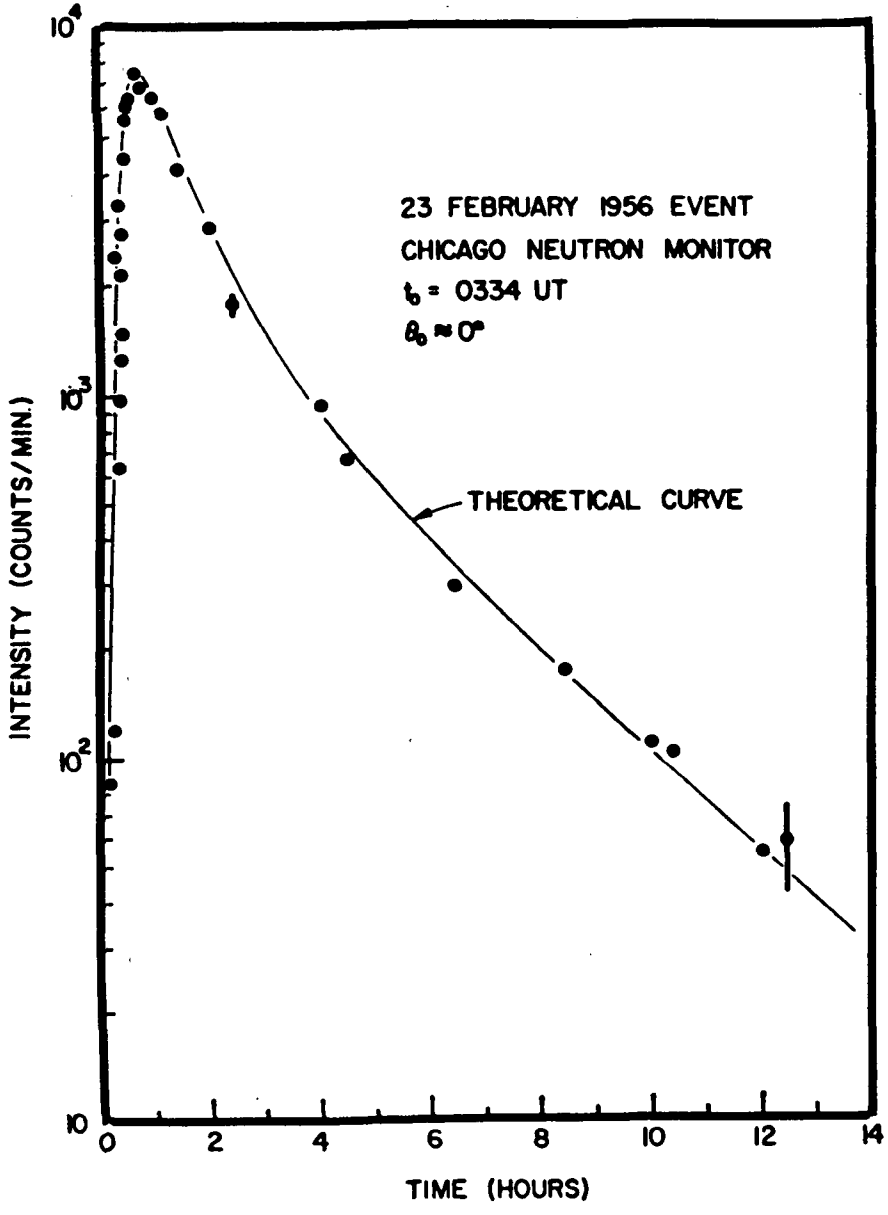
23 FEBRUARY 1956 EVENT
CHICAGO NEUTRON MONITOR
$t_0$ = 0334 UT
$\theta_0 \approx 0°$
THEORETICAL CURVE
INTENSITY (COUNTS/MIN.)
TIME (HOURS)

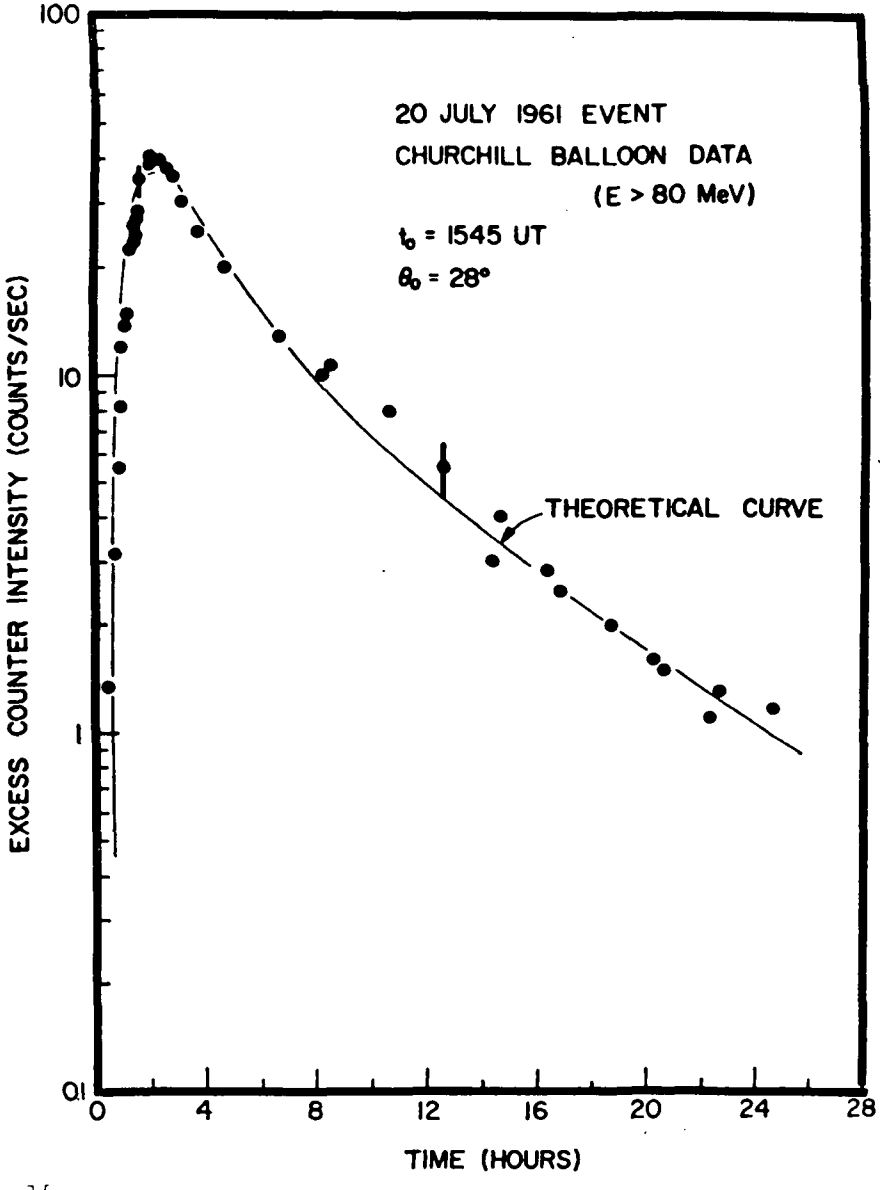
20 JULY 1961 EVENT
CHURCHILL BALLOON DATA
(E > 80 MeV)
$t_0$ = 1545 UT
$\theta_0$ = 28°
THEORETICAL CURVE
EXCESS COUNTER INTENSITY (COUNTS/SEC)
TIME (HOURS)

Figure 15

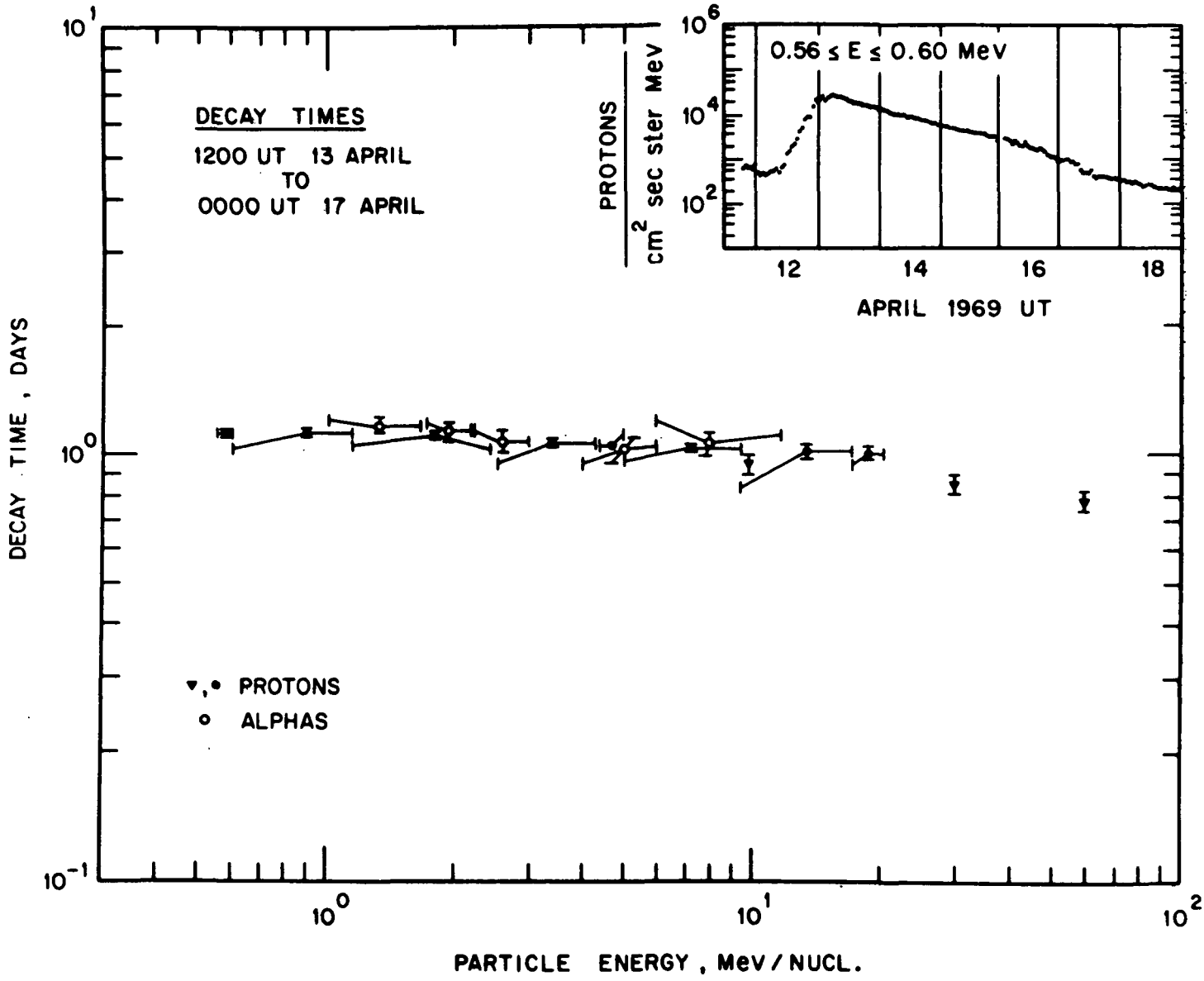
DECAY TIMES
1200 UT 13 APRIL
TO
0000 UT 17 APRIL
PROTONS
cm² sec ster MeV
0.56 ≤ E ≤ 0.60 MeV
APRIL 1969 UT
DECAY TIME, DAYS
▼,● PROTONS
○ ALPHAS
PARTICLE ENERGY, MeV/NUCL.

Figure 16

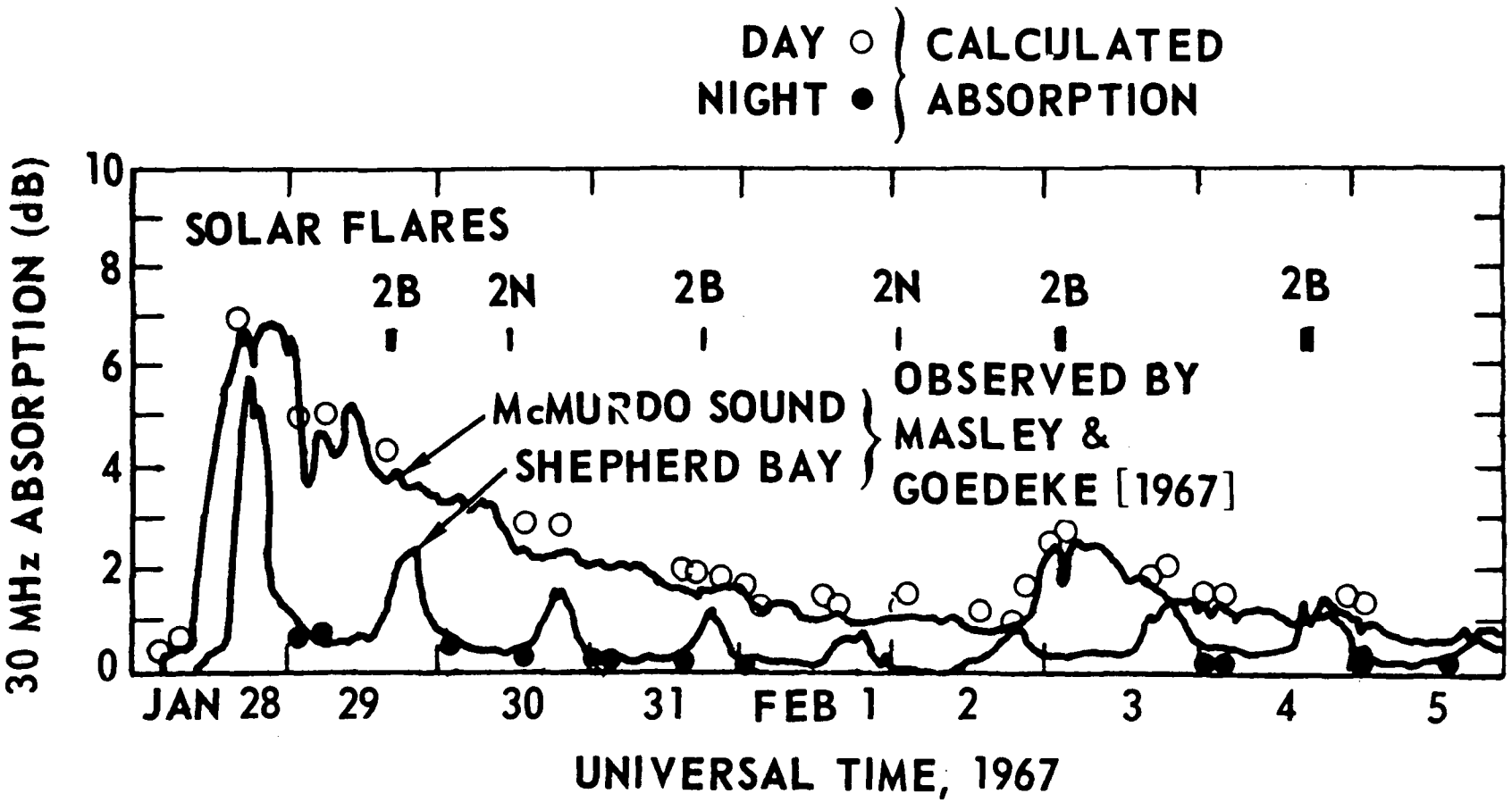
DAY ○
NIGHT ●
CALCULATED ABSORPTION
30 MHz ABSORPTION (dB)
10
8
6
4
2
0
SOLAR FLARES
2B
2N
2B
2N
2B
2B
McMURDO SOUND
SHEPHERD BAY
OBSERVED BY MASLEY & GOEDEKE [1967]
JAN 28
29
30
31
FEB 1
2
3
4
5
UNIVERSAL TIME, 1967

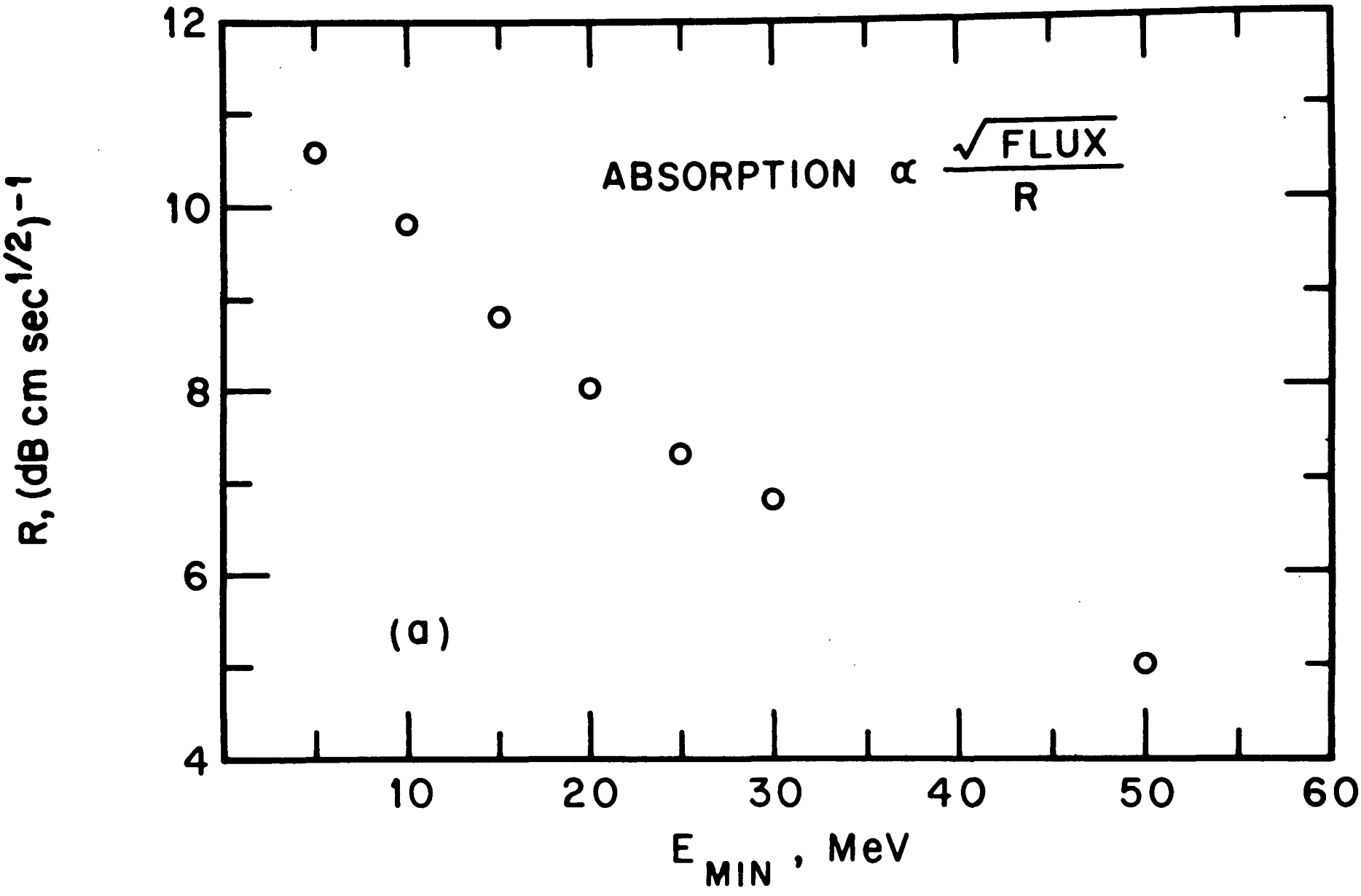
12
10
8
6
4
10
20
30
40
50
60
R, (dB cm sec^1/2)-1
E MIN , MeV
ABSORPTION α √FLUX / R
(a)

Figure 18

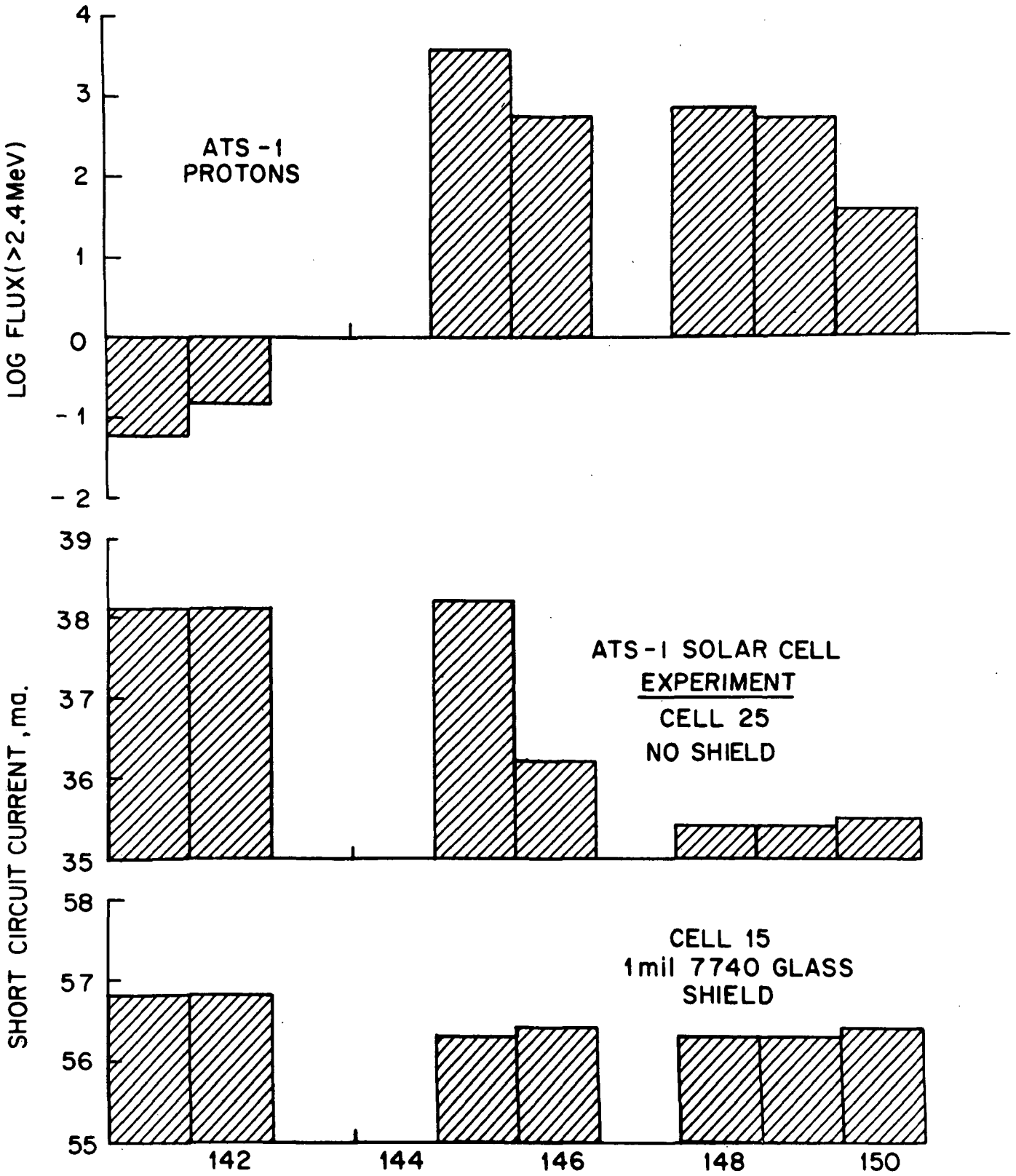
LOG FLUX(>2.4MeV)
4
3
2
1
0
-1
-2
ATS-1
PROTONS
SHORT CIRCUIT CURRENT, ma.
39
38
37
36
35
ATS-1 SOLAR CELL
EXPERIMENT
CELL 25
NO SHIELD
58
57
56
55
CELL 15
1mil 7740 GLASS
SHIELD
142
144
146
148
150
DAY 1967 UT

Figure 19